Study of the photobleaching mechanisms of the 5,10,15,20-tetrakis(m-hydroxyphenyl) bacteriochlorin (m-THPBC), in solution, in vitro and in vivo.

Henri-Pierre Lassalle

UNIVERSITE HENRI POINCARE-NANCY I

FACULTE DE MEDECINE

THESE

pour obtenir le grade de

DOCTEUR DE L'UNIVERSITE HENRI POINCARE-NANCY I

LABEL EUROPEEN

Discipline : Bio ingénierie

Présentée et soutenue publiquement

par **Henri-Pierre LASSALLE**

Le 07 juillet 2005

Etude des mécanismes du photoblanchiment de la 5,10,15,20-tetrakis(*m*-hydroxyphenyl)bactériochlorine, en solution, *in vitro* et *in vivo*.

Directeur de Thèse : Dr. L. Bezdetnaya-Bolotine

JURY

Jury : Dr. L.N. Bezdetnaya-Bolotine (Nancy, France)
Pr. F. Guillemin (Nancy, France), Président du Jury
Pr. J-F. Muller (Metz, France)
Pr. A.C. Tedesco (Sao Polo, Brésil)

Rapporteurs: Pr. R. Bonnett (Londres, UK)
Pr. H. Schneckenburger (Aalen, Allemagne)
Pr. P. de Witte (Leuven, Belgique)

UNIVERSITE HENRI POINCARE-NANCY I

FACULTE DE MEDECINE

THESE

pour obtenir le grade de

DOCTEUR DE L'UNIVERSITE HENRI POINCARE-NANCY I

LABEL EUROPEEN

Discipline : Bio ingénierie

Présentée et soutenue publiquement

par **Henri-Pierre LASSALLE**

Le 07 juillet 2005

Etude des mécanismes du photoblanchiment de la 5,10,15,20-tetrakis(*m*-hydroxyphenyl)bactériochlorine, en solution, *in vitro* et *in vivo*.

Directeur de Thèse : Dr. L. Bezdetnaya-Bolotine

JURY

Jury :	Dr. L.N. Bezdetnaya-Bolotine (Nancy, France)
	Pr. F. Guillemin (Nancy, France), Président du Jury
	Pr. J-F. Muller (Metz, France)
	Pr. A.C. Tedesco (Sao Polo, Brésil)
Rapporteurs:	Pr. R. Bonnett (Londres, UK)
	Pr. H. Schneckenburger (Aalen, Allemagne)
	Pr. P. de Witte (Leuven, Belgique)

Summary

TABLE OF CONTENTS

General Introduction

I GENERAL INTRODUCTION

Photodynamic therapy (PDT) has been developed as a treatment modality for a number of malignant and non-malignant disorders. PDT treatment is based on the presence of a drug with photosensitising and tumour localizing properties combined with visible light and oxygen. Separately, these three components are harmless, but in combination they may destroy tissue and inactivate cells.

Accurate dosimetry is necessary to ensure complete treatment and to allow for consistent and reproducible patient outcomes. It is widely accepted that the phototherapeutic effect of PDT is a result of the generation of singlet oxygen from the activation of a photosensitizer by light. The objective of PDT is to deliver a cytotoxic species dose that is sufficient and in the right place to kill or control the growth of malignant cells in a tumour. Dynamic variations of several parameters induced by irradiation: photosensitiser concentration, localisation and optical properties of the tissue makes the PDT treatment very complex. Therefore the understanding of the photodegradation mechanism, localisation and photodynamic reaction of a photosensitiser may provide information of paramount importance to adapt the photodynamic dose and receive the optimal treatment.

5,10,15,20-tetrakis(*m*-hydroxyphenyl)bacteriochlorin (*m*-THPBC) is a second generation photosensitiser, from the tetraphenylchlorin series. Even if several properties of the related sensitisers are now relatively well established, very little is known about the mechanisms of action of the *m*-THPBC. The first objective of the present study was to examine the photobleaching characteristics of *m*-THPBC in solution: the influence of the aggregation state of the photosensitiser on the photobleaching rate and the photodegradation yield, the nature of the photoproducts following laser irradiation and the identification of the species in charge of photobleaching. In a second part we examined some photobiological and photobleaching properties *in vitro* on WiDr adherent cells. And the third part of the work was an *in vivo* study assessing the *m*-THPBC potential in *nude* mice.

Introduction

II INTRODUCTION

II.1. Origin of Photodynamic Therapy

Light as been employed in the treatment of disease since antiquity. Phototherapy has been applied by humans for 3000 years and was known by the Egyptians, the Indians and the Chinese (Spikes, 1985). Herodotus (6C BC) is recorded as noticing the beneficial effect of sunlight on bone growth, and the eminent Hippocrates (460-375 BC) recommended the use of heliotherapy for various human diseases. But the first relevant "modern" scientist in the field of phototherapy was Niels Rydberg Finsen. From 1895 until 1903 he performed phototherapy on 800 patients, and in 1903 he was awarded the Nobel Prize for Physiology-Medicine for his work on the use of light from the carbon arc in the treatment of lupus vulgaris (skin tuberculosis) (Szeimies et al., 2001). The concept of cell death being induced by the interaction of light and chemicals has first been reported by a German medical student Oscar Raab. In the winter semester of 1897-1898 he started an investigation on the toxicity of acridine to paramecia. This work was carried out under the direction of Professor Dr. Hermann von Tappeiner. Initially, Raab found that the apparent toxicity of low concentrations of acridine varied significantly from day to day; however he soon noted that the toxicity depended on the intensity of sunlight in the laboratory. He was then able to show that low concentration of acridine and some other colored dyes such as eosin, that had no effect in the dark, provoked the rapid killing of paramecia in the presence of light (Raab, 1900). In 1902, C. Ledoux-Lebards observed that eosin killed paramecia more efficiently in open flask than in a closed bottle (Ledoux-Lebards, 1902), and he postulated that the presence of oxygen is essential for photoinactivation. It is in 1904 that von Tappeiner and Jodlbauer coined the term "photodynamische Wirkung "(von Tappeiner and Jodlbauer, 1904) which we translate as "photodynamic action" for oxygen-requiring photosensitized reactions in biological systems.

Although the mechanism of action was still unknown, it did not take long until this new therapeutic approach was tried out on patients. The first paper reporting a clinical trial was published in November 1903 by von Tappeiner and Jesionek (von Tappeiner and Jesionek, 1903). Several other trials were performed on patients, mainly by Dreyer and Neisser, unfortunately they were rapidly terminated because of severe side effects or because of temporary therapeutic effects. The photosensitisers used so far were dyes like chinidine, acridine and eosin, and further studies were devoted to develop new clinically relevant photosensitisers.

In 1911, Walter Hausmann injected 2 mg hematoporphyrin subcutaneously in mice, which were exposed to sunlight and he observed edema, erythema and skin necrosis (Haussman, 1911). The first report on the use of hematoporphyrin in humans was done by Meyer-Betz who injected himself with 200 mg hematoporphyrin and became extremely photosensitive during more than two months (Meyer-Betz, 1913). Accumulation and retention of hematoporphyrin in human neoplastic tissue was evidenced by Auler and Banzer in 1942 (Auler and Banzer, 1942). Interrupted by the Second World War clinical studies on photodynamic treatment were not performed in a major organized way until the middle 70's, largely through the efforts of Dougherty.

Photodynamic therapy uses the combination of a photosensitising drug and light to cause selective damage to the target tissue. The improved understanding of the tissue and cellular factors that control PDT and increased experience in the clinic has led to much larger, better-controlled clinical trials and the approval of drugs makes PDT a clinical reality. Photofrin® was the first approved in 1993 in Canada, now approved in more than 40 countries (1995 approval in USA, Canada, Japan and Europe) for advanced and early lung cancer, superficial gastric cancer, oesophageal adenocarcinoma, cervical cancer, and bladder cancer. Then the Levulan® got the FDA approval in 1999 for actinic keratosis, followed in 2001 by Foscan® (approved for advanced head and neck cancer, Europe, Norway and Iceland) and Metvix, approved for actinic keratosis, superficial basal-cell carcinoma, and basal-cell carcinoma in Europe. PDT has also indications for non-oncological diseases, such as wet age related macular degeneration (Visudyne®, FDA and European approval in 2000). Also a number of other conditions have also been treated including psoriasis, rheumatoid arthritis, menorrhagia and benign prostatic hyperplasia. In addition, PDT-mediated immune-modulation, bone marrow purging and PDT of certain bacterial, fungal and viral infections are being evaluated.

II.2. Photosensitization mechanisms.

2.1. Pathway of molecular excitation and deactivation

The absorption of light by a chromophore is the initial step in all photophysical and photochemical reactions, the energy of the absorbed light promotes molecules from their ground state, to states of higher energy (exited states). At room temperature, almost all the molecules are in their ground state, which is the electronic state associated with the lowest energy and a configuration where all electrons are orbitally paired. During an electronic transition one of the electrons is excited from an initially occupied orbital of low energy to a

previously unoccupied orbital of higher energy. This process transforms the molecule from its ground state into an excited state.

The excited state S_1 has a different electronic distribution than the ground state S_0, and is energetically less stable than S_0. De-excitation must take place to permit the release of the surplus of energy. Several physical pathways leading to deactivation can be followed, represented in the Jablonski diagram (figure 2.1.). A molecule in a high vibrational level of the excited state S_n will quickly fall to the lowest vibrational level of this state (Vibrational Relaxation: VR). Also, a molecule in a higher excited state S_n will finally fall to the first excited singlet state S_1 (Internal Conversion: IC). Then, the singlet state S_1 can rapidly return to the ground state level S_0 by two mechanisms, a radiative process which is fluorescence, or a non radiative process (IC). During this internal conversion, the excess of energy of the singlet state is released as heat, which dissipates usually into the tissue or the solvent. Concerning the radiative process, a photon is emitted with an energy equal to the energy gap between the ground state (S_0) and the excited singlet state (S_1) levels. This implies that the fluorescence does not depend on the excitation wavelength (Vavilov's rule). Emitted photons have lower energy than absorbed photons, so fluorescence emission maximum is red-shifted as compared to the absorption maximum, this is known as the Stokes-Lommel's law ($h\upsilon_{emission} > h\upsilon_{absorption}$).

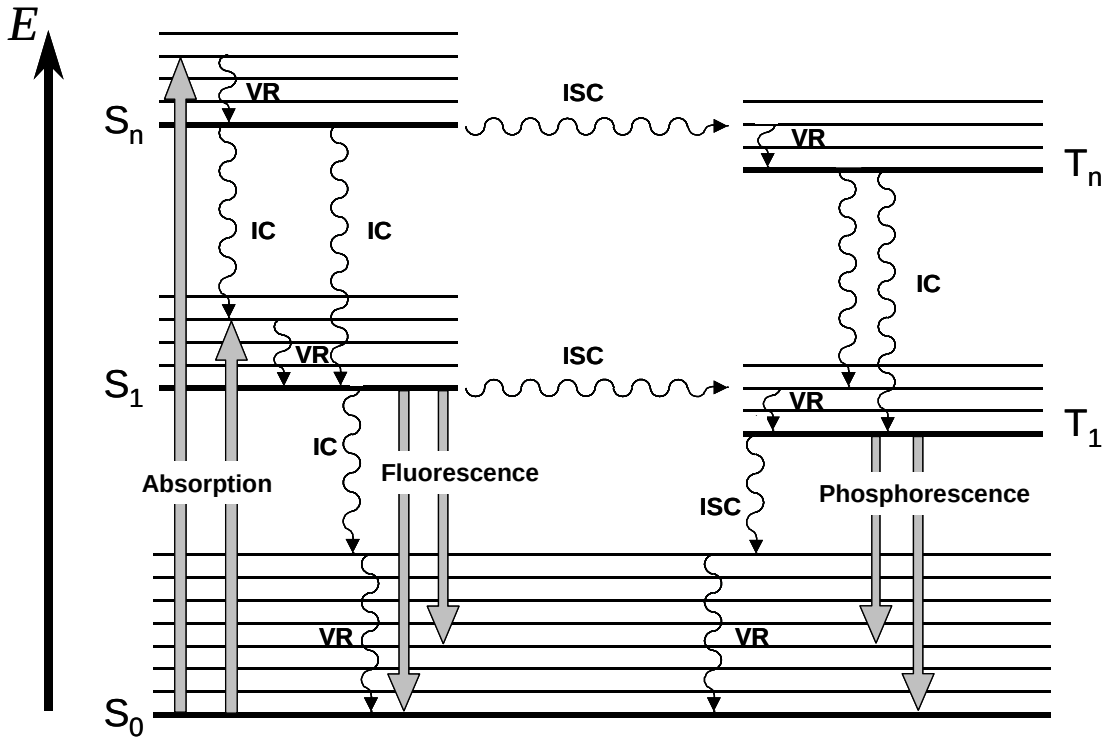

Figure 2.1 : Jablonski diagram, where IC stands for internal conversion, ICS for intersystem crossing and VR, for vibrational relaxation.

In addition to radiationless and radiative process, the singlet state can undergo a change to a triplet state T_1 via a pathway called intersystem crossing (ISC). The lifetime of the triplet state is much longer ($\tau \sim 10^{-7}$s) than the lifetime of the singlet state ($\tau \sim 10^{-10}$s), thus increasing dramatically the probability of a reaction with a neighbouring molecule. They are several pathways for the triplet state T_1 to return to a ground state S_0. De-excitation can occur with the emission of a photon, this is phosphorescence, but at room temperature and due to Vavilov's rule the phosphorescence is very weak and difficult to detect. The excited triplet state T_1 can alternatively deactivate by undergoing intersystem crossing followed by vibrational relaxation.

For most of the organic molecules, only the singlet state S1 and triplet state T1 of lowest energy can be considered as likely candidates for the initiation of photochemical and photophysical reactions. This is due to the fact that higher order electronic state ($n \geq 2$) undergo very rapidly internal conversion from S_n to S_1 and from T_n to T_1. This generalization (which was used here in the description of the Jablonski diagram fig. 2.1.) is known as Kasha's rule.

Table 2.1. : Photochemical processes involved in the activation and deactivation pathway of the photosensitizers and some of their characteristics

Processes	Reactions	Timescale	Constant
excitation	$h\upsilon + S_0 \rightarrow S_1, S_2, \ldots, S_n$	$\tau \sim 10^{-15}$-10^{-12} s	k_{abs}
internal conversion	$S_n, \ldots, S_2 \rightarrow S_1$ + heat	$\tau \sim 10^{-13}$-10^{-10} s	$k_{IC}[S_n]$
internal conversion	$S_1 \rightarrow S_0$ + heat	$\tau \sim 10^{-10}$ s	$k_{IC}[S_1]$
intersystem crossing	$S_1 \rightarrow T_1$ + heat	$\tau \sim 10^{-7}$ s	$k_{ISC}[S_1]$
photochemical reaction	$S_1 \rightarrow S_0$+ reaction		$k_R{}^S[S_1]$
fluorescence	$S_1 \rightarrow S_0 + h\upsilon_{fluor}$	$\tau \sim 10^{-11}$-10^{-8} s	$k_F[S_1]$
intersystem crossing	$T_1 \rightarrow S_0$ + heat	$\tau \sim 10^{-2}$-10^{2} s	$k_{ISC}{}^T[T_1]$
phosphorescence	$T_1 \rightarrow S_0 + h\upsilon_{phosphor}$	$\tau > 10^{-6}$ s	$k_{phosph}[T_1]$
chemiluminescence	Energy + $S_0 \rightarrow S_1 \rightarrow S_0 + h\upsilon_{chemilum}$	$\tau > 10^{-6}$ s	$k_{chemilum}[S_1]$
photochemical reaction	$T_1 \rightarrow S_0$+ reaction		$k_R{}^T[T_1]$

2.2 Mechanism of photosensitized reactions

Photosensitized reaction can be defined as a process in which light activation of a chromophore induces chemical changes in another molecule than the chromophore. The initial step of the reaction is the absorption of a photon by the photosensitiser, leading to the generation of an excited state (^{3}P). In the presence of oxygen the reaction can follow two competing pathways called Type I and Type II reactions (Sharman et al., 2000). According to the definition established by Foote (Foote, 1991) and as shown in Figure 2.2., a Type I mechanism involves the direct interaction of ^{3}P with a substrate (S), whereas in a type II process, ^{3}P reacts first with molecular oxygen to produce highly reactive oxygen intermediate that easily initiates further reactions.

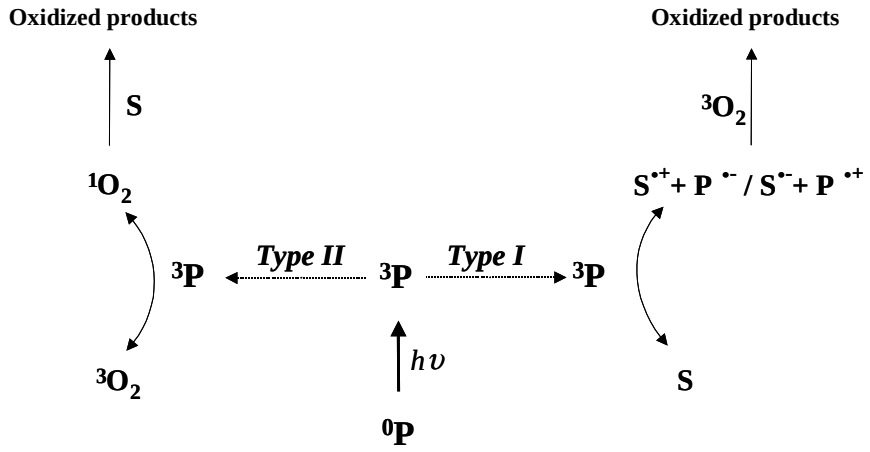

Figure 2.2. : Diagram of photosensitizations mechanisms occurring after absorption of photons by photosensitizer.

2.2.1. Type I photosensitization processes.

In a type I photochemical reaction, the exited triplet state of the photosensitiser (^{3}P*) interacts directly with the substrate molecule (S) and leads to the formation of pairs of neutral radicals or radical ions following an electron or hydrogen transfer as shown in the Eqs. 1& 2. Most biological substrates undergo an oxidation : (Eq. 1).

$$^3P^* + S \longrightarrow P^{\cdot -} + S^{\cdot +} \qquad (1)$$

$$^3P^* + S \longrightarrow P^{\cdot +} + S^{\cdot -} \qquad (2)$$

Both the excited photosensitiser and the ground state substrate can act as hydrogen donor (Eq. 3-4).

$$^3PH^* + S \longrightarrow P^{\cdot} + SH^{\cdot} \qquad (3)$$

$$^3P^* + SH \longrightarrow PH^{\cdot} + S^{\cdot} \qquad (4)$$

The resulting radical species from these Type I primary processes can subsequently participate in different kinds of reactions. In the presence of oxygen, for example, oxidized forms of the sensitiser or of the substrate readily react with O_2 to give peroxyl radicals, thus initiating a radical chain auto-oxidation (as described by Eqs (5) and (6)).

$$S^{\cdot} + O_2 \longrightarrow SOO^{\cdot} \qquad (5)$$

$$SOO^{\cdot} + SH \longrightarrow S^{\cdot} + SOOH \qquad (6)$$

Semireduced forms of the photosensitiser or of the substrate also interact efficiently with oxygen and the electron transfer which takes place between the reactants, generates superoxide radical anion (Eqs. 7).

$$\left.\begin{aligned} S^{\cdot -} + O_2 &\longrightarrow S + O_2^{\cdot -} \\ P^{\cdot -} + O_2 &\longrightarrow P + O_2^{\cdot -} \end{aligned}\right\} \qquad (7)$$

Any reaction that generates $O_2^{\cdot -}$ will also produce hydroperoxide H_2O_2 by spontaneous dismutation (eq. 8) or one-electron reduction (eq. 9).

$$O_2^{\cdot -} + O_2^{\cdot -} + 2H^+ \longrightarrow O_2 + H_2O_2 \qquad (8)$$

$$O_2^{\cdot -} + 2H^+ + e^- \longrightarrow H_2O_2 \qquad (9)$$

Hydroperoxide is a moderate oxidant, but when it accumulates, it can react with superoxide radical anion (eq. 10) or undergo ferrous ion catalysed reduction to give rise to an extremely reactive hydroxyl radical (Haber-Weiss reaction)(eqs. 11 & 12).

$$O_2^{\cdot -} + H_2O_2 \longrightarrow O_2 + OH^- + {}^{\cdot}OH \qquad (10)$$

$$O_2^{\cdot -} + Fe^{3+} \longrightarrow O_2 + Fe^{2+} \qquad (11)$$

$$H_2O_2 + Fe^{2+} \longrightarrow OH^- + {}^{\cdot}OH + Fe^{3+} \qquad (12)$$

Haber-Weiss reaction

2.2.2. Type II photosensitization processes.

This type of reaction requires the presence of molecular oxygen. In most cases, the reaction proceeds via energy transfer from the excited triplet state photosensitiser to the oxygen molecule in its triplet state. Singlet oxygen can only be generated by photosensitisers that possess an energy gap between the ground state and the excited triplet state which is higher than the energy $E\Delta$ needed to excite oxygen into its excited singlet state (Figure 2.3.). $E\Delta$ being very low (94 kJ mol-1 (van Lier and Spikes, 1989)), almost all the tetrapyrrolic photosensitisers can mediate generation of singlet oxygen. Theoretically all molecules absorbing light at wavelength $\lambda < 1260$ nm can mediate generation of $^1O_2$.

Due to the higher lifetime of triplet state of porphyrin-like photosensitiser compared to the singlet state, photochemical reactions most likely occur from the triplet state. The oxygen, is then excited from its ground state into excited single state:

$$P \xrightarrow{h\upsilon} {}^1P^* \longrightarrow {}^3P + O_2 \longrightarrow P + {}^1O_2 \qquad (13)$$

For pure Type II reaction, the quantum yield formation of singlet oxygen can be defined as: (for constant description see Table 2.1.)

$$\varphi_\Delta = \varphi_R^T = \frac{k_R^T[T_1] \,.\, [S]}{k_{phosph}[T_1] + k_{ISC}^T[T_1] + k_R^T[T_1] \,.\, [S]} \qquad (14)$$

Singlet oxygen is a very reactive species, it is much more electrophilic than its ground state and can oxidize biomolecules very rapidly. It is a metastable species with a lifetime varying from about 4 µs in water to 25-100 µs in non polar organic solutions, which can be considered as a model for lipid regions of the cell (Kohen et al., 1995). The life time of singlet oxygen decreases in biological environment due to the presence of various quenchers, and is calculated to be about 170-330 ns (Baker and Kanofsky, 1992). According to Moan and coworkers, this short lifetime allows the diffusion of singlet oxygen to a maximum distance of 50 nm at the sub-cellular level (Moan, 1990; Moan and Berg, 1991; Moan and Boye, 1981). Singlet oxygen can be either deactivated by returning to the ground state, or react with electron-rich regions of many biomolecules to give oxidized species.

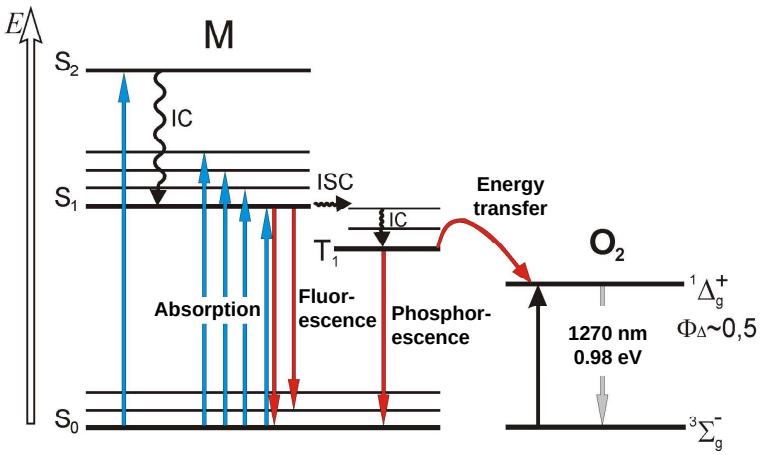

Figure 2.3. : Simplified Jablonski diagram, showing the activation and deactivation pathways during a Type II reaction.

2.3. Means to determine the reaction mechanisms

Irrespective to the reaction mechanisms, there are two distinct approaches to diagnose the relative participation of Type I and/or Type II processes. The first strategy relies upon the study of the effects of additives on biological or biochemical phenomena induced by light activation of a photosensitiser. For example the addition of sodium azide to a system should inhibit a singlet oxygen dependent biological phenomenon. The second approach is to detect, in a direct or indirect manner, the primary reactive species formed upon light activation of a photosensitiser in a biological system, e.g. the direct detection of singlet oxygen at 1268 nm.

2.3.1. Detection of radical species, type I mechanism

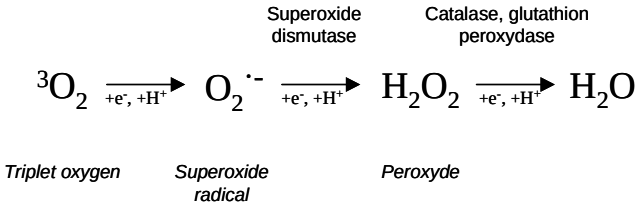

In order to detect the radical species of type I reaction, specific natural enzyme such as superoxide dismutase, catalase and glutathion peroxidase can be used. Superoxide dismutase (SOD) is known to scavenge the superoxide radical (McCord and Fridovich, 1969) with a rate constant of $2x10^9$ $M^{-1}s^{-1}$. SOD can detoxify the superoxide radical as follow (Fridovich, 1976) :

$$SOD\text{-}Me^{2+} + O_2^{\bullet -} \longrightarrow SOD\text{-}Me^{+} + O_2$$

$$SOD\text{-}Me^{+} + O_2^{\bullet -} + 2\ H^{+} \longrightarrow SOD\text{-}Me^{2+} + H_2O_2$$

SOD is a metallic oxydoreductase enzyme, the Cu^{2+}/Zn^{2+} SOD is cytoplasmic, while the Mn^{2+} enzyme is chiefly mitochondrial.

As mentioned above, Type I photodynamic reaction can generate hydrogen peroxide, this species can be scavenged by the catalase (Fridovich, 1976) according to the following reaction :

$$Cat\text{-}Fe^{3+} + 2\ H_2O_2 \longrightarrow Cat\text{-}Fe^{3+} + 2\ H_2O + O_2$$

Glutathione peroxidase, a cytosolic and mitochondrial seleno-cystein enzyme can eliminate hydrogen peroxide with the help of 2 glutathiones (GSH) (Fridovich, 1976):

$$H_2O_2 + 2\ GSH \longrightarrow 2\ H_2O + GSSG$$

Type I photodynamic reaction can also generate hydroxyl radical. In order to assess the role of this reactive oxygen species, the inhibitory action of hydrogen donors such as mannitol, ethanol, *tert*-butanol, acetate, formate and benzoic acid can be examined. These molecules

should be present in very high concentration in order to trap hydroxyl radical effectively (Foote, 1984).

Another method of detection of both superoxide and hydroxyl radicals is to trap them with spin traps like 5,5-dimethyl-pyrroline-1-oxide (DMPO), which upon reaction forms long-living characteristic spin adducts detectable by electron paramagnetic resonance (EPR) technique (Buettner and Oberley, 1978). DMPO spin label is, however, non specific and is belived to trap singlet oxygen forming essentially the same product (Foote, 1979) and these methods are unsuitable in the case of *in vivo* studies (Halliwell and Gutteridge, 1999).

2.3.2. Detection of singlet oxygen, type II mechanism

The gold standard of singlet oxygen identification is luminescence. As $^1O_2$ decays back to the ground state, some of the energy is emitted as light. There are two sorts of emission, and both are very weak in solution. The light from a single singlet oxygen molecule appears in the infrared as 1269 nm and 1588 nm (Krinsky, 1979), while two molecules can interact to produce emission at higher energy known as dimol luminescence (Cadenas et al., 1983).

$$O_2(^1\Delta_g) \longrightarrow O_2(^3\Sigma_g^-) \quad \begin{matrix} 1269\ \text{nm} \\ 1588\ \text{nm} \end{matrix}$$

$$O_2(^1\Delta_g) + O_2(^1\Delta_g) \longrightarrow O_2(^3\Sigma_g^-) + O_2(^3\Sigma_g^-) \quad \begin{matrix} 634\ \text{nm} \\ 703\ \text{nm} \end{matrix}$$

"dimol emission"

As for hydroxyl radicals, singlet oxygen can be detected with electron paramagnetic resonance (EPR). $^1O_2$ is a non-magnetic molecule and can thus not be detected directly by EPR. However, the reaction of $^1O_2$ with a stable molecule can generate a moderately long-lived free radical or a spin label whose structure as determined by EPR provides an unambiguous identification. The spin label 2,2,6,6-tetramethyl-4-piperidone (TEMP) has been

employed as a spin label probe. The reaction of $^1O_2$ with TEMP will lead to the free radical 2,2,6,6-tetramethyl-4-piperidone-N-oxyl (TEMPO) (Zang et al., 1990).

A new emerging technique to detect $^1O_2$ is a calorimetric method. This method is based on the efficient deactivation of $^1O_2$ on a cobalt coated platinum wire. The heat released during the deactivation corresponds to the excitation energy. Recently, a lower-cost laser deflection calorimeter (LDC) apparatus has been developed to determine $^1O_2$ quantitatively (Schneider et al., 2000). This method has been specially designed for the study of chemical and biochemical processes at interfaces by measuring low amounts of heat released.

The quenching of $^1O_2$ involves the deactivation of the excited singlet states of an oxygen molecule. It may be either physical or chemical quenching. Chemical quenching occurs when $^1O_2$ reacts with quencher (Q) to give product QO_2. Physical quenching leads only to the deactivation of $^1O_2$ to its ground state without oxygen consumption or product formation.

Deactivation by chemical quenching requires chemical traps such as 1,3-Diphenylisobenzofuran (DPBF), 9,10-Diphenylanthracene (DPA) or 2,5-Dimethylfuran. These substances are quite specific and react very rapidly with singlet oxygen.

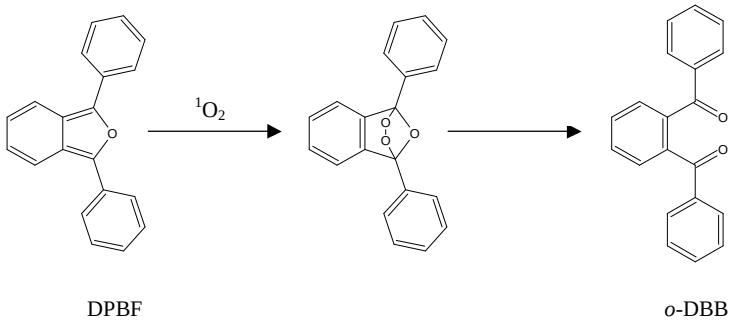

Figure 2.4. : Chemical quenching of singlet oxygen by DPBF

1,3-Diphenylisobenzofuran (DPBF), dissolved in organic solvents emits a strong fluorescence when excited at 410 nm. The intensity of fluorescence spectrum decreases when DPBF is exposed to singlet oxygen (Figure 2.4.).

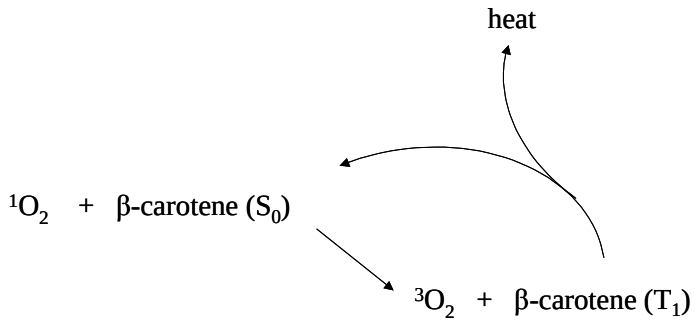

Figure 2.5. : Physical quenching of singlet oxygen by β-carotene

β-Carotene is one of the early discovered and a very well known $^1O_2$ physical quencher (Figure 2.5.) with a high efficacy ($k_q \approx 1.2 \times 10^{10}$ $M^{-1}s^{-1}$), which readily acts by energy transfer reaction with low triplet-energy species; whereas with 1,4-diazobicyclo[2,2,2]octane (DABCO) quenching reaction occurs via electron transfer. Several other physical quenchers such as azide ion N_3^-(Wilkinson and Brummer, 1981), and ascorbate quench singlet oxygen with a very high rate constant (Table 2.2.). D_2O can be used to detect $^1O_2$ presence because the lifetime of $^1O_2$ is 10 to 13 fold longer in D_2O than in H_2O (Gorman and Rodgers, 1989; Parker and Stanbro, 1984). So, if the reaction in aqueous solution is dependant on singlet oxygen, carrying it out in D_2O instead should greatly potentiate the reaction.

Table 2.2. : Bimolecular rate constants of the chemical (k_r) and chemical plus physical quenching ($k_r + k_q$) of $^1O_2$ by selected compounds.

Substrate	Solvent	k_r ($M^{-1}s^{-1}$)	$k_r + k_q$ ($M^{-1}s^{-1}$)	References
Trp	methanol	4×10^6	4×10^7	(Kohen et al., 1995)
His	methanol	7×10^6	5×10^7	(Kohen et al., 1995)
Met	methanol	5×10^6	3×10^7	(Kohen et al., 1995)
CystH	D_2O	—	8.9×10^6	(Kohen et al., 1995)
α-Tocopherol	methanol	4.6×10^7	6.2×10^8	(Kohen et al., 1995)
Vitamin C	D_2O	—	1.2×10^8	(Kohen et al., 1995)
Cholesterol	C_6D_6	—	5.7×10^4	(Vever-Bizet et al., 1989)
Linolenic acid	C_6D_6	—	1×10^5	(Vever-Bizet et al., 1989)
NADH	acetonitrle/methanol	—	7.4×10^7	(Monroe, 1985)
DPBF (1,3-Diphenylisobenzofuran)	methanol	9.8×10^8	1.2×10^9	(Monroe, 1985)
β-carotene	methanol	9.1×10^4	1.25×10^{10}	(Wilkinson and Ho, 1978)
N_3^-(azide ion)	water	—	$2\text{-}45 \times 10^8$	(Fernandez et al., 1997)
DABCO	water	—	2.4×10^7	(Monroe, 1985)

II.3. Photosensitisers.

3. 1. The profile of an ideal PDT drug.

Haematoporphyrin derivative (HpD) has been for a very long time the only photosensitiser used in clinical PDT. It belongs to the so called first generation photosensitisers. It was the first photosensitiser to receive regulatory approval from the Canada in 1993, and it is now approved in more than 40 countries. Many clinical trials have been realized with this drug, so that there is now a very large experience and the benefit of hindsight. Despite these advantages HpD presents several major drawbacks. It is a very complex mixture and the exact composition of a such mix is rather difficult to reproduce. The absorption band in the red is at 630 nm with a rather important tissue penetration, and is at the start of the "therapeutic window" and the molar extinction coefficient is rather low (about 1170 $M^{-1}cm^{-1}$). Although its photodynamic activity is acceptable, it is still modest. Finally, the selectivity for the target (tumour) is low, therefore inducing side effect such as skin sensitisation remaining for several weeks.

During the 80's it has becomes evident that HpD was not a perfect photosensitiser and Bonnett established several requirements for an ideal photosensitiser (Bonnett et al., 1989):

- Strong absorption in the red part of the visible spectrum (> 650nm)
- High quantum yield of triplet formation, with a triplet energy greater than 94 $kJmol^{-1}$, the excitation energy for Δ_g singlet oxygen
- High singlet oxygen quantum yield
- Lack of dark toxicity
- Pharmacokinetic profile with rapid clearing from the body
- High selectivity for the tumour tissue versus the healthy tissue
- Uniform stable composition, and preferably a single substance

3. 1. Photosensitisers of second and third generation.

Second generation photosensitisers have been developed so far as possible in agreement with the above requirements of the ideal photosensitiser. They are constituted by pure molecular

synthetic structure (Phthalocyanines, naphthalocyanines, benzoporphyrins, purpurins, chlorines and porphycenes) and natural porphyrinoids (pheophorbides, bacteriochlorins, bacterio-pheophorbides). Most of the second generation photosensitisers are tetrapyrrolic compounds with side chains added so as to stabilise and improve the absorption in the red. Phthalocyanines are tetrapyrrolic compounds where pyrrole groups are condensed with a benzenic group and where a nitrogenous bridge replaces a methene one, thus enhancing the molar absorption coefficient of these molecules and with a λ_{max} absorption around 700 nm. Texaphyrins are also synthetic relatives of porphyrins, due to their side chains these molecules are water soluble, and rapidly cleared from the circulation with a wide absorption band centred at 732 nm. However, one of the most active photosensitising agent appears to be 5,10,15,20-tetrakis(*m*-hydroxyphenyl)chlorin (*m*-THPC) (Figure 3.1). This sensitiser requires very low drug and light doses and strongly absorbs in the "therapeutic window" at 652 nm (Bonnett et al., 1989). Unfortunately 2nd generation sensitisers generally do not manifest a large tumour localizing selectivity. Therefore research has been focused on developing third generation photosensitisers. The 2nd generation photosensitiser are introduced in a vehicle (e.g. liposomes) which will drive the molecule until the desired target. Another method is to graft amino-acids, proteins, polymers, carbohydrates or anti-body on an existent photosensitiser (Moser, 1998).

3. 2. Tetraphenylchlorin series photosensitisers.

The photosensitisers of this series derive from the *meso*-tetra(hydroxyphenyl)porphyrins, they are namely the *meso*-tetra(hydroxyphenyl)chlorin and the *meso*-tetra(hydroxyphenyl)-bacteriochlorin (*m*-THPBC) (Figure 3.1). The discovery and the chemical synthesis pathway of these compounds was done by Bonnett *et al.* (Berenbaum et al., 1986; Bonnett et al., 1989). Basically the di-imide reduction of the tetra(hydroxyphenyl)porphyrins gives a mixture of the corresponding dihydro- and tetrahydroporphyrins. Dehydrogenation with o-chloranil cleanly removes the tetrahydro compound to produce the chlorines. Under more forcing conditions, di-imide reduction of the *m* isomer results mainly in the corresponding bacteriochlorin. The *ortho*, *meta* and *para* isomers of the porphyrin and the chlorin have been tested (Figure 3.2.). The *meta* isomer *m*-THPP was found to be the most active isomer in the *in vivo* assay (Berenbaum et al., 1986). The same *meta* isomer of the chlorin *m*-THPC was identified as the most active chlorin isomer (Bonnett et al., 1989).

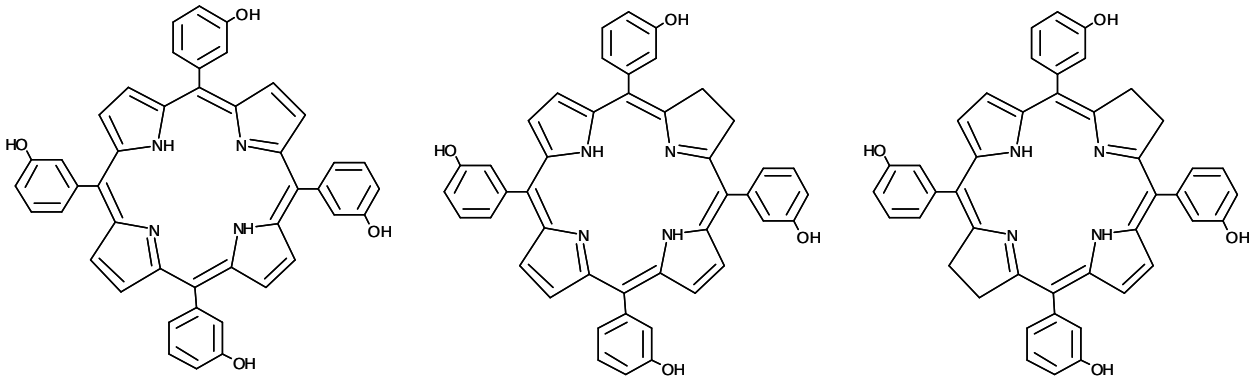

Figure 3.1. : Molecular structure of *m*-THPP, *m*-THPC and *m*-THPBC.

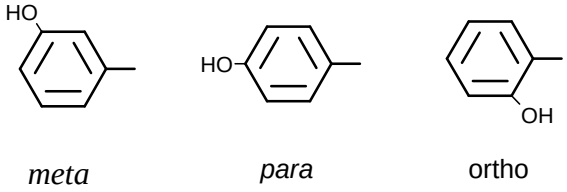

Figure 3.2. : *m*, *p* and *o* isomers of the hydroxyphenyl subsistent.

The attractive properties of this series are the strong absorption in the far red region. Where the molar extinction coefficient in ethanol is 1170 $M^{-1}cm^{-1}$ for Photofrin® at 630 nm, it is 3400 $M^{-1}cm^{-1}$ at 644 nm for *m*-THPP, 29600 $M^{-1}cm^{-1}$ at 650 nm for *m*-THPC and 91000 $M^{-1}cm^{-1}$ at 735 nm for *m*-THPBC (Table 3.1. and Figure 3.3.). They have a high triplet state quantum yield formation (Table 3.1.) ranging between 0.69-0.89 and a good quantum yield in singlet oxygen formation (0.43-0.45).

Because of these photophysical properties those photosensitisers were expected to be valuable compounds for PDT. Actually it has been shown that *m*-THPP was 25-30 times as potent as haematoporphyrin derivative in sensitising tumours (Berenbaum et al., 1986), and *m*-THPC considering global photodynamic doses (light doses x photosensitiser dose) was found to be 100 to 200 times as potent as haematoporphyrin derivative (Savary et al., 1998; Savary et al., 1997)

Table 3.1. : Some photophysical properties of *m*-THPP, *m*-THPC and *m*-THPBC in methanol from (Bonnett et al., 1999a).

	m -THPP	*m* -THPC	*m* -THPBC
λ_{max} Band I/nm	644	650	735
ε_{max}/M-1cm^{-1}	3400	29600	91000
λ_{max} fluorescence/nm	649, 715	653, 720	612, 653, 746
for excitation at λ/nm	415	415	500
Φ_f	0.12	0,089	0,11
Φ_T	0.69	0,89	0,83
τ_T/S	1.2x10^{-4}	0,50x10^{-4}	0,53x10^{-4}
O_2 quenching rate constant k_q/M^{-1}s^{-1}	1.9x10^9	1,8x10^9	2,5x10^9
Φ_Δ, air-saturated	0.46	0,43	0,43
Φ_Δ, oxygen-saturated	0.59	0,59	0,62

3.3. The 5,10,15,20-tetrakis(m-hydroxyphenyl)bacteriochlorin

m-THPBC has a strong absorbance in the red region (740 nm) (Bonnett et al., 1999b). In view of the weak absorbance of tissues at this wavelength, this offers promising therapeutic perspectives for PDT of deep tumours and pigmented tissues. Pre-clinical studies have demonstrated that in female BALB/c mice bearing PC6 tumour cells the depth of necrosis was 3.79 ± 0.28 mm for *m*-THPC and 5.22 ± 1.21 mm for *m*-THPBC for a nearly similar dose of administered photosensitiser, 0.375 and 0.39 µmol/kg for *m*-THPC and *m*-THPBC respectively (Bonnett et al., 1989). Another *in vivo* study demonstrated that area of necrosis is by far the largest after irradiation of *m*-THPBC-sensitised liver (93 ± 8 mm^2) compared to corresponding treatment with *m*-THPC (26 ± 4 mm^2) or with Photofrin (34 ± 11 mm^2) (Rovers et al., 2000a).

In vitro, Grahn et al demonstrated that the same toxicity was induced in cells incubated with *m*-THPC or *m*-THPBC and irradiated with a white light but concluded that, when the relative spectral activation of each compound was taken into account, the bacteriochlorin had about 0.6-0.7 fold the activity of the chlorin.

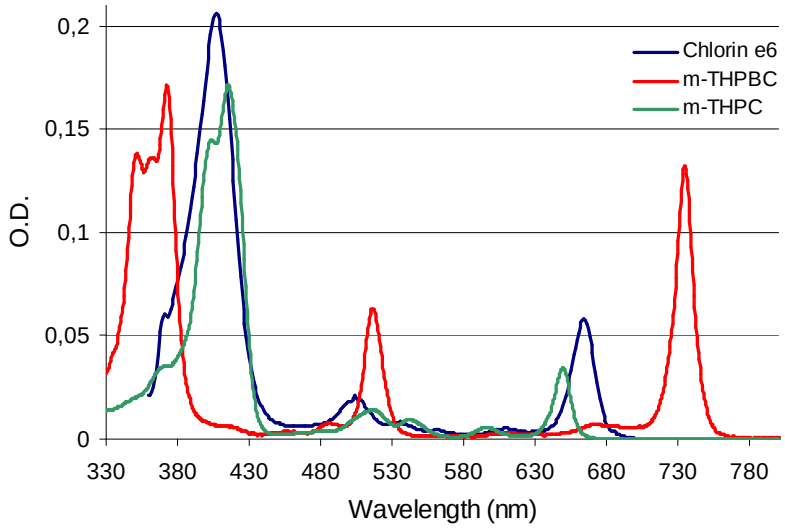

Figure 3.3. : Molar absorption spectra of *m*-THPBC and *m*-THPC in methanol and chlorin e6 in DMSO, the spectra presented here have been recorded in our laboratory.

m-THPBC has been reported to be a very photolabile compound. A comparative study of *m*-THPBC and *m*-THPC in methanol–water (3:2, v/v) solution demonstrated a 90 fold greater *m*-THPBC photobleaching rate (Bonnett et al., 1999b). Rovers *et al.* in an *in vivo* study on Colo 26 tumour bearing mice showed that the rate of bleaching of *m*-THPBC was approximately 20 times greater than that of *m*-THPC (Rovers et al., 2000b).

II.4. Photobleaching.

Degradation of dye is a subject that affects everybody, the visible expression of photobleaching are for example the bleaching of the hair in summer season or the fading of the tissues pigments. This phenomenon preoccupied the textile industry since a very long time. In the first books about dyeing, the sun was recognized as the cause of the fading of certain dyed textiles, and textile industry is currently making large efforts in order to find ingredients that can prevent bleaching. Plant life is also concerned by this phenomenon, adaptations and evolution occurs so as to prevent the photodegradation of chlorophyll and other vital pigments of the plants. The interest in the photodegradation of dyes and pigments has also been embraced by other fields which have appeared over the years with the advances of science and technology, so that nowadays, this phenomenon is relevant to a variety of fields, from laser technology to photomedicine.

The first relevant observation of photobleaching in the photodynamic therapy field was made in 1986 by Moan (Moan, 1986).

4.1. Photobleaching mechanisms

Ideally the photosensitiser should play the role of catalyst, it should be regenerated after its interaction with the substrate and should not interfere with the outcome of the reaction. Unfortunately, in addition to the reaction with biological substrate, self-photosensitization occurs, the reactive oxygen intermediates can interact with the photosensitiser, leading to its transformation and/or destruction. This phenomenon is called photobleaching.

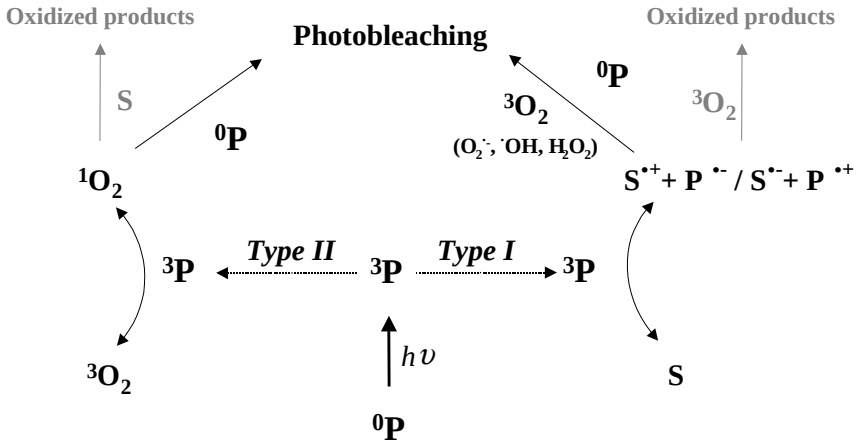

Figure 4.1. : Diagram of photobleaching mechanisms occurring after absorption of photons by photosensitizer.

The main reactions leading to photobleaching are presented in figure 4.1. The photosensitiser upon light irradiation undergoes Type I and/or Type II mechanisms, leading to the production of oxygen radical species. These oxygen radical species react with the neighbouring molecules, including the photosensitisers, leading to their destruction. Thus photobleaching can occurs via two pathways, the Type I way involving reactive oxygen species and Type II way involving singlet oxygen.

There are large differences in the photobleaching quantum yield of photosensitisers (Table 4.1), These differences be attributed to : oxidation potential, lipophilicity, presence of a metallic ion, kind of reactions involved (Type I or II).

Table 4.1. : Photobleaching quantum yield of some photosensitizers in PBS

Photosensitiser	Concentration (M)	Photobleaching quantum yield	References
MACE (Mono-L-aspartylchlorin e6)	5×10^{-6}	8.2×10^{-4}	(Spikes and Bommer, 1993)
Sn aspartyl chlorin e6	5×10^{-6}	5.7×10^{-6}	(Spikes and Bommer, 1993)
Zn aspartyl chlorin e6	5×10^{-6}	1.9×10^{-2}	(Spikes and Bommer, 1993)
Chlorin e6	5×10^{-6}	1.9×10^{-3}	(Spikes and Bommer, 1993)
Chlorin e6	10^{-4}	74.7×10^{-3}	(Rotomskis et al., 1997a)
Sn chlorin e6	5×10^{-6}	1.3×10^{-5}	(Spikes and Bommer, 1993)
Zn chlorin e6	5×10^{-6}	1.8×10^{-2}	(Spikes and Bommer, 1993)
Hematoporphyrin	10^{-4}	1.05×10^{-3}	(Rotomskis et al., 1997a)
Hematoporphyrin	5×10^{-6}	4.7×10^{-5}	(Spikes, 1992)
Photofrin®	10^{-4}	9×10^{-5}	(Rotomskis et al., 1997a)
Photofrin®	5×10^{-6}	5.4×10^{-5}	(Spikes, 1992)
$TSPP_4$	10^{-4}	2×10^{-4}	(Rotomskis et al., 1997a)
$TSPP_4$	5×10^{-6}	9.8×10^{-6}	(Spikes, 1992)
Uroporphyrin I	5×10^{-6}	2.8×10^{-5}	(Spikes, 1992)
BPD-MA		2.8×10^{-5}	(Aveline et al., 1994)

4.1.1. Effect of aggregation state, pH and ionic strength and miscellaneous agents on photobleaching.

Previous work in our laboratory demonstrated a different photosensitivity of monomeric and aggregated forms. In a first study, Bezdetnaya *et al.* (Bezdetnaya et al., 1996) demonstrated that for HpD and PpIX quantum yield of photobleaching obtained by matching fluorescence where higher than that obtained by matching absorbance (10 and 11 times for HpD and PpIX respectively). The authors concluded that this difference reflected the preferential photobleaching of photolabile monomeric forms compared to aggregates. In another study they demonstrated the preferential photobleaching of monomeric species of *m*-THPC as compared to aggregated forms (Belitchenko et al., 1998).

Several studies of Rotomskis and co-workers demonstrated that photobleaching efficiency of haematoporphyrin-like sensitisers seems to be consistent with their aggregation state and the presence of covalently linked structures. Dimethoxyhaematoporphyrin (DMHp) and Hp are present in an equilibrium of monomeric and aggregated forms in aqueous solution (Streckyte and Rotomskis, 1993a). Their absorption bleaching rate constants are two to four times higher

than that of HpD, a sensitiser containing mostly linear structures of porphyrins linked by ether, ester and/or carbon-carbon bonds (Dougherty et al., 1984), and 10 to 20 times higher than that of Photofrin® (PF), which contains covalently linked ”sandwich” type structure (Streckyte and Rotomskis, 1993b). In HpD, some of the side chains are involved in ether and ester linkages, and therefore this compound is more photostable than DMHp and Hp. In PF and Photosan-3 (PS) (highly aggregated “sandwich” type structure (Streckyte and Rotomskis, 1993b)), almost all side chains are involved in covalently linked structures, probably accounting for the high photostability of these sensitisers. The presence of a certain amount of protoporphyrin in PS is probably responsible for its lower photostability compared to PF.

Lowering the pH value of a photosensitiser solution results in a shift of both the absorption and the fluorescence spectrum as well as in a decrease of the fluorescence intensity, indicating an aggregation at low pH values (pH < 5) (Cunderlikova et al., 1999). Reddi *et al.* (Reddi and Jori, 1988) also demonstrated an aggregation of hematoporphyrin and Photofrin® when decreasing the pH from 7.4 to 5.0 and they also demonstrated the decrease of the photobleaching quantum yield to 70 % for hematoporphyrin and 30 % for Photofrin®, thus suggesting a resistance toward photobleaching of aggregated species.

Changing the ionic strength by varying the buffer concentration can affect the aggregation state of a sensitiser. An increase of the buffer concentration of a $TPPS_4$ solution increases the aggregation of the sensitiser and reduces the photobleaching quantum yield by 50 % (Davila and Harriman, 1990). Thus, it follows from all this studies that the quantum yield of photobleaching is inversely proportional to the aggregation state of the photosensitisers.

Streckyte *et al.* (Streckyte and Rotomskis, 1993a) showed that in micellar media (Triton X-100), which leads to the monomerisation of the photosensitisers, several dyes such as DMHp and HP had a different photostability and different photoproducts formation compared to aqueous media. Spikes (Spikes, 1992) reported that adding CTAB (cetyltrimethylammonium bromide) to PBS solution increases the quantum yield of PF photobleaching by 90%. The photobleaching of uroporphyrin I and hematoporphyrin in the same conditions was unchanged, and the bleaching of $TPPS_4$ decreased by 25%. Spectroscopic studies demonstrated that there was significant monomerisation of hematoporphyrin, $TPPS_4$, and PF in CTAB, however the reason for the opposite effect between $TPPS_4$ and PF was not clear. The authors proposed that $TPPS_4$ penetrates into the CTAB micelles (Reddi and Jori, 1988) and that it localizes in a low dielectric constant region and that under these conditions photobleaching would probably be slower.

4.1.2. Effect of oxygen concentration on photobleaching.

To provide evidence supporting the involvement of molecular oxygen in the photosensitisers photobleaching, the most unambiguous method is to remove the oxygen from the sample. This can be obtained through nitrogen bubbling. Bubbling with nitrogen during 30 minutes in a phosphate buffer reduces the concentration of oxygen from 22 µM to 2 µM (Spikes, 1992). The second method is argon flushing (König et al., 1993), and a third, called FPT (freeze-pump-thaw). It consists in the connexion of the sample to a high-vacuum line, the sample is frozen in a liquid nitrogen, and the system is brought at 1×10^{-4} mbar (<0.01% of atmospheric pressure) for 15 min. The valve of the vacuum pump is closed and the sample thawed. This cycle needs to be repeated five times in order to remove the oxygen. Spikes (Spikes, 1992) investigated the quantum yield of photobleaching of several porphyrins in phosphate buffer solution, and found that the bleaching was reduced by nitrogen bubbling. Also, Streckyte and co-workers demonstrated that the photobleaching process of ALA-induced PpIX in cells was slowed down by bubbling nitrogen trough the sample (Streckyte et al., 1994). König *et al.* also made the same observation for endogenously formed porphyrins in bacteria during argon flushing (König et al., 1993). An observation of the involvement of oxygen *in vivo* has been realised by Robinson and co-workers (Robinson et al., 1998). During a photobleaching experiment with ALA-induced PpIX the mice died and they observed a slowdown of the photobleaching. They correlated this bleaching decrease to the oxygen decline in the skin, due to the death of the animal.

4.1.3. Effect of antioxidant enzyme and quencher of type I on photobleaching

The most currently used type I quenchers or anti-oxidant enzymes are superoxyde dismutase (SOD) (Halliwell, 1978), catalase (CAT) (Fridovich, 1976) and deferoxamine which is an iron chelator (Halliwell and Gutteridge, 1986). In most cases, the addition of these kinds of Type I quenchers had no effects on the photobleaching quantum yield indicating a Type I independent photobleaching. Hadjur *et al.* (Hadjur et al., 1998) and Spikes (Spikes, 1992) used them to check whether the Type I radicals were involved in the photobleaching of the tetraphenylchlorin series in aqueous solution supplemented with foetal calf serum (FCS). They demonstrating that SOD and CAT had no effect on the photobleaching quantum yields of *m*-THPC (Table 4.2.), and thus concluded that free radicals were not involved to any significant extent in the photodegradation of *m*-THPC.

The studies of Spikes (Spikes, 1992) and Hongying (Hongying et al., 1999) are quite interesting. Indeed they have reported that the addition of SOD, CAT or a mix of both of them enhances the photobleaching quantum yield of chlorin e6 and different porphyrins (table 4.2.). The mechanism of the increased photobleaching yields produced by SOD and CAT is unexplained. We can suppose that it might be due to the fact that besides the enzymatic properties of those molecules, they are composed of amino-acids, known to be good photooxidizable substrates (cfr. § 4.1.6.), and that therefore the bleaching quantum yield is higher in the presence of such enzymes.

4.1.4. Means to determine the implication of singlet oxygen on photobleaching; Effect of $^1O_2$ quenchers and D_2O and rose bengal.

To determine whether singlet oxygen ($^1O_2$) is involved in the photobleaching mechanism of photosensitiser, the best way is to quench physically or chemically the $^1O_2$ immediately after his production. The most frequently used quenchers are physical quenchers (see § 2.3.2.) DABCO and sodium azide, and the chemical quencher histidine. In order to study the effect of $^1O_2$ quenchers on the photobleaching yield of photosensitisers, it is necessary to select $^1O_2$ scavengers that react with the triplet state of the sensitiser more slowly than oxygen to avoid the reaction between quenchers and the triplet state of photosensitisers.

For example, a hydrophilic $^1O_2$ quencher should be taken for the study of hydrophobic sensitisers. Another method is to enhance the activity of the $^1O_2$ with D_2O (D_2O increases 10 to 13 times the lifetime of $^1O_2$ compared to H_2O), thus if the singlet oxygen and his lifetime is a rate limiting factor in photosensitiser photobleaching, the quantum yield of photobleaching would be expected to increase significantly in D_2O. The addition of singlet oxygen photogenerator such as Rose Bengal in the reaction mixture can provide information about the effect of the singlet oxygen on the studied photosensitiser.

Bonnett and Martinez reported that DABCO and sodium azide slowed down the photobleaching rates of different porphyrins and phthalocyanine (Bonnett and Martinez, 2000), providing evidence for a singlet oxygen dependent bleaching (table 4.3.). The three tested compounds, di/tetrabenzoporphyrins and tetrabenzophtalocyanine, showed a large decrease in the reaction rate when adding 4 mM of DABCO or sodium azide, but this did not completely suppress the reaction.

Table 4.2. : Relative quantum yield of photobleaching of different photosensitizers in the presence of Type I quenchers

Photosensitiser	Solvent	Additive	Photobleaching quantum yield	References
Ce6	liposomes	—	1	(Hongying et al., 1999)
	liposomes	SOD (0.06 mg mL^{-1})	1,58	
	liposomes	Catalase (0.04 mg mL^{-1})	1,91	
	liposomes	SOD + Catalase	2,03	
Hematoporphyrin	PBS	—	4.7×10^{-5}	(Spikes, 1992)
	PBS	SOD (0.25 mg mL^{-1})	5.4×10^{-5}	
	PBS	Catalase (0.05 mg mL^{-1})	7.1×10^{-5}	
	PBS	SOD + Catalase	7.8×10^{-5}	
Photofrin II	PBS	—	5.4×10^{-5}	(Spikes, 1992)
	PBS	SOD (0.25 mg mL^{-1})	6.3×10^{-5}	
	PBS	Catalase (0.05 mg mL^{-1})	8.5×10^{-5}	
	PBS	SOD + Catalase	9.45×10^{-5}	
$TSPP_4$	PBS	—	9.8×10^{-6}	(Spikes, 1992)
	PBS	SOD (0.25 mg mL^{-1})	1.5×10^{-5}	
	PBS	Catalase (0.05 mg mL^{-1})	5.6×10^{-5}	
	PBS	SOD + Catalase	7.95×10^{-5}	
Uroporphyrin I	PBS	—	2.8×10^{-5}	(Spikes, 1992)
	PBS	SOD (0.25 mg mL^{-1})	2.9×10^{-5}	
	PBS	Catalase (0.05 mg mL^{-1})	1.2×10^{-4}	
	PBS	SOD + Catalase	1.4×10^{-4}	
m-THPP ($3x10^{-5}$)	Methanol/eau (3:2)	—	9.6×10^{-5}	(Bonnett et al., 1999b)
	Methanol/eau (3:2)	SOD (0.25 mg mL^{-1})	10.0×10^{-5}	
	Methanol/eau (3:2)	Catalase (0.15 mg mL^{-1})	10.2×10^{-5}	
m-THPC ($4x10^{-5}$)	Methanol/eau (3:2)	—	6.3×10^{-4}	(Bonnett et al., 1999b)
	Methanol/eau (3:2)	SOD (0.25 mg mL^{-1})	6.6×10^{-4}	
	Methanol/eau (3:2)	Catalase (0.15 mg mL^{-1})	7.7×10^{-4}	
m-THPBC ($2x10^{-5}$)	Methanol/eau (3:2)	—	5.7×10^{-2}	(Bonnett et al., 1999b)
	Methanol/eau (3:2)	SOD (0.25 mg mL^{-1})	5.3×10^{-2}	
	Methanol/eau (3:2)	Catalase (0.15 mg mL^{-1})	4.6×10^{-2}	
m-THPC ($2x10^{-6}$)	PBS-10% FCS	—	1.54×10^{-5}	(Hadjur et al., 1998)
	PBS-10% FCS	SOD (0.04 mg mL^{-1})	1.53×10^{-5}	
	PBS-10% FCS	Catalase (0.045 mg mL^{-1})	1.51×10^{-5}	

Another study of Bonnett and Martinez (Bonnett et al., 1999b) points out the efficiency of sodium azide in reducing the reaction rate of photobleaching for the compounds of the tetraphenylchlorin series *m*-THPP, *m*-THPC and *m*-THPBC. Moreover, the addition of Rose Bengal in the methanol solution leads to the large increase of photobleaching yield for all three compounds (table 4.3.). This result let the authors conclude that a Type II reaction pathway governs photobleaching for the tetraphenylchlorin series. This conclusion was in agreement with the earlier study of Hadjur *et al.* (Hadjur et al., 1998) showing the implication of a Type II mechanism in the bleaching of *m*-THPC in PBS supplemented with 10% FCS (Table 4.3.). Spikes and co-workers (Spikes, 1992; Spikes and Bommer, 1993) demonstrated that replacing H_2O by D_2O in a solution of PBS leads to a slight increase in the quantum yield of photobleaching of several porphyrins. 60% increases was observed for HP, 30% for PF II, 20% $TPPS_4$, 40% for URO and 50% for MACE. Adding sodium azide has little effect on the photobleaching quantum yield of those five sensitisers even with a high concentration of azide (0.10 M). These two observations together with the fact that molecular oxygen was required for the photobleaching (when nitrogen was bubbled in the solution the reaction rate of bleaching was considerably deacreased), and considering the lack of effect of Type I quenchers (table 4.2.) let the authors suggest that singlet oxygen was formed so close to the sensitiser that the probability to react with azide was very weak and that increasing the life time of singlet oxygen with D_2O has little effect.

4.1.5. Effect of organic solvents on photobleaching yields :

According to Spikes (Spikes, 1992) there is a strong correlation between the quantum yields of porphyrin photobleaching and the kind of organic solvent. There was no apparent correlation between molecular oxygen concentration or singlet oxygen lifetime in each solvent. However, the higher the dielectric constant, the more significant the photobleaching (Spikes and Bommer, 1993). Possibly the more polar solvents are stabilising polar and dipolar transition states involved in the reaction with singlet oxygen or other reactive oxygen species. This suggests that the photobleaching rate can be influenced by the polarity of the region where the photosensitisers are localised, and consequently the same photosensitiser would not photobleach to the same extent if it localises in the plasma membrane or in the cytoplasm for example.

Table 4.3.: Relative quantum yield of photobleaching of different photosensitizers in the presence of Type II quenchers

Photosensitiser	Solvent	Additive	Photobleaching quantum yield	References
Tetrabenzoporphyrin (1)	Acetonitrile	—	4.5×10^{-5}	(Bonnett and Martinez, 2000)
	Acetonitrile	DABCO (4mM)	1.7×10^{-5}	
Dibenzoporphyrin (2)	Methanol/formamide 1:1	—	4×10^{-5}	(Bonnett and Martinez, 2000)
	Methanol/formamide 1:1	NaN_3 (4mM)	1.8×10^{-5}	
Tetrabenzophthalocyanine (3)	Methanol	—	6.3×10^{-5}	(Bonnett and Martinez, 2000)
	Methanol	DABCO (4mM)	3.3×10^{-5}	
	Methanol	NaN_3 (4mM)	3.3×10^{-5}	
m-THPP ($3x10^{-5}$)	Methanol	—	3.3×10^{-5}	(Bonnett et al., 1999b)
	Methanol	NaN_3 (8mM)	1.6×10^{-5}	
	Methanol	Rose Bengal (3µM)	6.8×10^{-5}	
m-THPC ($4x10^{-5}$)	Methanol	—	1.7×10^{-4}	(Bonnett et al., 1999b)
	Methanol	NaN_3 (8mM)	6.7×10^{-5}	
	Methanol	Rose Bengal (3µM)	2.5×10^{-4}	
m-THPBC ($2x10^{-5}$)	Methanol	—	1×10^{-2}	(Bonnett et al., 1999b)
	Methanol	NaN_3 (8mM)	7.1×10^{-3}	
m-THPC ($2x10^{-6}$)	PBS-10% FCS	—	1.54×10^{-5}	(Hadjur et al., 1998)
	PBS-10% FCS	DABCO (1mM)	1.03×10^{-5}	
	PBS-10% FCS	histidine (1mM)	1.16×10^{-5}	
Hematoporphyrin	PBS	—	4.7×10^{-5}	(Spikes, 1992)
	PBS	D_2O	7.5×10^{-5}	
	PBS	NaN_3 (100mM)	5-8% decrease	
Photofrin II	PBS	—	5.4×10^{-5}	(Spikes, 1992)
	PBS	D_2O	7×10^{-5}	
	PBS	NaN_3 (100mM)	5-8% decrease	
$TSPP_4$	PBS	—	9.8×10^{-6}	(Spikes, 1992)
	PBS	D_2O	1.2×10^{-5}	
	PBS	NaN_3 (100mM)	5-8% decrease	
Uroporphyrin I	PBS	—	2.8×10^{-5}	(Spikes, 1992)
	PBS	D_2O	3.9×10^{-5}	
	PBS	NaN_3 (100mM)	5-8% decrease	
MACE	PBS	—	8.2×10^{-4}	(Spikes and Bommer, 1993)
	PBS	D_2O	$1,2 \times 10^{-3}$	
	PBS	NaN_3 (100mM)	5-8% decrease	

(1) zinc(II) tetra-*t*-butyltetrabenzoporphyrin; (2) Zinc(II) 13,17-Diethyl-12,18-dimethyl-5-azadibenzo[b,g] porphyrin; (3) Zinc(II) Tetra-t-butylphthalocyanine

4.1.6. Effect of photooxidizable substrates on photobleaching

Photosensitisers in solutions, cells, and tissues, can be bound to biomolecules such as proteins, amino-acids and lipids. The pattern of binding influences the mechanism of photosensitisers photobleaching. Krieg and Whitten showed that the photodegradation of porphyrins in biological systems is dependent on the presence of oxidizable amino acids or proteins (Krieg and Whitten, 1984b), moreover the authors demonstrated that the porphyrins in the presence of oxidizable amino acids were not degraded directly by the photogenerated singlet oxygen but by the oxidation products resulting from reactions between singlet oxygen and certain amino acids. Moan and co-workers in 1988 (Moan et al., 1988a) came to the conclusion that photobleaching of PF was mainly due to the production of singlet oxygen which oxidizes proteins and amino acids in the neighbourhood and further attack the parent molecule. The study of Spikes (Spikes, 1992) on several porphyrins did not evidence any clear rules concerning the effect of some photooxidizable compounds such as histidine, tryptophan, methionine, cysteine, HSA (human serum albumin) and furfuryl alcohol. In some cases the addition of one of these molecules to a porphyrin results in a higher bleaching rate, whereas the same photooxidizable molecules had no effect on another porphyrin. The author also noticed that adding HSA to the porphyrin solution leads to a 2 to 3 fold photobleaching rate increase, but the reasons for this increase are not so clear. It could be due to the monomerisation of the porphyrins rather than to the effect of the photooxidizable compounds.

4.2. Parameters affecting photobleaching kinetic characteristics

Kinetic parameters of photobleaching are mainly derived from spectroscopic measurements assessed by UV-Vis or fluorescence spectroscopy. Several important mechanistic issues of photobleaching were obtained from the detailed analysis of spectroscopic modifications. In the earlier studies on photobleaching of PDT molecules the kinetic decay of photosensitiser was considered as a mechanism depending only on the light dose delivered to the tissue, materialized by the mono-exponential decay $e^{-\alpha D}$, where α stands for the photobleaching constant and D stands for the fluence of irradiation ($J.cm^{-2}$). As became clear later, the photobleaching kinetic is a complex phenomenon which cannot be described by a single exponential decrease (Moan et al., 2000; Sørensen et al., 1998). Several parameters can

influence the kinetic decay such as the oxygen depletion during PDT, the presence of different types of binding sites for the sensitiser molecules in the tissues, the relocalisation of the dye during light exposure. For some photosensitisers the decay rates have been shown to be practically independent of the concentration of the dye during illumination (Mang et al., 1987; Moan, 1986; Sørensen et al., 1998); and thus exhibit a first order decay. However, for the majority of dyes the photobleaching decay is highly dependent on the initial concentration of the photosensitiser (Moan et al., 1988b), meaning that the photoproducts from the chromophore can cause the decay of a neighbouring chromophore (Moan et al., 1997). For example, the data in the Table 4.1. demonstrate that the QYs of photobleaching for the different concentrations of Ce6 are very different. The same holds true for other dyes (PF, hematoporphyrin and TSPP4) (table 4.1.).

4.2.1. Depletion of oxygen during the photodynamic treatment.

Several studies from the laboratory of TH. Foster documented the oxygen depletion during PDT. Oxygen consumption model was refined by Georgakoudi and co-workers (Georgakoudi and Foster, 1998; Georgakoudi et al., 1997) by taking into account the parameter of photobleaching of Photofrin in EMT6 spheroids. This improvement considerably changed the kinetic profile of the oxygen aspects of Photofrin-PDT. The authors observed a rapid decrease in oxygen concentration during irradiation followed by a progressive return to the values measured before the irradiation. The first phase is due to the photochemical oxygen consumption which is faster than the diffusion of the oxygen through the spheroid. The second phase, corresponding to the comeback of oxygen to the initial value, is due to a slowdown of the photochemical consumption of the oxygen explained by the decrease in photosensitiser concentration (photobleaching), together with the diffusion. This was in total agreement with the data from the mathematical model that they had developed assuming, that the photobleaching was based on a reaction between singlet oxygen and photosensitiser at the ground state. The validity of the developed model was confirmed by applying it to the experimental results on photobleaching in NHIK 3025 cells loaded with Photofrin from the study of Moan (Moan, 1986).

In their further studies Foster and co-workers investigated the impact of irradiance on dependant photobleaching (Finlay et al., 2001; Finlay et al., 2002). In a study reporting the photobleaching of ALA-induced Protoporphyrin IX (Pp IX) in normal rat skin (Finlay et al., 2001) it was demonstrated that the photobleaching kinetic was different with different irradiances (1, 5, 100 mW cm $^{-2}$). High irradiance led to rapid oxygen consumption and a slow

down of the photobleaching. In addition, the photoproducts of PpIX also exhibited an irradiance dependant photobleaching. In a second study, Finlay *et al.* (Finlay et al., 2002) showed that photobleaching kinetics of *m*-THPC on normal rat skin exhibits two distinct phases. The first phase was shown to be irradiance independent, whereas the second phase revealed an irradiance dependency consistent with an oxygen-dependant reaction process.

4.2.2. Different type of aggregation state for the sensitiser molecules in the tissues

Strauss and co-workers (Strauss et al., 1998) studied the photobleaching of protoporphyrin IX on endothelial cells from calf aorta (BKEz-7). Bi-exponential fluorescence decay was recorded using total internal reflection (TIR). The authors attributed the bi-exponential decay to the aggregation state of the molecule. The first, fast part of the decay was attributed to the monomers of PpIX mainly located in the plasma membrane and in the close vicinity of the membrane, and the second slower part of the curve was ascribed to the aggregated forms of PpIX which were localized in the cytoplasm and in the organelles. Several studies of Moan's group (Moan et al., 1997; Sørensen et al., 1998) also demonstrated that photobleaching kinetics were highly dependent on the sensitiser binding site in the tissue or in the cell. One of those studies (Moan et al., 1997) suggest that the bi-exponential decay of the PpIX in WiDr cells was due to two first order processes, one for PpIX bound to proteins and one for unbound PpIX.

4.2.3. Re-localisation during light exposure

During light exposure, photosensitisers can move from one binding site to another. This is also called light induced re-localisation. This has been shown for lysosomotropic dyes such as $TPPS_4$ (Berg et al., 1991; Rück et al., 1992), nile blue (Lin et al., 1993), $AlPcS_4$ and $AlPcS_2$ (Peng et al., 1991; Rück et al., 1996; Rück et al., 1990), which display a granular lysosomial distribution in a discrete perinuclear region (Rück et al., 1996). Moreover Ambroz *et al.* (Ambroz et al., 1994) reported a fluorescence redistribution and a monomerisation of $AlPcS_2$ during irradiation, which were coincidental with a change in the fluorescent decay from a bi-exponential to a mono-exponential one.

Moan also underlined the capability for PpIX to re-localise during light irradiation in WiDr cells (Moan et al., 1997). The surviving fraction was plotted against the relative values of the integrated number of PpIX fluorescence photons emitted during the irradiation. Three concentrations of ALA-induced PpIX were tested. The authors postulated that if the PpIX

molecules remained in their binding sites during light irradiation, the survival curves should be completely superimposable when plotted with exposures measured as the number of emitted photons. This was not what the authors observed, the survival curves became steeper than expected when the PpIX concentration was reduced, indicating a significant transfer of PpIX molecules from one binding site to another. Similar observations had been done earlier by Brun *et al.* on the transfer of PpIX from erythrocytes to other cells (Brun et al., 1990).

A remarkable transient relocalisation is observed when phthalocyanine sulphonates in tumor are exposed to light (Moan and Anholt, 1990; Moan et al., 1990). In this case the fluorescence intensity decreases during light exposure, but increases immediately afterwards. This indicates that light displaces the photosensitiser molecules from one type of binding site to another associated with fluorescence quenching.

More recently, Finlay *et al.* (Finlay et al., 2002) hypothesize that the two phases of *m*-THPC photobleaching observed *in vivo* were due to a redistribution of the photosensitiser in the tissue. However, *m*-THPC re-distribution in vitro was not detected (Melnikova et al., 1999b).

4.3. Photoproducts formation

Presently, two mechanisms of photobleaching are acknowledged (Bonnett and Martínez, 2001). The first one, true photobleaching, corresponds to the photodegradation of the porphyrin macrocycle with the formation of photoproducts, which do not absorb in the visible light region. The second mechanism is called photomodification, where the chromophore is retained in a modified form with the formation of new visible spectral bands. For the majority of photosensitisers the photoproducts arise from both photodegradation pathways.

4.3.1. Means to study photobleaching

-Fluorescence and absorbance spectroscopy

Fluorescence and absorbance spectroscopy are the most employed means to study photobleaching. These are high competitive tools, easy to use. These techniques can be used in solution and *in vitro*, when the spectrophotomer is equipped with an integrating sphere in order to avoid the light scattering phenomenon. *In vivo*, fluorescence will be investigated by a technique called light induced fluorescence (LIF). The *in vivo* absorbance can be examined by elastic scattering spectroscopy (ESS). These techniques give very useful information since the very large majority of the photosensitisers used in photodynamic therapy are fluorescent and absorb the visible light. Although fluorescence and absorbance are rather specific in the

identification and discrimination of the molecules, they can hardly be applied in the identification of slight modification on the molecules like hydroxylation which doesn't change the spectral characteristics of the molecules. Another limitation exists concerning photoproducts occurring during true photobleaching since those products don't fluoresce and do not absorb in the visible region. Thus the detection of these photoproducts by the means of visible spectrophotometry or spectrofluorimetry is rather complex.

-Mass spectrometry

Mass spectrometry is a very powerful tool in the structural analysis of organic compounds, this technique discriminates the molecules with respect to the mass/charge ratio. It is a very sensitive and useful instrument to study photobleaching, and it comes as a powerful complement to spectrophotometry or spectrofluorimetry.

4.3.2. Photoproducts as a result of photomodification and true photobleaching

Photomodification is featured by the loss of absorbance or fluorescence at some wavelength and the appearance of new spectral bands, this being in agreement with the photoformation of new compounds. For macrocyclic compounds, we are talking about photomodification when the rupture of the macrocycle doesn't occur. While true photobleaching leads to the destruction of the tetrapyrrolic cycle, and results in the formation of small products which do not absorb the visible light. It appears that, where photomodification occurs, true photobleaching often occurs concomitantly, also one should notice that photomodification can be mistaken for photorelocalisation.

PpIX was the first extensively studied dye because of its implication in the erythropoietic protoporphyria (EPP), an inherited disorder of porphyrin-heme metabolism with cutaneous and systemic manifestations. Mutations in the gene encoding ferrochelatase, the last enzyme of the heme biosynthetic pathway, result in partial deficiency of its activity. Reduced ferrochelatase activity causes accumulation of excess levels of Protoporphyrin. PpIX undergoes photooxydation during irradiation. Many studies report the formation of photoprotoporphyrins (two isomers called A and B) and formylporphyrins (Inhoffen et al., 1969). In organic solvent the phototransformation yield was between 25 and 51 %, with a formation of photoprotoporphyrin 10 times higher than the formation of formylporphyrins (Cox and Witten, 1982). Using type II quenchers they demonstrated that all photoproducts were diminished (Cox et al., 1982a), but formylporphyrins decreased less than

photoprotoporphyrin, implying that formylporphyrins formation could arise from non singlet oxygen mediated mechanism. While the addition of methyl viologen to the PpIX solution reduced the formation of photoprotoporphyrin, the formation yield of formylporphyrins was unaffected. The authors concluded that singlet oxygen attack was responsible for the photoformation of photoprotoporphyrins, whereas photoformation of formylporphyrins could also arise from a Type I mechanism. In organised assemblies such as micelles and vesicles (Cox et al., 1982b; Krieg and Whitten, 1984a), the phototransformation yield was shown to be lower than in an organic medium (15 to 28%), and PpIX was phototransformed, in opposition to the previous situation, to greater extent into formylporphyrins than into photoprotoporphyrins. Other work using PpIX dissolved in erythrocytes ghosts has shown that true photobleaching as a predominant photoreaction mechanism, perhaps resulting from the formation of reactive oxidized amino-acids contained in the ghosts, and their subsequent attack on the PpIX molecule (Krieg and Whitten, 1984a). In addition to true photobleaching, after prolonged irradiation, another visible-absorbing photoproduct was observed, and was postulated to be a photolabile biliverdine type product resulting from ring opening at the methylene bridge inside the porphyrin chromophore.

In vivo photobleaching of PpIX reveals mostly true photobleaching, however photoproduct formation was also largely observed. Photoprotoporphyrin was detected in mouse tumour and human skin lesions as a result of protoporphyrin phototransformation (Ahram et al., 1994). Other photoproducts where found and tentatively attributed to coproporphyrin, uroporphyrin and zinc(II) Protoporphyrin (Bagdonas et al., 2000; Juzenas et al., 2001; Moan et al., 1997).

Rotomskis was one of the most prominent researchers on the field of photobleaching and photoproducts formation of hematoporphyrin and related compounds. In a first study (Rotomskiene et al., 1988), Rotomskis and co-workers demonstrated that contingent on the aggregation state, the photosensitiser is either phototransformed into a red absorbing product or disrupted, i.e. aggregated porphyrins gives rise to photoproducts, whereas monomeric fraction of the dye undergoes true photobleaching. Later the same group refined the idea of photoproduct formation and aggregation state of the porphyrins, using hematoporphyrin dimethyl ether (DMHp) which is known to form “sandwich type” or H-type aggregates (blue shift of Soret and Q bands, usually marked broadening with decrease in absorbance), hematoporphyrin which forms both sandwich type and linear J-type aggregates (red shift of Soret and Q bands, either a slight band broadening or band sharpening), and Photosan, a mixture of highly aggregated H-type and covalently bonds aggregates. Photobleaching

experiments showed to the formation of a 660 nm absorbing product as a result of hematoporphyrin and Photosan irradiation, whereas photobleaching of DMHp gave rise to the formation of a 640 nm absorbing product. Consequently the authors suggested that the 660 nm photoproduct formation was due to the existence of J-type linear and covalently linked aggregates and the 640 nm photoproduct formation was due to the existence of H-type aggregates. In a series of studies from the same team (Rotomskis et al., 1996; Rotomskis et al., 1997a, b), the mechanism of hematoporphyrin like sensitiser was unfolded. A possible photobleaching mechanism is presented in the figure 4.2..

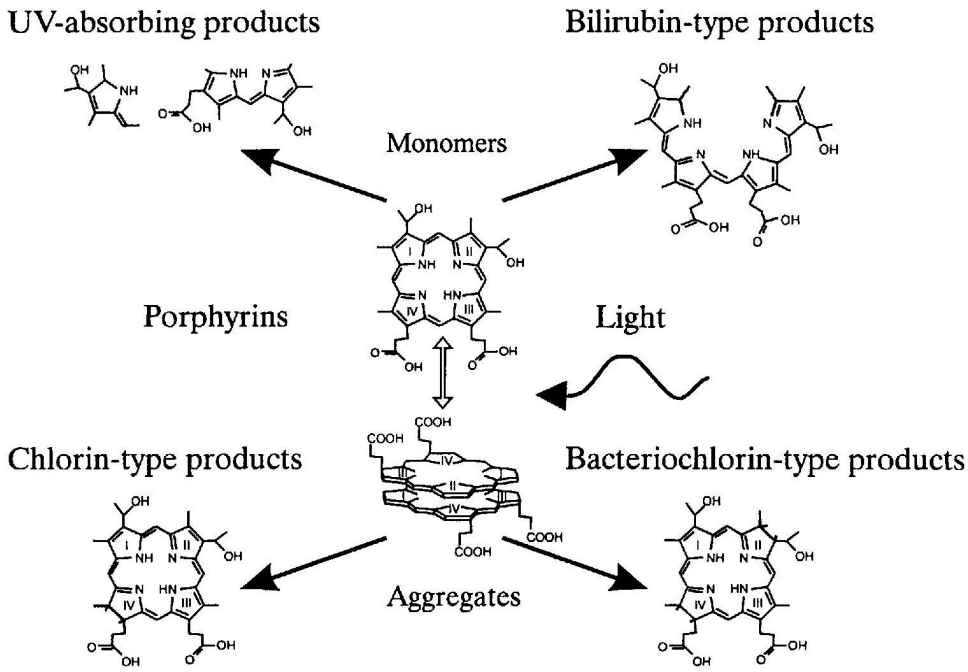

Figure 4.2. : possible phototransformation of hematoporphyrin like sensitisers from (Rotomskis et al., 1997b)

In a PBS solution, hematoporphyrin like sensitisers are under a dynamic equilibrium between aggregated and monomeric forms and irradiation of monomeric species gives rise to UV-absorbing photoproducts ($\lambda_{max} \approx$ 240-320 nm) and to bilirubin type products with an absorbtion band around 545 nm. The irradiation of aggregated (H-type) sensitisers leads to the formation of two distinct photoproducts with a λ_{max} at 640 and 660 nm supposed to be chlorin-type (640 nm) and bacteriochlorin-type products (660 nm). Moan and Kessel also identified two photoproducts formed after the irradiation of NHIK 3025 cells loaded with hematoporphyrin like sensitiser (Photofrin II). One photoproduct was characterised by a

fluorescence emission peak around 660-670 nm (λ_{ex} = 445 nm). This product is rapidly formed and then starts to decay after about 40 min of light exposure. The second photoproduct (with an emission maximum at 640-650 nm) is formed at slower rates but appears to be more stable during extended exposures. These two products were in all probability the porphyrins identified in the previous studies in solution.

The tetraphenylchlorin series sensitisers have been extensively studied because of the large clinical potential of the *m*-THPC and also because of their large absorption in the red region of the visible spectrum. Bonnett *et al.* have made a comparative study of the photobleaching of this sensitiser series by absorption measurements (Bonnett et al., 1999b). The authors demonstrated that in methanol-water solution *m*-THPC and *m*-THPBC underwent only true photobleaching and photomodification mainly occurs for *m*-THPP. The products formed after the irradiation of *m*-THPP methanol-water were hydroxylated *m*-THPP (mono-, di-, tri- and tetra-hydroxylated *m*-THPP) (Bonnett and Martinez, 2002) with mono-hydroxylated *m*-THPP being the major photoproduct (25%). While in pure methanol small photoproducts appeared such as maleimide and methyl-3-hydroxybenzoate, the mono-hydroxylated *m*-THPP was still photoproduced (Fig. 4.3.). A recent study of our group (Lourette et al., 2005) regarding the photobleaching of *m*-THPP in ethanol-water (1/99, v/v) solution revealed that using a pulsed laser as light source *m*-THPP undergoes phototransformation to a hydroxylated product and several covalent oligomeric structures as dimer, trimer, tetramer and pentamer of *m*-THPP.

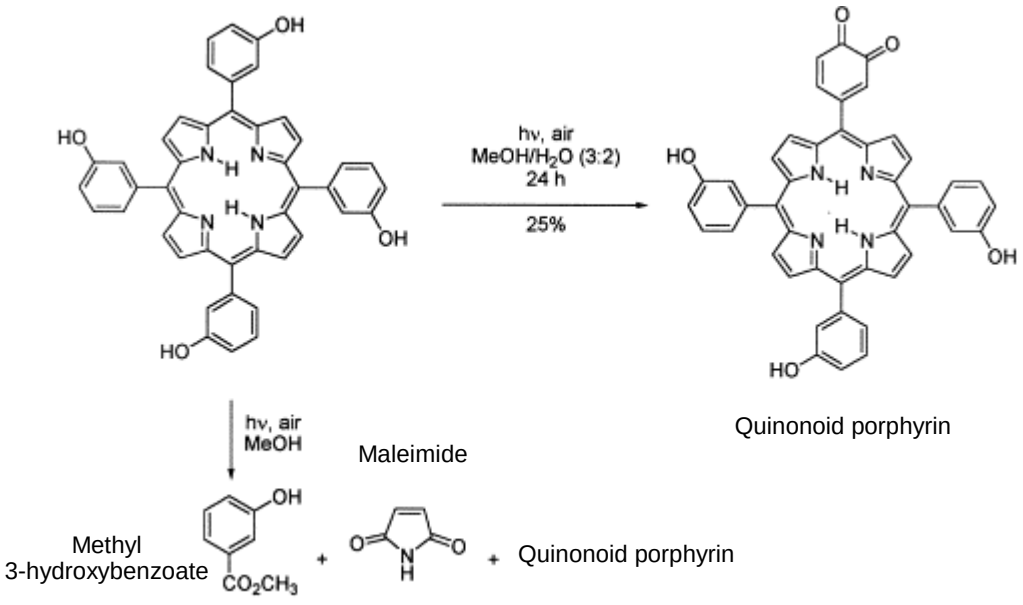

Figure 4.3. : Photoproducts formation upon light irradiation of m-THPP in methanol or methanol-water solution, from (Bonnett and Martínez, 2001).

Several studies on *m*-THPC photobleaching have been carried out in our laboratory together with the group of Professor J-F Muller (Angotti et al., 1999, 2001; Belitchenko et al., 1998) demonstrating a rapid true photobleaching of *m*-THPC (9.0×10^{-4}), accompanied by a photoproduct formation at λ_{abs} = 320 nm when the photosensitiser was in a PBS solution supplemented with 2% foetal calf serum (FCS). This result was confirmed by Hadjur *et al.*

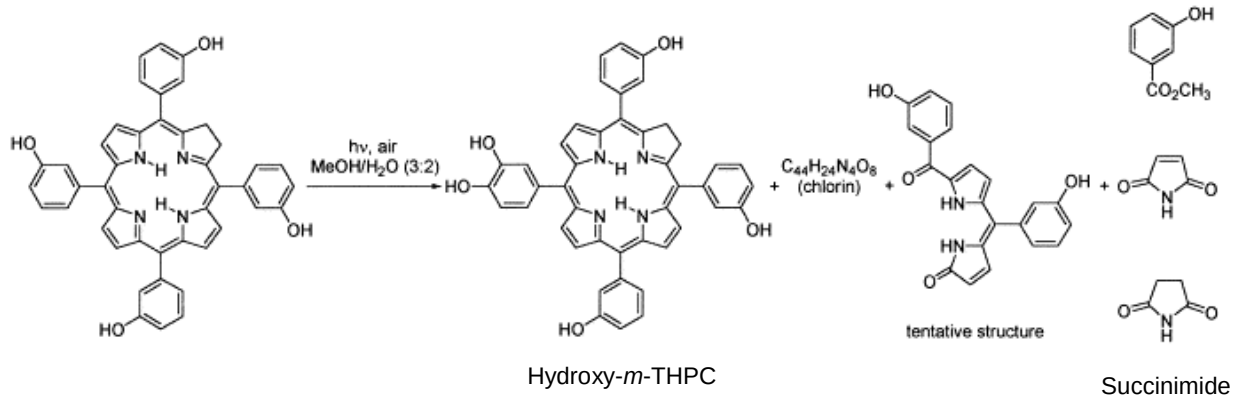

Figure 4.4. : Photooxidation of m-THPC in methanol-water from (Bonnett and Martínez, 2001).

(Hadjur et al., 1998) who showed a large formation of a 320 nm absorbing product in a 10% FCS solution. In methanol or methanol-water solution it appears that *m*-THPC undergoes photobleaching mainly via true photobleaching (Bonnett et al., 1999b), since no photoproduct at 320 nm was detected. These three observations, let us propose that the photoproduct formation correlates with the FCS concentration in the incubation solutions. Mass spectrometry studies were carried out to identify the spectroscopycally invisible photoproducts (Angotti et al., 1999, 2001; Jones et al., 1996; Kasselouri et al., 1999).The photobleaching was performed on *m*-THPC methanol solution or water-methanol solution and the products obtained are presented in the figures 4.4. and 4.5.

The major photoproducts observed were hydroxy- and di-hydroxy-*m*-THPC, hydroxy-*m*-THPP, still the position of the hydroxyl(s) group(s) is(are) not determined, these penta or hexahydroxylated chlorin have almost the same absorption peak than *m*-THPC (Jones et al., 1996; Kasselouri et al., 1999). Bonnett (Bonnett and Martinez, 2002) identified several products like a chlorin (molecular formula $C_{44}H_{24}N_4O_8$) and four minor products coming from true photobleaching. They are dipyrrin derivative, succinimide, and the two afore mentioned products maleimide and methyl-3-hydroxybenzoate, which were also photoproducts from *m*-THPP.

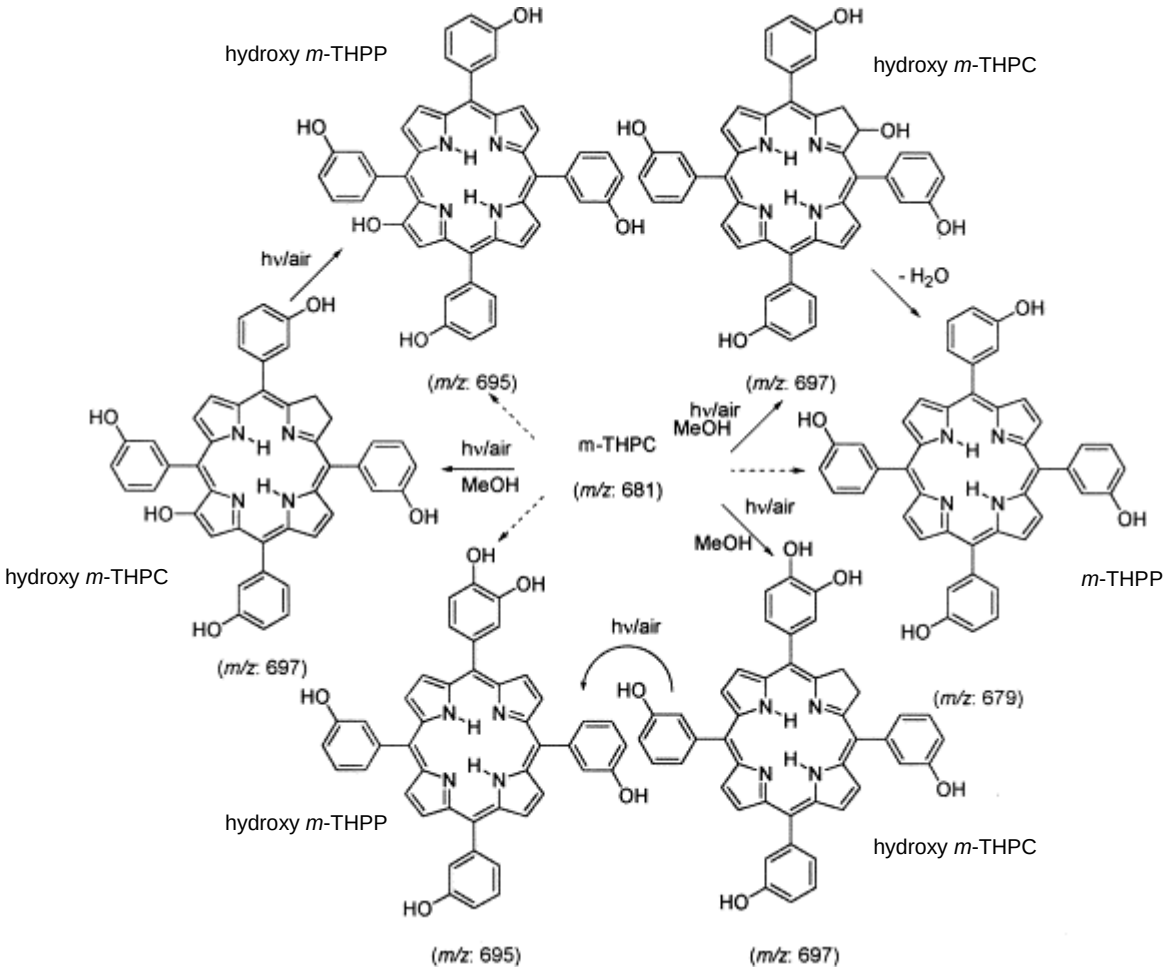

Figure 4.5. : Photooxidation products of *m*-THPC in methanol from (Bonnett and Martínez, 2001)

The last compound of the tetraphenylchlorin series is *m*-THPBC, it partly undergoes true photobleaching, with a bleaching rate 60 times faster than *m*-THPC. Angotti *et al.* (Angotti et al., 2001) demonstrated that in a methanol solution *m*-THPBC is phototransformed in *m*-THPC. Bonnett *et al.* (Bonnett and Martinez, 2002) also found that the bacteriochlorin was transformed into the chlorin, in addition the authors have found three others compounds, the succinimide and methyl-3-hydroxybenzoate, that were found in the photodegradation pattern of *m*-THPC and an orange red pigment identified as dipyrrin derivatives (Fig. 4.6.).

Steric effects are known to play a role in the ring opening of the tetraphenylporphyrin compounds. If the positions 2 and 6 of the phenyl ring are substituted the attack of the porphyrin macrocycle is prevented. However even though the phenyl rings of the *meso* tetraphenylchlorin series are not occupied in the position 2 and 6, they are no reports on the formation of ring opened photoproducts from those sensitisers. This observation could be

explained by a possible weakness of the macrocycle leading to the immediate disruption of the ring.

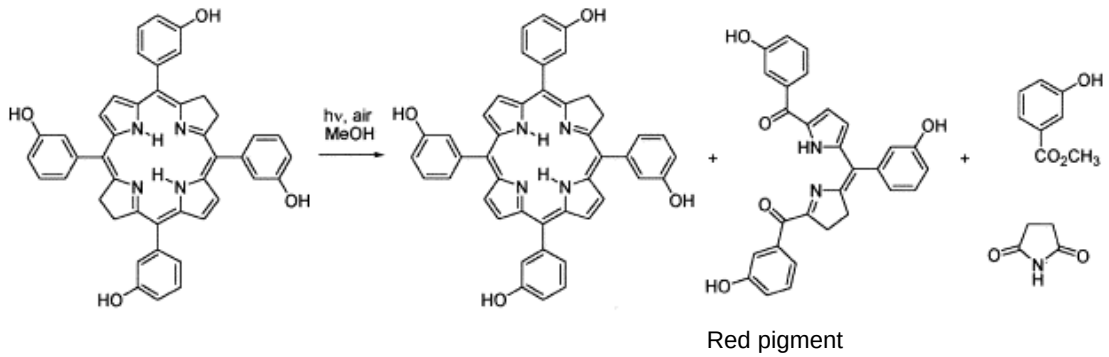

Figure 4.6. : m-THPBC photooxidation in methanol from (Bonnett and Martínez, 2001)

II.5. Significance of photobleaching in the dosimetry of photodynamic therapy.

In the clinical protocols, only the photosensitizer concentration in the tissue, the incident light dose, and the interval between drug application and light exposure are taken into account as dosimetry parameters, this dosimetry concept is named explicit dosimetry and was proposed by Wilson *et al.* (Wilson et al., 1997b). This approach can hamper PDT treatment outcome because of the biological variation between patients or pathological tissues. Overtreatment caused by too much light irradiation of the treatment sites may involve adverse effects such as strictures, fistulae, delayed healing, excessive scarring or cosmetic disfigurement, whereas in case of undertreatment the patients need to undergo additional treatment. Optimising PDT dosimetry is crucial for ensuring adequate treatment of the pathological tissue, at the same time minimising damage to surrounding normal tissues (Guillemin et al., 1995). Therefore it is easily understandable that during treatment it would be desirable to monitor the progress of therapy in real time. The question now is : what are the elements needed to be taken in account for an optimal PDT dosimetry? The answer becomes rather complex since more and more factors are identified to play a role in the outcome of the treatment. Wilson *et al.* (Wilson et al., 1997b) enumerate seven different factors which may influence the effective dose:

(1) The subject to subject variation in specific tumour uptake of photosensitisers.

(2) The large range of optical absorption and scattering coefficients of different tissues, which determine the light penetration and distribution in the target volume.
(3) The variability in tissue oxygenation, which affects the photodynamic efficiency.
(4) Change in light penetration during irradiation, due primarily to rapid PDT-induced blood flow changes.
(5) "Self shielding ", which occurs with second-generation photosensitisers of large molar extinction coefficient, and which limits the light penetration due to the added absorption of the photosensitiser itself in the tissue.
(6) Photobleaching, shown by many photosensitisers during light irradiation, which may reduce the concentration of (photo-active) photosensitiser in the tissue during irradiation.
(7) Photochemical depletion of oxygen in tissues under irradiation at high light fluence rates, leading to reduced photodynamic effect.

As we have seen before, many clinically relevant photosensitizer undergo modification during light irradiation and the resulting products are themselves photosensitizers, therefore it is possible to add an eighth factor:

(8) Photosensitisers undergo phototransformation leading to the formation of new active sensitisers.

Wilson and co-workers put forward the concept of implicit dosimetry, which as far as possible, incorporates all the response-determining elements (except the number 8) in order to compute the correct dosimetry. To be reliable each parameter should be measured during the PDT treatment.

Among the 8 points cited above, the points 5, 6, 7 and 8 are in direct relation with photobleaching of the photosensitisers. Therefore it seems essential to consider this phenomenon in the calculation of the dosimetry. The authors propose to monitor the photobleaching of the photosensitizer during the treatment, serving as a "biological dosimeter", the basic principle is that if the photosensitiser bleaches then it means that the treatment is efficient. This theory is not completely correct, since some sensitisers have a large bleaching with a poor photodynamic activity. For this reason the authors introduced the concept of $^1O_2$ coupling to photosensitiser photobleaching. Fully coupled photosensitiser will have a $^1O_2$ dependent photobleaching, in this case photobleaching indicates a strong photodynamic effect, whereas bleaching of an uncoupled sensitiser will not be representative of the photodynamic efficiency. The problem is that we don't know which sensitizer is

coupled and which one is uncoupled. Also, some results indicate that a photosensitiser can be found to be coupled in *in vitro* models and uncoupled for *in vivo* studies. This discrepancy points out the limitation of this model. In addition, during the treatment and the photobleaching of the sensitiser, transport and diffusion of the photosensitiser still occurs, perturbing measurements of the photobleaching.

Several alternatives have been proposed to monitor the efficiency of the treatment. The most unambiguous method consists in the measurement of the element presumed responsible for the photodamage : singlet oxygen. This can be done by monitoring the luminescence emission at 1270 nm as $^1O_2$ returns to the triplet ground state. However, this is routinely measurable in solution (Krasnovsky, 1998), but it has not been possible to measure the luminescence in cells or tissues in vivo due to the very short (around 100 ns) lifetime of the $^1O_2$ in biological environments (Moan, 1990; Moan and Berg, 1991; Schweitzer and Schmidt, 2003). The improvement of the detector sensitivity and/or temporal response of the near-infrared (NIR)-sensitive photomultiplier tube (PMT) allow to measure the $^1O_2$ life time in vitro and in vivo in the skin of hairless mice (Niedre et al., 2002a; Niedre et al., 2002b; Niedre et al., 2003; Niedre et al., 2005). These studies demonstrated that PDT cells killing correlated very strongly with the $^1O_2$ luminescence measured during treatment, regardless of initial photosensitiser concentration, irradiance or molecular oxygen concentration. A second alternative will be the measurement of the sensitiser triplet-state concentration and life time with laser flash photolysis techniques (Aveline et al., 1994), but there are several limitations of this method. The sensitivity may be insufficient for some sensitisers, since a significant fraction of these molecules must be excited during each light pulse in order to populate the triplet state. In order to distinguish the ground state and triplet state absorptions, the absorption spectra must have minimal spectral overlap, so that the method cannot be used for all the photosensitisers. And finally the pulsed laser technology is rather expensive and not suitable for routine clinical use. Another alternative is to monitor the changes in the tissue during irradiation by several means, radiological images, magnetic resonance imaging or high resolution ultrasound. The last alternative is to use fluorescent reporters, these are fluorophores which can be activated with some alterations generated by the treatment. Amongst the very well documented fluorescent reporters are the photoproducts formed during irradiation (Zeng et al., 2002).

II.6. Intracellular localisation of the photosensitisers.

6.1. Photosensitisers localisation techniques.

Epifluorescence microscopy

In the epifluorescence microscope, the light excitation pathway is the same as the observation optical pathway, the objective plays the role of a condenser as well as of the objective. The light sources used can be xenon lamps or mercury arc lamps (HBO). The light from the source is filtered (excitation filter), a specific excitation wavelength is selected, the excitation light is reflected on the sample with a dichroic mirror. The fluorescence emitted from the sample passes through the dichroic mirror and is filtered with an emission filter. Epifluorescence microscopy presents several advantages and drawbacks. The objective plays the role of condenser and objective, therefore the irradiated area perfectly fits the observed area. Full aperture of the objective for the excitation and the emission provide a maximal intensity to the fluorescence picture. However, the epifluorescence microscopy pictures are contaminated by information from outside the focal plane, leading to a decrease in contrast and clarity of the picture. The irradiated area corresponds to the observed area and for the whole thickness of the sample, thus observation of light sensitive molecules such as photosensitisers can be difficult. This technique has been widely used for photosensitisers observation in the past (Bour-Dill et al., 2000; Melnikova et al., 1999a; Morgan et al., 2000; Wood et al., 1997), but due to the major drawbacks, confocal microscopy is now the preferred method to look at the intra-cellular fluorochrome localisation.

Laser scanning confocal microscopy

The confocal microscope offers several advantages over the conventional epifluorescence microscope (Zucker and Price, 2001). Including elimination of out-of-focus glare, the decrease of depth of field and the ability to collect serial optical sections from thick specimens.

The illumination is achieved by scanning beams of light, usually from a laser, across the specimen, the configuration uses a pinhole placed in front of the light source, and another pinhole placed at the emission, with the same focus as the first pinhole (the two are confocal). The pinholes prevents light originating from above or below the focal plane in the specimen from reaching the photomultiplier. The confocal microscope does not avoid photobleaching, but reduces the irradiated area and therefore enables the study of light sensitive molecules.

Due to all these improvements confocal microscopy is preferred to epifluorescence microscopy in the localisation of photosensitisers (Chen et al., 2000; Delaey et al., 2001; Leung et al., 2002; Pogue et al., 2001; Scully et al., 1998; Zucker and Price, 2001).

Microspectrofluorimetry

Microspectrofluorimetry is usually coupled to confocal microscopy. This technique enables the spectral study of the molecules in a focal plane of a confocal microscope. The topographic resolution is very small (less than 1 μm^2), therefore it is possible to study the spectral signature of a molecule in a very localised area such as the organelles. In opposition to the imaging techniques such as epifluorescence and confocal microscope which gives subjective information, the microspectrofluorimetry gives objective data on the localisation or co-localisation of two fluorescent probes. Therefore, this technique has been widely used for the determination of the photosensitisers intra-cellular localisation sites (Matroule et al., 1999; Morliere et al., 1998; Ouedraogo et al., 1999).

6.2. Sub-cellular localisation of the photosensitisers.

Since singlet oxygen, the main cytotoxic species produced by PDT, is not able to diffuse over distances longer than 10–20 nm during its excited state lifetime and cell dimensions being approximately 20 µm, the primary sites of photodynamic action should be strictly related to the specific intracellular sensitiser distribution (Moan and Berg, 1991). The photosensitisers intra-cellular distribution are determined by the incorporation pathway of the molecules, by their physico-chemical properties (hydrophilic / hydrophobic), by the nature, number and position of the side chains, and by the aggregation state of the molecules (Rosenkranz et al., 2000).

Most of the photosensitisers including lipophilic ones, do localise in the plasma membrane except the most hydrophilic. It has been observed that for the short incubation time (less than 1 h) the damages to the plasma membrane were more important than for long incubation time (ref 158). This is explained by the fact that, depending on the incubation time the photosensitisers get deeper in the cells and is distributed to the cellular compartments, as was shown for Photofrin (Morgan et al., 2000).

Aggregated or hydrophilic photosensitisers enter the cell via endocytosis or pinocytosis and are captured by acidic compartments such as lysosomes. This has been observed for Photofrin

(Morliere et al., 1987), HpD (Malik et al., 1992), aluminium sulphonated phthalocyanines $AlPcS_4$ and $AlPcS_2$ (Moan et al., 1994; Moan et al., 1989), and MACE. The photochemical inactivation of cells through such photosensitisers is due to the release of lysosomal hydrolases. Photosensitisers with a lysosomal localisation seem to be less efficient than those localised in other organelles. Moreover the development of a new technology of macromolecule delivery into the cell is based on this properties, photochemical internalisation (PCI) consist in the uptake of a photosensitiser (with lysosomal localisation properties) and a drug. Light exposure induces a PDT effect and a release of the contents of these vesicles, including externally added macromolecules into the cytosol.

Mitochondria have been shown to be a localisation site of many photosensitisers such as Photofrin (Sharkey et al., 1993; Singh et al., 1987; Wilson et al., 1997a), ALA-PpXI (Iinuma et al., 1994; Wilson et al., 1997a), and HpD (Kessel, 1986). There is strong evidence that sensitisers with an acute localisation in mitochondria promote the release of cytochrome c upon irradiation (Marchal et al., 2005; Xue et al., 2001). This loss of cytochrome c can be lethal to cells either because of the disruption of the mitochondrial respiratory chain with the eventual reduction of cellular ATP levels or through caspase initiation with subsequent apoptotic cell death (Xue et al., 2001; Yow et al., 2000).

The ER and the Golgi apparatus are closely linked not only by their localisation in the perinuclear area of the cytoplasm, but also as they interact together in protein synthesis. Therefore it is conceivable to think that damaging those compartments can be lethal for the cells. Some photosensitisers were found to localise in the ER and the Golgi, for example, Photofrin (Candide et al., 1989), some analogues of hypericin (Delaey et al., 2001) and a recent study in our laboratory demonstrated that *m*-THPC mainly localises in these compartments.

Objectives

III OBJECTIVES

The first objective of our work was to study the effect of the photosensitiser aggregation on the photobleaching. By modifying the incubation time of *m*-THPBC solution in phosphate buffer solution supplemented with proteins we change the aggregation state of the photosensitiser. Therefore we were interested in:

- The photobleaching rate of *m*-THPBC with respect to the aggregation state. The difference between photobleaching rate assessed by UV/Vis absorption and by fluorescence.
- The kinetics profiles of the *m*-THPBC photobleaching in a monomerised form or in aggregated form.
- The nature of the photoproducts formed after irradiation with a 739 nm emitting laser diode, in aggregated or monomerised *m*-THPBC solutions.

The second objective is to compare photobiological properties of *m*-THPBC and the related photosensitiser *m*-THPC *in vitro*.

- Photobleaching kinetics have been examined in WiDr adherent cells.
- Phototoxicity of both photosensitisers was studied in the same conditions as photobleaching.
- Intracellular localisation was assessed by fluorescence microscopy.

The third part of the work consists in the *in vivo* evaluation of *m*-THPBC compared to the well documented *m*-THPC.

- Light penetration in mice liver.
- Biodistribution in different organs and tissues of BALB/c nude mice.
- Skin pharmacokinetics of *m*-THPBC.
- Photobleaching of *m*-THPBC and *m*-THPC in alive and dead mice skin.

Results

IV RESULTS

IV.1. Photobleaching characterisation of 5,10,15,20-tetrakis(m-hydroxyphenyl) bacteriochlorin (m-THPBC) in solution.

1.1. Photodegradation and phototransformation m-THPBC in solution.

The aim of this study was to examine the photobleaching characteristics of the *m*-THPBC in biologically relevant solution with different incubation condition leading to different aggregation state of the molecules. The preliminary step of this study was to determine the aggregation state of the photosensitiser in PBS solution supplemented with proteins and with different incubation time at 37°C. We find that incubation favors photosensitizer monomerisation, whereas *m*-THPBC is mostly aggregated in HSA–PBS immediately after being dissolved. Photobleaching study demonstrated faster rates for monomerised sensitiser compared to aggregated ones, also kinetic profiles are mono-exponential for freshly prepared solution and bi-exponential for incubated solution demonstrating that the kinetic profile is also in relation with the aggregation state of the sensitiser: for aggregated *m*-THPBC the kinetic is mono-exponential and for a mixture of bound to protein and aggregated *m*-THPBC the decay is bi-exponential. In the next step we addressed the photoproduct formation after *m*-THPBC irradiation. The only photoproduct detected by visible light absorption is m-THPC, and once again the aggregation state of the photosensitiser was found to be a determining factor in the phototransformation yield of the *m*-THPBC into *m*-THPC. Irradiation of the freshly prepared *m*-THPBC solution led to phototransformation of 50% of the bleached *m*-THPBC into *m*-THPC, and the phototransformation yield fall to 5% (mainly true photobleaching) for incubated *m*-THPBC.

This study was selected for an oral presentation at the European Society for Photobiology Congress 2003, and was published in *Photochemical & Photobiological Sciences*. This study is presented thereafter in its published form.

FULL PAPER

PPS www.rsc.org/pps

Photodegradation and phototransformation of 5,10,15,20-tetrakis(*m*-hydroxyphenyl)bacteriochlorin (*m*-THPBC) in solution†

Henri-Pierre Lassalle,[a,b] Lina Bezdetnaya,*[a] Vladimir Iani,[b] Asta Juzeniene,[b] François Guillemin[a] and Johan Moan[b]

[a] *Centre Alexis Vautrin, CRAN CNRS UMR 7039, Vandoeuvre-les-Nancy, France. E-mail: l.bolotine@nancy.fnclcc.fr; Fax: (33) 3 83 44 60 71; Tel: (33) 3 83 59 83 53*

[b] *Institute For Cancer Research, The Norwegian Radium Hospital, Oslo, Norway*

Received 6th April 2004, Accepted 15th October 2004
First published as an Advance Article on the web 10th November 2004

The kinetics of photobleaching and formation of photoproducts upon irradiation (735 nm) of 5,10,15,20-tetrakis(*m*-hydroxyphenyl)bacteriochlorin (*m*-THPBC) in phosphate buffer saline (PBS) supplemented with human serum albumin (HSA) were studied by means of absorption and steady-state fluorescence spectroscopy. Measurements were performed either immediately after the dye was dissolved in the HSA solution (0 h) or after six hours incubation in the HSA solution (6 h). Spectroscopic studies indicated that the dye was mainly present as aggregates in freshly prepared solutions, whereas incubation favored monomerisation. Irrespective to incubation time, the rates of photobleaching obtained by fluorescence measurements were higher than those obtained from absorbance measurements. Photobleaching of freshly prepared *m*-THPBC can be described by a single exponential decay, while the absorbance and fluorescence decays of the incubated dye solutions better fit a bi-exponential decay. Two photobleaching rates probably reflect differences in the photosensitivity of monomer (bound to proteins) and aggregated (non-bound) forms. Irradiation of the freshly prepared *m*-THPBC solution led to phototransformation of 50% of the bleached *m*-THPBC into 5,10,15,20-tetrakis(*m*-hydroxyphenyl)chlorin (*m*-THPC), a clinically used second generation photosensitizer. For irradiation 6 h after dissolving *m*-THPBC, different kinetics of *m*-THPC formation were found. A rapid decrease in concentration of *m*-THPBC was accompanied by a slow formation of *m*-THPC. The quantum yield of this process was small since only 5% of *m*-THPBC was transformed to *m*-THPC. The kinetics characteristics of *m*-THPBC photobleaching reported in the present study, together with the different kinetics of photoproduct formation during *m*-THPBC photobleaching, may provide important indications in the *m*-THPBC-based PDT dosimetry.

Introduction

Photodynamic therapy (PDT) is a new modality of cancer treatment that is based on the application of a tumour localizing and photosensitizing drug followed by exposure of the tumour area to light. Some of the photosensitizers used in PDT degrade rapidly upon irradiation, a phenomenon called photobleaching.[1] This is a field of significant interest in PDT, since it can influence the success of the treatment in several ways. A recent detailed review of the reactions leading to photobleaching of PDT sensitizers and to photoproduct formation focused on the complex character of both processes.[2] Two types of irreversible photobleaching should be considered:[2] true photobleaching, which involves fragmentation of the sensitizer that then loses its absorption in the visible region, and photomodification, where the chromophore is retained in a modified form with the formation of new visible spectral bands.

In the clinical protocols, only the administered photosensitizer dose, the incident light dose, and the interval between drug application and light exposure are taken into account as dosimetry parameters. A few years ago, Wilson *et al.* introduced the concept of implicit dosimetry,[3] which uses the yield of photosensitizer photobleaching as an index of the effective delivered fluence. A relevant PDT dosimetry can be also deduced by monitoring of the formation of photoproducts that accompanies photobleaching. A recent study by Zeng *et al.* demonstrated that a prediction of PDT treatment outcome based on the monitoring of photobleaching and photoproduct formation is an improvement compared to predictions based on conventional dosimetry.[4] Photobleaching also helps to increase the therapeutic ratio of PDT by reducing the level of sensitizer in normal tissue to below the threshold required for intolerable photochemical damage.[5]

5,10,15,20-Tetrakis(*m*-hydroxyphenyl)bacteriochlorin (*m*-THPBC) is the most reduced compound in the 5,10,15,20-tetrakis(*m*-hydroxyphenyl)porphyrin (*m*-THPP) series.[6] This dye has a strong absorbance in the red region (740 nm).[7] In view of the weak absorbance of tissues at this wavelength, this offers promising therapeutic perspectives for PDT of deep tumours and pigmented tissues. Pre-clinical model studies have demonstrated that the area of necrosis is by far the largest after irradiation of *m*-THPBC-sensitised liver (93 ± 8 mm^2) compared to corresponding treatment with 5,10,15,20-tetrakis(*m*-hydroxyphenyl)chlorin (*m*-THPC) (26 ± 4 mm^2) or with the conventionally used sensitizer Photofrin (34 ± 11 mm^2).[8] Presently, *m*-THPBC is under clinical investigation for PDT of patients with hepatic metastasis.[9]

m-THPBC has been reported to be a very photolabile compound. A comparative study of *m*-THPBC and *m*-THPC in methanol–water (3 : 2, v/v) solution demonstrated a 90 fold greater *m*-THPBC photobleaching rate.[10] Rovers *et al.* in an *in vivo* study on Colo 26 tumour bearing mice showed that the rate of bleaching of *m*-THPBC was approximately 20 times greater than that of *m*-THPC.[11]

† Presented at the 10th Congress of the European Society for Photobiology, Vienna, Austria, September 6th–11th, 2003.

DOI: 10.1039/b405138f

Recently, by using mass spectrometry, we demonstrated a photo-induced dehydrogenation of *m*-THPBC leading to transformation to *m*-THPC in ethanol–water (1 : 99, v/v) solution or in serum enriched aqueous solution.[12]

The phototransformation kinetic characteristics are rather complex and are defined by several factors (microenvironment, aggregation states, applied fluence, oxygen tension *etc.*).[13,14] Our previous studies.[15,16] have demonstrated that photobleaching kinetics are strongly influenced by aggregation of photosensitizers. Different rate constants were obtained depending on the detection methods. While the loss of fluorescence could be interpreted as loss of monomer species, the loss of absorbance represented both loss of aggregates and monomers.

The present study addresses the light induced spectral changes of *m*-THPBC in albumin-enriched solution at different incubation conditions leading to different aggregation states. Photobleaching measurements were monitored by absorbance and fluorescence decays. We also addressed the kinetics of photoproduct formation upon irradiation of *m*-THPBC in different aggregation states.

Materials and methods

Photosensitizer

The photosensitizer *m*-THPBC was kindly provided by Biolitec Pharma Ltd. (Edinburgh, UK). The chemical structure of *m*-THPBC is presented in Fig. 1. Stock solution of *m*-THPBC in methanol was stored in the dark at 4 °C at a concentration of 3 mM. Further dilution was performed in Phosphate Buffer Saline (PBS), in PBS supplemented with 1mg mL^{-1} Human Serum Albumin (HSA, Sigma-Aldrich Norway AS, Norway) or in methanol. The final concentration of *m*-THPBC in each solvent was 1,5 μM.

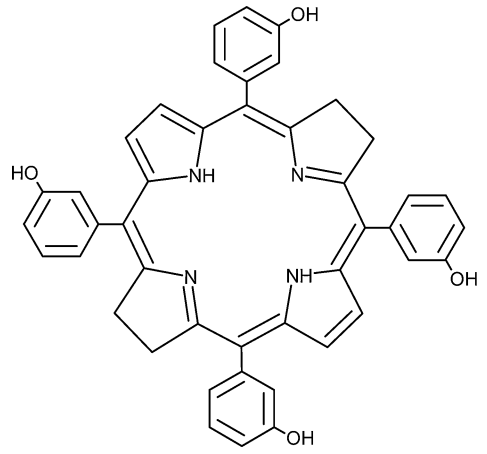

Fig. 1 Molecular structure of *m*-THPBC.

Light exposure

Prior to light exposure, *m*-THPBC solutions in HSA–PBS were kept for 0 or 6 h in the dark at 37 °C. Illumination was performed by exposing 2 mL of 1,5 μM *m*-THPBC solutions in a 10 mm quartz cuvettes to light from a 150 W halogen lamp equipped with a combination of three pass filters, one short wavelength (cut-off at 765 nm) and two long wavelength (cut-on at 520 and 700 nm). The spectral intensity distribution is presented in Fig. 2. The spectrum of the filtered lamp was in the wavelength region 700–765 nm with a peak at 735 nm. The incident fluence rate at the position of the sample was 55 mW cm^{-2}.

Absorption and fluorescence measurements

Absorption and fluorescence measurements were recorded using a Perkin Elmer (Norwalk, CT) Lambda 15 spectrometer and a Perkin-Elmer LS 50B luminescence spectrometer, respectively. For both photobleaching and photoproduct formation studies, the *m*-THPBC absorbance decay was recorded at 740 nm after different exposure times. The photoinduced formation of *m*-THPC was measured at 422 nm.

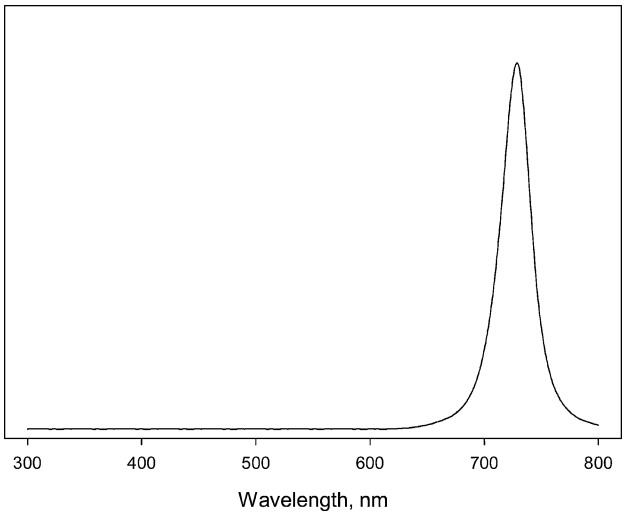

Fig. 2 Spectral intensity distribution of the 150 W halogen lamp equipped with a combination of one short wave (cut-off at 735 nm) and two long wave (cut-on at 520 and 735 nm) filters. A heat filter was used to reduce the heat effect of the lamp. The incident fluence rate was 55 mW cm^{-2}.

For fluorescence measurements, excitation was set at 378 nm, and the emission was scanned in the wavelength range between 700 and 800 nm. The fluorescence decay after *m*-THPBC irradiation was monitored by excitation at 378 nm, and the fluorescence emission was collected at 742 nm. The bandpasses of the excitation and emission slits were 5 and 10 nm, respectively.

Results

Spectroscopic studies

m-THPBC absorption spectra in methanol, in PBS and HSA–PBS are shown in Fig. 3A. Absoption maxima of the Soret band and of the red band along with corresponding molar absorption coefficients and a half-height bandwidth ($\Delta\nu$) of the first Q band are listed in Table 1. The absorption spectra of *m*-THPBC in methanol showed three main peaks: the Soret band at 373.5 nm, and two Q bands at 516 and 734 nm. In aqueous solutions the Soret band and Q-band peaks are red shifted to 383, 530 and 743 nm. This bathochromic shift was accompanied by a hypochromic effect in the Soret band (ε was 7313 M^{-1} cm^{-1} in PBS compared to that of 114 300 M^{-1} cm^{-1} in methanol). A half-height bandwidth amounted to 790 cm^{-1} compared to 350 cm^{-1} in methanol.

Absorption spectra of *m*-THPBC in PBS supplemented with HSA were measured either immediately (0 h) or after six hours of incubation (6 h). The presence of proteins reduced the bathochromic shift and the half-height bandwidth for both conditions (Fig. 3A). A 16% decrease in $\Delta\nu$ was observed in non-incubated *m*-THPBC HSA–PBS solution compared to *m*-THPBC-PBS (Table 1). This decrease was 50% for incubated *m*-THPBC HSA–PBS solution compared to *m*-THPBC-PBS (Table 1).

The steady-state fluorescence emission spectra of *m*-THPBC in HSA–PBS solutions are presented in Fig. 3B. The shapes of the spectra were similar for both incubation conditions and peaked at 742 nm. The relative fluorescence intensity, measured as integrated intensity of the emission band, was six times larger in incubated *m*-THPBC HSA–PBS solution than in the non-incubated solution. The emission band of *m*-THPBC-PBS

Table 1 Absorbance spectra characteristics of *m*-THPBC in different media[a]

	Soret band		Red band		
	λ/nm	ε/M^{-1} cm^{-1}	λ/nm	ε/M^{-1} cm^{-1}	$\Delta\nu$/cm^{-1}
Methanol	372	114 200	734	90 479	250
PBS + HSA, 0 h	378	19 479	740	11 123	667
PBS + HSA, 6 h	378	22 520	742	13 740	400
PBS	382	7213	742	4890	790

[a] Absorption maxima of the Soret and the red band (λ) with corresponding molar absorption coefficients (ε), $\Delta\nu$ is the half height bandwidth.

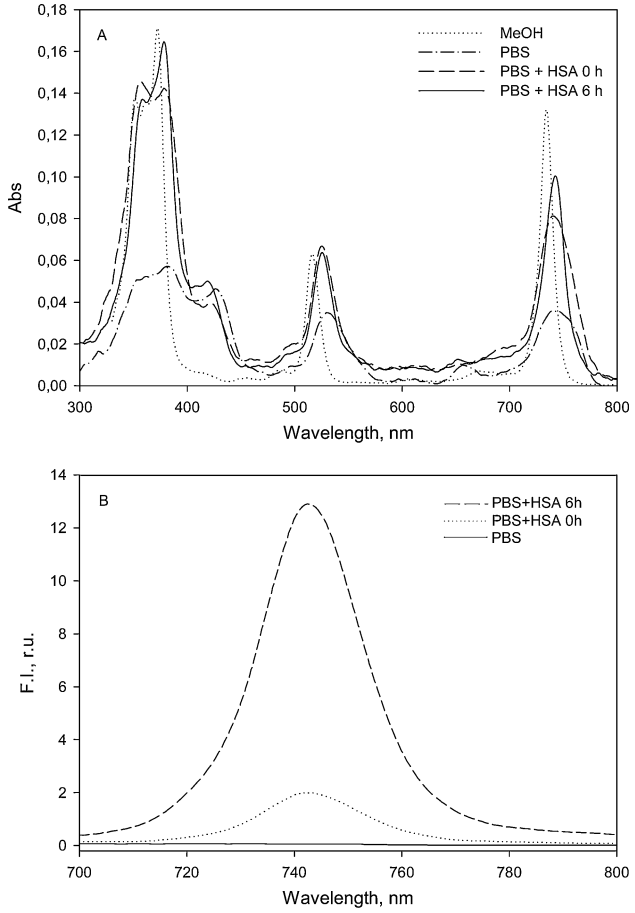

Fig. 3 Ground-state absorption spectra of *m*-THPBC (1.45 μM) (A) in methanol (· · ·), PBS (---) and in PBS supplemented with HSA (1 mg mL^{-1}) with (—) and without incubation (---). *m*-THPBC absorption spectra in PBS with and without HSA are magnified five times. Fluorescence spectra of 1.45 μM *m*-THPBC (B) in PBS (—), PBS supplemented with HSA (1 mg mL^{-1}) with (---) and without incubation (---). Excitation wavelength was 378 nm.

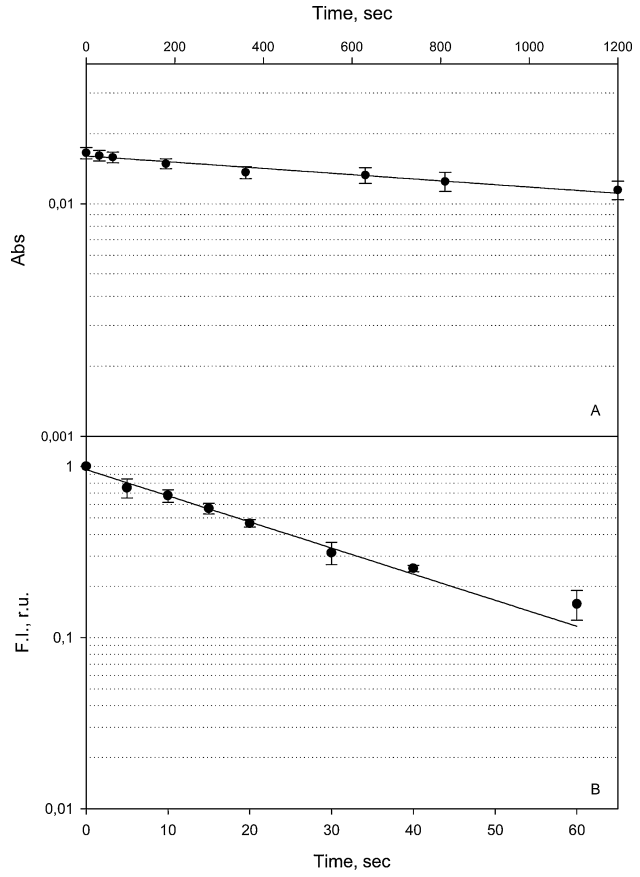

Fig. 4 Photobleaching kinetics of *m*-THPBC in PBS supplemented with HSA (1 mg mL^{-1}), measured by absorbance (A) and by fluorescence (B). Solutions were exposed to light immediately after the introduction of 1.45 μM of *m*-THPBC. Absorbance was measured at 740 nm. Fluorescence was monitored at an emission wavelength 742 nm using 378 nm excitation. Fluorescence values are normalized to the fluorescence of non-irradiated solution.

solution was not detectable under the experimental conditions of the present study.

Photobleaching studies

Incubated and non-incubated *m*-THPBC solutions in HSA–PBS were exposed to irradiation at 735 nm. After certain intervals of irradiation the bleaching processes were studied by measuring the absorbance at 740 nm, a wavelength which is not affected by interference of photoproducts, and the fluorescence decay was recorded at an emission wavelength of 742 nm.

The photobleaching kinetics of non-incubated *m*-THPBC HSA–PBS are shown in Fig. 4. Both the absorption and fluorescence decays are close to mono-exponential. The photobleaching rate calculated from absorption measurements was equal to 2.86×10^{-4} s^{-1}, and that obtained from fluorescence measurements was 3.51×10^{-2} s^{-1}

The bleaching kinetics of incubated *m*-THPBC HSA–PBS deviated from monoexponential, and the model fitting the experimental data best was a bi-exponential decay, as evidenced by regression analysis ($R = 0.998$) (Fig. 5). The absorption photobleaching rates calculated from the first and second parts of the curve were 6.82×10^{-2} and 1.68×10^{-4} s^{-1}, respectively, and the two fluorescent rate constants were 1.63×10^{-1} and 2.86×10^{-2} s^{-1}. The rate constants for the different incubation condition are presented in Table 2. It should be noted that the rates of photobleaching obtained from fluorescence measurements were three fold (6 h incubation) or two orders of magnitude (0 h incubation) larger than those obtained from absorbance measurements.

Photoproduct formation

Parallel to the fluence dependent decrease in absorption in the whole visible spectrum of *m*-THPBC, we observed a simultaneous increase in the spectral bands at 422 and 650 nm. As an

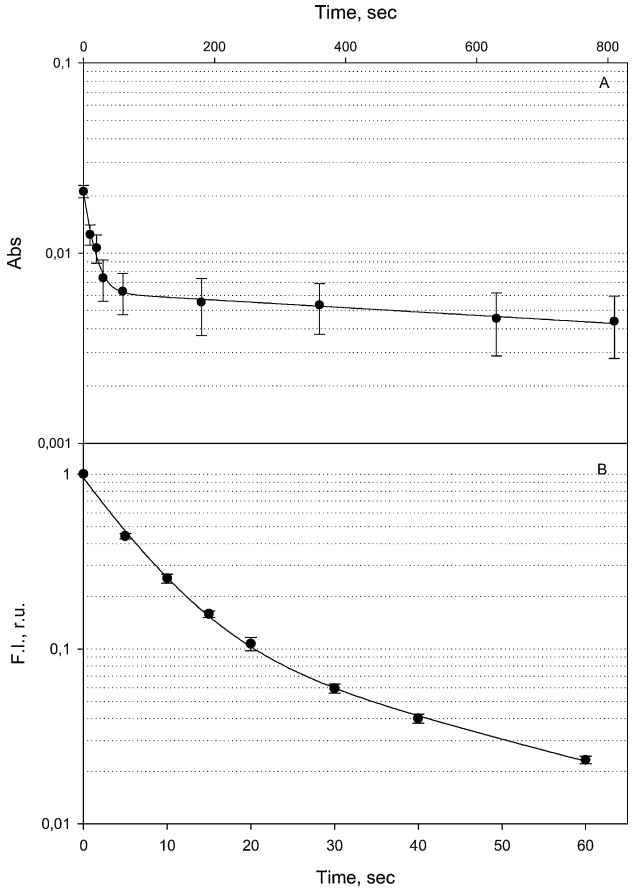

Fig. 5 Photobleaching kinetics of *m*-THPBC in PBS supplemented with HSA (1 mg mL^{-1}), measured by absorbance (A) and by fluorescence (B). Solutions were exposed to light 6 h after the introduction of 1.45 μM of *m*-THPBC. Absorbance was measured at 742 nm. Fluorescence was monitored at an emission wavelength 742 nm using 378 nm excitation. Fluorescence values are normalized to the fluorescence of non-irradiated solution.

Table 2 Photobleaching rate constants (k/s^{-1}) of *m*-THPBC incubated (6 h) and non-incubated (0 h) in an HSA–PBS solution, derived from absorbance and by fluorescence measurements (photobleaching rate constants from the second parts of the curves are shown in parentheses)

	0 h	6 h
Abs	2.68×10^{-4}	6.81×10^{-2} (1.68×10^{-4})
Fluo	3.51×10^{-2}	1.63×10^{-1} (2.86×10^{-2})

example, the spectra of incubated and non-incubated *m*-THPBC HSA–PBS solutions exposed to 44.5 J cm^{-2} (810 s) are presented in Fig. 6A and 7A. The insets in Figs. 6A and 7A represent the differential absorbance spectra (irradiated minus non-irradiated) and are characterized by the appearance of two peaks at 422 and 652 nm, which are characteristic for *m*-THPC. For a quantitative monitoring of the *m*-THPBC phototransformation to *m*-THPC, we measured the photoinduced *m*-THPBC loss of absorbance at 740 nm (non-incubated *m*-THPBC) and at 742 nm (incubated *m*-THPBC); the photoinduced growth in *m*-THPC absorbance was measured at 422 nm. The choice of the later wavelength was related to the difficulties encountered in spectral detection of *m*-THPC at 650 nm. The concentrations of the bleached *m*-THPBC and the formed *m*-THPC were calculated for different exposure times, on the assumption that the Beer–Lambert law is obeyed by both sensitizers under both incubation conditions. The molar extinction coefficients of *m*-THPBC in the red Q band for both incubation conditions are given in Table 1. The molar extinction coefficients of *m*-THPC at 422 nm were calculated from the absorption spectra of *m*-THPC (1.5 μM) in HSA–PBS measured either immediately or 6 h after bringing the dye into solution. The obtained values were 47 420 and 63 505 M^{-1} cm^{-1}, respectively, for non-incubated and incubated *m*-THPC HSA–PBS solutions. Fig. 6B and 7B show the fluence dependent variations in the concentrations of the photosensitizers.

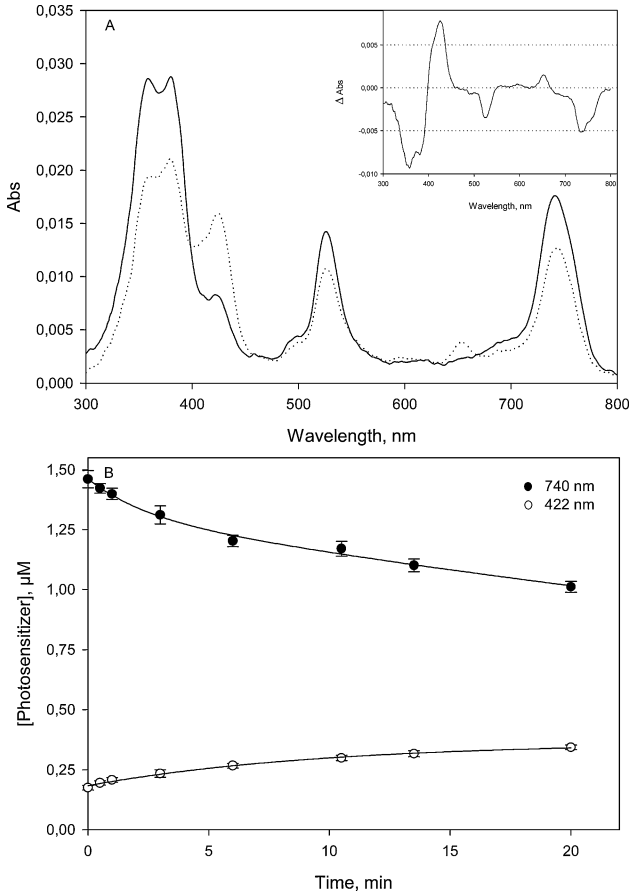

Fig. 6 Absorption spectra of *m*-THPBC solution in HSA–PBS without incubation before (—) and after 810 s irradiation (···) (A). The inset represents the differential spectra (illuminated minus non-illuminated). Fluence-dependent variations in *m*-THPBC and *m*-THPC concentrations (B). *m*-THPBC and *m*-THPC concentrations were derived from the Beer–Lambert law at each irradiation fluence considering the optical densities and the molar extinction coefficients at 740, 742 and 422 nm, respectively. Optical pathlength was 10 mm.

The ratio between growth of *m*-THPC and loss of *m*-THPBC at each irradiation time was defined as the yield of phototransformation (P_t, %)

$$P_t = \frac{[F]_t - [F]_{t_0}}{[B]_{t_0} - [B]_t}, \quad (1)$$

where $[B]_{t_0}$ is the initial concentration of *m*-THPBC in the solution, and $[B]_t$ and $[F]_t$ are the *m*-THPBC and *m*-THPC concentrations at a given irradiation time. Considering that the initial *m*-THPBC solution contains 10% of *m*-THPC (possibly as a result of dark oxidation), this value (1.45 μM) was assigned as $[F]_{t_0}$ in the calculations of P_t.

By applying this relation to the data shown in Fig. 6B, the phototransformation (P_t) for non-incubated *m*-THPBC varied from 38 to 53%, dependent on irradiation time, averaging to 43%. In other words, approximately half of the bleached *m*-THPBC was transformed into *m*-THPC at each irradiation time. For 6 h incubated *m*-THPBC (Fig. 7B), the yield of phototransformation was only 5%.

Discussion

It has been previously shown that *m*-THPBC, after prolonged incubation with cultured tumour cells, presents spectral properties

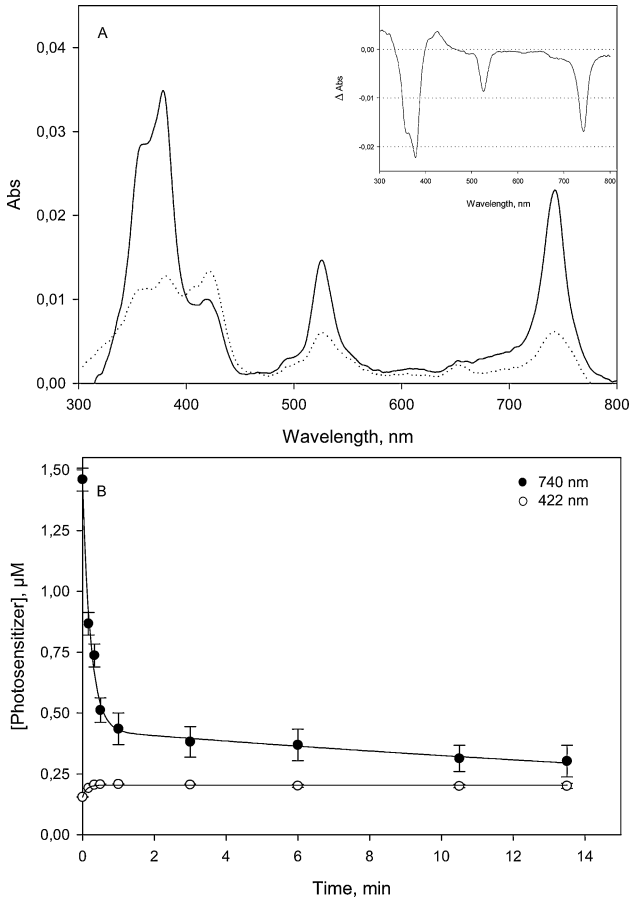

Fig. 7 Absorption spectra of *m*-THPBC solution in HSA–PBS subjected to 6h incubation before (—) and after 810 s irradiation (···) (A). The inset represents the differential spectra (illuminated minus non-illuminated). Fluence-dependent variations in *m*-THPBC and *m*-THPC concentrations (B). *m*-THPBC and *m*-THPC concentrations were derived from the Beer–Lambert law at each irradiation fluence considering the optical densities and the molar extinction coefficients at 740, 742 and 422 nm, respectively. Optical pathlength was 10 mm.

different from both the ethanol (monomeric forms) and aqueous (aggregated forms) reference spectra, suggesting that *m*-THPBC exists in more that one form within the cells.[17] The goal of the present study was an investigation of kinetic characteristics of *m*-THPBC photodegradation at different aggregation states. We also addressed the photoinduced formation of *m*-THPC, a clinically relevant second generation photosensitizer, as a result of *m*-THPBC photodegradation.

Spectroscopic studies

As with porphyrins and phthalocyanines, chlorin-type photosensitizers,[15,17–19] including *m*-THPBC, tend to aggregate in aqueous solutions. Compared to monomeric *m*-THPBC in methanol solution, a pronounced hypochromic effect, a bathochromic shift of the main spectral bands and an increase in the bandwidth $\Delta\nu$ were observed when *m*-THPBC was dissolved in PBS (Fig. 3A, Table 1). The changes in spectral characteristics, together with a barely detectable fluorescence, indicate aggregation of this dye in PBS solution. Similar spectral changes have previously been reported for *m*-THPBC in water compared to ethanol solutions and were considered to result from the aggregation of the dye in an aqueous environment.[17]

Aggregation is likely to occur immediately after the introduction of the *m*-THPBC in methanol stock solution into HSA–PBS. In comparison with monomeric *m*-THPBC in methanol solution, a non-incubated *m*-THPBC HSA–PBS solution exhibited a bathochromic shift of the visible spectral bands, an increase in the $\Delta\nu$ from 250 to 667 cm^{-1} and a considerable decrease in the molar extinction coefficient both in the Soret and red bands (Fig. 3A, Table 1).

Prolonged incubation of photosensitizers in the solutions with proteins results in monomerisation,[18] evidenced by a prominent increase in relative fluorescence intensity.[16,19] Our spectroscopic study demonstrated that *m*-THPBC fluorescence equilibrium in PBS solution supplemented with HSA is achieved two hours after the onset of incubation (data not shown). Six hours incubation of *m*-THPBC in HSA–PBS leads to several marked events compared to non-incubated dye solution. These are the reduction of $\Delta\nu$ from 667 to 400 cm^{-1} (Table 1), a 15% increase in the molar extinction coefficient in the Soret band (Table 1), and a six fold increase in the Soret band intensity in fluorescence excitation spectra (data not shown). Further, considering that only monomers fluoresce, and that a large increase in the relative fluorescence intensity was recorded for incubated *m*-THPBC HSA–PBS solution (Fig. 3B), we conclude that incubation favors photosensitizer monomerisation, whereas *m*-THPBC is mostly aggregated in HSA–PBS immediately after being dissolved.

Photobleaching studies

Generally, photobleaching rate constants depend on the aggregation state of the photosensitizing molecule.[13,15,16] For non-incubated *m*-THPBC HSA–PBS, the photobleaching rate calculated from fluorescence decay appears to be two orders of magnitude higher than photobleaching monitored by decay in absorbance (Table 2). The difference between absorbance and fluorescence measurements can be attributed to the preferential photobleaching of the fluorescing monomer forms as has been previously demonstrated in our studies using porphyrin and chlorin sensitizers.[15,16,20] While the photoinduced loss of fluorescence reflects photochemical activity of photolabile disaggregated forms of the photosensitizer, the decay in absorbance mainly result from aggregated forms which are more stable photochemically. Non-incubated *m*-THPBC HSA–PBS photobleaching can be described by a single exponential decay in terms of delivered light dose (Fig. 4). In contrast to non-incubated *m*-THPBC, the absorbance and fluorescence decays for the incubated dye solution deviate from first-order kinetics and fit better to a bi-exponential decay (Fig. 5). Similar to the photobleaching kinetic study with protoporphyrin IX (Pp IX) in cells,[21] two photobleaching rates could correspond to degradation of *m*-THPBC in two different environments, for example, bound and unbound to proteins. The first part of the photobleaching curve could be related to the rapid degradation of monomer species (bound to proteins) followed by the second exponent, corresponding to the photobleaching of aggregated bound or non-bound forms. This conclusion is supported by two facts. Firstly, the absorbance rate constant of photobleaching computed from the first exponent for incubated *m*-THPBC HSA–PBS is very close to that reported by Bonnett *et al.*[10] for monomeric *m*-THPBC in methanol–water solution. Secondly, the similarity between the absorbance rate constant of the second part of the curve for incubated and the absorbance rate constant for non-incubated *m*-THPBC HSA–PBS is consistent with the preferential photobleaching of aggregated species (Table 2). Another explanation for the bi-exponential decay might be a light-induced re-localisation between different binding sites on the protein, as has been postulated for other photosensitizers.[22]

Photoproducts formation

In addition to true photobleaching, most photosensitizers are phototransformed with the formation of photoproducts absorbing in visible light. Thus, photoproducts might themselves be photosensitizers, and behave differently with respect to photostability than the parent molecule.[23] Therefore, it might be advantageous to apply several wavelengths or modulate the irradiation parameters in order to increase the efficacy of PDT.

The nature of photoproducts formed during the photobleaching of *m*-THPBC in methanol was recently reported by Bonnett and Martinez.[24] True photobleaching was observed with the formation of colorless fragmentation products regarded as succinimide and methyl 3-hydroxybenzoate (the total recovered yield never exceeded 5%). Products of photomodifications were also identified, including the orange pyrrolic dipyrrin derivatives and a small but detectable amount of *m*-THPC. Rapid phototransformation of *m*-THPBC into *m*-THPC has been also reported in aqueous solution and *in vivo*.[12,17,25] Spectroscopic analysis of the present study demonstrated that photobleaching of *m*-THPBC in HSA–PBS solutions was accompanied by an increase in the 422 and 652 nm spectral bands (Fig. 6 and 7), and these spectral features correspond to the formation of *m*-THPC. A major finding of the present work is the influence of the aggregation state of *m*-THPBC on the kinetic of photoproducts formation. While in the aggregated/dimer state about 50% of bleached *m*-THPBC was transformed into *m*-THPC [Fig. 6, eqn. (1)], only 5% of disappeared *m*-THPBC yielded *m*-THPC when *m*-THPBC was bound to HSA [Fig. 7, eqn. (1)]. We further confirmed photoinduced *m*-THPC formation by the matrix assisted laser desorption ionisation coupled to time of flight mass spectrometer (MALDI-TOFMS). The details of MALDI-TOFMS will be reported elsewhere. Here we only note that the *m*-THPBC solutions before irradiation were characterised by a predominant mass peak at m/z 682 corresponding to $[m\text{-THPBC}]^{+\bullet}$. After irradiation (20 min, 66 J cm^{-2}) a new isotopic distribution was detected with an increase at m/z 680 and 681 identified respectively as $[m\text{-THPC}]^{+\bullet}$ and $[m\text{-THPC+H}]^{+}$ together with a concomitant decrease of ion signal at m/z 682. With respect to different *m*-THPBC aggregation states, MS studies were consistent with those obtained with UV-Vis spectroscopy and indicated much more efficient *m*-THPBC photodestruction with a less efficient *m*-THPC formation for *m*-THPBC bound to protein compared to aggregated *m*-THPBC. Along with the photoinduced formation of *m*-THPC, we did observe other photoproducts by applying MALDI-TOFMS. Mass spectrometry spectra of incubated *m*-THPBC HSA–PBS solution were characterized by the formation of dipyrrin derivatives as well as hydroxylated derivatives of *m*-THPC and *m*-THPBC. Unlike incubated, non-incubated *m*-THPBC HSA–PBS solution did not evidence any hydroxylated derivatives. Only dipyrrolic compounds and dipyrrin derivatives other those from incubated dye were detected.

Thus, analysis of photoproducts formed after *m*-THPBC irradiation, assessed by UV-Vis spectroscopy and mass spectrometry demonstrated that photoproduct transformation is significantly influenced by *m*-THPBC aggregation state. The hypothesis on the formation of different types of photoproducts from monomers and aggregates of porphyrin-like molecules was evoked in the studies of Rotomskis *et al.*[13] The afforded explanation was related to the different photobleaching pathways from different aggregation states of photosensitizer. Singlet-oxygen mediated mechanism of photobleaching has been extensively reported for many photosensitizers.[14,26–29] General considerations suggest that this pathway is preferred for photosensitizers bound to proteins.[23] In contrast, in aggregated forms the oxygen availability is restricted and therefore photobleaching *via* the classical $^1O_2$ pathway is limited. In that case, photobleaching mainly proceeds through reactions between the triplet state sensitizer (T_1) and cellular substrates.[30,31] Our ongoing experiments address the oxygen-dependent pathways of both the *m*-THPBC photobleaching and the formation of photoproducts.

In summary, kinetic characteristics of *m*-THPBC photobleaching, reported in the present study, together with the different kinetics of photoinduced formation of *m*-THPC, a clinically relevant photosensitizer, may provide important information to be taken into account in *m*-THPBC-based PDT dosimetry in the clinical context.

Abbreviations

HSA, human serum albumin; *m*-THPBC, 5,10,15,20-tetrakis(*m*-hydroxyphenyl)bacteriochlorin; *m*-THPC, 5,10,15,20-tetrakis-(*m*-hydroxyphenyl)chlorin; PDT, photodynamic therapy, Pp IX, protoporphyrin IX.

Acknowledgements

This work was supported by French Cancer Society, The Research Foundation of The Norwegian Radium Hospital (Oslo), Alexis Vautrin Cancer Centre Research Funds, French Ligue National Contre le Cancer (Comité de Meurthe et Moselle, Comité de Haute-Marne) and Conseil Régional de Lorraine. The authors are grateful to Professor J. F. Muller and N. Lourette from the LSMCL laboratory (Metz University, France) for their collaboration in the mass spectrometry study. The gift of *m*-THPBC from Biolitec Pharma Ltd. (Edinburgh, UK) is greatly appreciated.

References

1 J. D. Spikes, Quantum yields and kinetics of the photobleaching of hematoporphyrin, Photofrin II, tetra(4-sulfonatophenyl)-porphine and uroporphyrin, *Photochem. Photobiol.*, 1992, **55**, 797–808.
2 R. Bonnett and G. Martínez, Photobleaching of sensitisers used in photodynamic therapy, report number 591, *Tetrahedron*, 2001, **57**, 9513–9547.
3 B. C. Wilson, M. S. Patterson and L. Lilge, Implicit and explicit dosimetry in photodynamic therapy: a new paradigm., *Lasers Med. Sci.*, 1997, **12**, 182–199.
4 H. Zeng, M. Korbelik, D. I. McLean, C. MacAulay and H. Lui, Monitoring photoproduct formation and photobleaching by fluorescence spectroscopy has the potential to improve PDT dosimetry with a verteporfin-like photosensitizer, *Photochem. Photobiol.*, 2002, **75**, 398–405.
5 J. Moan, Effect of bleaching of porphyrin sensitizers during photodynamic therapy, *Cancer Lett.*, 1986, **33**, 45–53.
6 R. Bonnett, R. D. White, U. J. Winfield and M. C. Berenbaum, Hydroporphyrins of the meso-tetra(hydroxyphenyl)porphyrin series as tumour photosensitizers, *Biochem. J.*, 1989, **261**, 277–280.
7 R. Bonnett, P. Charlesworth, B. D. Djelal, S. Foley, D. J. McGarvey and T. G. Truscott, Photophysical properties of 5,10,15,20-tetrakis-(*m*-hydroxyphenyl)porphyrin (*m*-THPP), 5,10,15,20-tetrakis(*m*-hydroxyphenyl)chlorin (*m*-THPC) and 5,10,15,20-tetrakis(*m*-hydroxyphenyl) bacteriochlorin (*m*-THPBC): a comparative study, *J. Chem. Soc., Perkin Trans. 2*, 1999, **2**, 325–328.
8 J. P. Rovers, M. L. de Jode and M. F. Grahn, Significantly increased lesion size by using the near-infrared photosensitizer 5,10,15,20-tetrakis (*m*-hydroxyphenyl)bacteriochlorin in interstitial photodynamic therapy of normal rat liver tissue, *Lasers Surg. Med.*, 2000, **27**, 235–240.
9 K. Engelmann, M. G. Mack, K. Eichler, R. Straub, S. Zangos and T. J. Vogl, Interstitial photodynamic laser therapy for liver metastases: first results of a clinical phase I study, *RoeFo, Fortschr. Geb. Rontgenstr. Neuen. Bildgeb. Verfahr.*, 2003, **175**, 682–687.
10 R. Bonnett, B. D. Djelal, P. A. Hamilton, G. Martinez and F. Wierrani, Photobleaching of 5,10,15,20-tetrakis(*m*-hydroxyphenyl) porphyrin (*m*-THPP) and the corresponding chlorin (*m*-THPC) and bacteriochlorin(*m*-THPBC). A comparative study, *J. Photochem. Photobiol. B*, 1999, **53**, 136–143.
11 J. P. Rovers, M. L. de Jode, H. Rezzoug and M. F. Grahn, In vivo photodynamic characteristics of the near-infrared photosensitizer 5,10,15,20-tetrakis(M-hydroxyphenyl) bacteriochlorin, *Photochem. Photobiol.*, 2000, **72**, 358–364.
12 M. Angotti, B. Maunit, J. F. Muller, L. Bezdetnaya and F. Guillemin, Characterization by matrix-assisted laser desorption/ionizat ion Fourier transform ion cyclotron resonance mass spectrometry of the major photoproducts of temoporfin (*m*-THPC) and bacteriochlorin (*m*-THPBC), *J. Mass. Spectrom.*, 2001, **36**, 825–831.
13 R. Rotomskis, S. Bagdonas and G. Streckyte, Spectroscopic studies of photobleaching and photoproduct formation of porphyrins used in tumour therapy, *J. Photochem. Photobiol. B*, 1996, **33**, 61–67.
14 M. B. Ericson, S. Grapengiesser, F. Gudmundson, A. M. Wennberg, O. Larko, J. Moan and A. Rosen, A spectroscopic study of the photobleaching of protoporphyrin IX in solution, *Lasers Med. Sci.*, 2003, **18**, 56–62.

15 L. Bezdetnaya, N. Zeghari, I. Belitchenko, M. Barberi-Heyob, J. L. Merlin, A. Potapenko and F. Guillemin, Spectroscopic and biological testing of photobleaching of porphyrins in solutions, *Photochem. Photobiol.*, 1996, **64**, 382–386.
16 I. Belitchenko, V. Melnikova, L. Bezdetnaya, H. Rezzoug, J. L. Merlin, A. Potapenko and F. Guillemin, Characterization of photodegradation of meta-tetra(hydroxyphenyl)chlorin (*m*-THPC) in solution: biological consequences in human tumor cells, *Photochem. Photobiol.*, 1998, **67**, 584–590.
17 M. F. Grahn, A. McGuinness, R. Benzie, R. Boyle, M. L. de Jode, M. G. Dilkes, B. Abbas and N. S. Williams, Intracellular uptake, absorption spectrum and stability of the bacteriochlorin photosensitizer 5,10,15,20-tetrakis (*m*-hydroxyphenyl)bacteriochlorin (*m*-THPBC). Comparison with 5,10,15,20-tetrakis(*m*-hydroxyphenyl) chlorin (*m*-THPC), *J. Photochem. Photobiol. B*, 1997, **37**, 261–266.
18 B. M. Aveline, T. Hasan and R. W. Redmond, The effects of aggregation, protein binding and cellular incorporation on the photophysical properties of benzoporphyrin derivative monoacid ring A (BPDMA), *J. Photochem. Photobiol. B*, 1995, **30**, 161–169.
19 D. J. Ball, S. R. Wood, D. I. Vernon, J. Griffiths, T. M. Dubbelman and S. B. Brown, The characterisation of three substituted zinc phthalocyanines of differing charge for use in photodynamic therapy. A comparative study of their aggregation and photosensitising ability in relation to mTHPC and polyhaematoporphyrin, *J. Photochem. Photobiol. B*, 1998, **45**, 28–35.
20 J. Moan, The photochemical yield of singlet oxygen from porphyrins in different states of aggregation., *Photochem. Photobiol.*, 1984, **39**, 445–449.
21 J. Moan, G. Streckyte, S. Bagdonas, O. Bech and K. Berg, Photobleaching of protoporphyrin IX in cells incubated with 5-aminolevulinic acid, *Int. J. Cancer*, 1997, **70**, 90–97.
22 A. B. Uzdensky, V. Iani, L. W. Ma and J. Moan, Photobleaching of hypericin bound to human serum albumin, cultured adenocarcinoma cells and nude mice skin, *Photochem. Photobiol.*, 2002, **76**, 320–328.
23 J. Moan, P. Juzenas and S. Bagdonas, Degradation and transformation of photosensitizers during light exposure, *Recent Res. Dev. Photochem. Photobiol.*, 2000, **4**, 121–132.
24 R. Bonnett and G. Martinez, Photobleaching of compounds of the 5,10,15,20-tetrakis(*m*-hydroxyphenyl) porphyrin series (*m*-THPP, *m*-THPC and *m*-THPBC), *Org. Lett.*, 2002, **4**, 2013–2016.
25 L. W. Ma, J. Moan, M. F. Grahn and V. Iani, Comparison of meso-tetrahydroxyphenyl-chlorin and meso-tetrahydroxyphenyl-bacteriochlorin with respect to photobleaching and PCT efficiency in vivo, *Proc. SPIE*, 1996, **2924**, 219–224.
26 I. Georgakoudi, M. G. Nichols and T. H. Foster, The mechanism of Photofrin photobleaching and its consequences for photodynamic dosimetry, *Photochem. Photobiol.*, 1997, **65**, 135–144.
27 I. Georgakoudi and T. H. Foster, Singlet oxygen *versus* non-singlet oxygen-mediated mechanisms of sensitizer photobleaching and their effects on photodynamic dosimetry, *Photochem. Photobiol.*, 1998, **67**, 612–625.
28 C. Hadjur, N. Lange, J. Rebstein, P. Monnier, H. van den Bergh and G. Wagnières, Spectroscopic studies of photobleaching and photoproduct formation of meta(tetrahydroxyphenyl) chlorin (*m*-THPC) used in photodynamic therapy. The production of singlet oxygen by *m*-THPC, *J. Photochem. Photobiol. B*, 1998, **45**, 170–178.
29 S. Coutier, S. Mitra, L. N. Bezdetnaya, R. M. Parache, I. Georgakoudi, T. H. Foster and F. Guillemin, Effects of fluence rate on cell survival and photobleaching in meta-tetra-(hydroxyphenyl)chlorin-photosensitized Colo 26 multicell tumor spheroids, *Photochem. Photobiol.*, 2001, **73**, 297–303.
30 C. R. Shea, Y. Hefetz, R. Gillies, J. Wimberly, G. Dalickas and T. Hasan, Mechanistic investigation of doxycycline photosensitization by picosecond-pulsed and continuous wave laser irradiation of cells in culture, *J. Biol. Chem.*, 1990, **265**, 5977–5982.
31 B. W. Pogue, B. Ortel, N. Chen, R. W. Redmond and T. Hasan, A photobiological and photophysical-based study of phototoxicity of two chlorins, *Cancer Res.*, 2001, **61**, 717–724.

1.2. MALDI-TOF mass spectrometry analysis for the characterization of the 5,10,15,20-tetrakis(m-hydroxyphenyl)bacteriochlorin (m-THPBC) photoproducts in biological environment.

The first part of our work consisted in the study of the photobleaching characteristics of the *m*-THPBC in biologically relevant solution. We evidenced the photoformation of *m*-THPC consecutively to the *m*-THPBC irradiation, no other visible absorbing photoproducts were detected. In this second part of our work we have studied by the mean of MALDI-TOF mass spectrometry the products formed upon *m*-THPBC 739 nm laser diode irradiation. Aggregated and monomerised solution of *m*-THPBC were examined. Photoproducts such as di-hydroxylated *m*-THPBC and di-hydroxylated *m*-THPC were detected in both incubation conditions, however the formation of hydroxylated photoproducts was significantly greater in incubated solution. In addition small molecules arising from the degradation of the photosensitizer and identified as dipyrin derivatives were observed.

This part of the work was accepted for publication in the *Journal of Mass Spectrometry* and is presented thereafter in its uncorrected proofs.

JOURNAL OF MASS SPECTROMETRY
J. Mass Spectrom. 2005; **40**: 1149–1156
Published online 22 July 2005 in Wiley InterScience (www.interscience.wiley.com). DOI: 10.1002/jms.886

JMS

MALDI-TOF mass spectrometric analysis for the characterization of the 5,10,15,20-tetrakis-(*m*-hydroxyphenyl)bacteriochlorin (*m*-THPBC) photoproducts in biological environment

Henri-Pierre Lassalle,[1]* Natacha Lourette,[2] Benoît Maunit,[2] Jean-François Muller,[2] François Guillemin[1] and Lina Bezdetnaya-Bolotine[1]

[1] Centre Alexis Vautrin, CRAN CNRS UMR 7039-INPL-UHP, Vandœuvre-les-Nancy, France
[2] Laboratoire de Spectrométrie de Masse et de Chimie Laser, Metz, France

Received 4 March 2005; Accepted 3 May 2005

Photoproducts formation upon irradiation (739 nm) of 5,10,15,20-tetrakis(*m*-hydroxyphenyl)bacteriochlorin (*m*-THPBC) in phosphate buffer saline (PBS) supplemented with human serum albumin (HSA) were studied by means of absorption spectroscopy and MALDI-TOF mass spectrometry. The experiments were performed with a freshly prepared PBS–HSA solution of *m*-THPBC and with a PBS–HSA *m*-THPBC solution incubated for 6 h at 37 °C. The incubation of *m*-THPBC solution leads to the dye monomerisation, whereas in the freshly prepared solution, *m*-THPBC is under an aggregated form. Regardless of the incubation condition, photobleaching experiments carried out by absorption spectroscopy demonstrate the degradation of the photosensitizer and its phototransformation in *m*-THPC. Moreover, *m*-THPC was the sole photoproduct detected using absorption spectroscopy. Together with a degradation of *m*-THPBC and formation of *m*-THPC, MALDI-TOF mass spectrometry evidenced several other photoinduced modifications. Photoproducts such as dihydroxy *m*-THPBC and dihydroxy *m*-THPC were detected in both conditions; however, the formation of hydroxylated photoproducts was significantly greater in incubated solution. In addition, small molecules arising from the degradation of the photosensitizer and identified as dipyrin derivatives and dipyrrolic synthon were observed. Copyright © 2005 John Wiley & Sons, Ltd.

KEYWORDS: photodynamic therapy; mass spectrometry; MALDI-TOF-MS; photobleaching; photoproducts formation; *m*-THPBC

INTRODUCTION

Photodynamic therapy (PDT) of cancer is based on the use of a drug with photosensitizing and tumor localizing properties, combined with visible light and oxygen. Separately, these three components are harmless, but in combination they may destroy tissues and inactivate cells. By exposing the tumor area to light within the absorption spectrum of the drug, reactive oxygen species (ROS) including singlet oxygen are formed, and the tumor can be destroyed. Concomitantly, under light-exposure, the same species attack the photosensitisers; thus absorption and fluorescence properties of the photosensitizer are modified due to a phenomenon called *photobleaching*. The first relevant observation of photobleaching in the PDT field was made in 1986 by Moan.[1] Presently, two mechanisms of photobleaching are considered.[2] The first one, true photobleaching, corresponds to the photodegradation of the porphyrin macrocycle with the formation of photoproducts, which do not absorb in the visible region. The second mechanism is called *photomodification*, where the chromophore is retained in a modified form with the formation of new visible spectral bands. One of the main reasons to study photobleaching is that it leads to the decrease in the concentration and/or to the modification of the nature of the photosensitizer, thus playing a leading role in the dosimetry of the photodynamic treatment.

5,10,15,20-Tetrakis(*m*-hydroxyphenyl)bacteriochlorin (*m*-THPBC) is the most reduced compound in the tetraphenylchlorin series.[3] This dye has a strong absorbance in the red region (740 nm).[4] In view of the weak absorbance of tissues at this wavelength, this offers promising therapeutic perspectives for PDT of deep tumors and pigmented tissues. Presently, *m*-THPBC is under clinical investigation for PDT of patients with hepatic metastasis.[5]

Porphyrin-like compounds have been extensively studied in the past by mass spectrometry coupled with electron

*Correspondence to: Henri-Pierre Lassalle, Centre Alexis Vautrin, CRAN CNRS UMR 7039-INPL-UHP, Avenue de Bourgogne, 54511 Vandœuvre-les-Nancy, France. E-mail: h.lassalle@nancy.fnclcc.fr
Contract/grant sponsor: Alexis Vautrin Cancer Center Research Funds.
Contract/grant sponsor: French Ligue National Contre le Cancer (Comité de Meurthe et Moselle, Comité de Haute-Marne).

ionization (EI),[6] chemical ionization (CI),[7] fast atom bombardment (FAB),[8] plasma desorption,[9] laser desorption[10], electrospray (ESI)[11] and matrix assisted laser desorption (MALDI).[12,13] Among these ionization techniques, MALDI appears to be one of the most attractive and allows the analysis of complex media with salts and proteins. Likewise, MALDI-TOF-MS on porphyrins demonstrated a high sensitivity of detection (10^{-12} M)[14,15] and the possibility to control the fragmentation level by modifying the laser power.

Our recent study[16] demonstrated that the photobleaching rate constant and the phototransformation yield of *m*-THPBC were highly dependant on the aggregation state of this photosensitizer. Spectrophotometry and spectrofluorimetry studies allowed the detection of 5,10,15,20-tetrakis(*m*-hydroxyphenyl)chlorin (*m*-THPC) as the sole photoproduct after *m*-THPBC irradiation. To complete this study, we carried out the photoproducts identification by MALDI-TOF-MS after *m*-THPBC irradiation at 739 nm in an albumin-enriched solution under different incubation conditions corresponding to different aggregation states.

EXPERIMENTAL

Photosensitizer

The photosensitizer *m*-THPBC was kindly provided by Biolitec Pharma Ltd. (Edinburgh, UK). It was stored in the dark at 4 °C as a stock solution in methanol at a concentration of 3 mM. Further dilution was performed in phosphate buffer saline (PBS), in PBS supplemented with 1 mg ml^{-1} human serum albumin (HSA, Sigma-Aldrich, Saint-Quentin Fallavier, France) or in methanol. The final concentration of *m*-THPBC in each solvent was 10 μM.

Photoirradiation

Prior to irradiation, *m*-THPBC solutions in PBS-HSA were kept for 0 h or 6 h in the dark at 37 °C. Irradiation was carried out, under continuous magnetic stirring, by exposing 3 ml of 10 μM *m*-THPBC solution in a 10-mm quartz cuvette to light from a laser diode at 739 nm (Ceralas PDT 739, CeramOptec GmbH, Bonn, Germany). The incident radiance was 5 mW cm^{-2}.

Absorption measurements

Absorption spectra were recorded with a Perkin-Elmer Lambda 15 spectrophotometer using a 10-mm quartz cuvette. *m*-THPBC absorbance was recorded in the range 300–800 nm.

MALDI sample preparation

MALDI sample preparation was carried out by the standard thin layer technique. One μl of sample and 1 μl of a saturated α-cyano-4-hydroxy-*trans*-cinnamic acid (CHCA) solution in 50% acetonitrile, 0.1% of trifluoroacetic acid (TFA) were spotted on a stainless steel MALDI target. Thus, the molar ratio of analyte to matrix was 1 : 10^4. Mass spectra were acquired over the range 0–1200 Da. The porphyrin 5,10,15,20-tetra-(1-phenyl)-porphyrin (TPP, 614.74 g mol^{-1}) was used as internal control by adding 1 μl of a 10 μM TPP ethanol solution to each sample.

Time-of-flight mass spectrometer (TOF-MS)

Analyses were performed on a Bruker Reflex IV time-of-flight mass spectrometer (TOF-MS) (Bruker-Daltonic, Bremen Germany) equipped with the SCOUT 384 probe ion source. The system uses a pulsed nitrogen laser (337 nm, model VSL-337ND, Laser Science Inc., Boston, MA) with energy output of 400 μJ/pulse. The ions were accelerated under delayed extraction conditions (200 ns) in positive ion mode with an acceleration voltage of 20 kV and a reflector voltage of 23 kV. The detector signals were amplified and transferred to the XACQ program on a SUN work station (Sun Microsystems Inc. Palo Alto, CA). Spectra were processed with the XMass 5.1 program (Bruker Daltonics, Bremen, Germany). External calibration of MALDI mass spectra was carried out using PEG 600 Na^+ and K^+ cationized species. To achieve semiquantitative measurements, all experiments were performed under the same conditions (shots number, pressure, laser impact size and laser intensity), with TPP added as an internal control.

RESULTS AND DISCUSSION

Spectroscopic properties of *m*-THPBC in different media

The chemical structure of the molecule is presented in Fig 1. The *m*-THPBC visible absorption spectra in PBS supplemented with HSA (1 mg ml^{-1}) measured either immediately (0 h) or 6 h after incubation (6 h) are shown in Fig. 2. The main spectral characteristics of these solutions are summarized in Table 1. The absorption spectra in methanol displayed three peaks, one at 373 nm corresponding to the Soret band, and two at 517 nm and 734 nm corresponding to the Q bands. In HSA–PBS solutions these peaks are red shifted to 380 nm, 526 nm and 741 nm respectively. A hypochromic effect (decrease in absorbance) of *m*-THPBC in HSA–PBS solutions was evidenced (with or without incubation) compared to methanol ($\varepsilon \approx 15\,000$ M^{-1} cm^{-1} *vs* 103 591 M^{-1} cm^{-1}). A broadening of Q band (widening of the half maximum bandwidths; $\Delta\nu$), from 259 cm^{-1} to 368 cm^{-1} and further to 581 cm^{-1} for *m*-THPBC in methanol, incubated HSA–PBS and freshly prepared HSA–PBS, respectively was also observed. The bathochromic shift together with an hypochromic effect and a widening of the half maximum bandwidths are indicative of an aggregation of the photosensitizer in HSA–PBS solutions.[16–18] Presence of proteins results in monomerization of chlorin-type photosensitizers.[19] The spectroscopic *m*-THPBC properties presented in this study (Fig. 2, Table 1) together with the prominent increase in fluorescence intensity of incubated compared to freshly prepared *m*-THPBC (data not shown) show that incubation favors photosensitizer monomerisation, whereas *m*-THPBC is mostly aggregated immediately after being dissolved in HSA–PBS. These data are consistent with our previous study.[16]

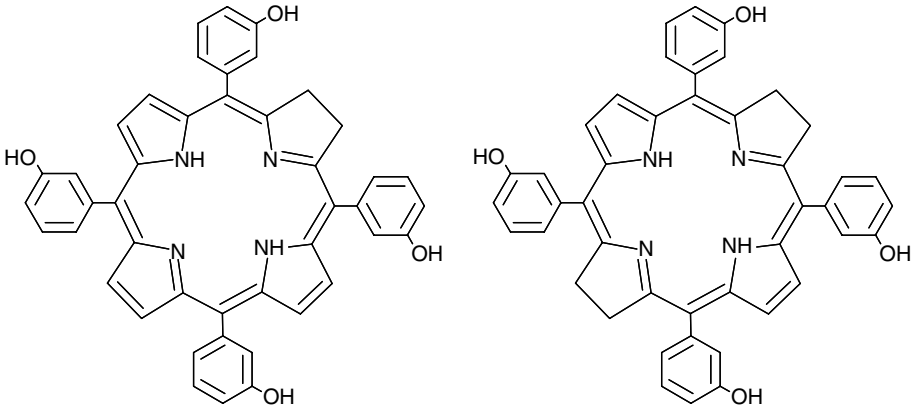

Figure 1. Molecular structure of *m*-THPC and *m*-THPBC.

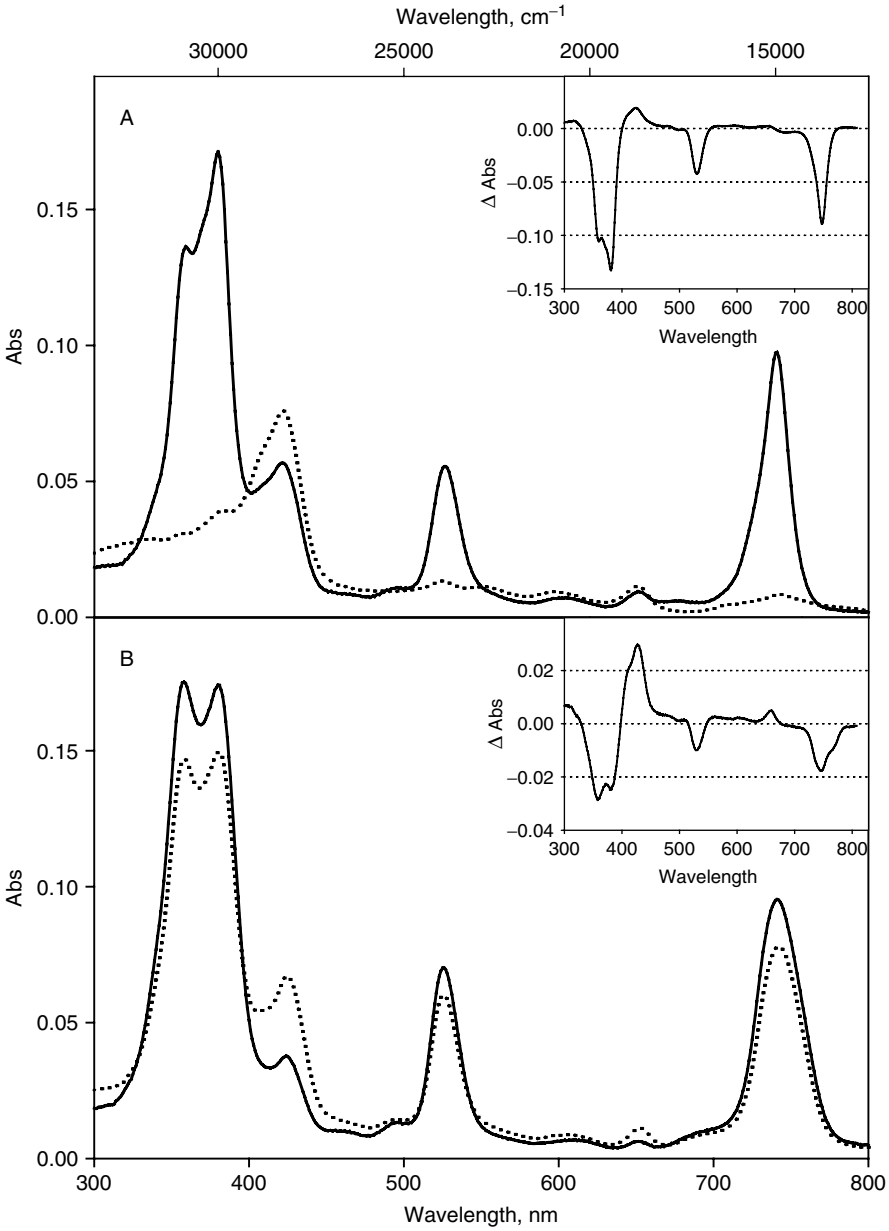

Figure 2. Absorption spectra of *m*-THPBC (10^{-5} M) before (full line), and after irradiation with 6 J cm^{-2} at 739 nm (dotted line). Absorption spectra of *m*-THPBC in HSA-PBS 6 h after incubation at 37 °C (A), and in freshly prepared HSA-PBS solution (B).

Table 1. Absorbance spectra characteristics of *m*-THPBC (10 μM) in different media[a]

	Soret band				Red band				
	λ (nm)	ε (M^{-1} cm^{-1})	Peak height prior irradiation	Peak height after irradiation	λ (nm)	ε (M^{-1} cm^{-1})	Δv (cm^{-1})	Peak height prior irradiation	Peak height after irradiation
Methanol	373	103 591	1.06	0.39	734	83 400	259	0.85	0.31
PBS + HSA 0h	380	15 587	0.16	0.13	741	8 676	581	0.09	0.07
PBS + HSA 6h	380	15 325	0.16	0.02	741	9 160	368	0.09	0.01

[a] Absorption maxima of the Soret and the red band (λ) with corresponding molar absorption coefficients (ε), Δv is the half height bandwidth.

Spectrophotometry data

m-*THPBC photobleaching and phototransformation*

Incubated or nonincubated solutions of *m*-THPBC were irradiated with a 739-nm laser diode for 20 min and with an output of 5 mW cm^{-2}. Figure 2 presents the visible absorbance spectra of the photosensitizer in different solutions, prior to (full lines) and after irradiation (dotted lines). Irrespective of the incubation of the solutions, the irradiation induces a significant decrease of the Soret bands and the Q bands I and II. Irradiation of *m*-THPBC in incubated solution (monomerised *m*-THPBC) leads to the decrease of 94% of the Q band I (Table 1), whereas it decreases only 20% for the nonincubated solution (aggregated *m*-THPBC).

Photobleaching rates depend strongly on the aggregation state of photosensitizers. It has been shown that photodegradation of porphyrins is much faster for monomerised photosensitizers.[20–22] The probable explanation could be related to the limited oxygen availability deep in the clusters of the aggregated species, thus explaining their weak photobleaching.[16,23]

The inset to the Figs 2A and 2B correspond to the differential absorbance spectra (illuminated minus nonilluminated) of *m*-THPBC. Corresponding to a decrease in the peaks at 378, 514 and 740 nm, these differential spectra evidence the formation of a compound absorbing visible light at 422 nm and 650 nm; these spectral features correspond to the formation of *m*-THPC (chemical structure in Fig. 1). Rapid phototransformation of *m*-THPBC in *m*-THPC has already been observed in aqueous solution and *in vivo*.[13,24,25]

Regarding the incubated, protein bound *m*-THPBC solution, we see a large decrease of the peaks corresponding to the *m*-THPBC (378, 514 and 740 nm) and a small but detectable formation of *m*-THPC (peaks at 422 and 650 nm) (Fig. 2). For nonincubated solution we observe a limited photobleaching of *m*-THPBC and a rather important formation of *m*-THPC. The photobleaching and photoproduct formation profiles observed in the present study are in good agreement with the previous one.[16]

Mass spectrometry studies

m-*THPBC photobleaching*

In a parallel set of experiments, we performed MALDI-TOF-MS analysis of *m*-THPBC photobleaching under the same experimental conditions as for spectroscopy studies. Both monomeric and aggregated nonilluminated *m*-THPBC solutions were characterized by a monoisotopic peak at *m*/*z* 682.25 corresponding to the $M^{+\bullet}$ radical species (Fig. 3 and Fig. 4). We also observed ions at *m*/*z* 680.25 and 681.25, corresponding respectively to the $M^{+\bullet}$ and $[M + H]^+$ ions of *m*-THPC. The presence of *m*-THPC in nonilluminated solutions is consistent with the presence of small but detectable absorbance at 422 nm in the absorption spectrum of *m*-THPBC (Fig. 2) and could be attributed to impurities (5%) arising from the synthesis pathway of *m*-THPBC.[3] Also, dark oxidation can occur giving rise to the formation of *m*-THPC up to 10%.[16] Figure 5 displays a control mass spectra of the HSA–PBS solution without *m*-THPBC, where irradiation did not modify the spectra. The nature of the peaks at *m*/*z* 682.00, 683.00 and 684.00 (Fig. 3 and Fig. 4) was derived from the MALDI-TOF-MS control experiment (Fig. 5) with a solution of HSA–PBS alone. Thus we identified these species as belonging to the HSA–PBS solution.

When both solutions were subjected to a 6 J cm^{-2} irradiation, a marked decrease of *m*-THPBC isotopic distribution was recorded (Fig. 3 and Fig. 4). All spectra were registered in the presence of an internal standard TPP (*m*/*z* 615.25 corresponding to $[M + H]^+$ ion), thus enabling the semi-quantitative estimation of *m*-THPBC signal intensity; the abundance standard error calculated from the experiments was 2.4%. Irradiation resulted in 82% decrease in *m*-THPBC signal for the incubated solution, whereas only 58% decrease was noticed for nonincubated solution. Absorption spectroscopy of protein-bound, photo-faded *m*-THPBC demonstrated a 94% decrease in the peak at 740 nm, and this value was very close to the 82% loss of signal at the *m*/*z* 682.25 in MALDI-TOF-MS experiments (Fig. 3). For aggregated photosensitizer (nonincubated solution) the decrease was, respectively, 20% for the absorbance at 740 nm and 58% for the *m*/*z* 682.25 signal (Fig. 4). This big discrepancy could be the consequence of the photoinduced formation of hydroxylated photoproducts (see the next section) that have the same absorption bands as the parent compound, which hampers a quantitative spectroscopic analysis.[12,26]

Photoproduct formation following laser irradiation

In contrast to the spectroscopy study, the mass spectra of *m*-THPBC solution after irradiation demonstrated a very different pattern of photoproducts formation. For both incubation conditions we observed a decrease in protonated and radical *m*-THPC signal intensity (*m*/*z* 680.25 and 681.25) (Fig. 3 and Fig. 4). However, this decrease was much more pronounced for the incubated (Fig. 3)

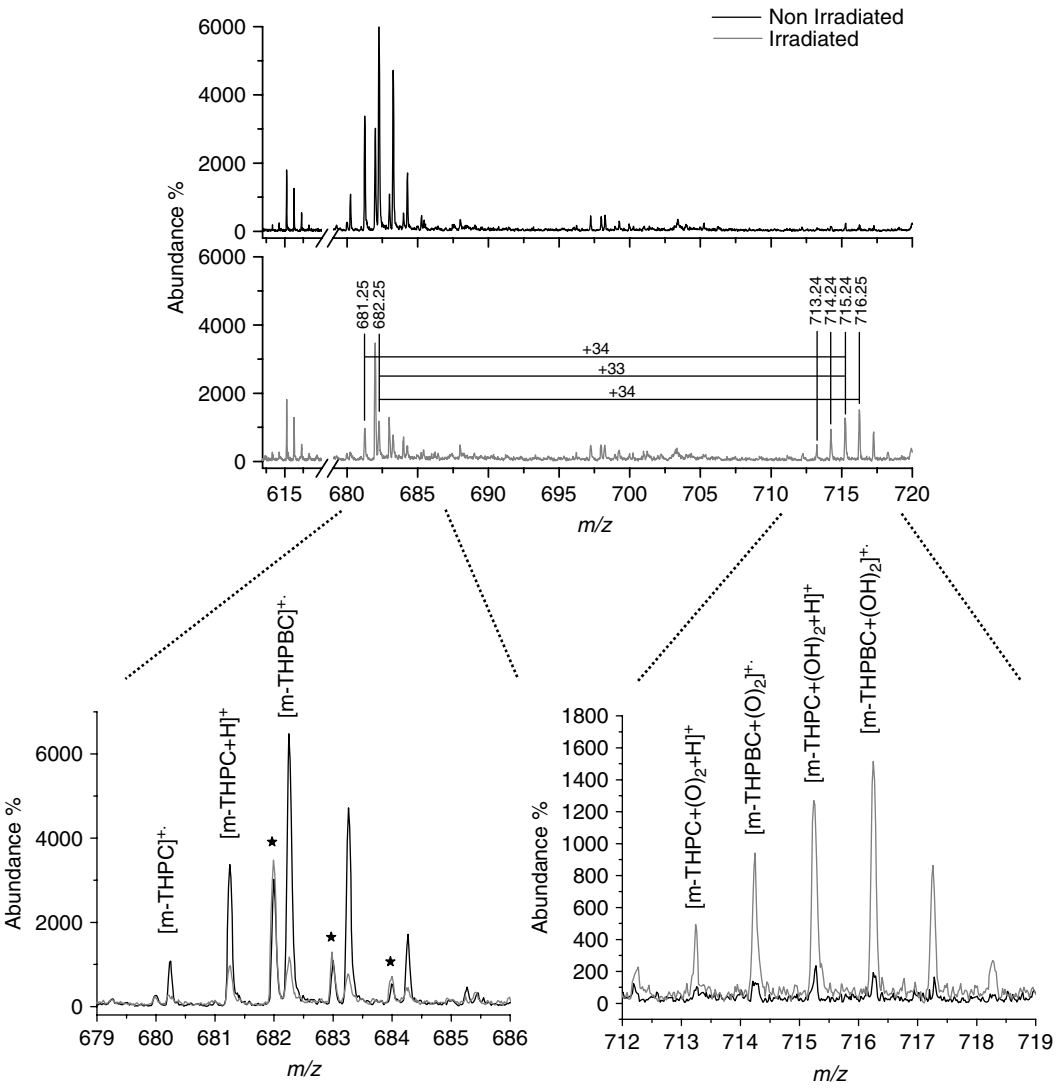

Figure 3. MALDI-TOF-MS spectra of nonirradiated and irradiated with 6 J cm^{-2} *m*-THPBC (10^{-5} M) in HSA-PBS solution incubated 6 h at 37 °C. The peaks marked with an asterisk are species relative to the HSA-PBS solution.

compared to nonincubated *m*-THPBC solution (Fig. 4), and is likely to reflect two simultaneously occurring processes: photoformation and photodestruction of *m*-THPC. Therefore photoformation for nonincubated solutions is higher and/or photodestruction is less than for incubated solutions. This profile of *m*-THPC formation significantly contrasts with a large *m*-THPC formation registered by spectroscopy (Fig. 2).

Irrespective of the incubation conditions, the signal around m/z 715 increases after 6 J cm^{-2} laser light exposure. For protein bound *m*-THPBC, we observed an intense ion signal with a predominant mass peak at m/z 716.25, and its intensity was about 8 times higher compared to nonirradiated solution. For aggregated *m*-THPBC, the formation of a signal with a predominant mass peak at m/z 715.24 was recorded after irradiation. However, the signal intensity did not increase more than 1.7 times compared to nonirradiated solution. This difference in the yield of photoinduced formation of hydroxylated derivatives is likely related to oxygen availability in monomer and aggregated fractions. The aggregated photosensitizers are packed, reducing the accessibility for the oxygen and thus limiting the photochemical production of singlet oxygen and other ROS. ROS, and especially singlet oxygen, are mainly responsible for the hydroxylation of tetrapyrrolic photosensitizers.[27] Several studies demonstrated monohydroxylation or/and di-hydroxylation of tetraphenylchlorin series upon irradiation[13,27] in methanol/water solution. Scarcity of oxygen could explain the weak photobleaching of aggregated molecules[28] together with the lower yield of photoformation of hydroxylated derivatives compared to those bound to the proteins.

We further attempted to identify the photoproducts between m/z 713 and 717 (Fig. 3 and Fig. 4). The ion at m/z 713.24 was attributed to the protonated dihydroxylated *m*-THPC ($[m\text{-THPC} + (O)_2 + H]^+$) as has been described by several authors[12,29] and the ion at m/z 714.24 was attributed to dihydroxy *m*-THPBC ($[m\text{-THPBC} + (O)_2]^{+\bullet}$) due to a photo-substitution mechanism. Two explanations can be proposed to clarify the nature of the ion at m/z 715.24: It could arise from the photo-addition (photo-hydratation) of the *m*-THPC, giving the protonated dihydro dihydroxy *m*-THPC

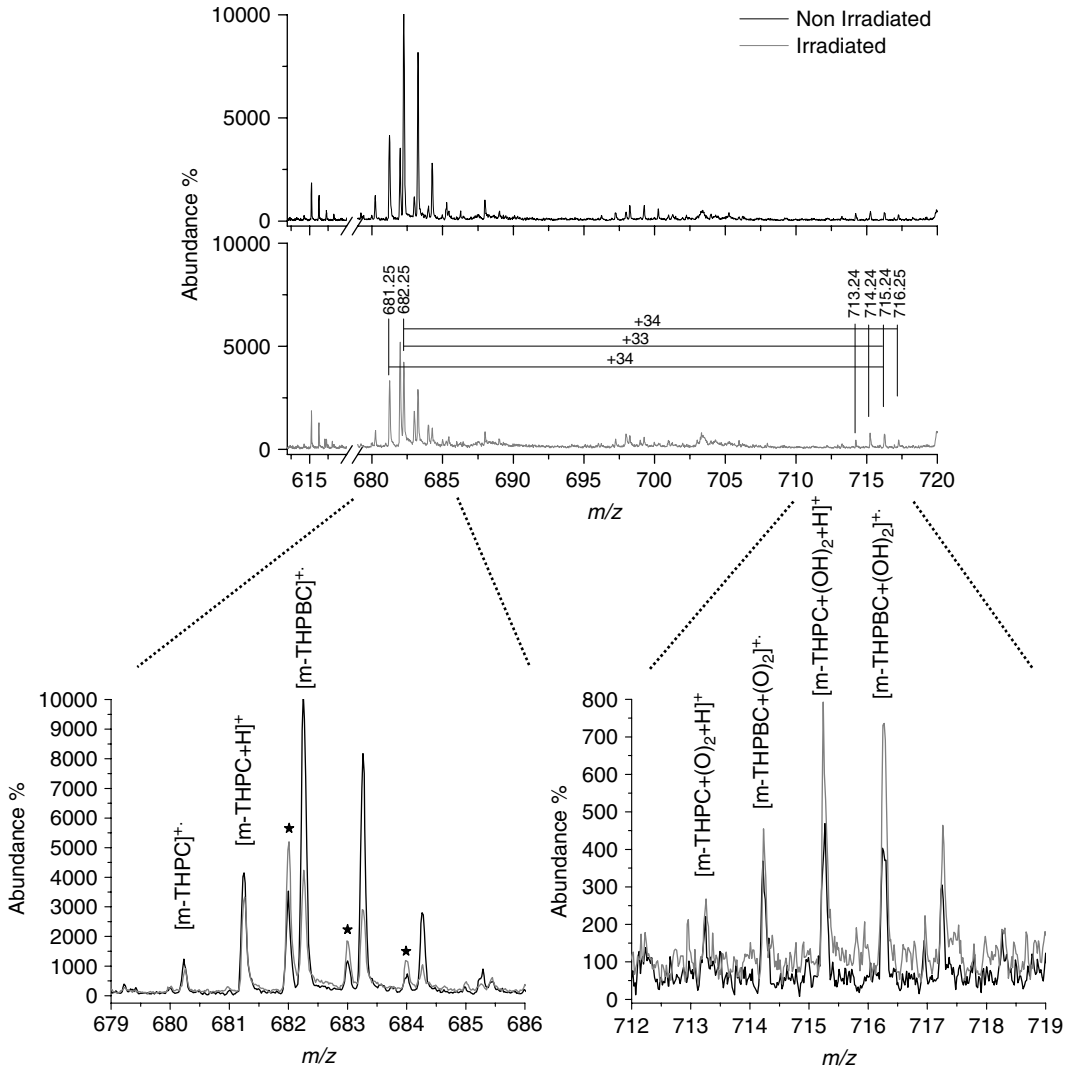

Figure 4. MALDI-TOF-MS spectra of nonirradiated and irradiated with 6 J cm^{-2} *m*-THPBC (10^{-5} M) in freshly prepared solution. The peaks marked with an asterisk are species relative to the HSA-PBS solution.

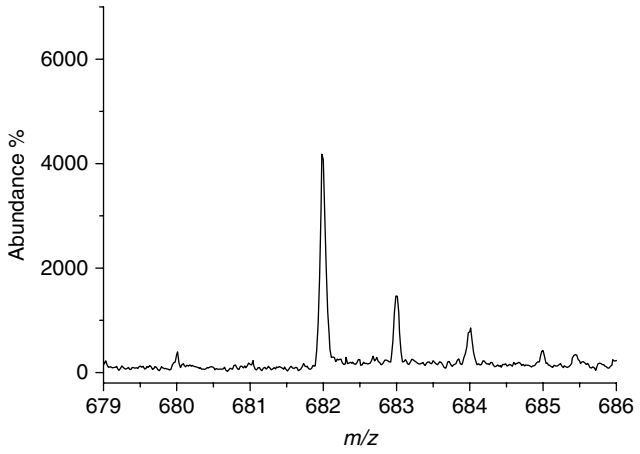

Figure 5. MALDI-TOF-MS spectra of HSA-PBS solution.

noted on the figures $[m\text{-THPC} + (OH)_2 + H]^+$. Another possibility is the dihydroxylation of the *m*-THPBC (photosubstitution) giving the protonated dihydroxy *m*-THPBC noted $[m\text{-THPBC} + (O)_2 + H]^+$. The ion at m/z 716.25 can be explained by the formation of the dihydro dihydroxylated *m*-THPBC ($[m\text{-THPBC} + (OH)_2]^{+\bullet}$) with the presence of the corresponding protonated ion ($[m\text{-THPBC} + (OH)_2 + H]^+$) at m/z 717.25, thus explaining that the peaks observed (m/z 716.25 and 717.25) are not consistent with the normal isotopic distribution. The above-mentioned mechanism of photoaddition has been reported in one of our recent studies.[30] The photoproducts generated after laser illumination of *m*-THPP have been investigated by MALDI-TOF-MS, indicating the major presence of protonated dihydro dihydroxylated *m*-THPP at m/z 713.25, formed by a photoaddition process. Considering that the difference between protonated *m*-THPC and *m*-THPBC radical is one m/z unit, it is reasonable to assume that protonated dihydro dihydroxylated *m*-THPC is detected at m/z 715.24 and that, correspondingly, the dihydro dihydroxylated *m*-THPBC is detected at m/z 716.25. Spectroscopic studies also tend to confirm this hypothesis. Aggregated *m*-THPBC solution demonstrated a significant phototransformation of *m*-THPBC into *m*-THPC (inset Fig. 2). In contrast with absorption spectroscopy where the signal of *m*-THPC after irradiation increased, the *m*-THPC signal (m/z 681) even decreased after irradiation of aggregated *m*-THPBC solution (Fig. 4). Along with this decrease, the signal at m/z

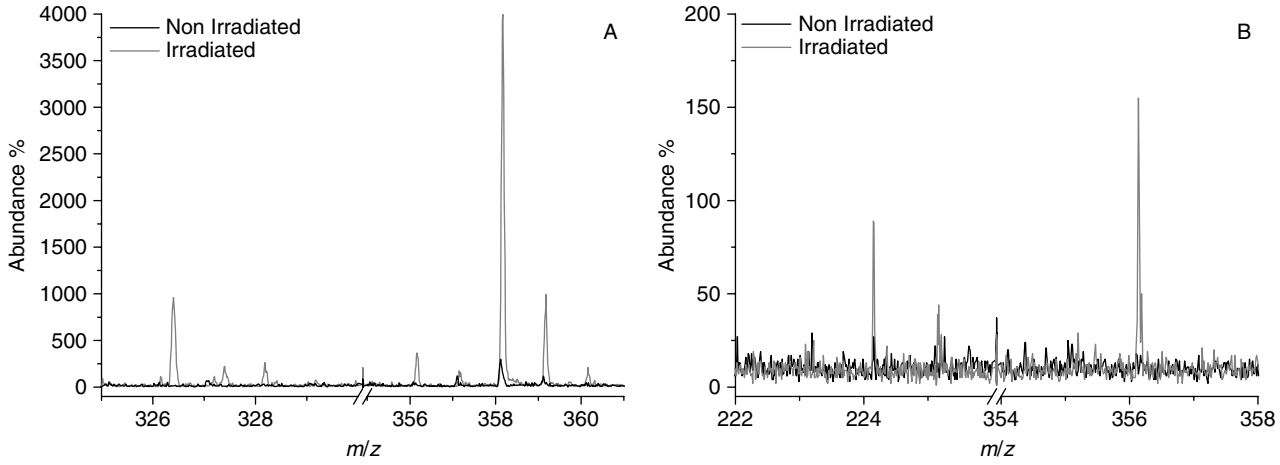

Figure 6. MALDI-TOF-MS spectra of nonirradiated and irradiated with 6 J cm^{-2} *m*-THPBC (10^{-5} M). Mass spectra of incubated *m*-THPBC solution in the *m/z* range 325–361 (A). Mass spectra of freshly prepared *m*-THPBC solution in the *m/z* range 222–358 (B).

715.24 increased after irradiation, reinforcing the hypothesis of photoformation of protonated dihydro dihydroxylated *m*-THPC (*m/z* 715.24). Indeed, absorption maxima of this compound peak at 422 nm and at 652 nm,[12] and therefore could be easily taken for the absorption peaks of *m*-THPC.

Singlet oxygen photogenerated from *m*-THPBC leads to the attack and scission of the porphyrin macrocycle, known as *true photobleaching*, and this is evidenced by the dramatic decrease of the *m*-THPCB absorption bands after the irradiation. The mass spectrometry study enables the detection of small, nonfluorescent photoproducts and nonabsorbing in the visible range, such as those originating from true photobleaching. Figure 6 shows the mass spectra prior to and after irradiation of freshly prepared and incubated HSA–PBS solutions. The photoproducts formed after irradiation of an incubated solution present signals at *m/z* 358.17, 356.18 and 326.4, while the signals of photoproducts formed after the irradiation of a nonincubated solution are detected at *m/z* 356.18 and 224.16. According to the previous study of Bonnett *et al.*,[31] the products at *m/z* 326.4, 356.18 and 358.17 were tentatively described as dipyrin derivatives and the signal at *m/z* 224.16 was tentatively attributed to a dipyrrolic synthon.

CONCLUSION

The present study, conceived as complementary to our previous investigation on *m*-THPBC photobleaching behavior, presents a description of a distinct unfolding of the photobleaching processes in aggregated and monomeric protein-supplemented *m*-THPBC solutions. Dihydroxylated tetraphenylchlorin compounds were detected regardless of the incubation time of the solution, with a much larger amount of dihydroxylated product for incubated solution compared to the nonincubated solution. When *m*-THPBC was subjected to prolonged incubation with proteins, and with the successive irradiation of this solution, the principal photoproduct was found to be dihydro dihydroxylated *m*-THPBC. Irradiation of freshly prepared *m*-THPBC yielded dihydro dihydroxylated *m*-THPC.

Acknowledgements

This work was supported by Alexis Vautrin Cancer Center Research Funds, French Ligue National Contre le Cancer (Comité de Meurthe et Moselle, Comité de Haute-Marne). The gift of *m*-THPBC from Biolitec Pharma Ltd. (Edinburgh, UK) is greatly appreciated. The authors are very grateful to Frédéric Aubriet and Marie-Ange D'Hallewin for their valuable comments and critical reading of the manuscript.

REFERENCES

1. Moan J. Effect of bleaching of porphyrin sensitizers during photodynamic therapy. *Cancer Lett.* 1986; **33**: 45.
2. Bonnett R, Martínez G. Photobleaching of Sensitisers Used in Photodynamic Therapy. *Tetrahedron.* 2001; **57**: 9513.
3. Bonnett R, White RD, Winfield UJ, Berenbaum MC. Hydroporphyrins of the meso-tetra(hydroxyphenyl)porphyrin series as tumour photosensitizers. *Biochem. J.* 1989; **261**: 277.
4. Bonnett R, charlesworth P, Djelal BD, Foley S, McGarvey DJ, Truscott TG. Photophysical properties of 5,10,15,20-tetrakis(m-hydroxyphenyl)porphyrin (m-THPP), 5,10,15,20-tetrakis(m-hydroxyphenyl)chlorin (m-THPC) and 5,10,15,20-tetrakis(m-hydroxyphenyl)bacteriochlorin (m-THPBC): a comparative study. *J. Chem. Soc., Perkin Trans. 2.* 1999; **2**: 325.
5. Engelmann K, Mack MG, Eichler K, Straub R, Zangos S, Vogl TJ. Interstitial photodynamic laser therapy for liver metastases: first results of a clinical phase I-study. *Rofo. Fortschr. Geb. Rontgenstr. Neuen. Bildgeb. Verfahr.* 2003; **175**: 682.
6. Beato B, Yost R, Quirke J. Doubly charged porphyrin ion tandem mass spectrometry: implications for structure elucidation. *Org. Mass. Spectrom.* 1989; **24**: 875.
7. Shaw GJ, Eglinton G, Quirke JME. Structural analysis of tetrapyrroles by hydrogen chemical ionization mass spectrometry. *Anal. Chem.* 1981; **53**: 2014.
8. Miller JM. Fast atom bombardment mass spectrometry of organometallic, coordination, and related compounds. *Mass Spectrom. Rev.* 1990; **9**: 319.
9. Lindsey JS, Chaudhary T, Chait BT. 252Cf plasma desorption mass spectrometry in the synthesis of porphyrin model systems. *Anal. Chem.* 1992; **64**: 2804.
10. Ha J, Hogan JD, Laude J, David A. Competitive ionization of tetraphenylporphyrin in a laser-generated metal ion plasma. *J. Am. Soc., Mass Spectrom.* 1993; **4**: 159.
11. McLuckey SA, Glish GL, Van Berkel GJ. Charge determination of product ions formed from collision-induced dissociation of multiply protonated molecules via ion/molecule reactions. *Anal. Chem.* 1991; **63**: 1971.
12. Kasselouri A, Bourdon O, Demore D, Blais JC, Prognon P, Bourg-Heckly G, Blais J. Fluorescence and mass spectrometry

studies of meta-tetra(hydroxyphenyl)chlorin photoproducts. *Photochem. Photobiol.* 1999; **70**: 275.
13. Angotti M, Maunit B, Muller JF, Bezdetnaya L, Guillemin F. Characterization by matrix-assisted laser desorption/ionization Fourier transform ion cyclotron resonance mass spectrometry of the major photoproducts of temoporfin (m-THPC) and bacteriochlorin (m-THPBC). *J. Mass Spectrom.* 2001; **36**: 825.
14. Bartlett MG, Busch KL, Wells CA, Schey KL. Use of 2-hydroxy-1-naphthoic acid as a matrix for matrix-assisted laser desorption/ionization mass spectrometry of low molecular weight porphyrins and peptides. *J. Mass Spectrom.* 1996; **31**: 275.
15. Green MK, Medforth CJ, Muzzi CM, Nurco DJ, Shea KM, Smith KM, Lebrilla CB. Application of matrix-assisted laser desorption/ionization Fourier transform mass spectrometry to the analysis of planar porphyrins and highly substituted nonplanar porphyrins. *Eur. J. Mass Spectrom.* 1997; **3**: 439.
16. Lassalle HP, Bezdetnaya L, Iani V, Juzeniene A, Guillemin F, Moan J. Photodegradation and phototransformation of 5,10,15,20-tetrakis-(m-hydroxyphenyl)bacteriochlorin (m-THPBC) in solution. *Photochem. Photobiol. Sci.* 2004; **3**: 999.
17. Brown SB, Shillcock M, Jones P. Equilibrium and kinetic studies of the aggregation of porphyrins in aqueous solution. *Biochem. J.* 1976; **153**: 279.
18. Bonnett R, Djelal BD, Nguyen A. Physical and chemical studies related to the development of m-THPC (FOSCAN®) for the photodynamic therapy (PDT) of tumours. *J. Porphyrins Phtalocyanines* 2001; **5**: 652.
19. Aveline BM, Hasan T, Redmond RW. The effects of aggregation, protein binding and cellular incorporation on the photophysical properties of benzoporphyrin derivative monoacid ring A (BPDMA). *J. Photochem. Photobiol. B.* 1995; **30**: 161.
20. Bezdetnaya L, Zeghari N, Belitchenko I, Barberi-Heyob M, Merlin JL, Potapenko A, Guillemin F. Spectroscopic and biological testing of photobleaching of porphyrins in solutions. *Photochem. Photobiol.* 1996; **64**: 382.
21. Belitchenko I, Melnikova V, Bezdetnaya L, Rezzoug H, Merlin JL, Potapenko A, Guillemin F. Characterization of photodegradation of meta-tetra(hydroxyphenyl)chlorin (mTHPC) in solution: biological consequences in human tumor cells. *Photochem. Photobiol.* 1998; **67**: 584.
22. Hadjur C, Lange N, Rebstein J, Monnier P, van den Bergh H, Wagnières G. Spectroscopic studies of photobleaching and photoproduct formation of meta(tetrahydroxyphenyl) chlorin (m-THPC) used in photodynamic therapy. The production of singlet oxygen by m-THPC. *J. Photochem. Photobiol. B.* 1998; **45**: 170.
23. Rotomskis R, Bagdonas S, Streckyte G. Spectroscopic studies of photobleaching and photoproduct formation of porphyrins used in tumour therapy. *J. Photochem. Photobiol. B.* 1996; **33**: 61.
24. Ma LW, Moan J, Grahn MF, Iani V. Comparison of meso-tetrahydroxyphenyl-chlorin and meso-tetrahydroxyphenyl-bacteriochlorin with respect to photobleaching and PCT efficiency in vivo. *Proc. SPIE* 1996; **2924**: 219.
25. Grahn MF, McGuinness A, Benzie R, Boyle R, de Jode ML, Dilkes MG, Abbas B, Williams NS. Intracellular uptake, absorption spectrum and stability of the bacteriochlorin photosensitizer 5,10,15,20-tetrakis (m-hydroxyphenyl)bacteriochlorin (mTHPBC). Comparison with 5,10,15,20-tetrakis(m-hydroxyphenyl)-chlorin (mTHPC). *J. Photochem. Photobiol. B.* 1997; **37**: 261.
26. Jones RM, Wang Q, Lamb JH, Djelal BD, Bonnett R, Lim CK. Identification of photochemical oxidation products of 5,10,15,20-tetra(m-hydroxyphenyl)chlorin by on-line high-performance liquid chromatography-electrospray ionization tandem mass spectrometry. *J Chromatogr., A.* 1996; **722**: 257.
27. Bonnett R. *Chemical Aspects of Photodynamic Therapy*. CRC Press: London, 2000.
28. Spikes JD. Quantum yields and kinetics of the photobleaching of hematoporphyrin, Photofrin II, tetra(4-sulfonatophenyl)-porphine and uroporphyrin. *Photochem. Photobiol.* 1992; **55**: 797.
29. Angotti M, Maunit B, Muller JF, Bezdetnaya L, Guillemin F. Matrix-assisted laser desorption/ionization coupled to Fourier transform ion cyclotron resonance mass spectrometry: a method to characterize temoporpfin photoproducts. *Rapid Commun. Mass Spectrom.* 1999; **13**: 597.
30. Lourette N, Maunit B, Bezdetnaya L, Lassalle HP, Guillemin F, Muller JF. Characterization of photoproducts of m-THPP in aqueous solution. *Photochem. Photobiol.* 2005; in press.
31. Bonnett R, Martinez G. Photobleaching of compounds of the 5,10,15,20-Tetrakis(m-hydroxyphenyl)porphyrin Series (m-THPP, m-THPC, and m-THPBC). *Org. Lett.* 2002; **4**: 2013.

1.3. m-THPC and m-THPBC photobleaching in the presence of different kinds of quenchers

1.3.1. Introduction

In order to contribute to the knowledge of *m*-THPC and *m*-THPBC photobleaching mechanisms, we have investigated the photodegradation of these two sensitisers in a phosphate buffer solution containing 10% foetal calf serum (FCS), which is close to a in vitro biologically relevant environment. Irradiation was performed with laser diodes in the red Q band of the photosensitisers to be consistent with the wavelength used in a clinical situation.
The goal of this study was to define the involvement of molecular oxygen, and reactive oxygen species including singlet oxygen in the photobleaching of *m*-THPC and *m*-THPBC.

1.3.2. Materials and methods

Chemicals: The photosensitizers *m*-THPC and *m*-THPBC were kindly provided by Biolitec Pharma Ltd. (Edinburgh, UK). They were stored in the dark at 4°C as a stock solution in methanol at a concentration of 3 mM. Further dilution were performed in Phosphate Buffer Saline (PBS) supplemented with 10% foetal calf serum (PAN Biotech GmbH, Aidenbach, Germany). The final concentration of *m*-THPC and *m*-THPBC in each solvent was 2 µM. Superoxide dismutase (SOD), Catalase (CAT), Histidine, 1,4-diazabicyclo[2,2,2] octane (DABCO) were purchased from Sigma (Saint Quentin Fallavier, France).
Photoirradiation. Prior to irradiation, *m*-THPC solutions in PBS-FCS were kept 6h in the dark at 37°C, and *m*-THPBC solutions in PBS-FCS were kept 3h in the dark at 37°C. Thereafter different chemicals (SOD, CAT, Histidine and DABCO) were added to the solution or oxygen was removed by nitrogen bubbling in the solution during 30 minutes. Illumination was performed under continuous magnetic stirring by exposing 3 mL of 2 µM photosensitisers solution in a 10 x 10 mm quartz cuvette to light from a laser diode at 739 nm (Ceralas PDT 739, CeramOptec GmbH, Bonn, Germany) for *m*-THPBC and light from a laser diode at 650 nm (F-System, Coherent, Saclay, France). The incident fluence rate was 10 mW cm^{-2} for both irradiation sources and the whole sample was irradiated.
Absorption measurements. Measurements were made in triplicate for each condition. Absorbance spectra were recorded with a Perkin-Elmer Lambda bio spectrophotometer with the same 10 x 10 mm quartz cuvette that was used for irradiation. The *m*-THPBC absorbance decay was recorded between 300 and 800 nm, and the *m*-THPC absorbance decay was

recorded between 300 and 700 nm. Based on the assumption that the *m*-THPBC photoproducts do not absorb at 740 nm, and that the *m*-THPC photoproducts do not absorb at 650 nm, the absorbance at those wavelengths can be used to compute the photobleaching quantum yield.

Photobleaching Quantum Yield Calculation. Quantum Yield of photodegradation (Φ_{Pb}) were calculated as a ratio of the decrease in quantity of sensitiser in a probe (mole) / amount of photons (mole) absorbed by the probe. Φ_{Pb} was calculated as follow (for the detailed calculations see Hadjur *et al.* (Hadjur et al., 1998)):

$$\Phi_{Pb} = \frac{(A_0 - A_1)V_s}{\varepsilon l N_{Ph} \int_0^t \left[1 - 10^{-A_0} \exp(-kt)\right] dt}$$

Where the numerator represents the decrease in quantity of sensitiser, with A_0 and A_t standing for the concentration of photosensitiser prior and after irradiation respectively, and V_s standing for the volume of the sample. The denominator correspond to the amount of photons absorbed by the sensitiser, where *k* is the photodegradation rate constant (in s^{-1}). For bi-exponential decay (m-THPC photobleaching) the first part of the curve was computed. ε stands for the molar extinction coefficient (in Mol^{-1} cm^{-1}) and *l* is the optical pathway (in cm). N_{Ph} the photon flux at the excitation wavelength λ, is equal to $I_0\lambda/N_A hc$ (in mol photons s^{-1}), where I_0 is the incident power (in J s^{-1}). c is the velocity of light, h is Planck's constant and N_A is Avogadro's number.

1.3.3. Results and discussion

-Photobleaching characteristics of m-THPC and m-THPBC

The *m*-THPBC and *m*-THPC were incubated during 3 and 6 hours respectively in PBS-FCS 10% solution in the dark at 37C° before irradiation. This incubation period allows to achieve equilibrium. Figures 3.1. and 3.2. show the kinetic of fluorescence emission spectra of *m*-THPBC and *m*-THPC during dark incubation at 37°C. *m*-THPBC fluorescence reach a plateau after 3 hours incubation, while the *m*-THPC fluorescence plateau is reached at 6 hours. These time points of pre-incubation were selected for photobleaching experiments.

The photobleaching quantum yield of the photosensitizers in PBS-FCS 10% solution are reported in the Table 3.1.. The Φ_{Pb} of *m*-THPBC is 5,76 x 10^{-4}, ±10 fold higher than the yield for most porphyrins like photosensitisers. (e.g. the yield for hematoporphyrin is 4,7 x 10^{-5} (Spikes, 1992)). Furthermore, Φ_{Pb} of m-THPC is 1,53 x 10^{-5}, meaning that *m*-THPBC is almost 38 times more sensitive to light than m-THPC.

The photobleaching kinetics are consistent with a mono-exponential decay for *m*-THPBC whether they better fit a bi-exponential decay for *m*-THPC (Figures 3.3. and 3.4.). This discrepancy in the photobleaching decay could be attributed to different aggregation state in the solutions, as has been previously demonstrated (see § IV.1.). Incubation of *m*-THPBC will result in a full monomerisation of the dye leading to a mono-exponential decay. At the same time *m*-THPC remains a mixture of aggregates and monomers even after reaching the equilibrium (fluorescence plateau), thus resulting in a bi-exponential decay. Different photobleaching kinetics could also be attributed to different distribution or re-distribution of *m*-THPC and *m*-THPBC among the constituting elements of FCS (proteins, apoproteins, HDL, LDL), and therefore have different bleaching kinetics due to the presence of oxidizable substrates or to photo-relocalisation as we already described in the chapter II.4.2.

Absorbance spectra evidenced photoproducts formation upon light irradiation (data not shown). Similar to several studies (Belitchenko et al., 1998; Hadjur et al., 1998) a 320 nm

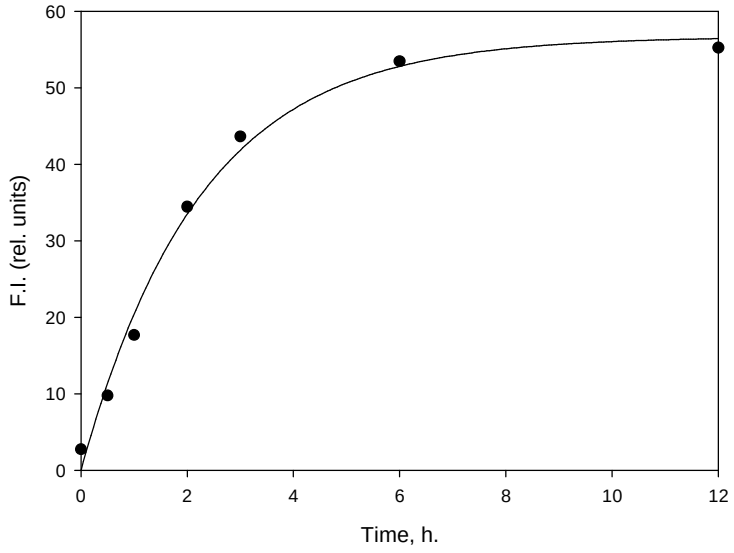

Figure 3.1. Fluorescence emission kinetic at 655 nm (λ_{ex} = 422nm) of m-THPC in PBS-FCS 10%; T = 37°C

absorbing product was detected following the *m*-THPC irradiation, while *m*-THPBC

irradiation exhibited the formation of m-THPC. The presence of the used Type I or Type II quenchers did not modify the phototransformation rate of the photosensitisers (data not shown).

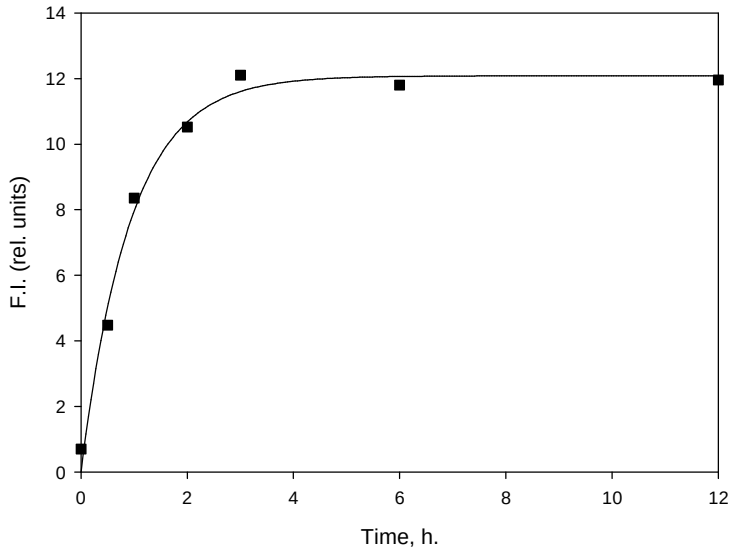

Figure 3.2. Fluorescence emission kinetic at 743 nm (λ_{ex} = 378 nm) of m-THPBC in PBS-FCS 10%; T = 37°C

-Effect of antioxidant enzymes on photobleaching

Several studies demonstrated the production of free radicals in addition to singlet oxygen upon irradiation of some sensitisers (Hadjur et al., 1994; Hadjur et al., 1997a; Hadjur et al., 1997b). In order to test the contribution of free radicals in photobleaching of *m*-THPC and *m*-THPBC, we examined the influence of antioxidant enzymes such as superoxide dismutase (SOD) and catalase (CAT). SOD is known to detoxify the superoxide radical anion ($O_2^{\cdot -}$) and form hydrogen peroxide (H_2O_2) and CAT protects against H_2O_2 (see §2.3.1. for detailed reaction mechanisms).

Neither *m*-THPC nor *m*-THPBC photobleaching quantum yield are changed by adding SOD or CAT to the solutions. Table 3.1. presents the quantum yield of photobleaching (Φ_{Pb}) of *m*-THPC and *m*-THPBC in different aqueous solution supplemented with FCS (10%). SOD and CAT were added to the concentration of 40 µg mL^{-1} and 45 µg mL^{-1} respectively. Figures 3.3. and 3.4. demonstrate that the two tested enzymes did not change the photobleaching rates and

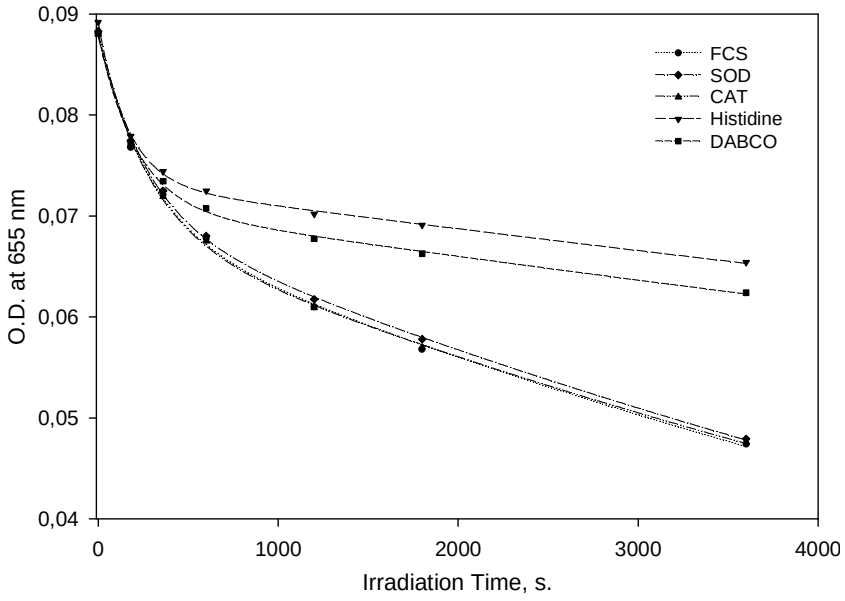

Figure 3.3. Effect of antioxidant enzyme and singlet oxygen quenchers on the photobleaching of m-THPC in PBS solution supplemented with 10% FCS. Histidine and DABCO were added to a final concentration of 1mM, SOD concentration was 40 µg mL^{-1}, and CAT concentration was 45 µg mL^{-1}.

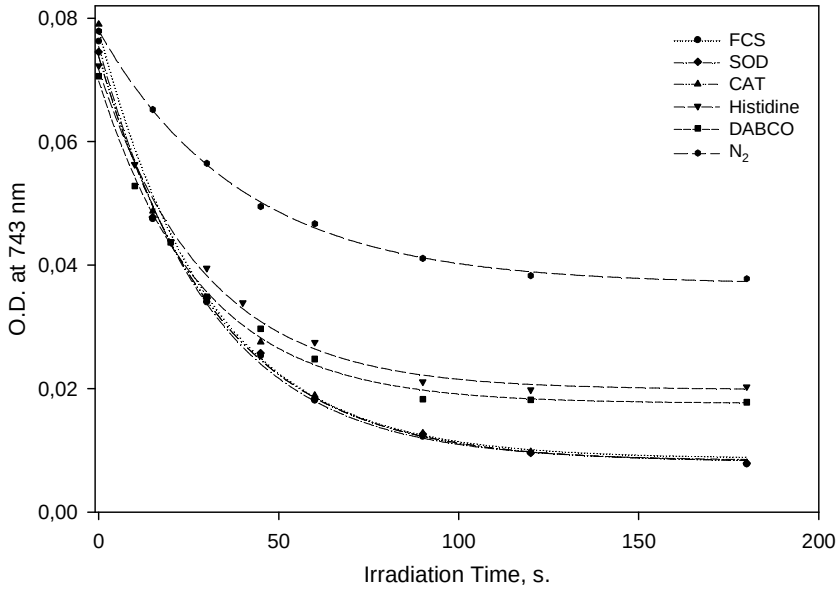

Figure 3.4. Effect of N_2, antioxidant enzyme and singlet oxygen quenchers on the photobleaching of m-THPBC in PBS solution supplemented with 10% FCS. Histidine and DABCO were added to a final concentration of 10mM, SOD concentration was 40 µg mL^{-1}, and CAT concentration was 45 µg mL^{-1}. Bubbling with nitrogen runs during 30 min.

the kinetic, and as a consequence Φ_{Pb} in the presence of SOD and CAT is not significantly different than the control Φ_{Pb} (less than ± 5%). These results point out that free radicals are not involved in the photobleaching of *m*-THPC and the *m*-THPBC in PBS-FCS solutions. The results concerning *m*-THPC are in total agreement with those of Hadjur and co-workers (Hadjur et al., 1998) who demonstrated that SOD and CAT did not change the Φ_{Pb} in identical conditions. Bonnett *et al.* (Bonnett et al., 1999b) also showed that these enzymes have no effect on the photobleaching yield of the *m*-THPC and the *m*-THPBC in methanol or in methanol-water (3:2) solutions.

Table 3.1. Photobleaching quantum yield (Φ_{Pb}) of *m*-THPC and *m*-THPBC in PBS-FCS (10%) solutions, the numbers in the brackets represent the variation of Φ_{Pb}.

Conditions	Φ_{Pb}			
	m-THPBC		*m*-THPC	
Control	$5{,}760 \times 10^{-4}$		$1{,}537 \times 10^{-5}$	
+SOD (40 µg mL^{-1})	$5{,}655 \times 10^{-4}$	(-1,8%)	$1{,}509 \times 10^{-5}$	(-1,8%)
+CAT (45 µg mL^{-1})	$5{,}967 \times 10^{-4}$	(+3,6%)	$1{,}516 \times 10^{-5}$	(-1,4%)
+Histidine*	$4{,}327 \times 10^{-4}$	(-25%)	$8{,}658 \times 10^{-6}$	(-44%)
+DABCO*	$4{,}373 \times 10^{-4}$	(-24%)	$9{,}473 \times 10^{-6}$	(-39%)
+N_2	$3{,}556 \times 10^{-4}$	(-38%)	(-90%) (Hadjur et al., 1998)	

*Concentration of Histidine and DABCO was 1 mM in m-THPC solution and 10 mM in *m*-THPBC solution

-Effect of singlet oxygen scavengers on photobleaching

The singlet oxygen quenchers used in this study are DABCO and Histidine (for detailed mechanisms see § 2.3.2.). As seen in Table 3.1. and in Figures 3.3. and 3.4. the addition of these chemicals significantly decrease the photobleaching of *m*-THPC and *m*-THPBC. The Photobleaching quantum yield decrease of m-THPC (44%) obtained using 1mM Histidine is in agreement with previous studies demonstrating similar decrease (Table 4.3., § II.4.) ranging between 35 and 46% (Hadjur et al., 1998; Spikes, 1992). Bleaching of *m*-THPC with DABCO also undergoes an important decrease (39%) and is consistent with previous studies reported in the literature (Hadjur et al., 1998; Spikes, 1992).

The *m*-THPBC photobleaching quantum yield also undergoes a decrease of 24 and 25% when adding histidine and DABCO, but to a less extent as compared to *m*-THPC or other photosensitisers cited in the literature. One hypothesis for the weak efficacy of these quenchers (despite the higher concentration used) on *m*-THPBC photobleaching as compared to *m*-THPC photobleaching might be that the *m*-THPBC molecule is oxidized more easily, even with a very low amount of singlet oxygen. This hypothesis is reinforced by the observation that by bubbling nitrogen through the sample, the bleaching rate decrease is only 38% compared to 90% for *m*-THPC (Table 3.1.) indicating that the small amount of O_2 remaining in the sample (2 µM instead of 22 µM) is enough to provoke an important photobleaching.

1.3.4. Conclusions

These results clearly evidence that photobleaching of both *m*-THPC and *m*-THPBC is mainly mediated via Type II reaction involving singlet oxygen. The results using Type I scavengers do not support the participation of free radicals in the bleaching of those sensitisers in PBS-FCS solutions.

IV.2. In vitro study of several photobiological properties of m-THPC and m-THPBC.

2.1. Introduction

The objective of this study was to examine the photobiological properties of *m*-THPBC in an *in vitro* model and compare them to the known *in vitro* properties of the *m*-THPC. These two sensitisers have similar structures and very close photophysical properties (see Chap.II, Fig. 3.1. and Table 3.1.), however their photobiological properties have been reported to be very different. The aim of this study was to better understand the reasons for this apparent discrepancy in PDT efficiency of these two photosensitisers.

2.2. Materials and methods

Chemicals. The photosensitisers *m*-THPC and *m*-THPBC were kindly provided by Biolitec Pharma Ltd. (Edinburgh, UK). Stock solutions were made in methanol at a concentration of 3 mM, and the molecules were kept at 4 °C in the dark. Further dilution was performed in RPMI 1640 (Gibco, Cergy Pontoise, France) supplemented with 2% heat inactivated FCS (PAN Biotech GmbH, Aidenbach, Germany). The final photosensitiser concentration was 1.5 µM.

Cell culture. WiDr Human colorectal adenocarcinoma cell line was used. The cells were maintained in RPMI 1640 supplemented with 10% heat inactivated FCS, penicillin (10000 UI) and streptomycin (10000 UI). Cells were kept at 37C° in a 5% CO_2 humidified atmosphere, trypsinised and reseeded to fresh medium every 7 days. For photobleaching experiments, cell suspension (5 x 10^4 cells mL^{-1}) were plated in 35 mm cell dishes (Corning, Avon, France). The cells were allowed to attach to the dishes and grow for 72 hours before being tested. WiDr cells were incubated during 24 h with *m*-THPC or *m*-THPBC. Two concentrations were used, 0.75 µM (0.5 $\mu g.mL^{-1}$) or 1.5 µM (1 $\mu g.mL^{-1}$). For photocytotoxicity assay the same protocol was used except for the cell concentration (500 cells per dishes).

Light sources. A laser diode emitting at 650 nm (F-System, Coherent, Saclay, France) for *m*-THPC irradiation and light from a laser diode at 739 nm (Ceralas PDT 739, CeramOptec GmbH, Bonn, Germany) for *m*-THPBC irradiation were used. The same frontal diffuser was

used and the incident fluence rate was 10 mW cm^{-2} for both irradiation sources and the whole dishes was irradiated.

Absorption spectra. The absorption spectra in methanol and in the cells were recorded using a Perkin Elmer Lambda 15 spectrophotometer equipped with an integrating sphere. The cell suspension or the methanol solution were introduced in a 10 x 10 mm quartz cuvette, the absorption was recorded from 330 nm to 800 nm.

Photobleaching experiments. Irradiation of the whole 35 mm cell culture dishes was performed and cellular fluorescence emission spectra were recorded using a Perkin Elmer LS 50 B spectrofluorimeter. Excitation wavelength was set at 378 nm and fluorescence was recorded between 600 and 800 nm for the *m*-THPBC photobleaching experiments; excitation was set at 422 nm and emission was recorded between 600 and 700 nm for the *m*-THPC experiments.

Cell survival. WiDr survival curves were determined by colony formation assay. 500 cells were inoculated in 35 mm cell dishes containing 2.5 ml of medium RPMI 1640 10% FCS. After 3 days, cells were incubated with 1.5µM of photosensitizer for 24 hours in the dark at 37 °C. Then the dye-containing medium was replaced by the fresh dye-free medium and the cells were irradiated. The numbers of surviving and colony-forming cells were scored 11 days after incubation.

Laser Confocal Scanning Microscope (LCSM). The cells double stained with *m*-THPC and organelle probes were examined with a confocal laser scanning microscope (SP-2 AOBS LCSM, Leica microsystem, Germany) equipped with a x 63, numerical aperture 1.3 oil immersion objective (Leica, Germany). A pinhole of 60.64 µm was used and each image recorded contained 512 x 512 pixels. An Ar/ArKr laser was used as excitation light at 488 nm for all organelle probes and He/Ne laser at 633 nm for *m*-THPC . Fluorescence of the organelles probes was detected on channel 1 with a 505–550nm band pass (BP) emission filter. Channel 2 was used to detect the red fluorescence of *m*-THPC with a 630 nm long pass emission filter. The fluorescence images were displayed in green and red 'false' colour output and electronically combined to visualise colocalisation in yellow. Controls (cells stained only with *m*-THPC or organelle probes) were conducted in parallel to optimise the staining protocol and the detecting parameters of LCSM.

Cells were incubated with 1.5 µM *m*-THPC for 24 h, and washed with phosphate-buffered saline (PBS) and incubated with a series of fluorescent probes to determine the identity of subcellular organelles targeted by *m*-THPC. For lysosomes identification, cells were incubated 30 min with 250 nM Lysotracker green. Mitotracker green FM was used at a final

concentration of 0.5 µM for 30 min to identify mitochondria. To visualise the Golgi apparatus, cells were labelled with 5 µM BODIPY FL C_5-ceramide (BPC) for 30 min. The ER was labeled with the lipophilic, cationic $DiOC_6$ dye applied for 1 min at a final concentration of 2.5 µg ml^{-1}. This marker, used in the concentration range 1–10 µg ml^{-1}, was reported to be highly specific for ER and, compared to other possible candidates, is the brightest with the slowest bleaching rate. At the end of the double staining, the labelling solution was removed by gentle rinsing with RPMI 1640 containing 25mM Hepes, except for BPC were the cells were washed with HBSS/HEPES buffer and observed by confocal fluorescence microscopy. All the fluorescent probes were purchased from Molecular Probes-Europe (Leiden, The Netherlands).

Epifluorescence Microscope. Intra-cellular localisation of *m*-THPBC was observed using a epifluorescence microscope (AX 70 PROVIS, Olympus, France) equipped with a 100 W mercury vapour lamp. Fluorescence images were recorded using a x40 oil immersion plan apochromatic objective, except for the images of mitochondrial staining. The same fluorescent probes were used to co-localise *m*-THPBC in the cells, with the same protocol except for lysotracker were the incubation concentration was 1µM and the $DiOC_6$ were the incubation time was shortened to 30 s. The filter set used for *m*-THPBC detection consisted of a 330-380 nm BP excitation filter associated with a 570 dichroic mirror and a 590 nm long pass filter. For all the fluorescent probes the same filters were used, the settings were a 460-490 nm BP filter for excitation, a 505 dichroic mirror and a 510-550 nm BP filter for emission.

2.3. Results and discussion

Spectroscopic study

Normalised absorbance spectra of *m*-THPC and *m*-THPBC in both methanol and intra-cellular (WiDr cells) solution are displayed in the figure 4.1. *m*-THPC in MeOH is characterised by 5 absorption bands. The Soret band is at 415 nm, and 4 Q bands at 517.5 nm, 543.5 nm, 596 nm and 649.5 nm respectively (Table 4.1.), and the half height bandwidths of the Q band 1 ($\Delta\upsilon$) is equal to 307.82 cm^{-1}. The solution of *m*-THPBC in MeOH has 3 absorption bands, the Soret band at 372.5 nm and the 2 Q bands at 516 nm and 734 nm (Table 4.2.). The $\Delta\upsilon$ is 252.21 cm^{-1}. The intra-cellular spectra for both sensitisers are slightly red shifted and the $\Delta\upsilon$ are almost the same in MeOH and in cells. Therefore we can conclude that *m*-THPC and *m*-THPBC are almost in the same aggregation state in MeOH and in the cells, namely under

monomeric form. This is in partial agreement with the observation of Grahn *et al*. (Grahn et al., 1997), who found that 60 h after incubation in cells as opposed to 24 h in our study, *m*-THPC had absorption spectra very similar to those in methanol solution, while intra-cellular *m*-THPBC spectra were found to be different. For *m*-THPBC they found 2 maxima, at 740 nm and 725 nm. They hypothesized that the photosensitizer was in a different aggregation state or intracellular location. We also observed this band (725 nm) in MeOH solutions stored for several days at room temperature and it seems likely that this peak corresponds to a dark oxidation product, rather than aggregated forms of photosensitiser.

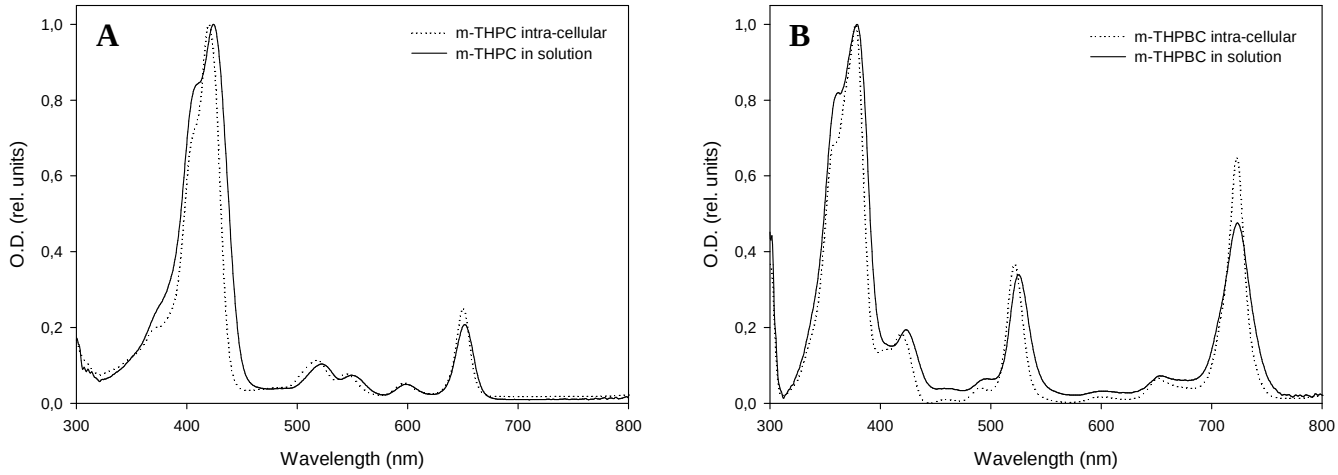

Figure 4.1. : Ground state absorption spectra of *m*-THPC (A) and *m*-THPBC (B), in MeOH (1.45 µM) or loaded in WiDr cells (24 h incubation, 1.45 µM)

Table 4.1. : Absorbance spectra characteristics of *m*-THPC in methanol solution and in WiDr cells.

	m-THPC					
	λ_{soret}/nm	λ_{Q4}/nm	λ_{Q3}/nm	λ_{Q2}/nm	λ_{Q1}/nm	$\Delta\nu$ /cm^{-1}
Methanol	415	517,5	543,5	596	649,5	307,82
Intra-cellular	419	516	541,5	596,5	650	333,21

Table 4.2. : Absorbance spectra characteristics of *m*-THPBC in methanol solution and in WiDr cells.

	m-THPBC			
	λ_{soret}/nm	λ_{Q2}/nm	λ_{Q1}/nm	$\Delta\nu$ /cm^{-1}
Methanol	372,5	516	734	252,21
Intra-cellular	377	520	740	264,99

Photobleaching

During light exposure the fluorescence of *m*-THPC and *m*-THPBC in the cells decayed, the decay rates being 3 to 5 times faster for *m*-THPBC than for *m*-THPC (Table 4.3.). This difference is smaller than the previous result of Rovers *et al.* (Rovers et al., 2000b), reporting a 7 fold greater rate of bleaching for *m*-THPBC. Unfortunately they did not precise the cell line neither the concentration of photosensitiser used. *m*-THPC fluorescence decay can be decomposed in two exponential curves as demonstrated in the figure 4.2., while *m*-THPBC fluorescence decay better fits a mono-exponential decay (Fig. 4.3.). This could be indicative of a different sub-cellular localization of the photosensitiser, or different environment, for example bound or unbound to proteins. Such possibility was proposed earlier for ALA-PpIX by Moan *et al.* (Moan et al., 1997).

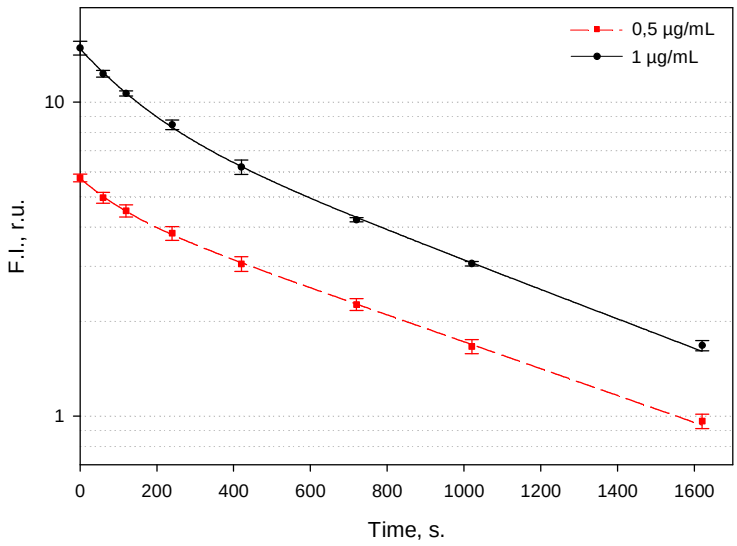

Figure 4.2. : Decay of the fluorescence of *m*-THPC in WiDr cells as a function of the irradiation time. Cells were loaded during 24 hours in the dark with either 0.75 µM (0.5 µg/mL) or 1.45 µM (1 µg/mL)

The two different concentrations of photosensitisers used give rise to different fluorescence levels in the cells, in all probability the concentration of the photosensitisers in the cells incubated with a 1.45 µM solution is higher than the concentration of sensitiser in the cells incubated with 0.75 µM. Table 4.3. presents the photobleaching rates for two different photosensitisers concentrations. *m*-THPC photobleaching rates are dependent on the initial concentration of the dye; the higher the initial concentration, the higher the photobleaching rate. While *m*-THPBC photobleaching is independent of the initial concentration of the sensitiser, indicating that photoproducts from one molecule of *m*-THPBC cannot cause the decay of a neighbouring molecule of *m*-THPBC. This is a first order decay kinetic. Thus, despite the weak difference in their structures (one double bound is reduced for *m*-THPBC) we can observe a large disparity in their photobleaching.

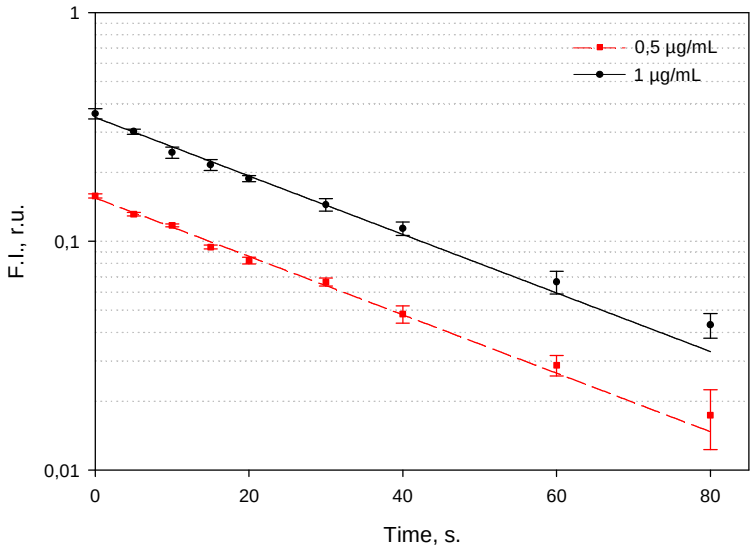

Figure 4.3. : Decay of the fluorescence of *m*-THPBC in WiDr cells as a function of the irradiation time. Cells were loaded during 24 hours in the dark with either 0.75 µM (0.5 µg/mL) or 1.45 µM (1 µg/mL)

The very different photobleaching properties of these 2 photosensitisers, especially single exponential versus bi-exponential and first order process versus non first order kinetic, might be indicative of different aggregation state and sub-cellular localisation (Rück et al., 1990; Strauss et al., 1998) or re-localisation pattern (Moan et al., 1997), or different binding properties.

Phototoxicity

Photocytotoxicity of both photosensitisers has been investigated with the same photosensitiser concentration (1.45 µM), the same fluence rate (10 mW cm^{-2}) and the same incubation time (24 hours).

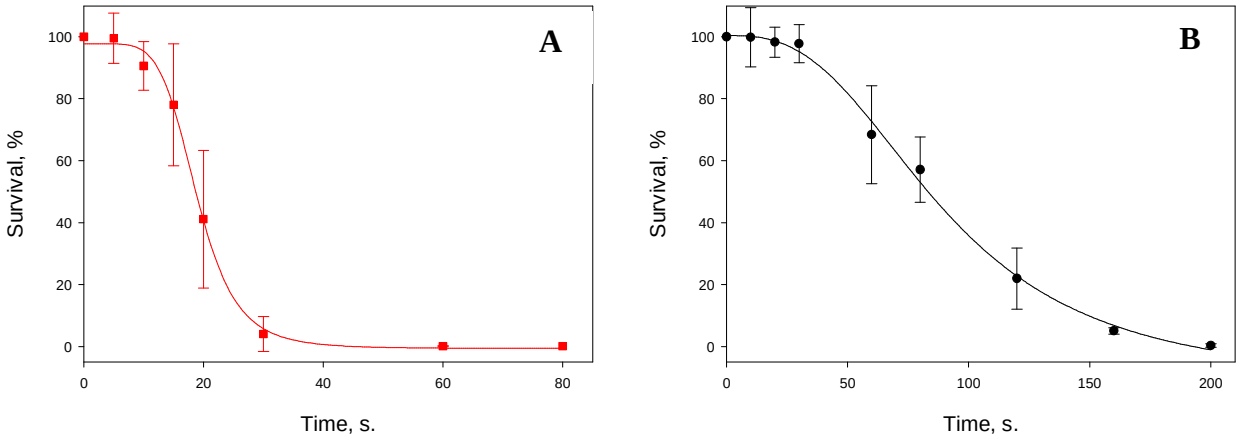

Figure 4.4. : Photocytotoxicity of m-THPC (A) and m-THPBC (B) on Widr cells. The cells were incubated with 1.45 µM of photosensitiser for 24 hours, the fluence rate was 10 mW cm^{-2}.

The photocytotoxicity curves obtained with colony forming assays are presented in figure 4.4. The LD_{50} (Light Dose required to kill 50% of the cells) are 0.17 J cm^{-2} for the *m*-THPC and 0.7 J cm^{-2} for *m*-THPBC. In other words the light dose required to kill 50% of the cells is 4 time higher for *m*-THPBC than for *m*-THPC.

Table 4.3. : Photobleaching rate constants (k/s^{-1}) of *m*-THPC and *m*-THPBC in WiDr cells, derived from fluorescence measurements (photobleaching rate constants from the second parts of the curves are shown in parentheses)

	k/s^{-1}	
	0,75 µM	1,5 µM
m-THPC	$8,7 \times 10^{-3}$ ($1,0 \times 10^{-3}$)	$6,4 \times 10^{-3}$ ($1,1 \times 10^{-3}$)
m-THPBC	$2,94 \times 10^{-2}$	$2,95 \times 10^{-2}$

Photoinactivation yield

Quantum yield of photoinactivation for each photosensitiser can be calculated by adapting the formula of Berg *et al.* (Berg and Moan, 1998), Φ_{in} is equal to (1):

$$\Phi_{in} = \frac{\text{number of cells photoinactivated } \left(N_{cells}\right)}{\text{number of photons absorbed by the chromophore } \left(I_{abs}\right)} \qquad (1)$$

By taking into account the photobleaching, the number of absorbed photons I_{abs} can be defined as equation (2):

$$I_{abs}(t) = (1\text{-}T)_{\lambda_1} \times I_{0\lambda_1} \times t = I_0 \int_0^t \left(1-10^{-D}\right) dt \qquad (2)$$

Where (1-T) is the percentage of absorbed light at the wavelength λ_1 and I_0 is the incident light irradiance at λ_1 and t the irradiation time in second.

Considering (3) and (4) :

$1-T = \left(1-10^{-D}\right)$ (3) , and $1-10^{-D} = 2.3D$ (4) for $D \leq 0.02$

The optical density D can be defined as (5):

$$D = \varepsilon \times c_0 \times e^{-kt} \qquad (5)$$

Therefore I_{abs} is equal to:

$$I_{abs}(t) = I_0 \varepsilon c_0 2.3 \int_0^t \left(e^{-kt}\right) dt$$

$$I_{abs}(t) = I_0 \varepsilon c_0 2.3 \left(-\frac{1}{k}\right) e^{-kt}$$

Knowing that *m*-THPC initial concentration is 1.5 times higher than *m*-THPBC concentration and using our previous photobleaching (Table 4.3.) and photocytotoxicity (Fig.4.4.) results we are able to compute the ratio of the relative photoinactivation yield of the photosensitisers to the LD_{50} (N_{cells} = 50%).

At the LD_{50} :

$$\frac{\Phi_{in,rel(Foscan)}}{\Phi_{in,rel(Bacteriochlorin)}} = \frac{I_{abs(Bacteriochlorin)}}{I_{abs(Foscan)}} = 6.2$$

This signify that in order to inactivate the same fraction of cells and in respect to the photobleaching, the *m*-THPC needs to absorb 6.2 times less photons than *m*-THPBC.

Fluorescence Microscopy

Considering that the intra-cellular localisation of the photosensitiser can influence the photobleaching and the phototoxicity outcome, we have been interested in the sub-cellular localisation of *m*-THPC and *m*-THPBC. The study was performed with the same incubation time (24 h) we used for the photobleaching and the photocytotoxicity experiments.

Intra-cellular localisation of the two photosensitisers was performed by using confocal microscopy for *m*-THPC and epifluorescence microscopy for *m*-THPBC, the confocal microscope was equipped with a non removable cut-off filter at 700 nm (I.R. filter), therefore localisation experiments of *m*-THPBC was not possible with confocal microscope (*m*-THPBC emission wavelength is at 740 nm).

Confocal fluorescence images of the double stained WiDr cells with *m*-THPC and the organelle markers are displayed in the Figures 4.5. to 4.8. For each figure, the upper row corresponds to the image of *m*-THPC in red and the organelle probe in green, the lower row displays the overlapped images and the microspectrofluorimetric topographic profile of a selected area (green line on the overlapped picture).

After 24 hours of incubation *m*-THPC presents a cytoplasmic distribution without distribution in the nucleus. Co-staining with organelle probes was carried out in order to determine the sub-cellular localisation of the photosensitiser. Mitotracker green (λ_{ex}= 490 nm; λ_{em}= 516 nm) was used to stain the mitochondria (Fig. 4.5.) and the images and the spectrofluorimetric profile do not favour *m*-THPC accumulation in the mitochondria. To assess the localisation of *m*-THPC in the Golgi apparatus cells were loaded with BPC (λ_{ex}= 505 nm; λ_{em}= 511 nm) (Fig. 4.6.), the co-localisation pattern of both markers indicates that *m*-THPC does not accumulate in the Golgi apparatus. Lysosomal localisation was assessed with lysotracker green (λ_{ex}= 504 nm; λ_{em}= 511 nm) and figure 4.7. points out that the staining pattern of

lysotracker and *m*-THPC partially overlap suggesting a slight co-localisation of *m*-THPC in lysosomes. Finally, we have used DiOC6 (λ_{ex}= 484 nm; λ_{em}= 501 nm) to stain the ER (Fig. 4.8.), and a clear overlapping of the spectra underlines a co-localisation of *m*-THPC in the ER. *m*-THPBC was distributed in compartments in the cytoplasm outside the nucleus. We have used the same 4 organelles probes as in the *m*-THPC study. The results are shown in the Figures 4.9. to 4.12. The figures are presented in the same way as *m*-THPC except for the microspectrofluorimetric profile which can not be obtained with a conventional epifluorescence microscope. The intra-cellular co-localisation profile of *m*-THPBC seems to be rather different compared to *m*-THPC. The *m*-THPBC has a weak localisation in the ER (Fig. 4.9.), whereas *m*-THPC has a strong distribution in the latter. Also *m*-THPBC was observed to localise slightly in the Golgi apparatus and the lysosomes (Fig. 4.10. and Fig. 4.11.). The unexpected results was a rather good accumulation of *m*-THPBC in the mitochondria, while *m*-THPC did not outline any localisation in the mitochondria (Fig. 4.12.). This different localisation pattern between *m*-THPC and *m*-THPBC is an important factor that could influence the photobleaching kinetics and the phototoxicity of the dyes, in so far as mitochondria are a key element in the cell death mechanism.

The *in vitro* localisation of the *m*-THPC has long be a subject of discussion. Several studies from our laboratory underline a ER and Golgi localisation in MCF-7 cells with 3 hours of incubation time (Teiten et al., 2003), and ER and mitochondrial accumulation with HT 29 cells, also after 3 hours of incubation (Melnikova et al., 1999a). Some other publications report lysosomal localisation (Colo 201 cells, 20 hours of incubation) (Leung et al., 2002). A recent study of our laboratory demonstrates a relocalisation of *m*-THPC during incubation. In the early time of incubation (3 hours) the photosensitiser is distributed in most of the organelles (ER, mitochondria and Golgi) except the lysosomes. During the incubation period from 3 to 24 hours (3-6-9-12-24 hours) *m*-THPC gradually relocalises from other organelles and accumulates mainly in the ER. These findings together with the results reported in the literature clearly demonstrate that the photosensitiser localisation is highly dependent on the incubation time and the cell lines.

To our knowledge no reports have been made on the sub-cellular localisation of *m*-THPBC. Considering the weak difference in the structure of the two molecules it could appear unusual to find a different localisation pattern, but knowing that the redistribution of *m*-THPBC among the proteins in solution is longer than for *m*-THPC (Sasnouski S., personal communication), it is possible to imagine a different endocytosis pathway and redistribution kinetic along the organelles, and eventually a different sub-cellular distribution of those two

photosensitisers. Nevertheless, it appears essential to carry out *m*-THPBC co-localisation experiments with a laser scanning confocal microscope to confirm the results observed by epifluorescence microscope.

2.4. Conclusions

As we have shown in the absorption studies in MeOH and in vitro, *m*-THPBC and *m*-THPC in WiDr cells are both under monomeric forms. Nevertheless their photobleaching kinetics are very different. *m*-THPBC follows a first order, mono-exponential decay while *m*-THPC follows a bi-exponential non-first order decay. The photobleaching rates have been shown to be 3 to 5 times faster for *m*-THPBC and the photocytotoxicity experiments reveal a 4 times higher toxicity for *m*-THPC than for *m*-THPBC. Knowing the photobleaching and photocytotoxicity of both photosensitisers we have been able to compute the photoinactivation yield ratio. This value represent the photocytotoxicity of both photosensitisers by taking into account their respective photobleaching, therefore it gives a good estimation of the absolute phototoxicity of the molecules. This calculation reveals that *m*-THPC is 6.2 times more photoactive than *m*-THPBC. Therefore we have been interested in the intra-cellular localisation pattern of the photosensitisers to explain the different observed photobleaching, phototoxicity and photoinactivation of the two molecules.

The intracellular localisation pattern after 24 h incubation demonstrate an accumulation of *m*-THPC in the ER whereas *m*-THPBC mainly localises in the mitochondria. Therefore it seems that damaging the ER does not have the same outcome as damaging the mitochondria.

Taken as a whole the results presented in this chapter demonstrate a good photocytotoxicity for *m*-THPBC, and a fast first order photobleaching. Thus, these observations are particularly attractive in terms of therapeutic ratio and selectivity of the treatment.

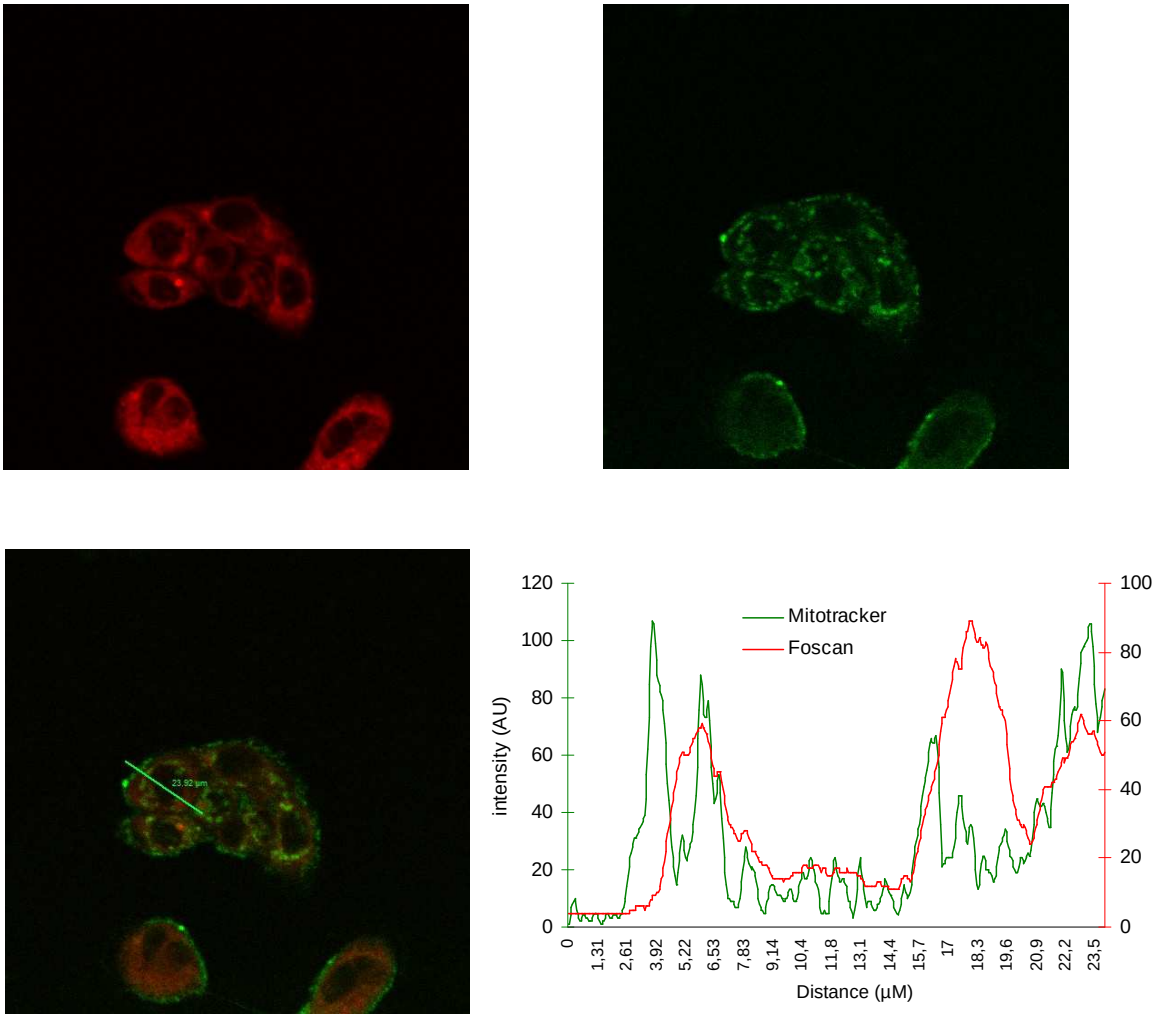

Figure 4.5. : Subcellular localisation of *m*-THPC in WiDr cells (1.45µM, 24 hours incubation). Mitochondria was stained with mitotracker green (0.5 µM).

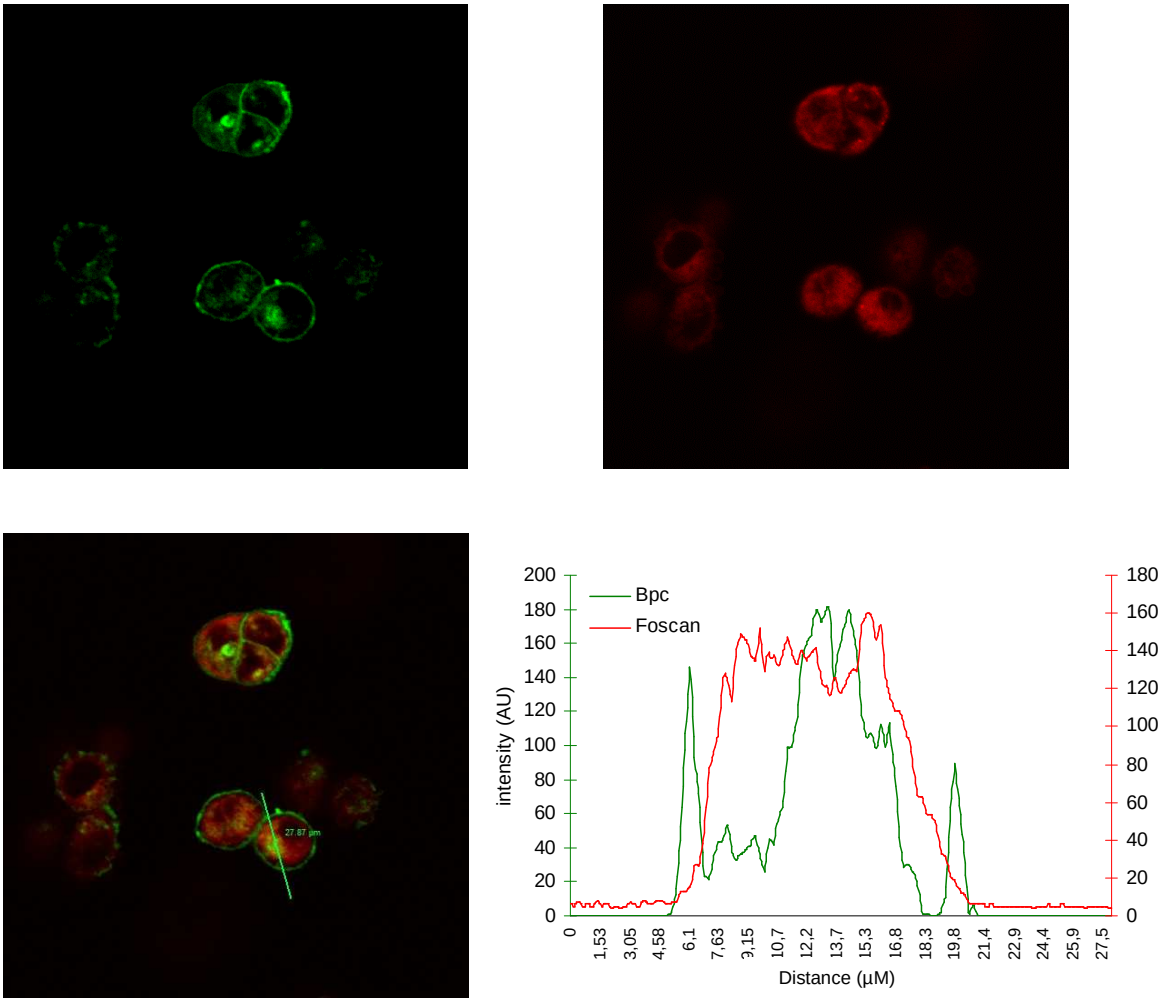

Figure 4.6. : Subcellular localisation of *m*-THPC in WiDr cells (1.45µM, 24 hours incubation). Golgi was stained with BPC (5µM).

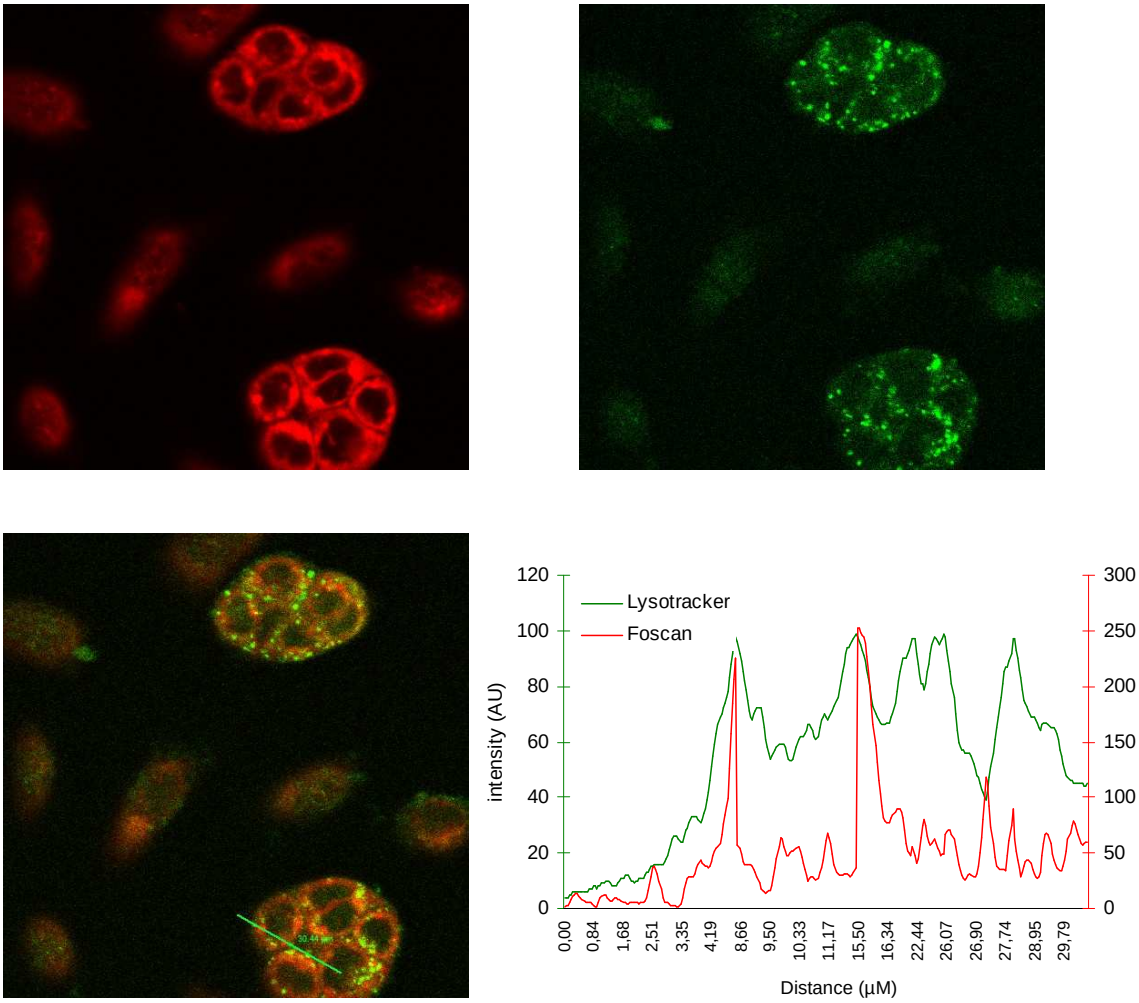

Figure 4.7. : Subcellular localisation of *m*-THPC in WiDr cells (1.45µM, 24 hours incubation). Lysosome was stained with lysotracker green (250 nM).

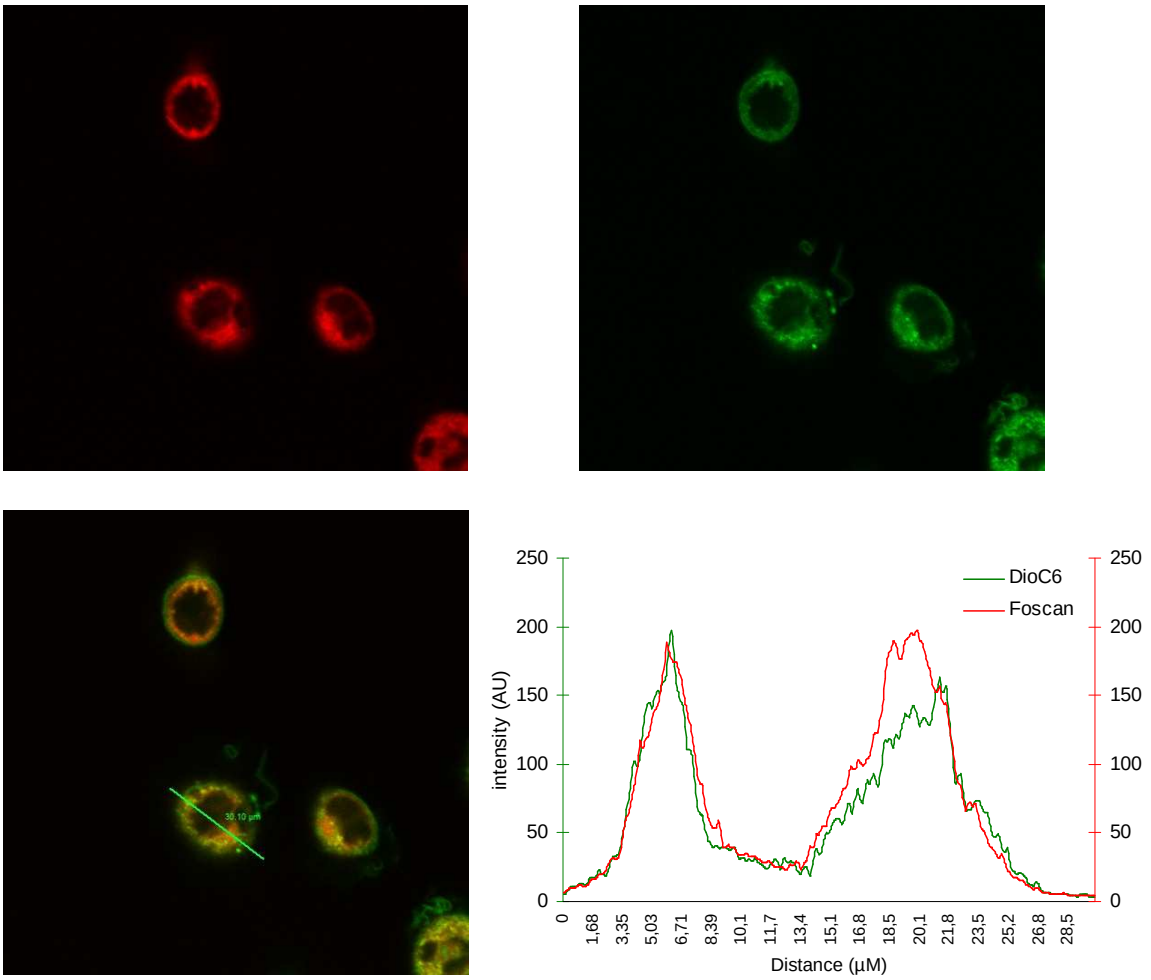

Figure 4.8. : Subcellular localisation of *m*-THPC in WiDr cells (1.45µM, 24 hours incubation). ER was stained with $DiOC_6$ (2.5 µg mL^{-1}).

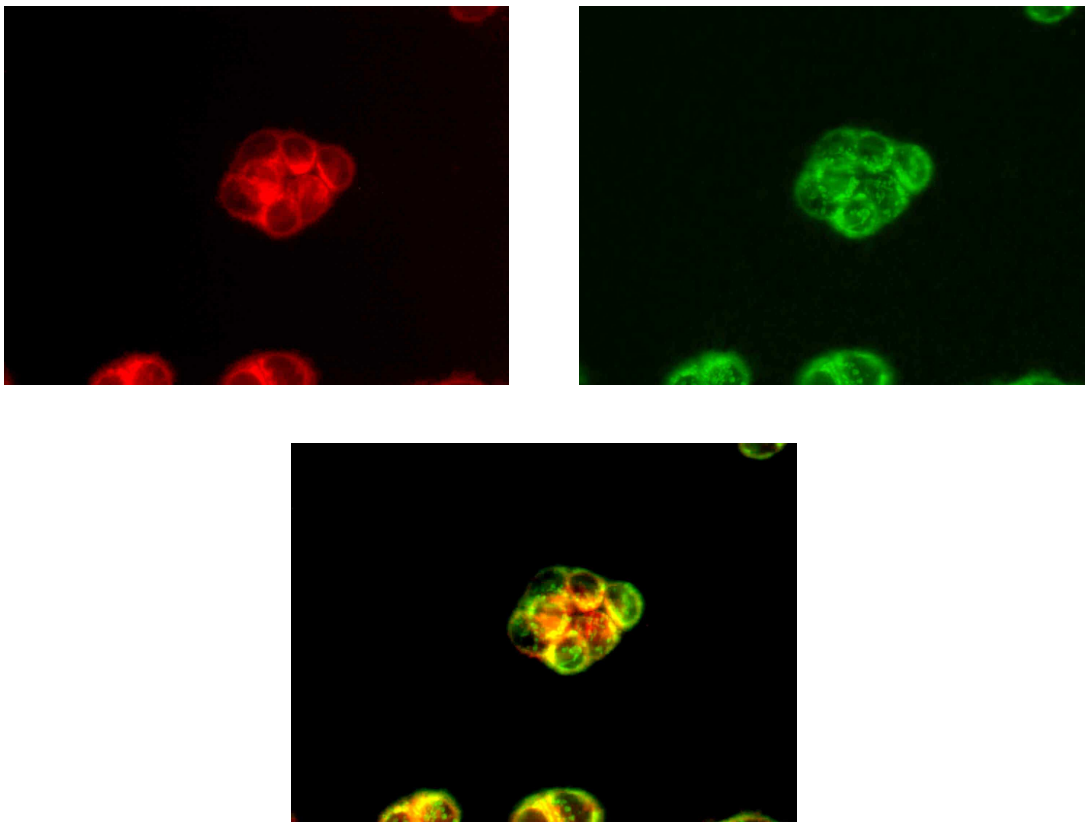

Figure 4.9. : Subcellular localisation of *m*-THPBC in WiDr cells (1.45µM, 24 hours incubation). Endoplasmic reticulum was stained with $DiOC_6$ (2.5 µg mL^{-1}).

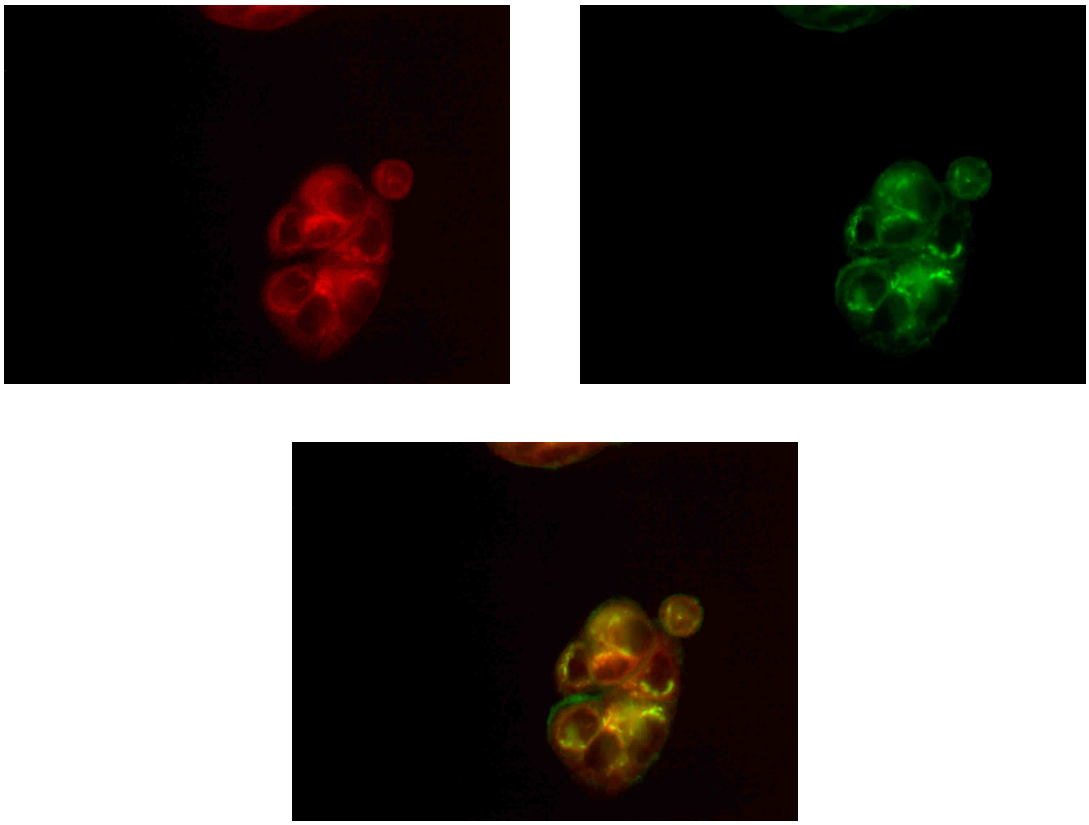

Figure 4.10. : Subcellular localisation of *m*-THPBC in WiDr cells (1.45µM, 24 hours incubation). Golgi apparatus was stained with BPC (5 µM).

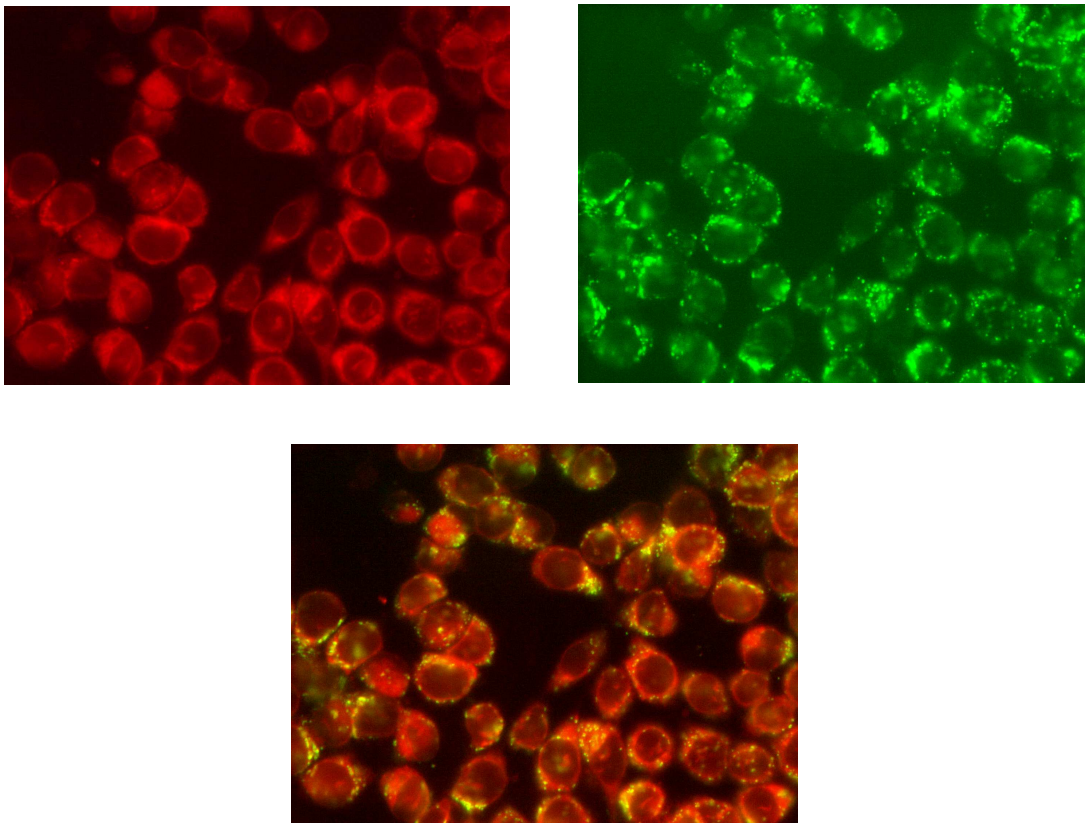

Figure 4.11. : Subcellular localisation of *m*-THPBC in WiDr cells (1.45µM, 24 hours incubation). Lysosome was stained with lysotracker green (1µM mL^{-1}).

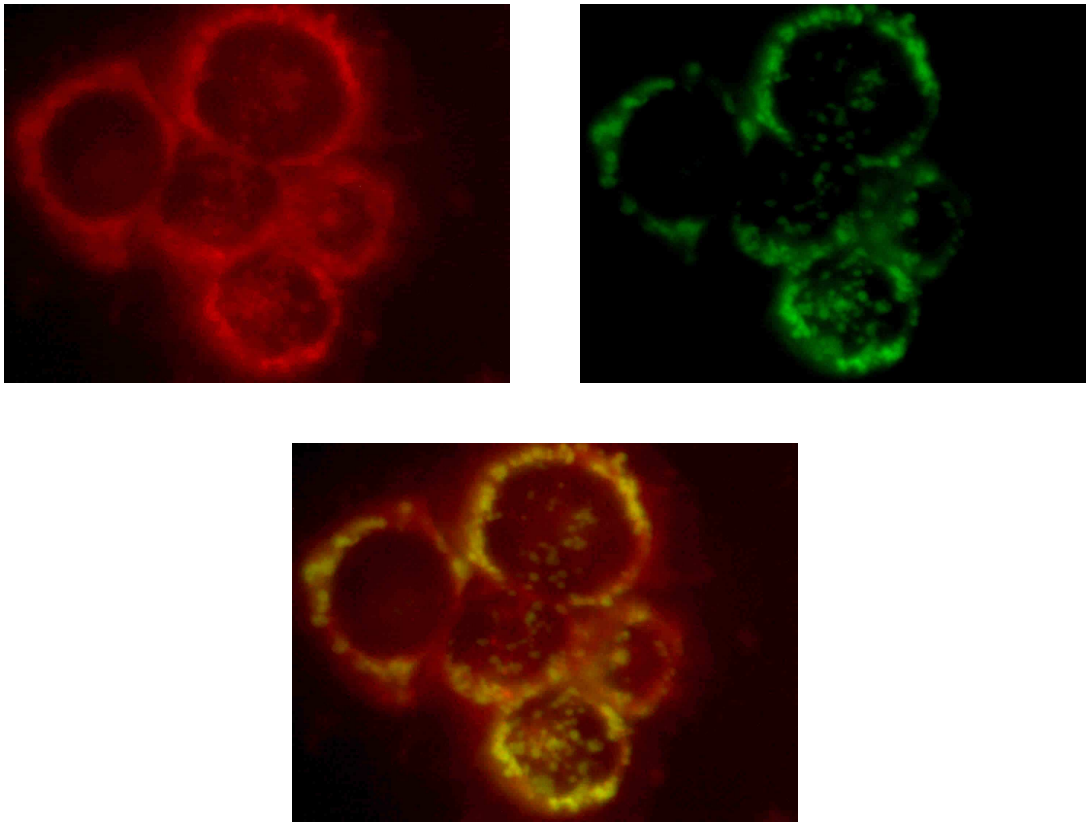

Figure 4.12. : Subcellular localisation of *m*-THPBC in WiDr cells (1.45µM, 24 hours incubation). Mitochondria was stained with mitotracker green (0.5 µM).

IV.3. In vivo evaluation of *m*-THPBC

3.1. Introduction

Few in vivo studies deal with the comparison of the photodynamic activity and the necrosis volume of *m*-THPBC-PDT compared to other active photosensitisers (Ma et al., 1996; Rovers et al., 2000a; Rovers et al., 2000b). In this part of the work we have compared the biodistribution, pharmacokinetics and photobleaching *in vivo* of *m*-THPBC and *m*-THPC. *m*-THPBC has a strong absorbance in the red region (740 nm), and with regard to the weak absorbance of tissues at this wavelength, this offers promising therapeutic perspectives for PDT of deep tumours and pigmented tissues. Therefore we focused some part of our study on the liver.

3.2. Materials and methods

Photosensitisers. *m*-THPBC and *m*-THPC were obtained as gifts from Biolitec Pharma Ltd. (Edinburgh, UK). 2 mg mL^{-1} stock solution were prepared in methanol and kept in the dark at 4°C. Mice were injected with 50µL of sensitiser solution (in PBS) at 0.5 mg kg^{-1} in the tail.

Animal model. Human colon adenocarcinoma cell lines, WiDr , were used in the present study. WiDr cells ($\approx 5 \times 10^6$) suspended in 0.04 ml of PBS were subcutaneously implanted in the flank of the mice. Non necrotic tumour material obtained by sterile dissection of large flank tumours was gently minced with a sterile surgical blade to make a tumour-tissue suspension, 0.02 ml of which was then injected into the dorsal side of the right hind foot of each syngeneic mouse. At this site the tumour was easily accessible to treatment and to assessment of response. Experiments were performed when tumours reached a surface diameter of about 4-5 mm, and a thickness of 2-3 mm.

Fluorescence measurements. Skin pharmacokinetic, biodistribution and photobleaching of *m*-THPBC and *m*-THPC were assessed by light-induced fluorescence spectroscopy (LIFS) by the means of a Perkin Elmer LS 50 B spectrofluorimeter equipped with a commercially available optic fibre (Perkin Elmer, Ref L2250144). Excitation wavelength was set at 378 nm and fluorescence was recorded at 740 nm for *m*-THPBC. For *m*-THPC experiments, excitation was set at 422 nm and emission was recorded at 650 nm.

Optical penetration depth in the liver. The light from a broadband xenon arc source was guided to the tissue. On the opposite side of the tissue a light collecting fibre was positioned at a known distances *x* from the end of a quartz rod and without applying significant pressure, the spectrum of light penetrating a lobe of the liver was measured. As shown in the inset of the figure 5.2. the light intensity collected by the fibre decreases in an exponential manner, and the penetration depth can be calculated from the slopes at all wavelengths within the lamp spectrum. The penetration depth δ is defined as the depth at which the irradiance is reduced from 1 to 1/e. The fibre optic set-up, using a commercially available spectrofluorimeter (Perkin Elmer LS 50 B), is described in the Figure 5.1. (for the detailed set-up see (Iani et al., 1996)).

Light sources. The light source used for photobleaching experiments of *m*-THPC was a CureLight BroadBand (Photocure, Norway), with an emission spectrum is 570-670 nm. The same light source with different filters was used for the *m*-THPBC irradiation (see chap. IV.1 for the details). The incident fluence rate was 55 mW cm^{-2} for both wavelengths.

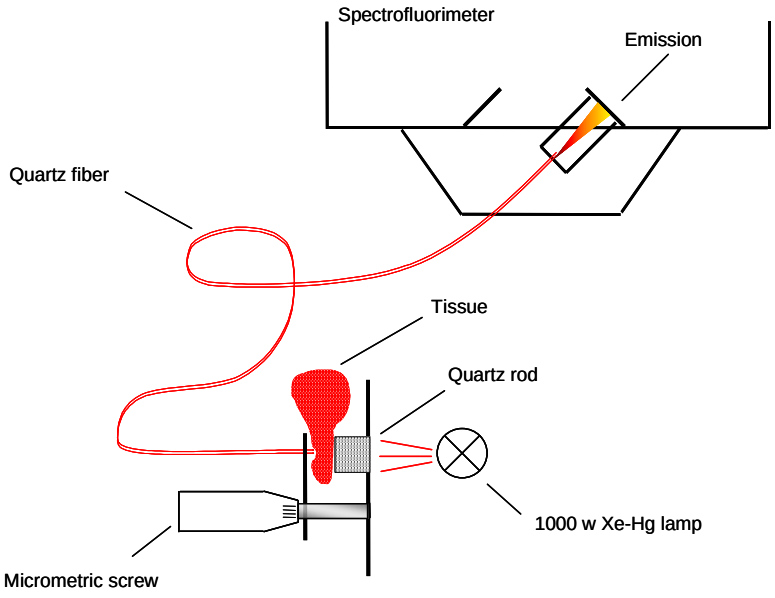

Figure 5.1. : Set-up for the determination of the optical penetration depth in the liver in vivo.

3.3. Results and discussion

Light penetration in the liver.

The Figure 5.2. clearly demonstrates the interest to use a far red excitation wavelength in the treatment of liver pathologies. The light penetration at 650 nm in a human ear is 3.6 mm (Moan et al., 1998a), in a WiDr tumour grown in a nude mouse it is 2.2 mm (Moan et al., 1998b) and due to the pigmentation of the liver the light penetration depth at 650 nm is 0,69 mm. This light penetration in the liver reaches 0,9 mm at 740 nm, with a 30% better penetration of light at 740 nm as compared to 650 nm.

Moreover the mouse liver presents a small area arround 740 nm which has a low tissue absorption. This makes the use of *m*-THPBC even more attractive than bacteriochlorophylls for example with an absorption band at 770-780 nm.

The shoulder around 500-600 nm is probably due to the absorption of haemoglobin and bilirubin. One can notice another shoulder around 760 nm. The absorbing species at this wavelength is unknown.

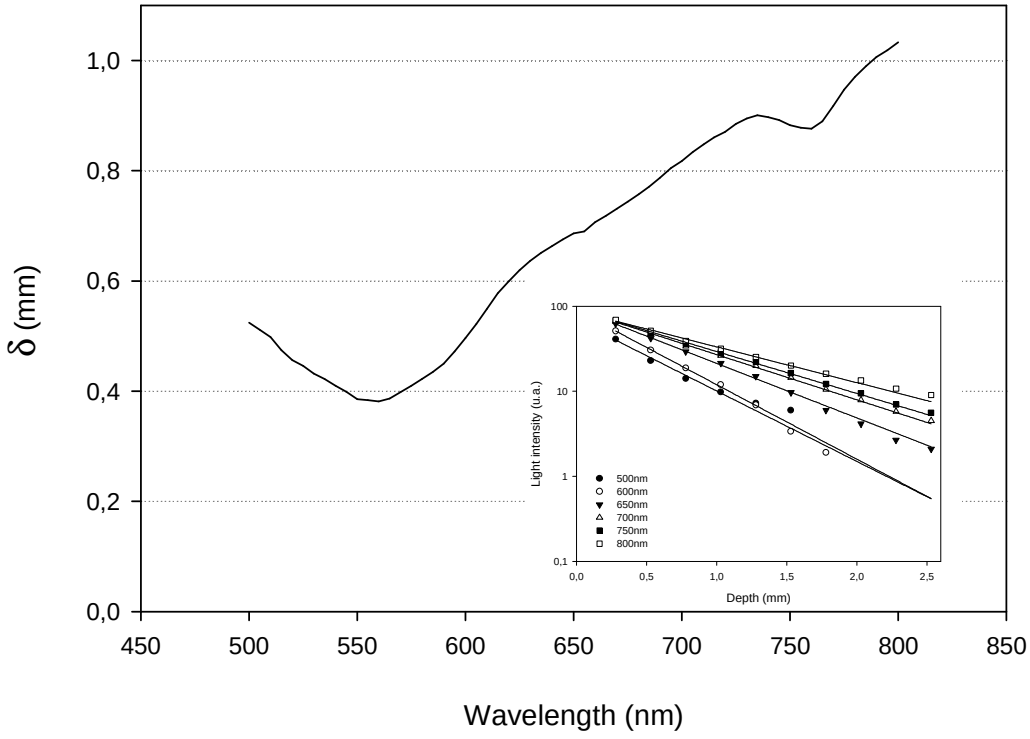

Figure 5.2. : Intensity of transmitted light through the liver of a BALB/c nude mice in vivo.

Biodistribution.

The biodistribution of the *m*-THPBC and the *m*-THPC in BALB/c nude mice is presented in Figure 5.3. *m*-THPBC and *m*-THPC fluorescence emission has been normalised in the skin and autofluorescence for each organ were subtracted.

Both photosensitisers were absent from the brain. This is in agreement with several studies on *m*-THPC biodistribution (Ronn et al., 1997; Whelpton et al., 1996). It also confirms that *m*-THPBC is not able to pass through the blood-brain barrier. The maximum of fluorescence was found in the tumour, ≈ 2 times more than in the skin and ≈ 4 times more than in the muscles, in all probability representative of a good accumulation of the photosensitisers in the WiDr tumour. *m*-THPBC and *m*-THPC almost have the same distribution in other studied organs except for the lungs and the liver where *m*-THPBC fluorescence far exceeds *m*-THPC fluorescence. This last observation bolsters the idea that *m*-THPBC is a good photosensitiser to treat liver disease. Due to the pigmentation and the absorbance of the liver, these LIFS results need to be confirmed with another technique. Chemical extraction and elastic scattering spectroscopy (ESS) study of the biodistribution of *m*-THPBC is carried out at the present time in our laboratory, and this study confirms the accumulation of this photosensitiser in the liver (Marchal F., personal communication).

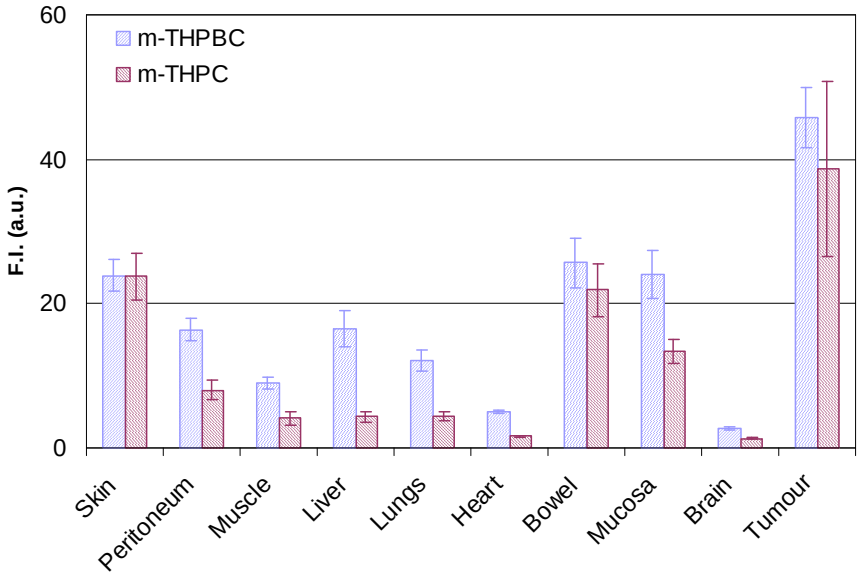

Figure 5.3. : Biodistribution of *m*-THPC and *m*-THPBC in a BALB/c nude mice after the injection of 0.5 mg kg^{-1} of photosensitisers.

Skin Pharmacokinetics.

Skin fluorescence of BALB/c nude mice was investigated by LIFS during 9 days following photosensitisers administration (Fig. 5.4.). Fluorescence kinetics of both photosensitisers are almost superimposable, with a fluorescence emission peak at 72 hours.

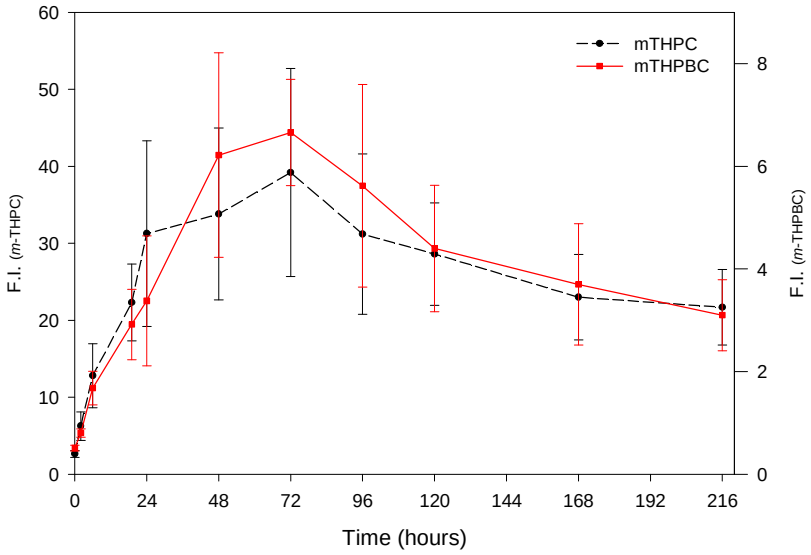

Figure 5.4. : Fluorescence intensity of *m*-THPC and *m*-THPBC in the skin of a BALB/c nude mice after the injection of 0.5 mg kg^{-1} of photosensitisers.

In the chapter IV.3. we have shown that the fluorescence emission in PBS-FCS 10% solution reaches a plateau 6 hours after the introduction of *m*-THPC (Fig. 3.1.), while the equilibrium was reached 3 hours after the addition of *m*-THPBC (Fig. 3.2.). Also a rather different redistribution rate among the plasma proteins exists for the two sensitisers (Sasnouski S., personal communication). Our present results seem to suggest that redistribution rates of the photosensitisers in the plasma proteins does not influence the skin Pharmacokinetics.

Photobleaching.

Photobleaching of *m*-THPC and *m*-THPBC was investigated in the skin of BALB/c nude mice 24 h after injection of 0.5 mg kg^{-1} of photosensitisers. Experiments were carried out with alive or dead mice to underline the oxygen effect on photobleaching in vivo. The figures 5.5. to 5.8. display the photobleaching curves in the skin of the mice of both photosensitisers for the alive and dead mice and the Table 5.1. summarizes the different photobleaching rates. One can notice that irrespective of the sensitisers and the status of the mice photobleaching kinetics rather fit a bi-exponential decay, suggesting that the two photosensitisers are both under monomeric and an aggregated form *in vivo* 24 hours post injection.

Table 5.1. : Photobleaching rate constants (k/s^{-1}) of *m*-THPC and *m*-THPBC in BALB/c mice (photobleaching rate constants from the second parts of the curves are shown in parentheses)

	Alive		Dead	
m-THPC	$2{,}63 \times 10^{-2}$	$(2{,}88 \times 10^{-3})$	$4{,}20 \times 10^{-3}$	$(2{,}05 \times 10^{-4})$
m-THPBC	$1{,}02 \times 10^{-1}$	$(2{,}84 \times 10^{-2})$	$1{,}58 \times 10^{-2}$	$(1{,}94 \times 10^{-3})$

In vivo photobleaching rate of *m*-THPBC appears to be 4 times higher than that of *m*-THPC for the first part of the curve and 10 times higher for the second exponential. These in vivo results are not so different as the in vitro result obtained on WiDr cells (Chapter IV.2.) where photobleaching rates were found to be around 3 to 4.5 times faster for *m*-THPBC than for *m*-THPC. Rovers *et al.* (Rovers et al., 2000b) report a *m*-THPBC photobleaching rate 20 times that of *m*-THPC in a Colo26 tumour bearing mice model. This large difference in photobleaching rate (20 times versus 4 times) might be due to the model used or to the fact that molecules concentration are very different (0.3 and 1.2 mg kg^{-1} for *m*-THPBC and *m*-THPC respectively) in the above mentioned study.

The blood flow in the dead mice is stopped as is the transport of oxygen to the tissues, therefore the tissue oxygenation is lower. Consistent with low oxygen levels, our results

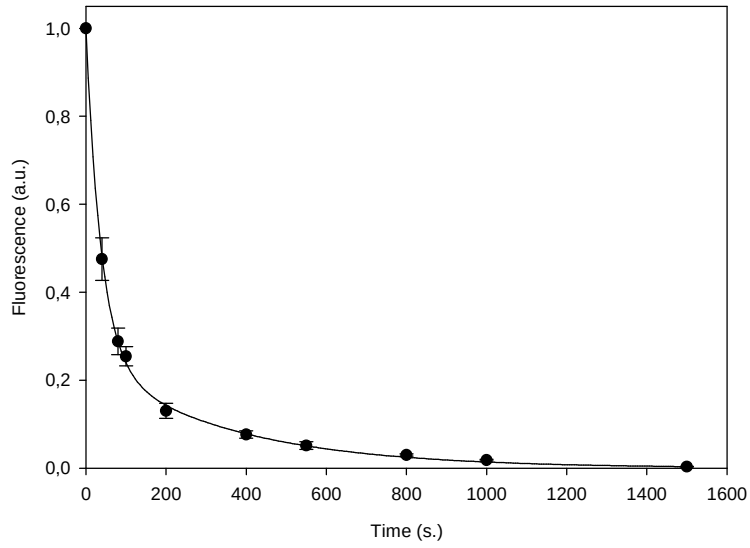

Figure 5.5. : Decay of the fluorescence of *m*-THPC in mouse skin as a function of the irradiation time.

demonstrate a 6 fold decrease in the photobleaching rates for both photosensitisers in the dead mice compared to the alive mice. This result demonstrates the implication of the oxygen in *m*-THPC and *m*-THPBC photobleaching *in vivo*. These *in vivo* results confirm our data obtained in solution showing the implication of the molecular oxygen in the photobleaching of *m*-THPBC (chapter IV.1.3.).

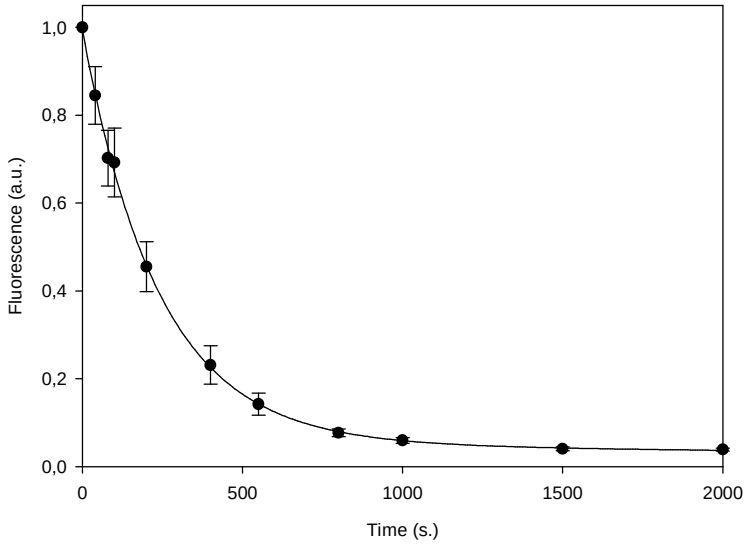

Figure 5.6. : Decay of the fluorescence of *m*-THPC in dead mouse skin as a function of the irradiation time.

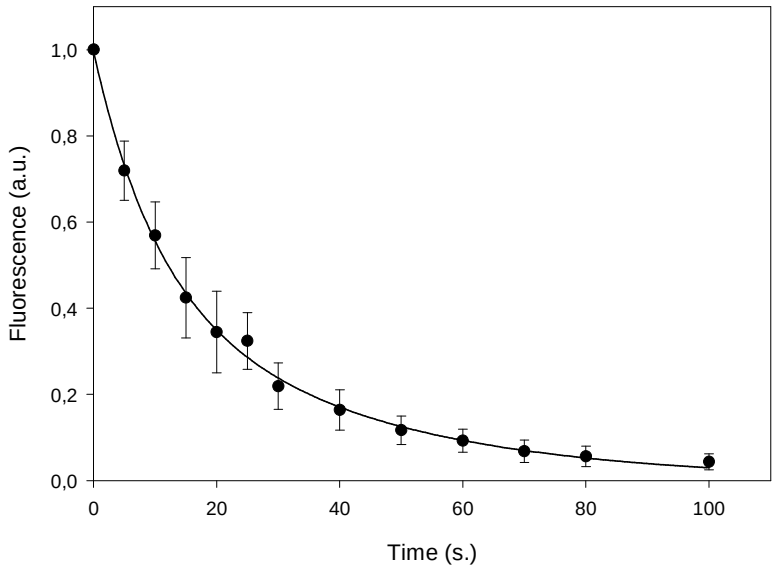

Figure 5.7. : Decay of the fluorescence of *m*-THPBC in mouse skin as a function of the irradiation time.

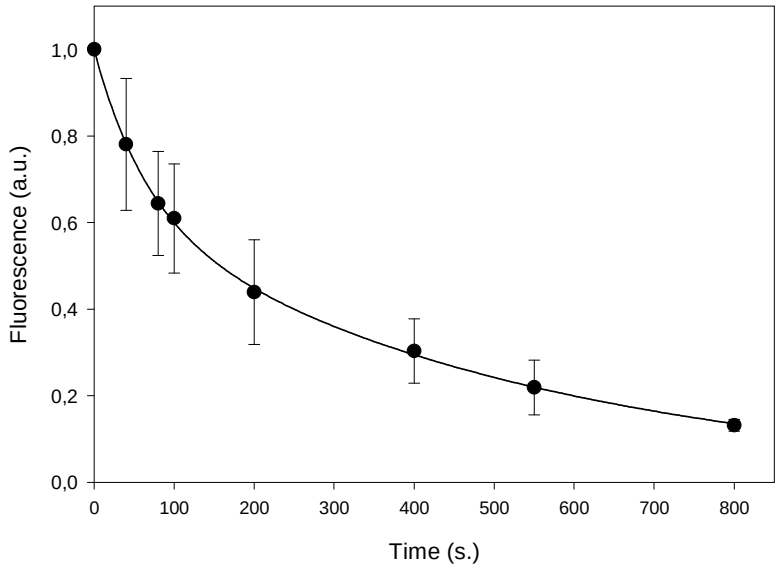

Figure 5.8. : Decay of the fluorescence of *m*-THPBC in dead mouse skin as a function of the irradiation time.

3.4. Conclusion

The rationale for taking advantage of the photobleaching effect is that since the level of sensitisers in normal tissues is lower than that in tumours (Fig. 5.3.), it may be possible to inject the sensitiser at a low dose, so that it is photobleached before it is able to cause any large photodynamic damage to normal tissue. The tumour, however, in which the concentration of the sensitiser is higher, may be completely photoinactivated. Another advantage of the photobleaching is that the two photosensitisers have the same distribution kinetic in the skin (Fig. 5.4.), and according to the higher photobleaching rates of *m*-THPBC, we can hypothesise that skin photosensitivity for *m*-THPBC will be less than for *m*-THPC.

General Discussion

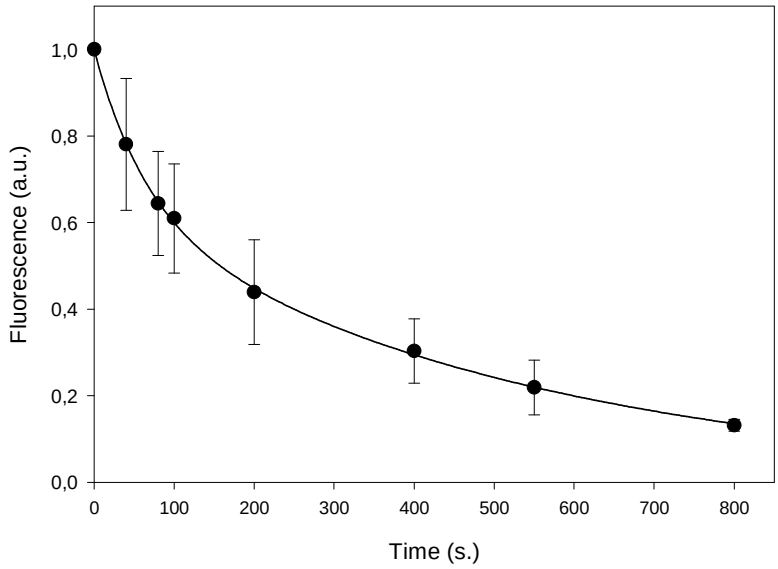

Figure 5.8. : Decay of the fluorescence of *m*-THPBC in dead mouse skin as a function of the irradiation time.

3.4. Conclusion

The rationale for taking advantage of the photobleaching effect is that since the level of sensitisers in normal tissues is lower than that in tumours (Fig. 5.3.), it may be possible to inject the sensitiser at a low dose, so that it is photobleached before it is able to cause any large photodynamic damage to normal tissue. The tumour, however, in which the concentration of the sensitiser is higher, may be completely photoinactivated. Another advantage of the photobleaching is that the two photosensitisers have the same distribution kinetic in the skin (Fig. 5.4.), and according to the higher photobleaching rates of *m*-THPBC, we can hypothesise that skin photosensitivity for *m*-THPBC will be less than for *m*-THPC.

V GENERAL DISCUSSION

Light exposure of photosensitisers results in a change in their absorbance and fluorescence spectra, demonstrating a photodegradation and phototransformation of the molecules. This might be seen as a disadvantage, since tumour destruction will be incomplete if the photosensitiser bleaches too rapidly during illumination (Mang et al., 1987; Moan et al., 1984). On the other hand, the unwanted damages to surrounding healthy tissue caused by PDT can probably be kept at tolerable level, if the injected drug dose is due to be photodegraded before it has been able to cause any large damage. Assuming that tumours contain much larger concentration of photosensitiser than the normal tissues surrounding the tumour, complete tumour inactivation could be expected, without excessive side effects. As today, the development of dosimetry for PDT has been mainly focused on the dosimetry of light and administered dose of photosensitiser. Although important progress has been made in this area during the last decade, state-of-the-art light dosimetry is still not a reliable predictor of the therapeutic PDT effect. All the recent dosimetry models are only taking into account the initial photosensitizer concentration. Wilson *et al.* introduced a new concept (Wilson et al., 1997b), named implicit dosimetry which recommended to use photosensitiser photobleaching as an index of the effective delivered dose. Therefore understanding the photodegradation mechanisms and the photoproducts formation of a photosensitiser is necessary to adapt the photodynamic dose and improve the treatment.

The photosensitiser aggregation state is an important field, which has been extensively studied. It is now well established that monomers and aggregates of photosensitisers have different photophysical, photobiological and photocytotoxic properties (Aveline et al., 1995; Belitchenko et al., 1998; Brown et al., 1976; Margalit et al., 1983). Inside tissues or cells photosensitisers can have different aggregation states (Hopkinson et al., 1999; Kelbauskas and Dietel, 2002). It has also been demonstrated in a study of our group, that in the presence of large amount of plasma proteins, a fraction of *m*-THPC still remains in an aggregated form (Sasnouski et al., in revision). Therefore we investigated the photobleaching properties of *m*-THPBC in two different solutions. We used freshly prepared *m*-THPBC solution in PBS-HSA, corresponding to an aggregated *m*-THPBC state and a PBS-HSA solution incubated during 6 hours corresponding to monomeric or bound to protein states. These two solutions can be considered to reproduce the biological situation. The photosensitiser concentration of

1.5 µM was chosen so as to be comparable to the photosensitiser plasma concentration. Aggregated *m*-THPBC photobleaching follows a mono-exponential decay, whereas the incubated solution corresponding to a mix of aggregates and monomers displays a bi-exponential fluorescence decrease. The rapid bleaching portion was attributed to the monomers and the slower to the aggregated forms as was reported in several studies for other photosensitisers (Moan et al., 1997; Strauss et al., 1998). Thus, the results of this study demonstrated that the photobleaching of *m*-THPBC was highly dependent on the aggregation state of the molecule.

Zeng *et al.* (Zeng et al., 2002) demonstrated that photoproduct formation dramatically improved the prediction of skin necrosis compared to light dose alone and as such photoproduct formation was identified as the best single parameter for predicting the PDT outcome. In addition, if the photoproduct also possesses photosensitising properties it is possible to improve the PDT efficiency by applying two wavelengths corresponding to excitation wavelengths of both the parent sensitiser and its photoproducts (Rotomskis et al., 1998). We investigated the photoproduct formation following the irradiation of *m*-THPBC in two different aggregation states. Identification of the photoproducts consecutive to the irradiation of *m*-THPBC was performed by mass spectrometry, along with spectroscopy. Hydroxylated compounds were detected irrespective of the aggregation state of the photosensitiser, with a much lower amount of hydroxylated product for aggregated *m*-THPBC solution. This is likely due to the scarcity of molecular oxygen in the aggregates or because of the low accessibility of singlet oxygen to *m*-THPBC. Photosensitiser molecules in the aggregated form are less subject to phototransformation and photodestruction. After the irradiation, mass spectrometry results demonstrated a decrease of the signal corresponding to *m*-THPC, in opposition to the spectroscopic study showing an increase of the peak intensity corresponding to *m*-THPC. This demonstrates that the main photoproduct formed is di-hydro di-hydroxylated *m*-THPC, which has almost the same spectrophotometric characteristic as *m*-THPC (Kasselouri et al., 1999) but a very different mass spectrometric signal (*m/z* + 34). This points out the limitations of spectroscopy techniques. We have emitted the hypothesis that the photobleaching behaviour of *m*-THPBC is strongly dependent on available oxygen. Indeed, oxygen replacement by nitrogen in m-THPBC solution considerably diminished the photoinduced decay. Therefore we investigated the involvement of reactive oxygen species in *m*-THPBC photobleaching in monomerised solution using ROS scavengers and *m*-THPC as a reference molecule. DABCO and Histidine, two singlet oxygen quenchers, inhibited *m*-THPBC and *m*-THPC photobleaching, indicating that Type II mechanisms are involved in the

bleaching of both photosensitisers. Type I scavengers, Catalase and Superoxide dismutase did not protect photosensitisers against photobleaching. These results are in agreement with the study of Bonnett et al. (Bonnett et al., 1999b) demonstrating the involvement of singlet oxygen in the *m*-THPBC photobleaching in methanol. In the *in vivo* part of our experiments we also demonstrated that molecular oxygen is required for the photobleaching of *m*-THPBC and *m*-THPC. Photobleaching experiments on alive and dead mice demonstrated, that the photobleaching rates for *m*-THPBC and for *m*-THPC were diminished 6 fold for dead mice, due to reduced oxygen levels.

In the second part of our work, we compared several photobiological properties of *m*-THPBC and *m*-THPC *in vitro*. The first step was to examine the aggregation state of the photosensitisers in the cells. Matching absorption spectra of *m*-THPBC and *m*-THPC in cells and comparing them with methanol reference spectra, we deduced that *m*-THPBC and *m*-THPC were mainly under monomerised form in the WiDr cells 24 hours after incubation. Despite the same aggregation state, the observed photobleaching kinetics were very different. *m*-THPBC follows a first order, mono-exponential decay while *m*-THPC follows a bi-exponential non-first order decay. The photobleaching rates have been shown to be 3 to 5 times faster for *m*-THPBC and the photocytotoxicity experiments demonstrate a four times greater LD_{50} for *m*-THPBC. In order to compare the "theoretical" efficiency of the two compounds we have computed the photoinactivation yield measured as the integrated number of photons absorbed by each photosensitiser, thereby implicating the photobleaching in the photocytotoxicity. The photoinactivation yield ratio revealed that *m*-THPBC needs to absorb 6 fold more photons to induce the same cell photoinactivation. Since these two photosensitisers had the same quantum yield of singlet oxygen formation (Bonnett et al., 1999a), we put forward the hypothesis that the two photosensitisers have different cell localisation sites. The intracellular localisation pattern after 24 h incubation studied by confocal fluorescence microscopy and microspectrofluorimetry demonstrates even better accumulation of *m*-THPC in the ER, compared to previously shown results of our laboratory (Teiten et al., 2003), whereas *m*-THPBC as assessed by epifluorescence microscopy mainly localises in the mitochondria. Therefore it seems that damaging the ER does not have the same outcome for the cell survival as mitochondrial damaging. To draw a final conclusion we need to confirm the mitochondrial cell localisation of *m*-THPBC by confocal microscopy and microspectrofluorimetry. Furthermore this different localisation pattern could help to explain the different photobleaching kinetics. Consistent with localisation, the bi-exponential decay

for *m*-THPC can correspond to the bleaching of the molecule in two different environments compared to *m*-THPBC which bleach in the same environment. Taken as a whole the results presented in the *in vitro* part of the work demonstrate a good photocytotoxicity for *m*-THPBC, along with fast first order photobleaching. These observations are particularly attractive in terms of therapeutic ratio and selectivity of the treatment. We further investigated the *in vivo* photobiological properties are as promising as the in vitro properties.

m-THPBC has a strong absorbance in the red region (740 nm) and with regard to the weak absorbance of tissues at this wavelength, this offers promising therapeutic perspectives for PDT of pigmented tissues. Several studies already demonstrated an increase necrotic area using *m*-THPBC in tumours (Bonnett et al., 1989) and liver (Rovers et al., 2000a) after irradiation at 740 nm. A study of light penetration in the liver showed a 30% increase of light penetration at 740 nm compared to 652 nm and in terms of volume it corresponds to a 120% increase. We also investigated the biodistribution of *m*-THPBC and *m*-THPC in the different organs of the mice, demonstrating a large accumulation of the photosensitisers in the tumours for both photosensitisers and a larger accumulation of *m*-THPBC in the liver. The *m*-THPBC skin pharmacokinetics reveal the same profile as *m*-THPC with a maximum peak at 72 hours after injection. We further examined photobleaching of *m*-THPBC and *m*-THPBC in the skin of the mice and irrespective of the sensitisers used, the bleaching kinetics better fit a bi-exponential decay, suggesting that the two photosensitisers are both under monomeric and aggregated forms *in vivo* 24 hours post injection. *m*-THPBC was found to bleach 4 to 10 times faster than *m*-THPC and this photobleaching profile could have important consequences. We observed that *m*-THPBC was present at higher concentrations in the tumours than in the surrounding healthy tissues, as do many others photosensitisers (Whelpton et al., 1995; Whelpton et al., 1996). Also, our *in vitro* results demonstrate a fast first order kinetic photobleaching meaning that the photobleaching rate is independent of the initial photosensitiser concentration in the tissue. Thus we assume that the photobleaching rate constant *in vivo* will also be subjected to a first order kinetic. This characteristic, together with the higher concentration in tumours tissues as opposed to healthy tissues and the fast photobleaching, offer the possibility to reduce the concentration of *m*-THPBC in the normal tissues to a level below the photodynamic threshold, while sufficient sensitiser could remain in the tumour to sensitise its photodestruction. Therefore using *m*-THPBC at an appropriate concentration could increase the therapeutic ratio and protect normal tissue from irreversible damages.

It has also been suggested that photobleaching could be used to decrease the concentration of photosensitiser in the skin and thus shorten the period of photosensitivity in patients following PDT (Roberts et al., 1989). This is actually carried out in clinical context. After a PDT treatment the patient is allowed, and even recommended to expose himself to a low dose of light and gradually increase light exposure until back to normal (Biolitec Pharma Ltd, Foscan®, light exposure guidelines). We have reported that skin pharmacokinetic of *m*-THPBC had the same characteristics as *m*-THPC and that skin photobleaching was 4 to 10 times faster for *m*-THPBC compared to *m*-THPC. These observations are promising regarding the skin photosensitivity during *m*-THPBC-PDT treatment, since we are expecting a much shorter skin photosensitivity than for *m*-THPC. The high molar extinction coefficient at 740 nm of *m*-THPBC compared to *m*-THPC excitation wavelength enables an increase in the treatment volume by 120% in the liver and this might be even higher for less pigmented tissues. Taken as a whole, the expected high therapeutic ratio, the low skin photosensitivity and the far-red excitation wavelength makes *m*-THPBC a very attractive photosensitiser and these findings might have potential clinical relevance.

Conclusion and Perspectives

VI CONCLUSION AND PERSPECTIVES

The examination of *m*-THPBC photobleaching in solution demonstrate a fast decrease of fluorescence and absorbance with irradiation, with a faster decrease of fluorescence attributed to the preferential photobleaching of the fluorescing monomer forms. For a solution of monomeric and aggregated *m*-THPBC species the photobleaching was found to be bi-exponential. The rapid portion was attributed to the photobleaching of monomeric species and the slow portion to the bleaching of aggregated portion. Aggregated solution of *m*-THPBC display a mono-exponential decay with a photobleaching rate equivalent to the one of the slow portion of the bi-exponential decay. Analysis of photoproducts formed after *m*-THPBC irradiation in phosphate buffer solution supplemented with proteins, assessed by UV-Vis spectroscopy and mass spectrometry demonstrated that *m*-THPBC was phototransformed into *m*-THPC and its hydroxylated derivatives and that photoproduct transformation was significantly influenced by *m*-THPBC aggregation state.

- *Perspectives*:

The photosensitisers in vitro and in vivo are known to be partly under aggregated state and partly monomerised, photobleaching of *m*-THPBC could gives rise to a sizeable amount of *m*-THPC. Therefore of it should be important to test if double wavelength irradiation (739 nm for *m*-THPBC activation, plus 652 nm for *m*-THPC activation) could improve the PDT treatment.

Mass spectrometry analysis enable the characterisation of the photoproducts formed after *m*-THPBC irradiation, it has been demonstrated that the main photoproducts where di-hydroxylated compounds such as di-hydroxy *m*-THPC, in opposition to spectrophotometric results showing photoformation of *m*-THPC due to the limitation of this technique in the discrimination of the hydroxylated products.

- *Perspectives :*

It could be interesting to isolate a sufficient amount of these hydroxylated products by chromatographic techniques to be able to test their photobiological properties such as their absorbance and fluorescence properties together with their photocytotoxicity.

Then we studied the involvement of reactive oxygen species in *m*-THPBC photobleaching in monomerised sensitiser solution using ROS scavengers and *m*-THPC as standard molecule. Singlet oxygen quenchers inhibited *m*-THPBC and *m*-THPC photobleaching, indicating that Type II mechanisms are involved in the bleaching of both photosensitisers. Type I scavengers did not protect photosensitisers against photobleaching.

- *Perspectives*:

Contribution of singlet oxygen in the photobleaching of *m*-THPBC has been demonstrated for monomerised or bound to proteins *m*-THPBC. It could be interesting to study the involvement of ROS for aggregated photosensitiser. We have emitted the hypothesis that due to the scarcity of molecular oxygen in the aggregates or because of the low accessibility of singlet oxygen to the *m*-THPBC, the photosensitiser molecules under an aggregated forms are less impacted by phototransformation and photodestruction. Therefore, it may be possible to know whether the photobleaching slow down is due to the difficulty for oxygen singlet to go inside the aggregates or if the mechanism involved is Type I dependent.

In vitro *m*-THPBC photobleaching was found to be a first order kinetic and to be 3 to 5 times faster than the non first order *m*-THPC bleaching, and the photocytotoxicity of *m*-THPBC was high (LD_{50} is 0.7 J cm^{-2}). It makes this photosensitiser attractive in terms of therapeutic ratio and protection of healthy tissues. The intracellular localisation pattern after 24 h incubation studied by confocal fluorescence microscopy and microspectrofluorimetry demonstrates an accumulation of *m*-THPC in the ER, whereas *m*-THPBC as assessed by epifluorescence microscopy mainly localises in the mitochondria.

- *Perspectives* :

It appears essential to carry out *m*-THPBC co-localisation experiments with a laser scanning confocal microscope and microspectrofluorimeter to confirm the observed results by epifluorescence microscope, and therefore be as reliable as the *m*-THPC localisation technique.

Also *m*-THPBC could serve as a good model to perform experiments on cell death mechanism after PDT treatment, since this sensitiser localises in the mitochondria. The modality of cell death following *m*-THPBC photosensitization should be further explored.

The *in vivo* results investigate the biodistribution by LIFS of *m*-THPBC and *m*-THPC in mice and demonstrated a large accumulation of the photosensitisers in the tumours for both photosensitisers and a larger accumulation of *m*-THPBC in the liver. Light penetration in the liver at *m*-THPBC excitation wavelength has been demonstrated to be 120% larger (in volume) than at *m*-THPC excitation wavelength. We have shown that skin pharmacokinetic of *m*-THPBC had the same characteristics as *m*-THPC and that skin photobleaching was 4 to 10 times faster for *m*-THPBC compared to *m*-THPC.

- *Perspectives* :

In the view of these results, we proposed to realize pre-clinical study of *m*-THPBC-PDT treatment on models such as hepatocarcinoma or liver metastasis. Also, skin photosensitivity following the treatment should also be evaluated, with the approach of minimal erythema doses.

References

REFERENCES

1. Ahram, M., Cheong, W.F., Ward, K., Kessel, D., 1994, Photoproduct formation during irradiation of tissues containing protoporphyrin. J Photochem Photobiol B 26, 203-204.

2. Ambroz, M., MacRobert, A.J., Morgan, J., Rumbles, G., Foley, M.S., Phillips, D., 1994, Time-resolved fluorescence spectroscopy and intracellular imaging of disulphonated aluminium phthalocyanine. J Photochem Photobiol B 22, 105-117.

3. Angotti, M., Maunit, B., Muller, J.F., Bezdetnaya, L., Guillemin, F., 1999, Matrix-assisted laser desorption/Ionization coupled to Fourier transform ion cyclotron resonance mass spectrometry: a method to characterize temoporpfin photoproducts. Rapid Commun. Mass Spectrom. 13, 597-603.

4. Angotti, M., Maunit, B., Muller, J.F., Bezdetnaya, L., Guillemin, F., 2001, Characterization by matrix-assisted laser desorption/ionization Fourier transform ion cyclotron resonance mass spectrometry of the major photoproducts of temoporfin (m-THPC) and bacteriochlorin (m-THPBC). J Mass Spectrom 36, 825-831.

5. Auler, H., Banzer, G., 1942, Untersuchungen über die Role der Porphyrine bei geschwultstkranken Menchen und Tieren. Z. Krebsforsch. 53, 65-68.

6. Aveline, B., Hasan, T., Redmond, R.W., 1994, Photophysical and photosensitizing properties of benzoporphyrin derivative monoacid ring A (BPD-MA). Photochem Photobiol 59, 328-335.

7. Aveline, B.M., Hasan, T., Redmond, R.W., 1995, The effects of aggregation, protein binding and cellular incorporation on the photophysical properties of benzoporphyrin derivative monoacid ring A (BPDMA). J. Photochem. Photobiol. B 30, 161-169.

8. Bagdonas, S., Ma, L.W., Iani, V., Rotomskis, R., Juzenas, P., Moan, J., 2000, Phototransformations of 5-aminolevulinic acid-induced protoporphyrin IX in vitro: a spectroscopic study. Photochem Photobiol 72, 186-192.

9. Baker, A., Kanofsky, J.R., 1992, Quenching of singlet oxygen by biomolecules from L1210 leukemia cells. Photochem Photobiol 55, 523-528.

10. Belitchenko, I., Melnikova, V., Bezdetnaya, L., Rezzoug, H., Merlin, J.L., Potapenko, A., Guillemin, F., 1998, Characterization of photodegradation of meta-tetra(hydroxyphenyl)chlorin (mTHPC) in solution: biological consequences in human tumor cells. Photochem Photobiol 67, 584-590.

11. Berenbaum, M.C., Akande, S.L., Bonnett, R., Kaur, H., Ioannou, S., White, R.D., Winfield, U.J., 1986, meso-Tetra(hydroxyphenyl)porphyrins, a new class of potent tumour photosensitisers with favourable selectivity. Br J Cancer 54, 717-725.

12. Berg, K., Madslien, K., Bommer, J.C., Oftebro, R., Winkelman, J.W., Moan, J., 1991, Light induced relocalization of sulfonated meso-tetraphenylporphines in NHIK 3025 cells and effects of dose fractionation. Photochem Photobiol 53, 203-210.

13. Berg, K., Moan, J., 1998, Optimization of wavelength in photodynamic therapy, In: Moser, J.G. (Ed.) Photodynamic tumor therapy. 2nd and 3rd generation photosensitizers. Harwood Academic Publishers, Amsterdam, pp. 151-168.

14. Bezdetnaya, L., Zeghari, N., Belitchenko, I., Barberi-Heyob, M., Merlin, J.L., Potapenko, A., Guillemin, F., 1996, Spectroscopic and biological testing of photobleaching of porphyrins in solutions. Photochem. Photobiol. 64, 382-386.

15. Bonnett, R., Charlesworth, P., Djelal, B.D., Foley, S., McGarvey, D.J., Truscott, T.G., 1999a, Photophysical properties of 5,10,15,20-tetrakis(m-hydroxyphenyl)porphyrin (m-THPP), 5,10,15,20-tetrakis(m-hydroxyphenyl)chlorin (m-THPC) and 5,10,15,20-tetrakis(m-hydroxyphenyl)bacteriochlorin (m-THPBC): a comparative study. J. Chem. Soc., Perkin Trans. 2 2, 325 - 328.

16. Bonnett, R., Djelal, B.D., Hamilton, P.A., Martinez, G., Wierrani, F., 1999b, Photobleaching of 5,10,15,20-tetrakis(m-hydroxyphenyl)porphyrin (m-THPP) and the corresponding chlorin (m-THPC) and bacteriochlorin(m-THPBC). A comparative study. J. Photochem. Photobiol. B 53, 136-143.

17. Bonnett, R., Martinez, G., 2000, Photobleaching studies on azabenzoporphyrins and related systems: a comparison of the photobleaching of the zinc(II) complexes of the tetrabenzoporphyrin, 5-azadibenzo[b,g]porphyrin and phthalocyanine systems. Journal of Porphyrins and Phthalocyanines 4, 544-550.

18. Bonnett, R., Martinez, G., 2002, Photobleaching of compounds of the 5,10,15,20-Tetrakis(m-hydroxyphenyl)porphyrin Series (m-THPP, m-THPC, and m-THPBC). Org. Lett. 4, 2013-2016.

19. Bonnett, R., Martínez, G., 2001, Photobleaching of sensitisers used in photodynamic therapy. Tetrahedron report number 591 57, 9513-9547.

20. Bonnett, R., White, R.D., Winfield, U.J., Berenbaum, M.C., 1989, Hydroporphyrins of the meso-tetra(hydroxyphenyl)porphyrin series as tumour photosensitizers. Biochem J 261, 277-280.

21. Bour-Dill, C., Gramain, M.P., Merlin, J.L., Marchal, S., Guillemin, F., 2000, Determination of intracellular organelles implicated in daunorubicin cytoplasmic sequestration in multidrug-resistant MCF-7 cells using fluorescence microscopy image analysis. Cytometry 39, 16-25.

22. Brown, S.B., Shillcock, M., Jones, P., 1976, Equilibrium and kinetic studies of the aggregation of porphyrins in aqueous solution. Biochem J 153, 279-285.

23. Brun, A., Western, A., Malik, Z., Sandberg, S., 1990, Erythropoietic protoporphyria: photodynamic transfer of protoporphyrin from intact erythrocytes to other cells. Photochem Photobiol 51, 573-577.

24. Buettner, G.R., Oberley, L.W., 1978, Considerations in the spin trapping of superoxide and hydroxyl radical in aqueous systems using 5,5-dimethyl-1-pyrroline-1-oxide. Biochem Biophys Res Commun 83, 69-74.

25. Cadenas, E., Sies, H., Nastainczyk, W., Ullrich, V., 1983, Singlet oxygen formation detected by low-level chemiluminescence during enzymatic reduction of prostaglandin G2 to H2. Hoppe Seylers Z Physiol Chem 364, 519-528.

26. Candide, C., Maziere, J.C., Santus, R., Maziere, C., Morliere, P., Reyftmann, J.P., Goldstein, S., Dubertret, L., 1989, Photosensitization of Wi26-VA4 transformed human fibroblasts by low density lipoprotein loaded with the anticancer porphyrin mixture photofrin II: evidence for endoplasmic reticulum alteration. Cancer Lett 44, 157-161.

27. Chen, J.Y., Mak, N.K., Yow, C.M., Fung, M.C., Chiu, L.C., Leung, W.N., Cheung, N.H., 2000, The binding characteristics and intracellular localization of temoporfin (mTHPC) in myeloid leukemia cells: phototoxicity and mitochondrial damage. Photochem Photobiol 72, 541-547.

28. Cox, G.S., Bobillier, C., Whitten, D.G., 1982a, Photooxidation and singlet oxygen sensitization by protoporphyrin IX and its photooxidation products. Photochem Photobiol 36, 401-407.

29. Cox, G.S., Krieg, M., Whitten, D.G., 1982b, Self-sensitized photooxidation of protoporphyrin IX derivatives in aqueous surfactant solutions; product and mechanistic studies. J. Am. Chem. Soc. 104, 6930 - 6937.

30. Cox, G.S., Witten, D.G., 1982, Mechanisms for the photooxidation of protoporphyrin IX in solution. J. Am. Chem. Soc. 104, 516 - 521.

31. Cunderlikova, B., Gangeskar, L., Moan, J., 1999, Acid-base properties of chlorin e6: relation to cellular uptake. J Photochem Photobiol B 53(1-3), 81-90.

32. Davila, J., Harriman, A., 1990, Photoreactions of macrocyclic dyes bound to human serum albumin. Photochem Photobiol 51, 9-19.

33. Delaey, E.M., Obermueller, R., Zupko, I., De Vos, D., Falk, H., de Witte, P.A., 2001, In vitro study of the photocytotoxicity of some hypericin analogs on different cell lines. Photochem Photobiol 74, 164-171.

34. Dougherty, T.J., Gomer, C.J., Henderson, B.W., Jori, G., Kessel, D., Korbelik, M., Moan, J., Peng, Q., 1998, Photodynamic therapy. J Natl Cancer Inst 90, 889-905.

35. Dougherty, T.J., Potter, W.R., Weinshaupt, K.R., 1984, The structure of the active component of hematoporphyrin derivative, In: Andreoni, A., Cubeddu, R. (Eds.) Porphyrins in Tumor Phototherapy. Plenum, New-York, pp. 23-35.

36. Fernandez, J.M., Bilgin, M.D., Grossweiner, L.I., 1997, Singlet oxygen generation by photodynamic agents. J Photochem Photobiol B 37, 131-140.

37. Finlay, J.C., Conover, D.L., Hull, E.L., Foster, T.H., 2001, Porphyrin bleaching and PDT-induced spectral changes are irradiance dependent in ALA-sensitized normal rat skin in vivo. Photochem Photobiol 73, 54-63.

38. Finlay, J.C., Mitra, S., Foster, T.H., 2002, In vivo mTHPC photobleaching in normal rat skin exhibits unique irradiance-dependent features. Photochem Photobiol 75, 282-288.

39. Foote, C.S., 1979, Detection of singlet oxygen in complex systems: a critique, In: Biochemical and Clinical Aspect of Oxygen. Academic Press, New York.

40. Foote, C.S., 1984, Mechanisms of photooxygenation, In: Doiron, D.R., Gomer, C.J. (Eds.) Porphyrin Localisation and Treatment of Tumors. Alan R. Liss Inc., New YorK, pp. 3-18.

41. Foote, C.S., 1991, Definition of type I and type II photosensitized oxidation. Photochem Photobiol 54, 659.

42. Fridovich, I., 1976, Oxygen Radicals, Hydrogen Peroxide, and Oxygen Toxicity., In: Pryor, W.A. (Ed.) Free Radicals in Biology. Academic Press, New York, pp. 239-277.

43. Georgakoudi, I., Foster, T.H., 1998, Singlet oxygen- versus nonsinglet oxygen-mediated mechanisms of sensitizer photobleaching and their effects on photodynamic dosimetry. Photochem. Photobiol. 67, 612-625.

44. Georgakoudi, I., Nichols, M.G., Foster, T.H., 1997, The mechanism of Photofrin photobleaching and its consequences for photodynamic dosimetry. Photochem. Photobiol. 65, 135-144.

45. Gorman, A.A., Rodgers, M.A., 1989, Singlet oxygen, In: Scaiano, J.C. (Ed.) Handbook of organic photochemistry. CRC Press, Boca Raton, pp. 229-247.

46. Grahn, M.F., McGuinness, A., Benzie, R., Boyle, R., de Jode, M.L., Dilkes, M.G., Abbas, B., Williams, N.S., 1997, Intracellular uptake, absorption spectrum and stability of the bacteriochlorin photosensitizer 5,10,15,20-tetrakis (m-hydroxyphenyl)bacteriochlorin (mTHPBC). Comparison with 5,10,15,20-tetrakis(m-hydroxyphenyl)chlorin (mTHPC). J. Photochem. Photobiol. B 37, 261-266.

47. Guillemin, F., A'Amar, O.M., Rezzoug, H., Lignon, D., Jaffry, F., Abdulnour, C., Muller, L., Yvroud, E., Merlin, J.L., Granjon, Y., Bolotina-Bezdetnaya, L., Zeghari, N., Khemis, K., Barberi-Heyob, M., Meunier-Reynes, A., Potapenko, A., Notter, D., Vigneron, C., 1995, Optical instrumentation suitable for a real-time dosimetry during photodynamic therapy. Proc. SPIE 2627, 92-99.

48. Hadjur, C., Jeunet, A., Jardon, P., 1994, Photosensitization by hypericin: Electron spin resonance (ESR) evidence for the formation of singlet oxygen and superoxide anion radicals in an in vitro model. J. Photochem. Photobiol. B. 26, 67-74.

49. Hadjur, C., Lange, N., Rebstein, J., Monnier, P., van den Bergh, H., Wagnières, G., 1998, Spectroscopic studies of photobleaching and photoproduct formation of meta(tetrahydroxyphenyl) chlorin (m-THPC) used in photodynamic therapy. The production of singlet oxygen by m-THPC. J. Photochem. Photobiol. B 45.

50. Hadjur, C., Wagnieres, G., Ihringer, F., Monnier, P., van den Bergh, H., 1997a, Production of the free radicals O2.- and .OH by irradiation of the photosensitizer zinc(II) phthalocyanine. J Photochem Photobiol B 38, 196-202.

51. Hadjur, C., Wagnieres, G., Monnier, P., van den Bergh, H., 1997b, EPR and spectrophotometric studies of free radicals ($O_2^{\cdot -}$, $^{\cdot}OH$, BPD-$MA^{\cdot -}$) and singlet oxygen ($^1O_2$) generated by irradiation of benzoporphyrin derivative monoacid ring A. Photochem Photobiol 65, 818-827.

52. Halliwell, B., 1978, Biochemical mechanisms accounting for the toxic action of oxygen on living organisms: the key role of superoxide dismutase. Cell Biol Int Rep 2, 113-128.

53. Halliwell, B., Gutteridge, J.M., 1986, Oxygen free radicals and iron in relation to biology and medicine: some problems and concepts. Arch Biochem Biophys 246, 501-514.

54. Halliwell, B., Gutteridge, J.M.C., 1999, Free Radicals In Biology and Medicine. Oxford University Press, UK.

55. Haussman, W., 1911, Die sensibilisierende Wirkung des hämatoporphyrins. Biochem. Z. 30, 276-316.

56. Hongying, Y., Fuyuan, W., Zhiyi, Z., 1999, Photobleaching of chlorins in homogeneous and heterogeneous media. Dyes and Pigments 43, 109-117.

57. Hopkinson, H.J., Vernon, D.I., Brown, S.B., 1999, Identification and partial characterization of an unusual distribution of the photosensitizer meta-tetrahydroxyphenyl chlorin (temoporfin) in human plasma. Photochem Photobiol 69, 482-488.

58. Iani, V., Moan, J., Ma, L., 1996, Measurements of light penetration into human tissue in vivo. SPIE 2625, 378-383.

59. Iinuma, S., Farshi, S.S., Ortel, B., Hasan, T., 1994, A mechanistic study of cellular photodestruction with 5-aminolaevulinic acid-induced porphyrin. Br J Cancer 70, 21-28.

60. Inhoffen, H.H., Brockmann, H., Bliesener, K.M., 1969, Photoprotoporphyrine und ihre Umwandlung in Spirographis-sowie Isospirographis-Porphyrin. Justus Liebigs Ann. Chem. 730, 173–185.

61. Jones, R.M., Wang, Q., Lamb, J.H., Djelal, B.D., Bonnett, R., Lim, C.K., 1996, Identification of photochemical oxidation products of 5,10,15,20-tetra(m-hydroxyphenyl)chlorin by on-line high-performance liquid chromatography-electrospray ionization tandem mass spectrometry. J Chromatogr A 722, 257-265.

62. Juzenas, P., Iani, V., Bagdonas, S., Rotomskis, R., Moan, J., 2001, Fluorescence spectroscopy of normal mouse skin exposed to 5-aminolaevulinic acid and red light. J Photochem Photobiol B 61, 78-86.

63. Kasselouri, A., Bourdon, O., Demore, D., Blais, J.C., Prognon, P., Bourg-Heckly, G., Blais, J., 1999, Fluorescence and mass spectrometry studies of meta-tetra(hydroxyphenyl)chlorin photoproducts. Photochem Photobiol 70, 275-279.

64. Kelbauskas, L., Dietel, W., 2002, Internalization of aggregated photosensitizers by tumor cells: subcellular time-resolved fluorescence spectroscopy on derivatives of pyropheophorbide-a ethers and chlorin e6 under femtosecond one- and two-photon excitations. Photochem Photobiol 76, 686-694.

65. Kessel, D., 1986, Sites of photosensitization by derivatives of hematoporphyrin. Photochem Photobiol 44, 489-493.

66. Kessel, D., Woodburn, K., 1993, Biodistribution of photosensitizing agents. Int J Biochem 25, 1377-1383.

67. Kohen, E., Santus, R., Hirschberg, J., 1995, Photobiology. Academic Press, San Diego.

68. König, K., Meyer, H., Schneckenburger, H., Rück, A., 1993, The study of endogenous porphyrins in human skin and their potential for photodynamic therapy by laser induced fluorescence spectroscopy. Lasers Med Sci 8, 127-132.

69. Krasnovsky, A.A., Jr., 1998, Singlet molecular oxygen in photobiochemical systems: IR phosphorescence studies. Membr Cell Biol 12, 665-690.

70. Krieg, M., Whitten, D.G., 1984a, Self-sensitized photooxidation of protoporphyrin IX and related free-base porphyrins in natural and model membrane systems. Evidence for novel photooxidation pathways involving amino acids. J. Am. Chem. Soc. 106, 2477 - 2479.

71. Krieg, M., Whitten, D.G., 1984b, Self-sensitized photooxidation of protoporphyrin IX and related porphyrins in erythrocytes ghosts and microemulsions: a novel photooxidation pathway involving singlet oxygen. J Photochem 25, 235-252.

72. Krinsky, N.I., 1979, Biological role of singlet oxygen, In: Singlet oxygen. Academic Press, New-York, pp. 597-641.

73. Ledoux-Lebards, C., 1902, Annales de l'institut Pasteur 16, 593.

74. Leung, W.N., Sun, X., Mak, N.K., Yow, C.M., 2002, Photodynamic effects of mTHPC on human colon adenocarcinoma cells: photocytotoxicity, subcellular localization and apoptosis. Photochem Photobiol 75, 406-411.

75. Lin, C.W., Shulok, J.R., Kirley, S.D., Bachelder, C.M., Flotte, T.J., Sherwood, M.E., Cincotta, L., Foley, J.W., 1993, Photodynamic destruction of lysosomes mediated by Nile blue photosensitizers. Photochem Photobiol 58, 81-91.

76. Lourette, N., Maunit, B., Bezdetnaya, L., Lassalle, H.P., Guillemin, F., Muller, J.F., 2005, Characterization of Photoproducts of m-THPP in Aqueous Solution. Photochem Photobiol 81, 691-696.

77. Ma, L.W., Moan, J., Grahn, M.F., Iani, V., 1996, Comparison of meso-tetrahydroxyphenyl-chlorin and meso-tetrahydroxyphenyl-bacteriochlorin with respect to photobleaching and PCT efficiency in vivo. Proc. SPIE 2924, 219-224.

78. MacRobert, A.J., Bown, S.G., Phillips, D., 1989, What are the ideal photoproperties for a sensitizer? Ciba Found Symp 146, 4-12; discussion 12-16.

79. Malik, Z., Faraggi, A., Savion, N., 1992, Ultrastructural damage in photosensitized endothelial cells: dependence on hematoporphyrin delivery pathways. J Photochem Photobiol B 14, 359-368.

80. Mang, T.S., Dougherty, T.J., Potter, W.R., Boyle, D.G., Somer, S., Moan, J., 1987, Photobleaching of porphyrins used in photodynamic therapy and implications for therapy. Photochem Photobiol 45, 501-506.

81. Marchal, S., Fadloun, A., Maugain, E., D'Hallewin, M.A., Guillemin, F., Bezdetnaya, L., 2005, Necrotic and apoptotic features of cell death in response to Foscan photosensitization of HT29 monolayer and multicell spheroids. Biochem Pharmacol 69, 1167-1176.

82. Margalit, R., Shaklai, N., Cohen, S., 1983, Fluorimetric studies on the dimerization equilibrium of protoporphyrin IX and its haemato derivative. Biochem J 209, 547-552.

83. Matroule, J.Y., Bonizzi, G., Morliere, P., Paillous, N., Santus, R., Bours, V., Piette, J., 1999, Pyropheophorbide-a methyl ester-mediated photosensitization activates transcription factor NF-kappaB through the interleukin-1 receptor-dependent signaling pathway. J Biol Chem 274(5), 2988-3000.

84. McCord, J.M., Fridovich, I., 1969, Superoxide dismutase. An enzymic function for erythrocuprein (hemocuprein). J Biol Chem 244, 6049-6055.

85. Melnikova, V.O., Bezdetnaya, L.N., Bour, C., Festor, E., Gramain, M.P., Merlin, J.L., Potapenko, A., Guillemin, F., 1999a, Subcellular localization of meta-tetra

(hydroxyphenyl) chlorin in human tumor cells subjected to photodynamic treatment. J Photochem Photobiol B 49, 96-103.

86. Melnikova, V.O., Bezdetnaya, L.N., Potapenko, A.Y., Guillemin, F., 1999b, Photodynamic properties of meta-tetra(hydroxyphenyl)chlorin in human tumor cells. Radiat Res 152, 428-435.

87. Meyer-Betz, F., 1913, Untersuchungen über die biologische (photodynamische) Wirkung des Hämatoporphyrins und andere Derivate des Blut- und Gallenfarbstoffes. Dtsch. Arch. Klin. Med. 112, 476-503.

88. Moan, J., 1986, Effect of bleaching of porphyrin sensitizers during photodynamic therapy. Cancer Lett 33, 45-53.

89. Moan, J., 1990, On the diffusion length of singlet oxygen in cells and tissues. J Photochem Photobiol B 6, 343-344.

90. Moan, J., Anholt, H., 1990, Phthalocyanine fluorescence in tumors during PDT. Photochem Photobiol 51, 379-381.

91. Moan, J., Anholt, H., Peng, Q., 1990, A transient reduction of the fluorescence of aluminium phthalocyanine tetrasulphonate in tumours during photodynamic therapy. J Photochem Photobiol B 5, 115-119.

92. Moan, J., Berg, K., 1991, The photodegradation of porphyrins in cells can be used to estimate the lifetime of singlet oxygen. Photochem Photobiol 53, 549-553.

93. Moan, J., Berg, K., Anholt, H., Madslien, K., 1994, Sulfonated aluminium phthalocyanines as sensitizers for photochemotherapy. Effects of small light doses on localization, dye fluorescence and photosensitivity in V79 cells. Int J Cancer 58, 865-870.

94. Moan, J., Berg, K., Iani, V., 1998a, Action spectra of dyes relevant for photodynamic therapy, In: Moser, J.G. (Ed.) Photodynamic tumor therapy. 2nd and 3rd generation photosensitizers. Harwood Academic Publishers, Amsterdam, pp. 169-181.

95. Moan, J., Berg, K., Kvam, E., Western, A., Malik, Z., Ruck, A., Schneckenburger, H., 1989, Intracellular localization of photosensitizers., In: Bock, G., Harnett, S. (Eds.)

Photosensitizing compounds: their Chemistry, Biology and Clinical Use. Wiley, Chichester, pp. 95-107.

96. Moan, J., Boye, E., 1981, Photodynamic effect on DNA and cell survival of human cells sensitized by hematoporphyrin. Photobiochem. Photobiophys. 2, 301-307.

97. Moan, J., Christensen, T., Jacobsen, P.B., 1984, Porphyrin-sensitized photoinactivation of cells *in vitro*, In: Doiron, D.R., Gomer, C.J. (Eds.) Porphyrin Localization and Treatment of Tumors. Alan R. Liss, New-York, pp. 419-442.

98. Moan, J., Juzenas, P., Bagdonas, S., 2000, Degradation and transformation of photosensitizers during light exposure. Recent Res. Devel. Photochem. Photobiol. 4, 121-132.

99. Moan, J., Peng, Q., Sorensen, R., Iani, V., Nesland, J.M., 1998b, The biophysical foundations of photodynamic therapy. Endoscopy 30, 387-391.

100. Moan, J., Rimington, C., Malik, Z., 1988a, Photoinduced degradation and modification of Photofrin II in cells in vitro. Photochem Photobiol 47, 363-367.

101. Moan, J., Streckyte, G., Bagdonas, S., Bech, O., Berg, K., 1997, Photobleaching of protoporphyrin IX in cells incubated with 5-aminolevulinic acid. Int J Cancer 70, 90-97.

102. Moan, J., Western, A., Rimington, C., 1988b, Photomodification of porphyrins in biological systems., In: Moreno, G., Pottier, R.H., Truscott, T.G. (Eds.) Photosensitization. Springer-Verlag, Berlin, Heidelberg, New York, London, Paris, Tokyo, pp. 407-418.

103. Monroe, B.M., 1985, Singlet oxygen in solution: lifetimes and reaction rate constants, In: Frimer, A.A. (Ed.) Singlet oxygen. CRC Press, Boca Raton, pp. 177-221.

104. Morgan, J., Potter, W.R., Oseroff, A.R., 2000, Comparison of photodynamic targets in a carcinoma cell line and its mitochondrial DNA-deficient derivative. Photochem Photobiol 71, 747-757.

105. Morliere, P., Kohen, E., Reyftmann, J.P., Santus, R., Kohen, C., Maziere, J.C., Goldstein, S., Mangel, W.F., Dubertret, L., 1987, Photosensitization by porphyrins

delivered to L cell fibroblasts by human serum low density lipoproteins. A microspectrofluorometric study. Photochem Photobiol 46, 183-191.

106. Morliere, P., Maziere, J.C., Santus, R., Smith, C.D., Prinsep, M.R., Stobbe, C.C., Fenning, M.C., Golberg, J.L., Chapman, J.D., 1998, Tolyporphin: a natural product from cyanobacteria with potent photosensitizing activity against tumor cells in vitro and in vivo. Cancer Res 58, 3571-3578.

107. Moser, J.G., 1998, Definition and general properties of 2nd and 3rd generation photosensitizers, In: Moser, J.G. (Ed.) Photodynamic tumor therapy. 2nd and 3rd generation photosensitizers. Harwood Academic Publishers, Amsterdam, pp. 3-7.

108. Niedre, M., Patterson, M.S., Wilson, B.C., 2002a, Direct near-infrared luminescence detection of singlet oxygen generated by photodynamic therapy in cells in vitro and tissues in vivo. Photochem Photobiol 75, 382-391.

109. Niedre, M.J., Patterson, M.S., Boruvka, N., Wilson, B.C., 2002b, Measurement of singlet oxygen luminescence from AML5 cells sensitized with ALA-induced PpIX in suspension during photodynamic therapy and correlation with cell viability after treatment. Proc. SPIE 4612, 93-101.

110. Niedre, M.J., Secord, A.J., Patterson, M.S., Wilson, B.C., 2003, In vitro tests of the validity of singlet oxygen luminescence measurements as a dose metric in photodynamic therapy. Cancer Res 63, 7986-7994.

111. Niedre, M.J., Yu, C.S., Patterson, M.S., Wilson, B.C., 2005, Singlet oxygen luminescence as an in vivo photodynamic therapy dose metric: validation in normal mouse skin with topical amino-levulinic acid. Br J Cancer 92, 298-304.

112. Ouedraogo, G., Morliere, P., Bazin, M., Santus, R., Kratzer, B., Miranda, M.A., Castell, J.V., 1999, Lysosomes are sites of fluoroquinolone photosensitization in human skin fibroblasts: a microspectrofluorometric approach. Photochem Photobiol 70, 123-129.

113. Parker, J.G., Stanbro, W.D., 1984, Opitical detemination of the rates of formation and decay of O2 in H2O, D2O and other solvents. J Photochem 25, 545-547.

114. Peng, Q., Farrants, G.W., Madslien, K., Bommer, J.C., Moan, J., Danielsen, H.E., Nesland, J.M., 1991, Subcellular localization, redistribution and photobleaching of sulfonated aluminum phthalocyanines in a human melanoma cell line. Int J Cancer 49, 290-295.

115. Peng, Q., Moan, J., Nesland, J.M., 1996, Correlation of subcellular and intratumoral photosensitizer localization with ultrastructural features after photodynamic therapy. Ultrastruct Pathol 20, 109-129.

116. Pogue, B.W., Ortel, B., Chen, N., Redmond, R.W., Hasan, T., 2001, A photobiological and photophysical-based study of phototoxicity of two chlorins. Cancer Res 61, 717-724.

117. Raab, O., 1900, Ueber die Wirkung fluorescirender Stoffe auf Infusorien. Z. Biol (Munich) 39, 524-546.

118. Reddi, E., Jori, G., 1988, Steady state and time resolved spectroscopic studies of photodynamic sensitizers: porphyrins and phthalocyanines. Recv. Chem. Intermed. 10, 241-268.

119. Roberts, W.G., Smith, K.M., McCullough, J.L., Berns, M.W., 1989, Skin photosensitivity and photodestruction of several potential photodynamic sensitizers. Photochem Photobiol 49, 431-438.

120. Robinson, D.J., de Bruijn, H.S., van der Veen, N., Stringer, M.R., Brown, S.B., Star, W.M., 1998, Fluorescence photobleaching of ALA-induced protoporphyrin IX during photodynamic therapy of normal hairless mouse skin: the effect of light dose and irradiance and the resulting biological effect. Photochem Photobiol 67, 140-149.

121. Ronn, A.M., Batti, J., Lee, C.J., Yoo, D., Siegel, M.E., Nouri, M., Lofgren, L.A., Steinberg, B.M., 1997, Comparative biodistribution of meta-Tetra(Hydroxyphenyl) chlorin in multiple species: clinical implications for photodynamic therapy. Lasers Surg Med 20, 437-442.

122. Rosenkranz, A.A., Jans, D.A., Sobolev, A.S., 2000, Targeted intracellular delivery of photosensitizers to enhance photodynamic efficiency. Immunol Cell Biol 78, 452-464.

123. Rotomskiene, J., Kapociute, R., Rotomskis, R., Jonusauskas, G., Szito, T., Nizhnik, A., 1988, Light-induced transformations of hematoporphyrin diacetate and hematoporphyrin. J. Photochem. Photobiol. B 2, 373-379.

124. Rotomskis, R., Bagdonas, S., Streckyte, G., 1996, Spectroscopic studies of photobleaching and photoproduct formation of porphyrins used in tumour therapy. J. Photochem. Photobiol. B 33, 61-67.

125. Rotomskis, R., Bagdonas, S., Streckyte, G., Wendenburg, R., Dietel, W., Didziapetriene, J., Ibelhauptaite, A., Staciokiene, L., 1998, Phototransformation of sensitisers: 3. Implications for Clinical Dosimetry. Lasers Med Sci 13, 271-278.

126. Rotomskis, R., Streckyte, G., Bagdonas, S., 1997a, Phototransformations of sensitizers 1. Significance of the nature of the sensitizer in the photobleaching process and photoproduct formation in aqueous solution. J. Photochem. Photobiol. B 39, 167-171.

127. Rotomskis, R., Streckyte, G., Bagdonas, S., 1997b, Phototransformations of sensitizers 2. Photoproducts formed in aqueous solutions of porphyrins. J. Photochem. Photobiol. B 39, 172-175.

128. Rovers, J.P., de Jode, M.L., Grahn, M.F., 2000a, Significantly increased lesion size by using the near-infrared photosensitizer 5,10,15,20-tetrakis (m-hydroxyphenyl)bacteriochlorin in interstitial photodynamic therapy of normal rat liver tissue. Lasers Surg Med 27, 235-240.

129. Rovers, J.P., de Jode, M.L., Rezzoug, H., Grahn, M.F., 2000b, In vivo photodynamic characteristics of the near-infrared photosensitizer 5,10,15,20-tetrakis(M-hydroxyphenyl) bacteriochlorin. Photochem. Photobiol. 72, 358-364.

130. Rück, A., Beck, G., Bachor, R., Akgun, N., Gschwend, M.H., Steiner, R., 1996, Dynamic fluorescence changes during photodynamic therapy in vivo and in vitro of hydrophilic A1(III) phthalocyanine tetrasulphonate and lipophilic Zn(II) phthalocyanine administered in liposomes. J Photochem Photobiol B 36, 127-133.

131. Rück, A., Hildebrandt, C., Kollner, T., Schneckenburger, H., Steiner, R., 1990, Competition between photobleaching and fluorescence increase of photosensitizing

porphyrins and tetrasulphonated chloroaluminiumphthalocyanine. J Photochem Photobiol B 5, 311-319.

132. Rück, A., Kollner, T., Dietrich, A., Strauss, W., Schneckenburger, H., 1992, Fluorescence formation during photodynamic therapy in the nucleus of cells incubated with cationic and anionic water-soluble photosensitizers. J Photochem Photobiol B 12, 403-412.

133. Sasnouski, S., Zorin, V., Khludeyev, I., D'Hallewin, M.A., Guillemin, F., Bezdetnaya, L., in revision, Investigation of Foscan interactions with plasma proteins. Biochim Biophys Acta.

134. Savary, J.F., Grosjean, P., Monnier, P., Fontolliet, C., Wagnieres, G., Braichotte, D., van den Bergh, H., 1998, Photodynamic therapy of early squamous cell carcinomas of the esophagus: a review of 31 cases. Endoscopy 30, 258-265.

135. Savary, J.F., Monnier, P., Fontolliet, C., Mizeret, J., Wagnieres, G., Braichotte, D., van den Bergh, H., 1997, Photodynamic therapy for early squamous cell carcinomas of the esophagus, bronchi, and mouth with m-tetra (hydroxyphenyl) chlorin. Arch Otolaryngol Head Neck Surg 123, 162-168.

136. Schneider, T., Gugliotti, M., Politi, M.J., Baptista, M.S., 2000, Quantitative determination of singlet oxygen by laser deflection calorimeter. Analytical Letters 33, 297-305.

137. Schweitzer, C., Schmidt, R., 2003, Physical mechanisms of generation and deactivation of singlet oxygen. Chem Rev 103, 1685-1757.

138. Scully, A.D., Ostler, R.B., MacRobert, A.J., Parker, A.W., de Lara, C., O'Neill, P., Phillips, D., 1998, Laser line-scanning confocal fluorescence imaging of the photodynamic action of aluminum and zinc phthalocyanines in V79-4 Chinese hamster fibroblasts. Photochem Photobiol 68, 199-204.

139. Sharkey, S.M., Wilson, B.C., Moorehead, R., Singh, G., 1993, Mitochondrial alterations in photodynamic therapy-resistant cells. Cancer Res 53, 4994-4999.

140. Sharman, W.M., Allen, C.M., van Lier, J.E., 2000, Role of activated oxygen species in photodynamic therapy. Methods Enzymol 319, 376-400.

141. Singh, G., Jeeves, W.P., Wilson, B.C., Jang, D., 1987, Mitochondrial photosensitization by Photofrin II. Photochem Photobiol 46, 645-649.

142. Sørensen, R., Iani, V., Moan, J., 1998, Kinetics of photobleaching of protoporphyrin IX in the skin of nude mice exposed to different fluence rates of red light. Photochem Photobiol 68, 835-840.

143. Spikes, J.D., 1985, The historical development of ideas on applications of photosensitised reactions in health sciences, In: Bergasson, R.V., Jori, G., Land, E.J., Truscott, T.G. (Eds.) Primary photoprocesses in Biology and Medicine. Plenum Press, New York, New York, pp. 209-227.

144. Spikes, J.D., 1992, Quantum yields and kinetics of the photobleaching of hematoporphyrin, Photofrin II, tetra(4-sulfonatophenyl)-porphine and uroporphyrin. Photochem. Photobiol. 55, 797-808.

145. Spikes, J.D., Bommer, J.C., 1993, Photobleaching of mono-L-aspartyl chlorin e6 (NPe6): a candidate sensitizer for the photodynamic therapy of tumors, In: Photochem Photobiol. pp. 346-350.

146. Strauss, W.S., Sailer, R., Gschwend, M.H., Emmert, H., Steiner, R., Schneckenburger, H., 1998, Selective examination of plasma membrane-associated photosensitizers using total internal reflection fluorescence spectroscopy: correlation between photobleaching and photodynamic efficacy of protoporphyrin IX. Photochem Photobiol 67, 363-369.

147. Streckyte, G., Berg, K., Moan, J., 1994, Photomodification of ALA-induced protoporphyrin IX in cells *in vitro*. SPIE Photodynamic of Cancer II 2325, 58-65.

148. Streckyte, G., Rotomskis, R., 1993a, Phototransformation of porphyrins in aqueous and micellar media. J Photochem Photobiol B 18, 259-263.

149. Streckyte, G., Rotomskis, R., 1993b, Phototransformation of porphyrins under clinically relevant light irradiation. Biology 3, 26-31.

150. Szeimies, R.M., Dräger, J., Abels, C., Landthaler, M., 2001, History of photodynamic therapy in dermatology, In: Calzavara-Pinton, P., Szeimies, R.M., Ortel, B. (Eds.) Photodynamic therapy and fluorescence diagnosis in dermatology. Elsevier Science.

151. Teiten, M.H., Bezdetnaya, L., Morliere, P., Santus, R., Guillemin, F., 2003, Endoplasmic reticulum and Golgi apparatus are the preferential sites of Foscan localisation in cultured tumour cells. Br J Cancer 88, 146-152.

152. van Lier, J.E., Spikes, J.D., 1989, The chemistry, photophysics and photosensitizing properties of phthalocyanines. Ciba Found Symp 146, 17-26; discussion 26-32.

153. Vever-Bizet, C., Dellinger, M., Brault, D., Rougee, M., Bensasson, R.V., 1989, Singlet molecular oxygen quenching by saturated and unsaturated fatty-acids and by cholesterol. Photochem Photobiol 50, 321-325.

154. von Tappeiner, H., Jesionek, A., 1903, Terapeutische versuche mit fluoreszierenden Stoffen. Münch. Med. Wochenschr. 50, 2042-2044.

155. von Tappeiner, H., Jodlbauer, A., 1904, Ueber die Wirkung der photodynamischen (fluorescierenden) Stoffe auf Protozoen und Enzyme. Arch. Klin. Med. 80, 427-487.

156. Whelpton, R., Michael-Titus, A.T., Basra, S.S., Grahn, M., 1995, Distribution of temoporfin, a new photosensitizer for the photodynamic therapy of cancer, in a murine tumor model. Photochem Photobiol 61, 397-401.

157. Whelpton, R., Michael-Titus, A.T., Jamdar, R.P., Abdillahi, K., Grahn, M.F., 1996, Distribution and excretion of radiolabeled temoporfin in a murine tumor model. Photochem Photobiol 63, 885-891.

158. Wilkinson, F., Brummer, J.G., 1981, Rate constants for the decay and reactions of the lowest electronically excited singlet state of molecular oxygen in solution. J Phys Chem Ref Data 10, 809-999.

159. Wilkinson, F., Ho, W.T., 1978, Electronic energy transfer from singlet molecular oxygen to carotenoids. Spectrosc. Lett. 11, 455-457.

160. Wilson, B.C., Olivo, M., Singh, G., 1997a, Subcellular localization of Photofrin and aminolevulinic acid and photodynamic cross-resistance in vitro in radiation-induced

fibrosarcoma cells sensitive or resistant to photofrin-mediated photodynamic therapy. Photochem Photobiol 65, 166-176.

161. Wilson, B.C., Patterson, M.S., Lilge, L., 1997b, Implicit and explicit dosimetry in photodynamic therapy: a new paradigm. Lasers Med. Sci. 12, 182-199.

162. Wood, S.R., Holroyd, J.A., Brown, S.B., 1997, The subcellular localization of Zn(II) phthalocyanines and their redistribution on exposure to light. Photochem Photobiol 65, 397-402.

163. Xue, L.Y., Chiu, S.M., Oleinick, N.L., 2001, Photodynamic therapy-induced death of MCF-7 human breast cancer cells: a role for caspase-3 in the late steps of apoptosis but not for the critical lethal event. Exp Cell Res 263, 145-155.

164. Yow, C.M., Chen, J.Y., Mak, N.K., Cheung, N.H., Leung, A.W., 2000, Cellular uptake, subcellular localization and photodamaging effect of temoporfin (mTHPC) in nasopharyngeal carcinoma cells: comparison with hematoporphyrin derivative. Cancer Lett 157, 123-131.

165. Zang, L.Y., Zhang, Z.Y., Misra, H.P., 1990, EPR studies of trapped singlet oxygen (1O2) generated during photoirradiation of hypocrellin A. Photochem Photobiol 52, 677-683.

166. Zeng, H., Korbelik, M., McLean, D.I., MacAulay, C., Lui, H., 2002, Monitoring photoproduct formation and photobleaching by fluorescence spectroscopy has the potential to improve PDT dosimetry with a verteporfin-like photosensitizer. Photochem. Photobiol. 75, 398-405.

167. Zucker, R.M., Price, O., 2001, Evaluation of confocal microscopy system performance. Cytometry 44, 273-294.

Annexes

APPENDIX

French Summary

Introduction

La Thérapie photodynamique est devenue une modalité de traitement de certaines maladies cancéreuses et non cancéreuses. Le traitement PDT est basé sur la présence d'une molécule avec des propriétés photosensibilisantes et de localisation tumorale, de lumière et d'oxygène. Séparément ces trois éléments sont inoffensifs, mais peuvent acquérir un pouvoir destructeur lorsqu'ils sont administrés de façon concomitante.

Une dosimétrie précise est nécessaire pour assurer l'efficacité et la reproductibilité du traitement. Il est largement accepté que l'espèce assurant l'efficacité du traitement est l'oxygène singulet et qu'il résulte de l'irradiation d'un photosensibilisant à une longueur d'onde appropriée. Les variations de plusieurs paramètres au cours du traitement tels que : la concentration et la localisation du photosensibilisant, ainsi que les propriétés optiques des tissus font de la dosimétrie un élément très difficile à maîtriser.

La *m*-THPBC est photosensibilisant de seconde génération, appartenant à la famille des tetraphenylchlorines. Bien que beaucoup de propriétés des photosensibilisants appartenant à cette famille soient connues, les propriétés de la *m*-THPBC ont été très peu étudiées. Le premier objectif de cette étude a été d'évaluer les propriétés de photoblanchiment de la *m*-THPBC en solution. Puis nous avons effectué un travail *in vitro* afin de comparer certaines propriétés de la *m*-THPBC avec celles de la *m*-THPC.

Introduction Bibliographique

1. Généralités

La thérapie photodynamique (PDT) est un traitement alternatif employé à des fins curatives pour des tumeurs solides de petites tailles, telles que les tumeurs du poumon, vessie, tête et cou, œsophage, et de la peau. Elle est aussi utilisée à visée palliative dans le cas de grosses tumeurs infiltrantes ou récidivantes.

Cette technique est basée sur l'activation par la lumière d'une molécule, appelée photosensibilisant, se répartissant de manière prépondérante dans le tissu néoplasique (Kessel and Woodburn, 1993). Le photosensibilisant non toxique à l'obscurité, génère sous l'effet

d'une irradiation lumineuse des processus photochimiques produisant des espèces chimiques cytotoxiques.

Trois mécanismes essentiels sont impliqués dans la destruction tumorale par PDT (Dougherty et al., 1998; Peng et al., 1996) :
(i) *destruction directe des cellules tumorales*, conséquence de l'altération des fonctions des organelles cellulaires et des systèmes biomembranaires par effet direct de la PDT ; (ii) *destruction indirecte des cellules tumorales* qui se produit par la destruction première de la néo-vascularisation tumorale ; le processus est suivi par l'hypoxie et finalement aboutit à la mort des cellules néoplasiques dans la tumeur; (iii) *destruction par effets immunologiques*, parce que la PDT cause la libération de cytokines et d'autres médiateurs inflammatoires par les cellules traitées produisant une réponse inflammatoire et recrutant des cellules immunocompétentes (lymphocytes et phagocytes). La contribution de chaque mécanisme à la réponse tumorale générale dépend du photosensibilisant et de la tumeur. Il semble probable que *tous ces mécanismes s'associent pour assurer le contrôle tumoral à long terme*.

2. Les réactions photochimiques

Les réactions photochimiques caractérisent l'effet direct de la PDT. Après absorption d'un photon d'énergie hν, le photosensibilisant est excité et passe d'un niveau d'énergie fondamental à un niveau singulet excité.
Le retour au niveau singulet fondamental s'effectue en quelques nanosecondes sauf dans le cas d'une transition inter-système, où par rotation de spin le photosensibilisant passe d'un état singulet excité à un état triplet de moindre énergie avec une durée de vie allant jusqu'à la milliseconde. Ce délai permet au photosensibilisant de réagir avec les molécules de son environnement proche avant de redescendre à son niveau d'énergie fondamental.

Ces réactions photochimiques peuvent être de deux types :

La réaction photochimique de type I :

Elle conduit le photosensibilisant dans son état triplet ($^3P^*$) à réagir avec un substrat en produisant des radicaux libres, chargés ou neutres. Ces réactions consistent, soit en un transfert d'hydrogène vers le photosensibilisant avec formation de radicaux libres neutres, soit en un transfert d'électron avec formation d'une forme ionique chargée. Les radicaux formés réagissent avec l'oxygène moléculaire ($^3O_2$), aboutissant à la formation de produits de

photooxydation très puissants. Les espèces réactive de l'oxygène ainsi produites sont l'anion superoxide, le peroxyde d'hydrogène et le radical hydroxyle .

La réaction photochimique de type II :

Ce phénomène est préférentiel dans les tissus bien oxygénés, par transfert d'énergie il y a réaction entre le photosensibilisant dans son état triplet ($^3P^*$) et l'oxygène moléculaire ($^3O_2$), pour aboutir à l'oxygène singulet ($^1O_2$). Ce dernier est une molécule très réactive, hautement toxique et de faible durée de vie. Ce qui lui permet de réagir dans un rayon de 10 à 20 nm avec des substrats cellulaires pour donner principalement des peroxydes.

3. Les photosensibilisants

3.1. Généralités

On dénombre aujourd'hui trois classes de photosensibilisants: ceux de première, seconde et troisième génération. Ce qui caractérise les photosensibilisants de seconde génération par rapport à leurs prédécesseurs est une modification des substituants du noyau tétrapyrolique, ce qui à pour effet de changer le spectre d'absorption de la molécule et d'augmenter la sélectivité tumorale. Quant aux photosensibilisants de troisième génération ils sont généralement couplés à une autre molécule (BSA, EGF…) ou encapsulés (liposomes…).

3.2. Le photosensibilisant idéal en Thérapie Photodynamique

Bonnett et Mac Robert en 1989 ont défini les caractéristiques d'un photosensibilisant idéal afin aboutir à une action photodynamique efficace (Bonnett et al., 1989; MacRobert et al., 1989).

- Le photosensibilisant recherché en PDT doit avoir un rendement quantique en oxygène singulet élevé, afin d'induire des réactions photochimiques importantes.
- Il doit posséder une absorption optimale dans le rouge entre 650 et 800 nm, là où les tissus sont les plus transparents à la lumière. Son absorption doit être faible dans les longueurs d'ondes du rayonnement solaire.
-Il doit être sélectif vis-à-vis de la tumeur, en étant de préférence amphiphile, pour une solubilité satisfaisante dans milieux hydrophiles et hydrophobes. Cette caractéristique va lui permettre de s'incorporer dans les organites cellulaires, ainsi que dans les membranes de ces organites.

- Il doit être pur et non toxique en absence de lumière, pour que la photosensibilisation cutanée soit faible et courte. Le photosensibilisant doit avoir une clairance rapide.

4. Le Photoblanchiment

La plupart des photosensibilisants utilisés en PDT, tels que les molécules de type porphyrines, chlorines et phtalocyanines, ne sont pas photostables. En solution ou dans un environnement complexe, ils subissent des modifications induites par la lumière qui se traduisent par une diminution de leur intensité initiale d'absorption, et de ce fait une diminution de leurs activités phototoxiques.

Les modifications spectrales de la fluorescence des porphyrines dans les cellules peuvent être dues à trois phénomènes (Bonnett et al., 1999b; Bonnett and Martínez, 2001; Moan et al., 2000) :

-La photodégradation ou « *true photobleaching* » , c'est à dire la conversion du photosensibilisant en produits qui n'absorbent pas la lumière visible de manière significative, accompagnée de la destruction de structure macrocyclique.

-La phototransformation ou « *photomodification* », modification photochimique sans destruction du macrocycle, qui conduit à la formation de nouveaux photoproduits absorbant dans le rouge.

4.1. Mécanismes de photoblanchiment.

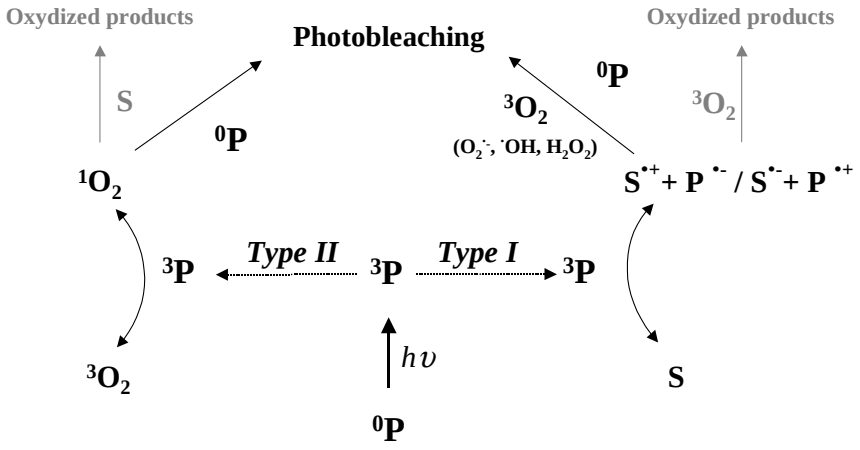

Figure 1. : Mécanismes de photoblanchiment intervenant après l'absorption d'un photon par le photosensibilisant.

Les mécanismes de photoblanchiment empruntent les même voies que les mécanismes de cytotoxicité, c'est à dire les mécanismes de Type I et de Type II, dans ce cas le substrat oxydé se trouve être le photosensibilisant.

De nombreux éléments influencent les mécanismes de photoblanchiment, à savoir :

- L'état d'agrégation, le pH, la force ionique et les surfactants.
- La concentration en oxygène.
- Les « quenchers » de Type I & II.
- Les substrats photo-oxidables.

4.2. Paramètres affectant la cinétique photoblanchiment.

Le photoblanchiment a longtemps été considéré comme étant un mécanisme uniquement dépendant de la dose de lumière délivrée au tissu, décrit par une décroissance mono-exponentielle de type $e^{-\alpha D}$, ou α représente la constante de photoblanchiment et D représente la fluence (J cm^{-2}) de l'irradiation. Or il est apparu que les cinétiques de photoblanchiment sont des phénomènes complexes qui ne peuvent pas être décrits par une simple décroissance mono-exponentielle (Moan et al., 2000; Sørensen et al., 1998). Plusieurs paramètres peuvent influencer la cinétique du photoblanchiment tels que la présence de différent sites de liaison des photosensibilisants dans les tissus ou cellules, la relocalisation du photosensibilisant pendant l'irradiation et la déplétion en oxygène durant le traitement.

4.3. Formation de Photoproduits.

La plupart des photosensibilisants utilisés en thérapie photodynamique, tels que les porphyrines et leurs dérivés, subissent une dégradation progressive au cours de l'irradiation, appelée photoblanchiment, qui se traduit par une diminution de leur capacité à absorber la lumière (Rotomskis et al., 1996; Spikes, 1992).

Le phénomène de photoblanchiment est communément évalué par la mesure de la décroissance de fluorescence photoinduite du photosensibilisant. Cependant, les résultats obtenus par cette méthode doivent être interprétés avec précaution. En effet, la mesure de fluorescence ne reflète pas uniquement la photodégradation et les photomodifications subies par le photosensibilisant mais également les changements d'environnement du photosensibilisant. La migration du photosensibilisant d'un site de liaison à un autre au cours de l'irradiation, la photorelocalisation, contribue ainsi à la diminution de l'intensité

d’émission de fluorescence et aux modifications observées dans la forme du spectre (Moan et al., 1997).

Objectifs

L’objectif principal de ce travail était d’appréhender les mécanismes du photoblanchiment de la *m*-THPBC et son rôle dans le résultat du traitement PDT. Le travail s’est organisé en deux parties :

Une première approche du photoblanchiment de la *m*-THPBC en solution a été realisée. La vitesse, la cinétique, les photoproduits du photoblanchiment ainsi que les espèces responsables du phénomène ont été étudiés.

Dans un deuxième temps une étude in vitro a été réalisée sur cellules WiDr. Une étude comparative a été effectuée entre la *m*-THPBC et la *m*-THPC, un photosensibilisant de deuxième génération très actif. Les caractéristiques du photoblanchiment ont été déterminées, ainsi que la toxicité des photosensibilisants et leurs localisation intra-cellulaires dans nos conditions expérimentales.

Résultats

Photodégradation et phototransformation de la m-THPBC en solution.

Les cinétiques de photoblanchiment et la formation de photoproduits lors de l’irradiation (735 nm) de la 5,10,15,20-tetrakis(m-hydroxyphényl)bactériochlorine (*m*-THPBC) dans une solution de tampon phosphate supplémentée avec de l’albumine de sérum humain (HSA) ont été étudiées par spectroscopie d’absorption et spectroscopie de fluorescence. Les mesures ont été réalisées soit immédiatement après que le photosensibilisant a été dissout dans la solution HSA (0h), soit après 6 heures d’incubation dans la solution HSA (6h). Les études spectroscopiques ont indiqué que la molécule était principalement présente sous forme d’agrégats dans les solutions fraîchement préparées, alors que l’incubation favorise la monomérisation. Indépendamment du temps d’incubation, les taux de photoblanchiment obtenus par mesures de fluorescence ont été plus élevés que ceux obtenus par mesures d’absorbance. Le photoblanchiment de *m*-THPBC fraîchement préparée peut être décrit

comme une décroissance mono-exponentielle, alors que les baisses d'absorbance et de fluorescence des solutions de photosensibilisant incubé correspondent à une décroissance bi-exponentielle. Les deux taux de photoblanchiment reflètent probablement les différences dans la photosensibilité des formes monomères (liées aux protéines) et agrégées (non liées).

L'irradiation de la solution de *m*-THPBC fraîchement préparée a induit la phototransformation de 50% de *m*-THPBC photoblanchie en 5,10,15,20-tetrakis(m-hydroxyphényl)chlorine (*m*-THPC), un photosensibilisant de seconde génération utilisé en clinique. Pour une irradiation 6 h après dissolution de la *m*-THPBC, différentes cinétiques de la formation de *m*-THPC ont été observées. Une baisse rapide dans la concentration de la *m*-THPBC a été accompagnée par une formation lente de *m*-THPC. Le rendement quantique de ce processus était faible puisque 5% de *m*-THPBC ont été transformés en *m*-THPC.

Les caractéristiques cinétiques du photoblanchiment de la *m*-THPBC rapportées dans cette étude, ainsi que les différentes cinétiques de formation de photoproduits pendant le photoblanchiment de la *m*-THPBC peuvent fournir des indications importantes dans la dosimétrie de la *m*-THPBC-PDT.

Analyse en MALDI-TOFMS des photoproduits issu de la dégradation de la m-THPBC.

La formation de photoproduits lors de l'irradiation (739 nm) de la 5,10,15,20-tetrakis (m-hydroxyphényl) bactériochlorine (*m*-THPBC) dans un tampon phosphate (PBS) supplémenté d'albumine de sérum humain (HSA) a été étudiée par spectroscopie d'absorption et par spectrométrie de masse MALDI-TOF. Les expérimentations ont été réalisées avec une solution fraîchement préparée de PBS-HSA de *m*-THPBC et avec une solution *m*-THPBC PBS-HSA incubée pendant 6 heures à 37°C. L'incubation de la solution de *m*-THPBC induit la monomérisation du colorant alors que dans la solution fraîchement préparée, la *m*-THPBC est sous forme agrégée. Indépendamment des conditions d'incubation, les expérimentations de photoblanchiment effectuées par spectroscopie d'absorption démontrent la dégradation du photosensibilisant et sa phototransformation en *m*-THPC. De plus, la *m*-THPC est le seul photoproduit détecté en utilisant la spectroscopie d'absorption. La spectrométrie de masse MALDI-TOF a non seulement mis en évidence la dégradation de la *m*-THPBC et la formation de *m*-THPC, mais aussi d'autres modifications photoinduites. Les photoproduits comme la di-hydroxy *m*-THPBC et la di-hydroxy *m*-THPC ont été détectées dans les deux conditions d'incubation, cependant la formation de photoproduits hydroxylés a été significativement plus élevée dans la solution incubée. Nous avons en outre observé de petites molécules provenant

de la fragmentation du photosensibilisant et identifiées comme dérivés dipyrines et synthon dipyrolique.

Photoblanchiment de la m-THPC et de la m-THPBC en présence de différents types de quenchers

Le photoblanchiment intervient par l'intermédiaire de deux types de réaction, le Type I et le Type II. Comme nous l'avons déjà évoqué, le Type I met en jeux les espèces réactives de l'oxygène, alors que le Type II fait intervenir exclusivement l'oxygène singulet. Afin de déterminer l'implication de chacun des mécanismes dans le processus de photoblanchiment de la *m*-THPC et de la *m*-THPBC, nous avons réalisé des expériences de photoblanchiment en présence ou non de « quenchers » de Type I ou de Type II. Il s'agissait des enzymes anti-oxydante superoxyde dismutase (SOD), et catalase (CAT) pour les quenchers de type I. Le DABCO et l'histidine ont été utilisé comme quenchers de type II. Les résultats obtenus étaient une absence d'impact des quenchers de type I sur le photoblanchiment des photosensibilisant alors que l'ajout de quenchers de type II conduisait à une réduction de la vitesse de photoblanchiment de 40% pour la *m*-THPC et de 25% pour la *m*-THPBC signifiant que l'oxygène singulet était l'espèce responsable du photoblanchiment de la *m*-THPC et de la *m*-THPBC.

Etude in vitro des propriétés photobiologiques de la m-THPC et de la m-THPBC.

Après avoir étudié le photoblanchiment de la *m*-THPBC en solution, nous nous sommes intéressés aux propriétés photobiologiques de ce photosensibilisant *in vitro*. Nous avons tout d'abord démontré par une étude en spectrophotométrie que les photosensibilisants *m*-THPC et *m*-THPBC étaient sous forme monomère dans les cellules WiDr lorsque celles-ci étaient incubées pendant 24 heures avec 1.45 µM de photosensibilisant. Il a ensuite été montré que les cinétiques de photoblanchiment intra-cellulaire des ces photosensibilisants étaient très différentes. La cinétique de photoblanchiment de la *m*-THPBC est apparue rapide, de premier ordre et mono-exponentielle, alors que la cinétique de photoblanchiment de la *m*-THPC a été montré comme étant de deuxième ordre, bi-exponentielle et plus lente (3 à 5 x moins) que celle de la *m*-THPBC. La phototoxicité de ces photosensibilisants a été étudiée dans les mêmes conditions que le photoblanchiment. La *m*-THPC s'est révélée être 4 fois plus active que la *m*-THPBC, les doses de lumière nécessaire pour détruire 50% des cellules (LD_{50}) étaient 0.7 J cm^{-2} pour la *m*-THPBC et 0.17 J cm^{-2} pour la *m*-THPC.

La différence de photoblanchiment ne peut pas s'expliquer par une différence d'état d'agrégation de la molécule, il a été montré auparavant que les deux photosensibilisants étaient tous deux dans des formes monomères, mais une différence de localisation du photosensibilisant dans la cellule entraînant une différence d'environnements expliquerait la disparité au niveau des propriétés de photoblanchiment de ces deux photosensibilisants. Dans ce but nous avons effectué une étude de la distribution intra cellulaire de la *m*-THPBC et de la *m*-THPC dans les cellules WiDr par microscopie de fluorescence et microspectrofluorimetrie. Ceci a montré un localisation surtout dans le réticulum endoplasmique pour la *m*-THPC, alors que la *m*-THPBC s'accumule préférentiellement dans les mitochondries. Cette différence de localisation intra-cellulaire est très intéressante puisqu'elle peut expliquer d'une part la différence de photoblanchiment observée ainsi que la différence de photocytotoxicité.

Conclusion et perspectives

L'analyse des photoproduits formés après l'irradiation de la *m*-THPBC a été évaluée par spectroscopie UV-Vis et par spectrométrie de masse. Les résultats obtenus ont montré que la formation de photoproduits était influencée significativement par l'état d'agrégation de la *m*-THPBC. En sachant que le photosensibilisant se trouve sous forme monomérisée mais aussi sous forme agrégée dans la cellule, il serait intéressant de réaliser des expérimentations avec une double longueur d'onde d'irradiation (739 nm pour la *m*-THPBC et 652 nm pour le photoproduit : la *m*-THPC). Les études menées en MALDI-TOF MS ont révélé la présence de produits di-hyroxylés. La séparation de ces composés permettrait de tester leurs propriétés photobiologiques telle que leur fluorescence, absorbance et photocytotoxicité. Les expérimentations in vitro avec la *m*-THPBC ont démontré une importante phototoxicité et un photoblanchiment rapide, de premier ordre. Ces résultats, accompagné des résultats obtenus in vivo, à savoir une bonne accumulation de la *m*-THPBC dans les tissus tumoraux, ainsi qu'un photoblanchiment rapide de ce photosensibilisant permet d'envisager des résultats prometteurs dans l'utilisation de la *m*-THPBC en clinique. Ces propriétés pourraient être utilisées pour effectuer des expérimentations afin de trouver la dose optimale de lumière et de photosensibilisant à administrer dans le but de limiter les effets secondaire sur les tissus sains environnants.

Abbreviations

AMD	age related macular degeneration
CAT	catalase
DABCO	1,4-diazobicyclo[2,2,2]octane
DMPO	5,5-dimethyl-pyrroline-1-oxide
DPA	9,10-Diphenylanthracene
DPBF	1,3-Diphenylisobenzofuran
EPR	electron paramagnetic resonance
FCS	fœtal calf serum
FDA	Food and Drug Administration
GSH	glutathione
HpD	Haematoporphyrin derivative
HSA	human serum albumin
IC	internal conversion
ISC	intersystem crossing
LDC	laser deflection calorimeter
m-THPBC	5,10,15,20-tetrakis(*m*-hydroxyphenyl)bacteriochlorin
m-THPC	5,10,15,20-tetrakis(*m*-hydroxyphenyl)chlorin
m-THPP	5,10,15,20-tetrakis(*m*-hydroxyphenyl)porphyrin
PBS	phospate buffer saline
PDT	photodynamic therapy
SOD	superoxide dismutase
TEMP	2,2,6,6-tetramethyl-4-piperidone
TEMPO	2,2,6,6-tetramethyl-4-piperidone-N-oxyl
VR	vibrational relaxation
MeOH	Methanol

Scientific Works

Publications

Photodegradation and phototransformation of 5,10,15,20-tetrakis(m-hydroxyphenyl) bacteriochlorin (*m*-THPBC) in solution.
Henri-Pierre Lassalle, Lina Bezdetnaya, Vladimir Iani, Asta Juzeniene, François Guillemin and Johan Moan, *Photochem. Photobiol. Sci*., 2004, 3, 999-1005.

Characterization of photoproducts of *m*-THPP in aqueous solution.
Natacha Lourette, Benoît Maunit, Lina Bezdetnaya, Henri-Pierre Lassalle, François Guillemin, and Jean-François Muller, *Photochem Photobiol*., 2005, 81, 3, 691-696.

MALDI-TOF mass spectrometry analysis for the characterization of the *m*-THPBC photoproduct formation in a biological environment.
Henri-Pierre Lassalle, Natacha Lourette, Benoît Maunit, Jean-François Muller, François Guillemin and Lina Bezdetnaya, *J. Mass Spectrom*. 2005, 40, 9, 1149-1156.

Oral presentations

Photodegradation and phototransformation of 5,10,15,20-tetrakis(m-hydroxyphenyl) bacteriochlorin (*m*-THPBC) in solution.
Henri-Pierre Lassalle, Lina Bezdetnaya, François Guillemin and Johan Moan, *European Society for Photobiology Congress* (Vienna, 6-11 September 2003).

Photobiological properties of Foscan® (*m*-THPC) and Bacteriochlorin (*m*-THPBC) in cells.
Henri-Pierre Lassalle, Johan Moan, François Guillemin and Lina Bezdetnaya, *American Society for Photobiology Congress* (Seattle, 10-14 July 2004).

Photobleaching and photocytotoxicity of Foscan® (*m*-THPC) and the corresponding Bacteriochlorin (*m*-THPBC) in cells.
Henri-Pierre Lassalle, Johan Moan, François Guillemin and Lina Bezdetnaya, *Joint meeting of the Italian and French photobiology society* (Pisa, 9-10 September 2004).

Posters

Influence of constitutive NF-kB activity on photodynamic therapy efficiency in head and neck carcinoma cell lines.

H.-P. Lassalle, M. Barberi-Heyob, J.-L. Merlin, C. Didelot, P. Becuwe, M. Dauça, and F. Guillemin, *American Association for Cancer research*, vol. 43, 2002.

Photodégradation et phototransformation de la 5,10,15,20-tetrakis(m-hydroxyphenyl) bacteriochlorin (*m*-THPBC), photosensibilisant utilisé en thérapie photodynamique.

Lassalle H-P, Moan J, Bezdetnaya L, Guillemin F, *Eurocancer Congress 2003* (Paris, 8-10 july 2003).

Photodégradation et phototransformation de la 5,10,15,20-tetrakis(m-hydroxyphenyl) bacteriochlorin (*m*-THPBC), photosensibilisant utilisé en thérapie photodynamique.

Lassalle H-P, Moan J, Bezdetnaya L, Guillemin F, *Paris-Biophotonique Symposium 2003* (Paris, 22 octobrer 2003).

Photochemistry and Photobiology, 2005, 81: 691–696

Characterization of Photoproducts of *m*-THPP in Aqueous Solution¶

Natacha Lourette[1], Benoît Maunit[1], Lina Bezdetnaya[2], Henri-Pierre Lassalle[2], François Guillemin[2] and Jean-François Muller*[1]

[1]Laboratoire de Spectrométrie de Masse et de Chimie Laser (LSMCL), Université Paul Verlaine-Metz, Institut de Physique et d'Electronique de Metz (IPEM), Metz, France
[2]Centre Alexis Vautrin, Centre de Recherche en Automatique de Nancy (CRAN) National de la Recherche Scientifique (CNRS) Unité Mixte de Recherche (UMR) 7039, Cedex, France.

Received 9 June 2005; accepted 28 January 2005

ABSTRACT

This study examined the nature of photoproducts after pulse laser irradiation (647.5 nm) of 5,10,15,20-tetrakis(*meso*-hydroxyphenyl)porphyrin (*m*-THPP) (10 μmol/L) in ethanol-water (1/99, vol/vol) solution. Spectroscopic measurements (UV-visible absorption and fluorescence) and mass spectrometry techniques (matrix-assisted laser desorption-ionization [MALDI] coupled with time-of-flight mass spectrometer [TOF-MS] or tandem time of flight mass spectrometer [TOF/TOF-MS]) were used to follow photomodifications. Spectroscopic measurements evidenced photomodification as the main process after *m*-THPP irradiation. Three oxidized photoproducts at m/z 693.25, 695.24 and 713.25 were characterized by MS. After prolonged irradiation new isotopic distributions were registered at m/z 1355.41, 2031.57, 2707.80 and 3383.98 with MALDI-TOF-MS and TOF/TOF-MS. These new photoproducts were attributed to covalent oligomeric structures as dimer, trimer, tetramer and pentamer of *m*-THPP.

INTRODUCTION

Photodynamic therapy (PDT) (1–5), a minimally invasive procedure, is applied for the treatment of *in situ* and microinvasive, light-accessible tumors. A photosensitizer preferentially retained by diseased tissue upon visible light-induced activation and interaction with molecular oxygen induces a cytotoxic activity and microvascular damage due to the production of reactive oxygen species such as singlet oxygen ($^1O_2$).

Most of the photosensitizers used in PDT degrade rapidly upon irradiation, a phenomenon called photobleaching, which is characterized by a light-induced loss of absorption or emission intensities (6,7). There are two types of irreversible photobleaching that lead to a chemical change (1) photomodification in which the chromophore is retained in a modified form; and (2) true photobleaching characterized by the formation of small fragments that no longer have appreciable absorption in the visible region (8). Photobleaching kinetic characteristics and the nature of photoproducts are strongly influenced by the nature of the photosensitizer and therefore should be established for the given dye.

The 5,10,15,20-tetrakis(*meso*-hydroxyphenyl)porphyrin (*m*-THPP), the corresponding chlorin (*m*-THPC) and bacteriochlorin (*m*-THPBC) represent the class of potent photosensitizers. Evidence was found for the involvement of singlet oxygen in the mechanism of photobleaching of all three molecules (8). True photobleaching was reported for the methanol/water (3:2 vol/vol) solutions of *m*-THPC and *m*-THPBC after irradiation with two Philips MLU 300 W lamps (Philips Lighting, Eindhoven, The Netherlands), whereas the corresponding porphyrin reacted more slowly with photomodification (9).

Mass spectrometry (MS) has been shown to be an effective tool for characterizing photomodification products (9–13). Our recent study reported *m*-THPBC and *m*-THPC photomodification products after laser irradiation in ethanol/water (1:99 vol/vol) solution by using matrix-assisted laser desorption-ionization (MALDI) Fourier transform ion cyclotron resonance (FTICR) MS (10). We observed the photoinduced transformation of *m*-THPBC into *m*-THPC, and finally into *m*-THPP by dehydrogenation.

To complete the study of photodegradation of this series of compounds, we have performed MALDI-MS analysis of photoproducts formed after laser light irradiation of ethanol/water (1:99 vol/vol) solutions of *m*-THPP.

MATERIALS AND METHODS

Reagents. *M*-THPP (M_r 678.23 g • mol^{-1}) was kindly provided by Biolitec Pharma Ltd. (Edimbourg, UK) as crystalline powder. The photosensitizer was dissolved in ethanol (Prolabo, Fontenay sous Bois, France) to a concentration of 10^{-3} M. This stock solution of *m*-THPP was further diluted with water to obtain a final concentration of 10^{-5} M in ethanol/water (1/99 vol/vol) mixture. The prepared solution was kept 30 min in the dark at room temperature before being subjected to laser light irradiation.

¶Posted on the website on 2 February 2005
*To whom correspondence should be addressed: Laboratoire de Spectrométrie de Masse et de Chimie Laser (LSMCL), Université de Metz, Institut de Physique et d'Electronique de Metz (IPEM) 1 Bd Arago, Metz-Technopôle, F-57078 Cedex 03, Metz, France. Fax: 33-387-31-5851; e-mail: jfmuller@sciences.univ-metz.fr

Abbreviations: CHCA, α-cyano-4-hydroxy-*trans*-cinnamic acid; DCM, 4-dicyanomethylene-2-methyl-6-(*p*-dimethylaminostyryl)-4*H*-pyran; FTICR, Fourier transform ion cyclotron resonance; LIFT, laser-induced forward transfer; MALDI, matrix-assisted laser desorption-ionization; MS, mass spectrometry; MS/MS, tandem mass spectrometry; *m*-THPBC, 5,10,15,20-tetrakis(*meso*-hydroxyphenyl)bacteriochlorin; *m*-THPC, 5,10,15,20-tetrakis(*meso*-hydroxyphenyl)chlorin; *m*-THPP, 5,10,15,20-tetrakis(*meso*-hydroxyphenyl)porphyrin; *m*-TPP, *meso*-tetraphenylporphyrin; PDT, photodynamic therapy; PSD, postsource decay; TTP, tetraphenylporphyrin; TFA, trifluoroacetic acid; TOF, time of flight; TOF/TOF, tandem time of flight; UV-vis, ultraviolet-visible.

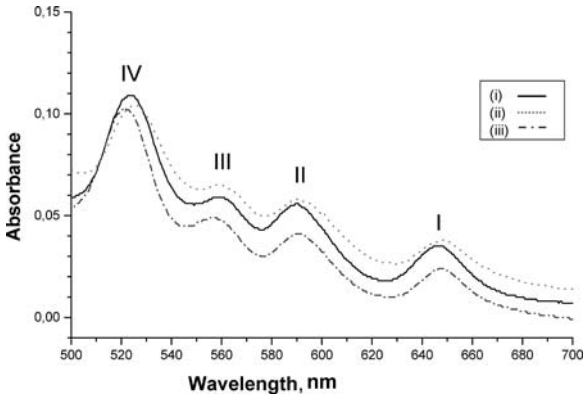

Figure 1. Electronic absorption spectra of *m*-THPP at 10^{-5} M in aqueous solvent (ethanol/water 1:99 vol/vol). i) Non-illuminated *m*-THPP solution. ii) Immediately after 11 min of laser illumination (λ 647.5 nm, output power 270 mW). iii) Immediately after 225 min of laser illumination (λ 647.5 nm, output power 270 mW).

Laser irradiation. The illumination of 3.5 mL of a photosensitizer solution (7 μg/mL, 10^{-5} mol • L^{-1}) in quartz cuvette (path length 0.95 cm) was performed with a dye laser (model TDL 50, Quantel SA, Les Ulis, France) pumped with the second harmonic of a Nd-YAG laser (λ = 532 nm; pulse duration 12 ns; frequency = 10 Hz; output power 3.7 W). For laser irradiation, the dye used was 4-dicyanomethylene-2-methyl-6-(*p*-dimethylaminostyryl)-4*H*-pyran (DCM) (Exciton, Inc, Dayton, OH) to obtain the irradiation wavelength of 647.5 nm; output power was 270 mW, frequency [f] = 10 Hz; and impact diameter was 4 mm. Illumination periods of 11 min and 225 min (t_{ill}) correspond to a total effective illumination time of 0.8 ms and 1.62 ms respectively (total time = $t_{ill} \cdot f \cdot T_p$; $t_{ill} = 225 \times 60 = 13\,500$ s; f = 10 Hz; T_p = 12 ns). Sample irradiation was performed under continuous stirring.

UV-visible (UV-vis) absorption and fluorescence spectra. The absorption spectra were registered using a Lamba 14 UV-vis spectrometer (Perkin-Elmer, Boston, MA) that operates in the spectral range between 190 and 1100 nm. Other parameters were as follows: scan speed 240 nm • min^{-1}, slit widths 2 nm and smooth bandwidth 4 nm. Fluorescence emission spectra were recorded on a fluorolog-2 spectrofluorometer (SPEX Industries, Metuchen, NJ) with excitation wavelength equal to 525 nm. The xenon source is focused onto the entrance slit (2 mm) of the excitation monochromator. Precision cells (Hellma, Müllheim, Germany) made of Quartz SUPRASIL (Shin-Etsu Chemical Co., Tokyo, Japan) with a path length of 0.95 cm were used for absorption and fluorescence measurements.

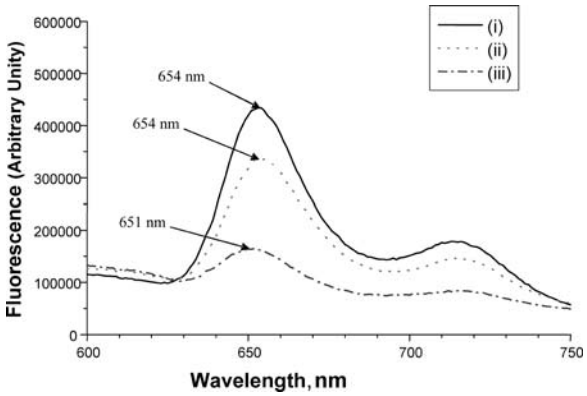

Figure 2. Fluorescence spectra (λ_{exc} 415 nm) of *m*-THPP at 10^{-5} M in aqueous solvent (ethanol/water 1:99 vol/vol). i) Non-illuminated *m*-THPP solution. ii) Immediately after 11 min of laser illumination (λ 647.5 nm, output power 270 mW). iii) Immediately after 225 min of laser illumination (λ 647.5 nm, output power 270 mW).

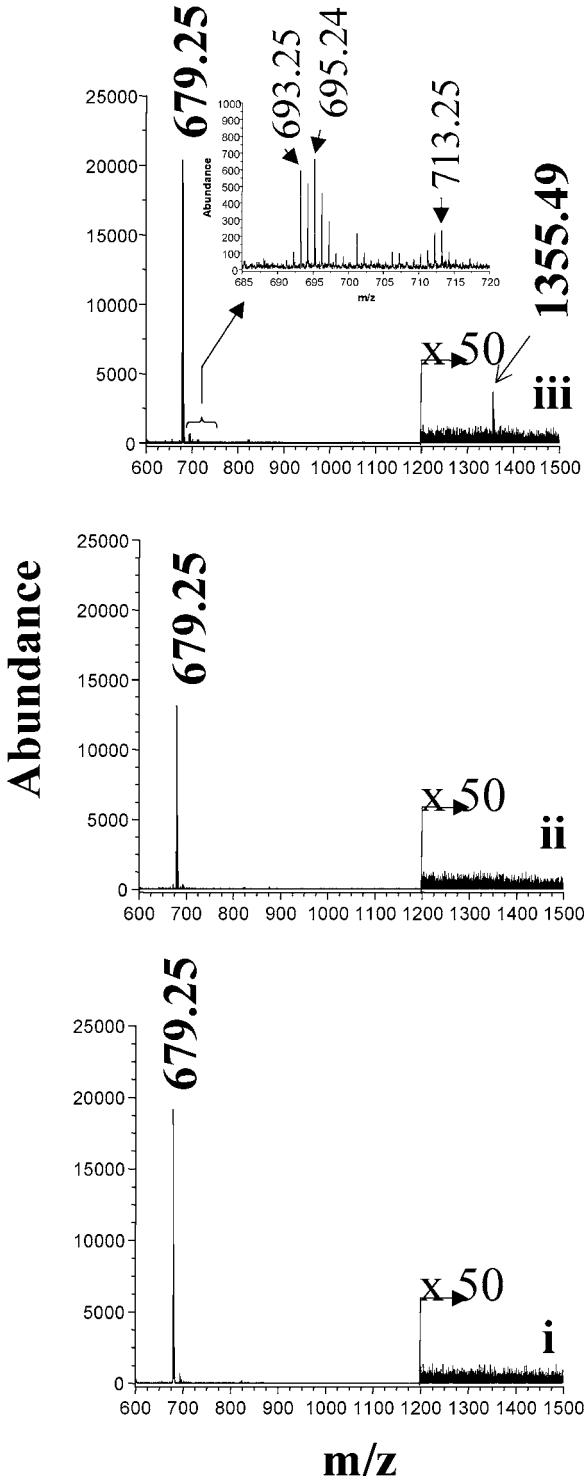

Figure 3. MALDI–TOF MS spectrum of *m*-THPP at 10^{-5} M in aqueous solvent (ethanol/water 1:99 vol/vol). i) Non-illuminated *m*-THPP solution. ii) Immediately after 11 min of laser illumination (λ 647.5 nm, output power 270 mW). iii) Immediately after 225 min of laser illumination (λ 647.5 nm, output power 270 mW).

MALDI sample preparation. The sensitizer solutions were prepared by the standard dried droplet procedure. A 1 μL sample of saturated α-cyano-4-hydroxy-*trans*-cinnamic acid (CHCA) solution in 50% acetonitrile and 0.1% of trifluoroacetic acid (TFA) were spotted on the stainless steel

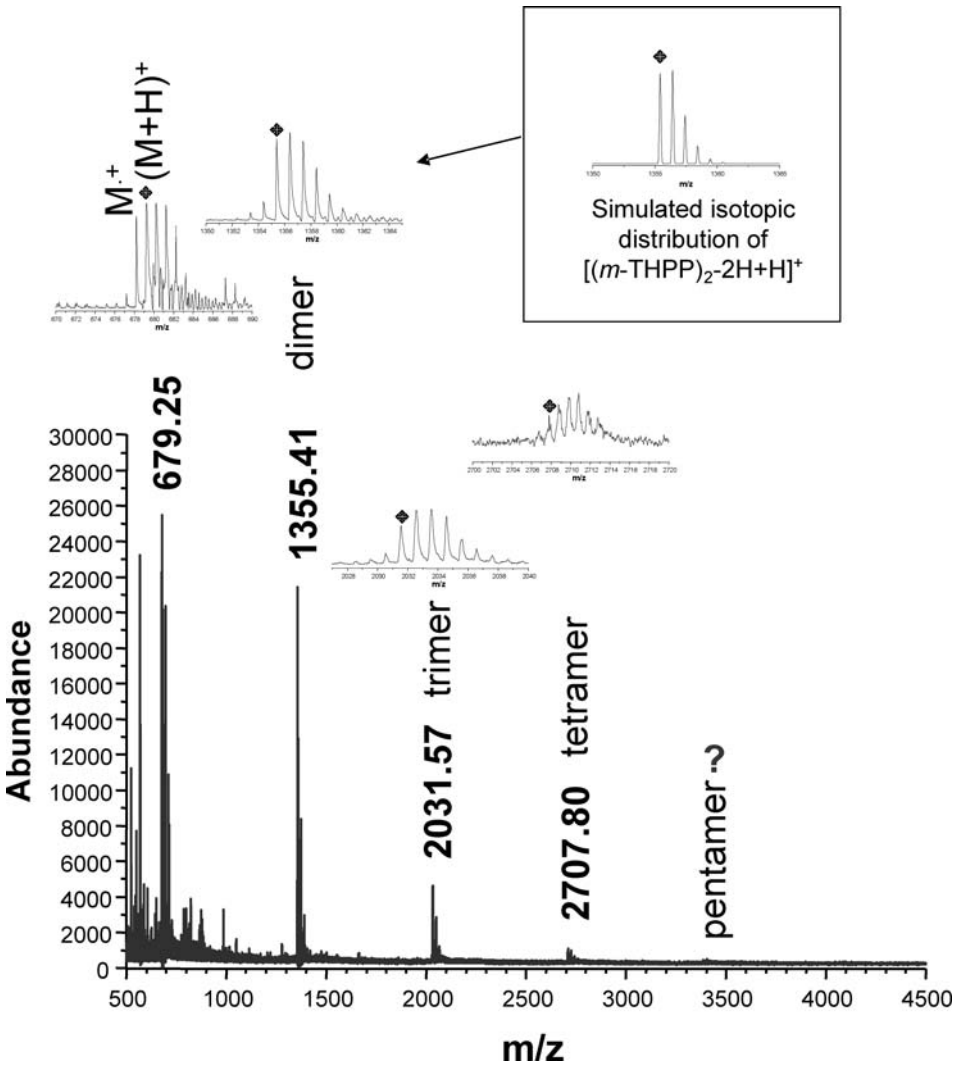

Figure 4. MALDI–TOF MS spectrum of *m*-THPP (10^{-5} M) irradiated at 647.5 nm, during 6 h (monoisotopic ion) and zooms of the isotopic distributions around m/z A: 679.25. B: 1355.41. C: 2031.57 and 2707.80.

MALDI targets. Thus the molar ratio of analyte to matrix was 1:10^4. The solvent was evaporated before insertion in the source.

Time-of-flight (TOF) MS. The sensitizer solutions were prepared by the standard dried droplet procedure. A 1 μL sample of saturated CHCA solution in 50% acetonitrile and 0.1% TFA were spotted on the stainless steel MALDI targets. Thus the molar ratio of analyte to matrix was 1:10^4. The solvent was evaporated before insertion in the source. Mass spectra were acquired over the range of 0–1500 Da.

RESULTS AND DISCUSSION

Spectroscopic measurements of photobleaching of *m*-THPP in ethanol/water solution

The ordered structures of porphyrin pigments formed as a result of nonvalence interactions are now extensively studied. Several studies have shown that porphyrins and related compounds tend to aggregate in aqueous conditions (14–19). Udal'tsov *et al.* presented evidence for self-assembly of large-scale *meso*-tetraphenylporphyrine (*m*-TPP) aggregates resulting from water–porphyrin interactions in aggregates (20). The aggregation is relevant to the biological situation because even in the presence of serum proteins a large fraction of photosensitizers are still present in aggregated form (21,22) and as such could serve as the pool of monomers.

Under our experimental conditions, the absorption spectrum of the ethanol/water (1:99 vol/vol) solution of *m*-THPP (10^{-5} M) compared with that in ethanol displayed a bathochromic shift in the wavelength of the Soret band ($\Delta\lambda = 11.5$ nm) and a broadening of the Soret band with a concomitant reduction in its intensity ($\Delta\varepsilon = 1.76\ 10^5$ L · cm^{-1} · mol^{-1}) (data not shown). Those factors are in favor of an aggregated state of *m*-THPP molecules in aqueous solution. Unfortunately, *m*-THPP aggregates could not be detected by MALDI–TOF MS, probably because noncovalent bonds of *m*-THPP were not preserved.

Table 1. Comparison between calculated and measured isotopic distributions around m/z 1355.41 for *m*-THPP (10^{-5} M) irradiated at 647.5 nm for 6 h

Isotopic ion	First	Second	Third	Fourth	Fifth
$[(m\text{-THPP})_2-2H]^+$, calculated	1354.44	1355.44	1356.44	1357.44	1358.43
$[(m\text{-THPP})_2-2H+H]^+$, calculated	1355.45	1356.45	1357.45	1358.45	1359.46
Experimental	1355.41	1356.48	1357.42	1358.47	1359.46

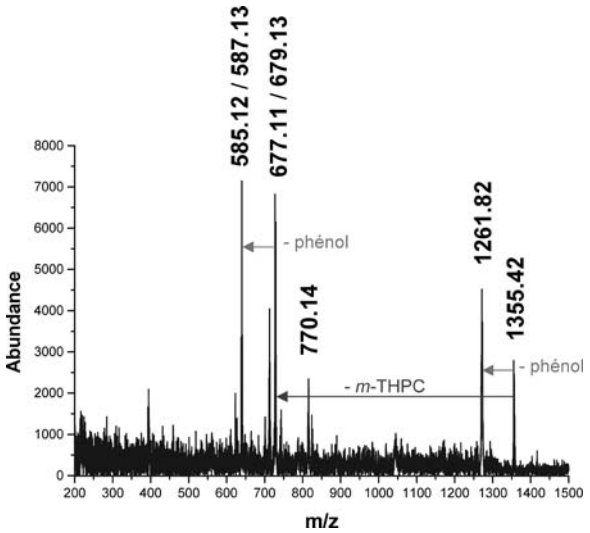

Figure 5. MALDI LIFT MS/MS spectrum of the parent ion at m/z 1355.4 (*m*-THPP, 10^{-5} M, irradiated at 647.5 nm for 6 h).

m-THPP solutions were exposed to irradiation at 647.5 nm and absorption and fluorescence spectra were recorded after 11 minutes and 225 minutes of irradiation (Figs. 1 and 2). Changes in the visible spectrum of *m*-THPP ethanol/water solution are presented in Fig. 1. A moderate decrease was observed at all Q-bands after 225 min of irradiation whereas 11 minutes of irradiation did not differ significantly from nonirradiated spectrum. It is worthwhile to note that a slight redshift was observed for band IV after 11 min of irradiation (Fig. 1). These spectral changes are consistent with the study of Bonnett *et al*. (7) on *m*-THPP photobleaching in methanol/water (3:2, vol/vol) solution indicating that the main process is photomodification rather than true photobleaching.

The fluorescence measurements (Fig. 2) show the gradual decrease in intensity of the two bands (0–0 and 0–1) (λ_{em} = 654 nm and λ'_{em} = 714 nm) with the increase in irradiation time thus revealing a photobleaching process (8).

Mass spectrometry

MALDI–TOF MS experiments were performed at 337 nm, the wavelength that did not correspond to a noticeable absorption of *m*-THPP. Figure 3 shows the variation in MALDI–TOF MS signals with respect to irradiation time. Without illumination (Fig. 3a) a predominant mass peak is observed at m/z 679.25 corresponding to $[m\text{-THPP+H}]^+$. Eleven minutes of irradiation was characterized by the same pattern of signal distribution as nonirradiated solution. This result is consistent with absorbance measurements (Fig. 1).

However, after 225 min of irradiation a new isotopic distribution of mass peaks is detected at peak monoisotopic m/z 1355.49. We could also observe the increase in signals at m/z 693.25, 695.24 and 713.25. The ion at m/z 693.25 could be attributed to *meso*-ben-zoquinonylporphyrin ($C_{44}H_{28}N_4O_5$) formed by addition of one oxygen atom to *m*-THPP molecule, which may be further reduced to dihydroxyphenylporphyrin ($C_{44}H_{30}N_4O_5$) at m/z 695.24. The singlet oxygen–mediated formation of *p*-benzoquinones from phenols has been previously reported by Saito *et al.* (23). The signal at m/z 713.25 corresponds to $C_{44}H_{32}N_4O_6$ due to the addition of the second oxygen atom. The photooxidation of *m*-THPP has been described by Bonnett (9) after unspecific irradiation (two Philips MLU 300W lamps). Authors have shown that the photooxidation of phenolic porphyrin gives benzoquinonylporphyrins and have explained that the photooxidation of *m*-THPP is slower in methanol than in methanol-water (60:40).

After 225 min of irradiation we can observe the appearance of a new isotopic distribution around m/z 1355.49. The intensity of this peak increases with illumination time (data not shown). This ionic distribution at m/z 1355.49 could correspond to $[(m\text{-THPP})_2\text{–2H+H}]^+$. To confirm the hypothesis of a dimeric structure, a postsource decay (PSD) experiment was performed (data not shown). The PSD method is used to increase the laser power beyond the threshold value that is needed to generate a traditional MALDI spectrum, and the energy excess induces molecule fragmentation. The parent ion at m/z 1355.49 gave only a fragment at m/z 1261.15; this loss of 94 atomic units (u) could be explained by the loss of phenolic group. We did not succeed in completely rupturing the parent ion so we presume that the dimeric structure is linked by a strong bond.

To provide more energy and higher sensitivity, MALDI tandem time of flight (TOF/TOF) MS was used to characterize this new photoproduct. To increase the signal of the distribution at m/z 1355.49, these experiments were performed with a solution of *m*-THPP (10^{-5} M) irradiated for 6 h (Fig. 4).

The analysis in reflector mode showed four isotopic distributions around m/z 1355.41, 2031.57, 2707.80 and 3383.98. After comparison with isotopic simulations performed by XMASS 5.1 software (Bruker Daltonics, Billerica, MA) four structures can be proposed corresponding to the above-mentioned isotopic distributions: $[(m\text{-THPP})_2\text{–2H+H}]^+$ (calculated m/z = 1355.45); $[(m\text{-THPP})_3\text{–4H+H}]^+$ (calculated m/z = 2031.66); $[(m\text{-THPP})_4\text{–6H+H}]^+$ (calculated m/z = 2707.87); and $[(m\text{-THPP})_5\text{–8H+H}]^+$ (calculated m/z = 3384.08) (Table 1).

The fragmentation of these distributions was performed by MALDI laser-induced forward transfer (LIFT) tandem mass spectrometry (MS/MS) (Fig. 5). LIFT technology measures MS/MS spectra with rapid precursor ion selection, which allows fragmenting of the dimeric structure. For the distribution around 1355.41, four fragments groups at m/z (1) 1261.82; (2) 770.14; (3) 679.13 and 677.11; and (4) 585.12 and 587.13 are mainly distinguished. The third group (m/z = 679.13 and 677.11) is related to the ion of $[m\text{-THPP+H}]^+$ and $[m\text{-THPP-2H} + \text{H}]^+$. This result demonstrates that the compound at m/z 1355.42 is constituted by two monomeric units of *m*-THPP. For the first and fourth groups (ions at m/z 1261.82 and at m/z 585.12 and 587.13) may correspond to the loss of a radical of hydroxybenzyne from $[(m\text{-THPP})_2\text{–2H+H}]^+$ and from $[m\text{-THPP–2H+H}]^+$ and $[m\text{-THPP+H}]^+$ respectively.

Finally, the ion at m/z 770.14 may correspond to $[m\text{-THPP} + 91\text{ u} + \text{H}]^+$ with molecular formula of ($C_{50}H_{33}N_4O_5$) and suggests that the phenolic group would influence the covalent bond. We suggest that photo-Claisen rearrangement to ortho-alkylphenol (Fig. 6a) has occurred (24,25), and Fig. 6b represents a structural proposition for the dimeric structure that is formed from a photochemical reaction. To confirm the hypothesis, we performed an additional set of experiments on irradiation of tetraphenylporphyrin (TPP) under the same experimental conditions (10^{-5} M, methanol/aqueous solution, 1:99, vol/vol; pulsed laser irradiation for 225 min). TPP lacks hydroxyl groups, thus preventing dimer formation after irradiation. We did not observe the formation of dimers after irradiation of 225 min or even longer (data not shown). This observation supports the hypothesis that hydroxyl groups form the covalent bond between both monomer units of *m*-THPP.

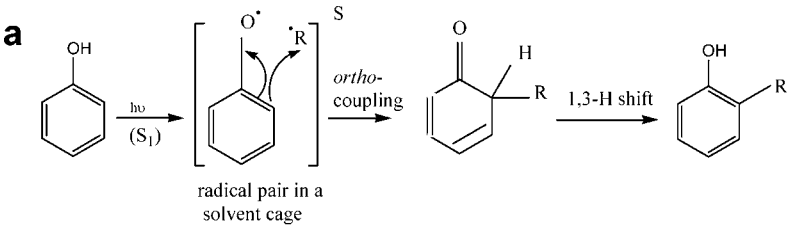

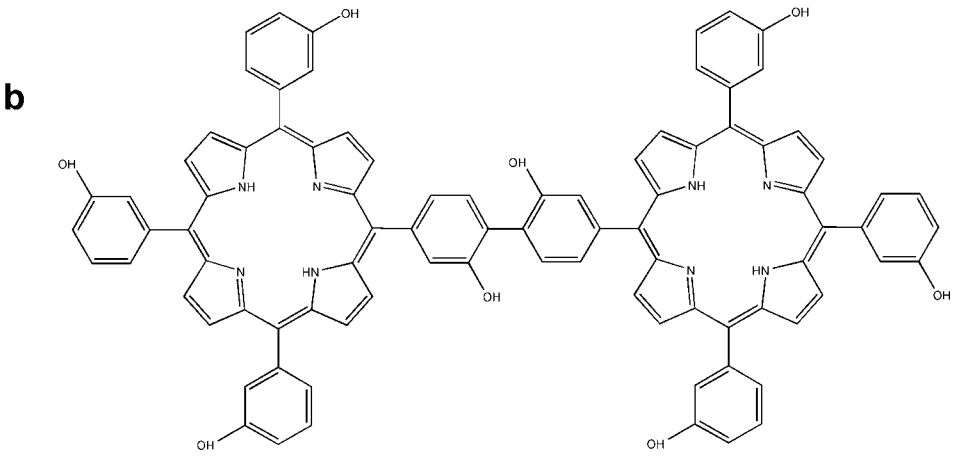

Figure 6. a: Schema of the photo-Claisen rearrangement to *ortho*-alkylphenol. b: Proposed dimer structure.

The same experiments were performed for trimer and tetramer and revealed that they are also constituted by *m*-THPP units (data not shown). The electronic spectrum of the covalent dimer (side to side) is not very different from monomeric species because the π electron system is not noticeably modified.

An important issue is the relevance of the irradiation light doses used in the present study when compared with those applied for cell photoinactivation. The comparison between effective dosimetry for the pulsed and continuous wave lasers is not obvious. A possible approach could be to compare both light sources in relation to the selected photobiological effect. With regard for the previous experience of Belitchenko *et al*. (22) with the photobleaching of m-THPC, we compared the photobleaching rates of this dye after irradiation with both light sources. Five times longer exposure time was needed with a continuous wave diode laser at 652 nm (40 J • cm^{-2}) to induce 50% loss of *m*-THPC absorbance as opposed to the pulsed laser at 652 nm used in this study (data not shown).

CONCLUSION

The MALDI MS technique employed in this study demonstrated the formation of photooxidized phenolic porphyrins and new photoproducts with an isotopic distribution around m/z 1355.5. MALDI–LIFT–TOF/TOF MS experiments revealed the photoproduct was a dimer, probably composed of two covalent linked *m*-THPP units. MALDI MS measurements also established the trimeric and tetrameric structures after prolonged laser light illumination.

To assess the *m*-THPP photobleaching pathway in a cellular environment, further studies should be undertaken in different biological medium.

Acknowledgements—We are indebted to the French Ligue Nationale contre le Cancer, the Region Lorraine and the Pole Européen de Santé for their support. The gift of *m*-THPP from Biolitec (Germany) is greatly appreciated. We would like to thank Miss Hecka and Mr. Dodeller for their help. We are grateful to Dr. Frochot and Mr. Di Stasio (Departement de Chimie Physique des Reactions) for the fluorescent spectroscopy experiments as well as Dr. Leize-Wagner and Mrs. Diemer (Laboratoire de Spectrométrie de Masse Bio-Organique) for allowing us to use the Ultraflex TOF/TOF mass spectrometer.

REFERENCES

1. MacDonald, I. J. and T. J. Dougherty (2001) Basic principles of photodynamic therapy. *J. Porphyrins Phthalocyanines* **5**, 105–129.
2. Hopper, C. (2000) Photodynamic therapy: a clinical reality in the treatment of cancer—review. *Lancet Oncol.* **1**, 212–219.
3. Pandey, R. K. (2000) Recent advances in photodynamic therapy. *J. Porphyrins Phthalocyanines* **4**, 368–373.
4. Bonnett, R. (1995) Photosensitizers of the porphyrin and phthalocyanine series for photodynamic therapy. *Chem. Soc. Rev.* **24**, 19–32.
5. Konan, Y. N., R. Gurny and E. Allemann (2002) State of the art in the delivery of photosensitizers for photodynamic therapy. *J. Photochem. Photobiol. B Biol.* **66**, 89–106.
6. Ma, L. W., J. Moan and K. Berg (1994) Comparison of the photobleaching effect of three photosensitizing agents: *meso*-tetra(*m*-hydroxyphenyl)chlorin, *meso*-tetra(*m*-hydroxyphenyl)porphyrin and photofrin during photodynamic therapy. *Lasers Med. Sci.* **9**, 127–132.
7. Bonnett, R., B. D. Djelal, P. A. Hamilton, G. Martinez and F. Wierrani (1999) Photobleaching of 5,10,15,20-tetrakis(*m*-hydroxyphenyl)porphyrin (*m*-THPP) and the corresponding chlorin (*m*-THPC) and bacteriochlorin (*m*-THPBC): a comparative study. *J. Photochem. Photobiol. B Biol.* **53**, 136–143.
8. Bonnett, R. and G. Martinez (2001) Photobleaching of sensitisers used in photodynamic therapy. *Tetrahedron* **57**, 9513–9547.
9. Bonnett, R. and G. Martinez (2002) Photobleaching of Compounds of the 5,10,15,20-tetrakis(*m*-hydroxyphenyl)-porphyrin series (*m*-THPP, *m*-THPC, and *m*-THPBC). *Org. Lett.* **4**, 2013–2016.

10. Angotti, M., B. Maunit, J.-F. Muller, L. Bezdetnaya and F. Guillemin (2001) Characterization by matrix-assisted laser desorption/ionization Fourier transform ion cyclotron resonance mass spectrometry of the major photoproducts of temoporfin (*m*-THPC) and bacteriochlorin (*m*-THPBC). *J. Mass Spectrom.* **36**, 825–831.
11. Angotti, M., B. Maunit, J.-F. Muller, L. Bezdetnaya and F. Guillemin, (1999) Matrix-assisted laser desorption/ionization coupled to Fourier transform ion cyclotron resonance mass spectrometry: a method to characterize temoporphin photoproducts. *Rapid Commun. Mass Spectrom.* **13**, 597–603.
12. Jones, R. M., Q. Wang, J. H. Lamb, B. D. Djebal, R. Bonnett and C. K. Lim (1996) Identification of photochemical oxidation products of 5,10,15,20-tetra(*m*-hydroxyphenyl)chlorin by on-line high-performance liquid chromatography-electrospray ionization tandem mass spectrometry. *J. Chromatogr. A.* **722**, 257–265.
13. Kasselouri, A., O. Bourdon, D. Demore, J. C. Blais, P. Prognon, G. Bourg-Heckly and J. Blais (1999) Fluorescence and mass spectrometry studies of *meta-tetra*(hydroxyphenyl)chlorin photoproducts. *Photochem. Photobiol.* **70**, 275–279.
14. Rotomskis, R., S. Bagdonas and G. Streckyte (1996) Spectroscopic studies of photobleaching and photoproduct formation of porphyrins used in tumour therapy. *J. Photochem. Photobiol. B Biol.* **33**, 61–67.
15. Margalit, R. and M. Rotenberg (1984) Thermodynamics of porphyrin dimerization in aqueous solutions. *Biochem. J.* **219**, 445–450.
16. Brown, S. B., M. Shillcock and P. Jones (1976) Equilibrium and kinetic studies of the aggregation of porphyrins in aqueous solution. *Biochem. J.* **153**, 279–285.
17. Margalit, R., N. Shaklai and S. Cohen (1983) Fluorimetric studies on the dimerization equilibrium of protoporphyrin IX and its haemato derivative. *Biochem. J.* **209**, 547–552.
18. Streckyte, G. and R. Rotomskis (1993) Phototransformations of porphyrins in aqueous and micellar media. *J. Photochem. Photobiol. B Biol.* **18**, 259–263.
19. Bonnett, R., B. D. Djelaln and A. Nguyen (2001) Physical and chemical studies related to the development of *m*-THPC (FOSCAN) for the photodynamic therapy (PDT) of tumors. *J. Porphyrins Phthalocyanines* **5**, 652–661.
20. Udal'tsov, A. V., L. A. Kazarin, V. A. Sinani, A. and A. Sweshnikov (2002) Water–porphyrin interactions and their influence on self-assembly of large-scale porphyrin aggregates. *J. Photochem. Photobiol. A Chem.* **151**, 105–119.
21. Bezdetnaya, L., N. Zeghari, I. Belitchenko, M. Barberi-Heyob J. L. Merlin, A. Potapenko, and F. Guillemin (1996) Spectroscopic and biological testing of photobleaching of porphyrins in solutions. *Photochem Photobiol.* **64**, 382–386.
22. Belitchenko I., V. Melnikova, L. Bezdetnaya, H. Rezzoug, J. L. Merlin, A. Potapenko and F. Guillemin (1998) Characterization of photo-degradation of meta-tetra(hydroxyphenyl)chlorin (mTHPC) in solution: biological consequences in human tumor cells. *Photochem Photobiol.* **67**, 584–590.
23. Saito, I. and T. Matsuura (1979) In *Singlet Oxygen, Organic Chemistry*. Vol. 40. (Edited by H. H. Wasserman, R. W. Murray), pp. 511. Academic Press, New York.
24. Galindo, F., M. A. Miranda and R. Tormos (1998) Coupling of phenoxy and alkyl radicals derived from the photolysis of phenol/ketone pairs: an intermolecular approach to the photo-Claisen rearrangement. *J. Photochem. Photobiol. A Chem.* **117**, 17–19.
25. Kajiyama, T. and Y. Ohkatsuic (2001) Effect of para-substituents of phenolic antioxidants. *Polym. Degrad. Stab.* **71**, 445–452.

MONSIEUR HENRI-PIERRE LASSALLE a soutenu le 7 juillet 2005
une thèse de DOCTORAT DE L'UNIVERSITE HENRI POINCARE NANCY I

TITRE DE LA THESE :
"ETUDE DES MECANISMES DU PHOTOBLANCHIEMENT DE LA 5,10,15,20-TETRAKIS(*M*-HYDROXYLPHENYL) BACTERIOCHLORINE, EN SOLUTION, *IN VITRO* ET *IN VIVO*".

RAPPORTEURS :

R. BONNETT	Professeur, Department of Chemistry, Queen Mary, University of London UK
H. SCHNECKENBURGER	Professeur, Institut für Angewandte Forschung, Aalen, Allemagne
P. De WITTE	Professeur, Faculty of Phamaceutical Sciences, Lab. Farmaceutische biologie, Leuven, Belgique

JURY :

R. BONNETT	Professeur, Department of Chemistry, Queen Mary, University of London UK
H. SCHNECKENBURGER	Professeur, Institut für Angewandte Forschung, Aalen, Allemagne
A.C. TEDESCO	Professeur, FFCLRP-Sao Paulo University, Sao Paulo, Brésil
J.F. MULLER	Professeur, LSMCL, IPEM, Metz-Technopôle, Metz, France
F. GUILLEMIN	Professeur, Centre Alexis Vautrin, Vandoeuvre, France
L.N. BEZDETNAYA-BOLOTINE	Docteur, Centre Alexis Vautrin, Vandoeuvre, France

Le jury ayant reconnu que toutes les conditions étaient remplies,

il est décerné à MONSIEUR HENRI-PIERRE LASSALLE
le DOCTORAT DE L'UNIVERSITE HENRI POINCARE NANCY I avec le label
DOCTORAT EUROPEEN

Date : 26 septembre 2005

Le Vice - Président
du Conseil Scientifique,

Patrick ALNOT

Le Président de l'Université
Henri Poincaré, NANCY I,

UNIVERSITÉ HENRI POINCARÉ, NANCY I
LE PRESIDENT

Jean-Pierre FINANCE

DOCTOR
COMMUNITATIS
EUROPEAE

UNIVERSITÉ HENRI POINCARÉ NANCY 1
24-30, rue Lionnois B.P. 60120 54003 Nancy cedex - Tél. 03 83 68 20 00 - Fax 03 83 68 21 00
Adresse électronique : _____ @uhp-nancy.fr

Université Henri Poincaré, Nancy 1
FACULTÉ DE MÉDECINE

RAPPORT DE SOUTENANCE

Concernant la thèse de **Doctorat de l'Université Henri Poincaré, Nancy 1,**
en BIOLOGIE SANTÉ ENVIRONNEMENT - Spécialité : Bioingénierie

Présentée par : **Monsieur Henri-Pierre LASSALLE**
Date de la soutenance : **JEUDI 7 JUILLET 2005**

Sur le sujet suivant : **"ÉTUDE DES MÉCANISMES DU PHOTOBLANCHIMENT DE LA 5, 10, 15, 20-TETRAKIS(m-HYDROXYPHENYL)BACTÉRIOCHLORINE, UNE ÉTUDE EN SOLUTION, IN VITRO ET IN VIVO ".**

Compte tenu du label européen de la thèse d'université, la soutenance s'est tenue en anglais. On a pu apprécier la qualité de l'anglais parlé du candidat. L'exposé oral était clair, bien présenté, didactique, montant par ailleurs une bonne appréhension des autres champs scientifiques d'intérêt.
A des questions parfois difficiles, les réponses étaient argumentées, parfois prudentes, témoignant d'une bonne capacité de réflexion.
Le candidat a montré une excellente connaissance de ses références bibliographiques qui par ailleurs étaient soigneusement choisies. Il a su mettre en exergue sa contribution personnelle à l'amélioration des connaissances sur le sujet. Tant dans le document écrit que dans la présentation orale puis dans les questions, il a valorisé ses conclusions et a mis en perspective d'autres voies de recherche. Il a montré une réelle réflexion scientifique et un potentiel pour la recherche.

Fait à VANDOEUVRE LES NANCY, le 7 juillet 2005

Signatures :
Président du Jury : Nom et signature (autre que le Directeur de Thèse)

Pr François GUILLEMIN

Membres du Jury :

Pr R. BONNET - Pr H. SCHNECKENBURGER - Pr F. GUILLEMIN

Pr L.N. BEZDETNAYA-BOLOTINE - Pr J.F. MULLER - Pr A. TEDESCO

À retourner au Service des Spécialités de la Faculté de Médecine dans les meilleurs délais.

La thérapie photodynamique (PDT) est une modalité de traitement des petites tumeurs localisées accessibles à la lumière. Son principe repose sur l'action conjuguée d'un photosensibilisant, de la lumière et de l'oxygène.
Une dosimétrie correcte est nécessaire pour assurer le traitement complet et des résultats reproductibles. Un élément clé de la dosimétrie à prendre en compte est le photoblanchiment, étant donné qu'il diminue la concentration du photosensibilisant au cours du traitement. Il est donc indispensable d'appréhender les mécanismes du photoblanchiment pour maîtriser au mieux le traitement.
Le rendement quantique de photoblanchiment de la *m*-THPBC en solution avec des protéines est de 5.7×10^{-4}, les formes agrégées de photosensibilisants photoblanchissent plus lentement que les formes monomérisées. La *m*-THPBC se transforme sous l'effet de la lumière en *m*-THPC, ce rendement de phototransformation est influencé par l'état d'agrégation de la molécule. D'autres photoproduits tels que la *m*-THPBC di-hydroxylée et la *m*-THPC di-hydroxylée ainsi que des dérivés dipyrines ont été observés. L'espèce responsable du photoblanchiment a été identifiée comme étant l'oxygène singulet. *In vitro*, la LD_{50} de la *m*-THPBC est 0.7 J cm^{-2}. Le photoblanchiment est 3 à 5 fois plus sensible que celui de la *m*-THPC. L'étude de la localisation intra-cellulaire des photosensibilisants a montré une différence, la *m*-THPC s'accumulant dans le réticulum endoplasmique alors que la *m*-THPBC se localise dans les mitochondries. *In vivo*, la *m*-THPBC possède un photoblanchiment 4 à 10 fois plus élevé que la *m*-THPC, ainsi qu'une bonne accumulation tumorale. Ces résultats *in vitro* et *in vivo* sont particulièrement intéressants en terme de ratio thérapeutique, de sélectivité du traitement et de photosensibilité cutanée.

Study of the photobleaching mechanisms of the 5,10,15,20-tetrakis(m-hydroxyphenyl) bacteriochlorin (*m*-THPBC), in solution, in vitro and in vivo.

Photodynamic therapy (PDT) has been developed as a treatment modality for a number of malignant and non-malignant disorders. PDT treatment is based on the presence of a drug with photosensitising and tumour localizing properties combined with visible light and oxygen. Accurate dosimetry is necessary to ensure complete treatment and to allow for consistent and reproducible patient outcomes. One of the key element which needs to be considered in dosimetry is photobleaching since it decrease the photosensitiser concentration during the treatment. It seems therefore important to understand the photobleaching mechanisms to adapt the photodynamic dose and receive the optimal treatment.
The photobleaching quantum yield in solution supplemented with proteins is 5.7×10^{-4}, the aggregated forms of the photosensitiser bleach slower than the monomerised forms. Under light exposure the *m*-THPBC is transformed in *m*-THPC, the phototransformation yield is influenced by the aggregation state of the molecule. Some other photoproducts such as di-hydroxy *m*-THPBC, di-hydroxy *m*-THPC, dipyrin derivatives were observed. Singlet oxygen was found to be responsible of the photobleaching of both *m*-THPBC and *m*-THPC. *In vitro*, the *m*-THPBC LD_{50} is 0.7 J cm^{-2}, and the photobleaching 3 to 5 times faster than *m*-THPC. Fluorescence microscopy study exhibits a discrepancy in the photosensitisers localisation, *m*-THPC is localised is the endoplasmic reticulum and *m*-THPBC accumulates in mitochondria. In vivo *m*-THPBC photobleaching is 4 to 10 times faster than *m*-THPC, with a good tumour accumulation. Taking as a whole these observations are particularly attractive in terms of therapeutic ratio and selectivity of the treatment and skin photosensitivity.

MOTS CLES: Thérapie Photodynamique (PDT), *m*-THPBC, photoblanchiment, photodegradation.

DISCIPLINE : Bio Ingénierie

Centre Alexis Vautrin, CRAN CNRS UMR 7039-INPL-UHP, avenue de Bourgogne, 54511 Vandœuvre-les-Nancy